Electrocatalytic Nanoparticle Based Sensing for Diagnostics

By

Marisa Maltez da Costa

Thesis dissertation to apply for the PhD in
Biochemistry, Molecular Biology and Biomedicine

Directors: Prof. Arben Merkoçi and Dr. Alfredo de la Escosura

Nanobioelectronics and Biosensors Group,
Institut Català de Nanotecnologia

University Tutor: Ester Boix

Departament de Bioquímica i Biologia Molecular,
Universitat Autònoma de Barcelona

Bellaterra (Barcelona), Spain
May 2012

The present work entitled "*Electrocatalytic Nanoparticle Based Sensing for Diagnostics*", presented by Marisa Maltez da Costa to obtain the degree of doctor by the Universitat Autònoma de Barcelona, was performed at the Nanobioelectronics and Biosensors Group in the Institut Català de Nanotecnologia (ICN), under the supervision of Prof. Arben Merkoçi Hyka, ICREA Professor and Group Leader, and Dr. Alfredo de la Escosura Muñiz, Post-doctoral Researcher.

Bellaterra, May 2012

The supervisors

-

Prof. Arben Merkoçi Hyka

-

Dr. Alfredo de la Escosura Muñiz

The present thesis was performed under the doctoral program studies "Doctorado en Bioquimica, Biologia Molecular i Biomedicina" at Universitat Autònoma de Barcelona, under the tutorship of Prof. Ester Boix.

The university tutor

-

Prof. Ester Boix Borràs

PREFACE

The present PhD thesis research was carried out at Nanobioelectronics and Biosensors Group at Catalan Institute of Nanotechnology (ICN-CIN2) under the doctoral program of Biochemistry, Molecular Biology and Biomedicine at Autonomous University of Barcelona (UAB).

The research work accomplished, resulted in several publications and manuscripts that were submitted to international peer-reviewed scientific journals, and also in a book chapter by invitation of the editor.

According to the decision of the PhD Commission of the Autonomous University of Barcelona (UAB), this PhD thesis is presented as a compendium of publications.

A manuscript that was published in 2009, prior to the inscription in the PhD doctoral program and for this reason does not fulfill the UAB PhD-commission rules was allowed to be included in the "Additional manuscripts" section.

Another manuscript in which the UAB-affiliation of the PhD student is not explicit, and for this reason does not fulfill the UAB PhD-commission rules was allowed to be included in the "Additional publications and manuscripts" section.

Other two manuscripts that were sent to peer-revision in 2012, and that are not yet accepted, are also included in the "Additional publications and manuscripts" section.

Publications presented to the UAB-PhD commission on February 22nd, 2012:

Publication 1. "Electrochemical quantification of gold nanoparticles based on their catalytic properties toward hydrogen formation: application in magneto immunoassays" M. Maltez-da Costa, A. de la Escosura-Muñiz, A. Merkoçi *Electrochemistry Communications* **2010**, 12, 1501-1504

Publication 2. "Gold nanoparticle-based electrochemical magnetoimmunosensor for rapid detection of anti-hepatitis B virus antibodies in human serum" A. de la Escosura-Muñiz, M. Maltez-da Costa, C. Sánchez-Espinel, B. Díaz-Freitas, J. Fernández-Suarez, A. González-Fernández, A. Merkoçi, *Biosensors and Bioelectronics* **2010**, 26, 1710-1714.

Publication 3. "Nanoparticle-induced catalysis for electrochemical DNA biosensors" book chapter from "Electrochemical DNA Biosensors" M. Maltez-da Costa, A. de la Escosura-Muñiz, A. Merkoçi, edited by Mehmet Ozsoz (Pan Stanford Publishing, i*n press*, **2012**)

Publication 4. "Aptamers based electrochemical biosensor for protein detection using carbon nanotubes platforms" P. Kara, A. de la Escosura-Muñiz, M. Maltez-da Costa, M. Guix, M. Ozsoz, A. Merkoçi, *Biosensors and Bioelectronics*, **2010**, 26, 1715-1718.

Additional publications and manuscripts

Publication 5. “Controlling the electrochemical deposition of silver onto gold nanoparticles: reducing interferences and increasing the sensitivity of magnetoimmuno assays” A. de la Escosura-Muñiz, M. Maltez-da Costa, A. Merkoçi, *Biosensors and Bioelectronics* **2009**, 24, 2475-2482.

Publication 6. “Rapid identification and quantification of tumor cells using an electrocatalytic method based on gold nanoparticles” A. de la Escosura-Muñiz, C. Sánchez-Espinel, B. Díaz-Freitas, A. González-Fernández, M. Maltez-da Costa, A. Merkoçi, *Analytical Chemistry* **2009**, 81, 10268-10274.

Publication 7. “Detection of Circulating Tumor Cells Using Nanoparticles” M. Maltez-da Costa, A. de la Escosura-Muñiz, Carme Nogués, Leonard Barrios, Elena Ibáñez, A. Merkoçi, *submitted to Small* **2012.**

Publication 8. “Magnetic cell assay with electrocatalytic gold nanoparticles for rapid CTCs electrochemical detection” M. Maltez-da Costa, A. de la Escosura-Muñiz, Carme Nogués, Leonard Barrios, Elena Ibáñez, A. Merkoçi, *submitted to Nature Methods* **2012**.

ACKOWLEDGEMENTS FOR FINANCIAL SUPPORT

In first, I would like to acknowledge Catalan Institute of Nanotechnology (ICN) for the financial support that I personally received to develop the research work here presented, and also for the funding of my master and doctoral studies.
Acknowledgments are also given for the financial support obtained from several programs:

MEC / MICINN (Madrid) for the projects:

MAT2008-03079/NAN, MAT2008-03079/NAN, CSD2006-00012 ‘‘NANOBIOMED’’ (Consolider-Ingenio 2010), PIB2010JP-00278 and IT2009-0092.

Xunta de Galicia for PGIDIT06TMT31402PR and INBIOMED, 2009/63.

SUDOE-FEDER (Immunonet-SOE1/P1/E014.

E.U.’s support under FP7 contract number 246513 ‘‘NADINE”.

NATO Science for Peace and Security Program’s support under the project SfP 983807.

GLOSSARY OF TERMS, ACRONYMS AND ABBREVIATIONS

Ab	Antibody
AgNPs	Silver nanoparticles
AuNPs	Gold nanoparticles
Anti-CEA	Carcinoembryonic antibody
Caco2	Human colon adenocarcinoma cell
CE	Counter electrode
CEA	Carcinoembryonic antigen
CCRF-CEM	Human leukemic lymphoblast
CNTs	Carbon nanotubes
CoA	Concanavalin A
CTCs	Circulating tumor cells
CV	Cyclic voltammetry
DNA	Deoxyribonucleic-acid
DPV	Differential pulse voltammetry
E	Potential
EIS	Electrochemical impedance spectroscopy
ELISA	Enzyme-linked immunosorbent assay
et al.	And other people
e.g.	For example
Fc	6-ferrocenylhexanethiol
Fc-D	Ferrocenyl tethered dendrimer
GC	Glassy carbon
H2O2	Hydrogen peroxide
HepB	Hepatitis B
HER	Hydrogen evolution reaction
HMy2	Human Lymphoblastoid B cell
HRP	Horseradish peroxidase
i	current
IgE	Immunoglobulin E
IgG	Immunoglobulin G
IgM	Immunoglobulin M
ITO	Indium-tin-oxide
LOD	Limit of detection
MBs	Magnetic microparticles
MCF-7	Human breast carcinoma cell
MWCNTs	Multiwall carbon nanotubes
NaBH4	Sodium boruhydride
NO	Nitric Oxide gas
PC-3	Human prostate carcinoma cell

PdNPs	Palladium nanoparticles
PSA	Prostate specific antigen
PtNPs	Platinum nanoparticles
QDs	Quantum dots
QCM	Quartz crystal microbalance
RNA	Ribonucleic acid
RE	Reference electrode
RSD	Relative standard deviation
RT-PCR	Reverse transcriptase polymerase chain reaction
SEM	Scanning electron microscopy
SPCE	Screen printed carbon electrodes
SPR	Surface plasmon resonance
TEM	Transmission electron microscopy
UV-Vis	Ultraviolet-visible
WE	Working electrode
ΔE	Potential variation

TABLE OF CONTENTS

Chapter 1

General introduction

Chapter 1

Electrocatalytic nanomaterial-based sensing for biomarker detection

1. Sensing and biosensing using nanomaterials

Several nanomaterials, including carbon nanotubes, nanoparticles, magnetic nanoparticles, and nanocomposites, are being used to develop highly sensitive and robust biosensors and biosensing systems [1] with a special emphasis on the development of electrochemical-based (bio)sensors [2] due to their simplicity and cost efficiency.

One of the main requirements for a good performance of a biosensor is the high sensitivity of the response. This is of great importance when, for example, it is required to use the biosensor in clinical diagnostics for the detection of low levels of clinical biomarkers in human fluids [3], because in most cases the biomarker to be detected is present in very low concentrations. The need for biosensing systems that can detect these markers with high sensitivity without loss of selectivity, that is, low detection limits with high reliability and superior reproducibility, is an important challenge. To accomplish all these requirements the signal amplification and noise reduction are significant strategies that have been greatly explored by the incorporation of nanomaterials.

The amplified detection of biorecognition events stands out of the biosensing field, because it is one of the most important objectives of the current bioanalytical chemistry. In this context, approaching the catalytic properties of some (bio)materials appears to be a promising way to enhance the sensitivity of the bioassays.

Several publications explain the use of nanoparticles in sensing and biosensing systems, enunciating the several detection techniques employed. One of the ways to classify them is by the nature of the transducer system used. Briefly, this classification results in Optical (light absorption, light scattering (SPR) and fluorescence), Electrical (QCM, EIS) or Electrochemical techniques (Potentiometry, Stripping Voltammetry), and each one has its own advantages. Globally they can all profit from the inclusion of nanomaterials in the most diverse configurations or assemblies, but owing to the central focus of this review from this point on, only the electrochemical sensing techniques are going to be addressed.

Electrochemical biosensors are very interesting for point-of-care devices due to the possibilities that they display. They are portable, easy to use, cost-effective and in most cases disposable. The most widely used example of an electrochemical biosensor is the glucose sensor that is based on a screen-printed amperometric disposable electrode. This sensor illustrates the miniaturization and portability features and the genuine “on-site” analysis that electrochemical biosensors ideally display.

Most electrochemical biosensors still require the use of an enzymatic label that act as reporter label. The traditional coupling of enzymes as biocatalytic amplifying labels is a generated paradigm in the development of bioelectronic sensing devices. The biocatalytic generation of a redox product upon binding of the label to the recognition event, the incorporation of redox mediators into biomolecules assemblies that activate bioelectrocatalytic transformations, or the use of enzyme labels that yield an insoluble product on electrode surfaces has been extensively used to amplify biorecognition events. Enzymatic biosensors represent an already consolidated class of biosensors, with glucose biosensors among the most successful on the market. Nevertheless, research is still needed to find novel alternative strategies and materials, so that affinity biosensors (immunosensors and genosensors) could be used in more successful applications in everyday life.[4]

2. Nanomaterials as catalysts: electrocatalytic sensing

Catalysts are materials that change the rate of chemical reactions without being consumed in the process. Because of their huge economical contribution, by lowering the costs of several processes, they are actually one of most wanted materials and can be found in manufacturing processes, fuel cells, combustion devices, pollution control systems, food processing, and sensor systems. Catalysts are generally prepared from transition metals, most of them from the platinum group, but this fact still represent a high cost due to the material expensiveness, and thus a reduction in used amounts would be appreciated. [5,6]

By definition an electrocatalyst is a catalyst that participates in an electrochemical reaction. The electrocatalyst assists in the electron transfer between the electrode and the reactants and/or facilitates an intermediate reaction/transformation /state.

An electrochemical reaction at an electrode is a heterogeneous reaction process that occurs at the electrode–electrolyte interface. The rate of the electrochemical reactions depend either on mass transfer of the ions from bulk of the solution to the electrode surface (diffusion limited) or on rate of heterogeneous electron transfer (kinetically limited).

In electrochemical sensors, electrocatalytic procedures can be approached in two ways, either by using an electrode that have highly or moderately electrocatalytic properties, or by exploiting a significant change in the electrocatalytic activity of an electrode during the detection process. Gold and platinum are commonly employed as highly electrocatalytic electrodes. Although these electrodes allow fast electron-transfer kinetics for most electroactive species, their background currents are high and fluctuate with

the applied potential, which may inhibit the high signal-to-background ratios, required to obtain low detection limits.

In recent years, moderately electrocatalytic electrodes have been used to obtain high signal-to-background ratios. Such electrodes can be prepared by modifying a poorly electrocatalytic electrode with a low coverage of a highly electrocatalytic material. For example, indium-tin oxide (ITO) electrodes modified with a partial monolayer of ferrocene, carbon nanotubes, or gold NPs (AuNPs) have been employed [7, 11].

The actual knowledge concerning the special properties of NPs arises from the numerous studies related to the effects of changes in shape and size on the general properties of materials. From the electroanalysis point of view the major features resulting from these studies are enhancement of mass transport, high catalytic activity, high effective surface area, and control over local microenvironment at the electrode surface [8, 12, 13, 14].

The development of nanotechnology during the last decades has led the scientists to fabricate and analyze catalysts at the nanoscale. These nanostructured materials are usually high-surface-area metals or semiconductors in the form of NPs with excellent catalytic properties due to the high ratio of surface atoms with free valences to the cluster of total atoms. The catalysis takes place on the active surface sites of metal clusters in a similar mechanism as the conventional heterogeneous catalysis [12] and in general, this is a process that occurs at the molecular or atomic level independent of the catalyst dimensions [6, 14]. There is a considerable amount of research articles and interesting reviews in what concerns to the study of NP-catalyzed reactions, but the application of these reactions in electrochemical biosensing is not so well documented.

Employing NPs in electroanalysis can lead to more sensitive and selective sensors as well as more cost-effective and portable detection systems. Their application as catalysts in electroanalytical systems can decrease overpotentials of many important redox species, induce discrimination between different electroactive analytes, and also allow the occurrence and reversibility of some redox reactions, which are irreversible at commonly modified electrodes [15]. The catalytic effect can be explained through the enhancement of electron transfer between the electrode surface and the species in solution, by enhancement of mass transport or also by the NP's high surface energy that allows the preferred adsorption of some species that by this way suffer a change in their overpotentials (Fig. 1).

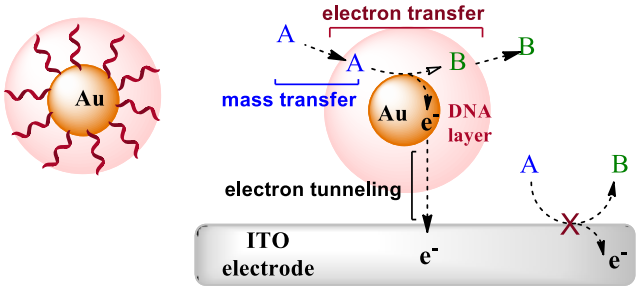

Figure 1. Schematic illustration of the processes that affect the electrocatalytic oxidation by AuNP when functionalized with DNA strands. Adapted from ref. ([7]

Nanoparticles can be employed in biosensing systems as electrocatalytic electrode modifiers or as electrocatalytic labels of biomolecules. The presence of nanoparticles on the electrotransducer surface promotes the direct electron transfer between the electrode and the electroactive species in solution, improving the electrochemical response from potentiometric or conductimetric signals. The same effect can be obtained when the nanoparticles are used as electrochemical report-labels for biomolecules, where the signal comes directly from the nanoparticles (like AuNPs and semi-conductor QDs) or when they are used as electrocatalytic enhancer-labels of redox biomolecules.

2.1. Nanomaterials as modifiers of electrotransducer surfaces

In biosensors, NPs can be assembled on conventional electrode surfaces using several methods and different nanoparticles. Nanoparticles can be integrated in the electrode base constituting material, for example in carbon paste electrodes, [8,9] they can be included in biopolymer-composites as for example the Chitosan/AuNPs composite membrane [10,11] or they can also be conjugated with proteins and then be assembled in 3D sol-gel networks [12] or Layer-by-Layer assemblies [13,14] through electrostatic interactions .

The most exploited materials in catalysis are the metals from platinum group, but with the introduction of nanotechnology some other elements that in bulk state did not attract a lot of attention, either due to their lack of reactivity toward some analytes or due to their high costs in production, are now emerging.

Metallic gold was thought to be very stable and useless for some catalytic systems, but by the reduction of size to the nanoscale range, gold was proved to be a very reactive element and it has been extensively used in sensing and biosensing systems as a catalyst for some interesting electroanalytical applications. For instance, a sensitive Nitric Oxide (NO) sensor was developed through the modification of a platinum microelectrode by AuNPs in which they catalyze the electrochemical oxidation of NO with an overpotential

decrease of about 250 mV [15]. A Sulphur Dioxide (SO2) gas sensor was also developed using AuNPs to catalyze the electrochemical oxidation of SO2 when the gas diffuses through the pores of the working electrode [23].

Raj and co-worker reported an ultrasensitive electrochemical detection of hydrazine using AuNPs self-assembled on a sol–gel-derived 3D silicate network, followed by seed-mediated growth of gold. The system proved to be highly sensitive toward the electrochemical oxidation of hydrazine. A very large decrease in the overpotential (∼800 mV) and significant enhancement in the peak currents with respect to the bulk Au electrode were observed without using any redox mediator. The nanostructured platform showed excellent sensitivity with an experimental detection limit of 200 pM.[15]

AgNPs are not so commonly used as AuNPs but nevertheless their catalytic properties in electrochemical detection have also been exploited. For instance, they were reported as promoters for electron transfer between the graphite electrode and hemoglobin in a NO sensor system where they also act as a base to attach the hemoglobin onto a pyrolytic graphite electrode while preserving the hemoglobin natural conformation and therefore its reactivity [46].

Platinum Nanoparticle (PtNPs) can also be used as electrocatalists. Despite the high cost of this metal in the bulk state, the subsequent saving that reducing the metal size implies placed PtNPs in the center of attention of scientists due to their ability to be used as catalyst for many industrial processes [13]. PtNPs are used as catalysts for electrochemical hydrogen peroxide (H2O2) detection, where they act as modifiers of the electrode surface and electrocatalyze the oxidation of H2O2 observed by a lower oxidation peak potential when compared with the bulk platinum electrode [30]. As the H2O2 is a product of many enzymatic reactions, this electrode has a vast potential application as an electrochemical biosensor for many substances [15]. PtNPs have also been used as catalysts in gas sensors like nitric oxide (NO) sensor making use of the electrocatalytic effect in the oxidation of this specie [31]

Metal oxides are emerging as important materials because of their versatile properties such as high-temperature superconductivity, ferroelectricity, ferromagnetism, piezoelectricity, and semiconductivity [38].

Recently, nanostructured TiO2 particle (TiO2-NPs) preparation and their applications in photovoltaic studies, photocatalysis, and environmental studies have attracted much attention mostly in the emerging sensor technology based on NPs and nanocomposites with chemical and biological molecules [33].

2.2. Nanomaterials as labels

Nanoparticles, especially small and round shape nanoparticles, such as metal and semi-conductor particles, can be easily applied as labels for electrochemical biosensors.(Castañeda, Alegret, & Merkoçi, 2007; de la. Escosura-Muñiz, Ambrosi, & Merkoçi, 2008)

When these nanoparticles are used as electrochemical report-labels for biomolecules, using a voltammetric method the signal comes straight from the nanoparticles with or without their previous dissolution. The direct methods, without previous dissolution, offer advantages for sensing applications due to the fast response, procedure simplification and the reduced cost o analysis. However this type of detection needs a direct contact between the electrode surface and the nanoparticle, therefore indirect methods are very often reported as better options when an exceptional sensitivity is necessary.[17]. A very comprehensive review was assembled by Merkoçi's group were several nanoparticle direct and indirect detection methods are described and classified.

Although considerable amounts of research papers have been published in last five years, the review by Welch and Compton [18] is another good summary of the investigations carried out in the use of nanoparticles in electroanalysis. The authors reviewed several examples that inspired much of the work that is still being done nowadays. Most work describe the use of gold, silver and platinum metals, however, iron, nickel and copper are also reviewed with some examples of other metals such as iridium, ruthenium, cobalt, chromium and palladium. Some bimetallic nanoparticle modifications are also mentioned because they can cause unique catalysis through the mixing of the properties of both metals. Later on, they published an updated review that complements the first. [19]

Nucleic acid-functionalized Pt nanoparticles (Pt-NPs) were use as catalytic labels for the amplified electrochemical detection of aptamer/protein recognition. The association of aptamer-functionalized Pt- NPs to a thrombin aptamer/thrombin complex associated with an electrode allowed the amplified, electrocatalytic detection of thrombin with a sensitivity limit corresponding to 1×10^{-9} M.[20]

Another example of ultrasensitive detection of protein was reported by Das et al. by signal amplification combined with noise reduction: the signal was amplified both by the catalytic reduction of p-nitrophenol to p-aminophenol, by gold-nanocatalyst labels, and by the chemical reduction of p-quinone imine to p-aminophenol by sodium borohydride ($NaBH_4$); the noise was reduced by employing an indium tin oxide electrode modified with a ferrocenyl-tethered dendrimer and a hydrophilic immunosensing layer.[21]. A more recent work from the same group reported an enhancement of the electrocatalytic activity

of AuNPs after $NaBH_4$ and its application to H_2O_2 detection. They also showed the same effect for the electro-oxidation of glucose and formic acid. The authors claim that adsorption/absorption of great amounts of hydrogen species on the AuNPs forming an activated state that remains even after hydrogen species are removed.

2.3. Nanomaterials as carrier/enhancers of redox proteins

In protein-based biosensors the efficient electrical communication between redox proteins and solid electrode surfaces is still an important request, and many methods have been tried in order to obtain direct electrochemical responses of proteins embedded in surface modifier films.

An example for the latter is the work presented by Zhou et al. [39] where the photovoltaic effect of TiO2-NPs, induced by ultraviolet light, can greatly improve the catalytic activity of hemoglobin as a peroxidase with increased sensitivity when compared to the catalytic reactions in the dark, which indicates a possible method to tune the properties of proteins for development of photocontrolled protein-based biosensors. The method claims an enhancement in the catalytic activity of hemoglobin, by a specific interaction with 35-nm TiO2-NP, toward the H2O2 reduction. This catalytic effect was not observed by other comparative experiments with films containing nanostructured CdS or ZnO2.

3. Electrocatalysis applied for biomarker sensing systems

A biomarker is an indicator of a biological state of disease or physiological condition that can be used as marker to target the specific conditions which it is related to. [22–24] In medicine, biomarkers can be specific molecules, DNA or RNA fragments or sequences, hormones, enzymes, proteins, fragments of a protein or cells associated with any medical condition with clinical interest. These biomarkers can be present in human fluids like blood, serum, urine or other, and must be detected and/or quantified to perform or complement a medical diagnostic, or to evaluate the progression of a disease.

Therefore there is a high variability in terms of the nature and size of biomarkers and they can be classified by innumerous ways. In agreement their detection can also be performed by several different techniques, but there is a general claim in the diagnostic field for more accurate detection systems that can operate with low amounts of sample and offer also the possibility of multiplexing without compromising the costs and the time of analysis.

Catalytic nanoparticles are introduced here as tools for enhancing the detection of biomarkers. Because of their small size, surface charge, stability and ability to bee functionalized by biomolecules, their use can be extremely advantageous. Their nanometric size allow for fast interaction with similar sized biomolecules, resulting in lower interaction time to produce nanoparticle bioconjugates, where nanoparticles are coated with DNA and RNA sequences, antibodies, antigens and enzymes, between many others. These conjugates can be used as detection labels for other biomolecules like proteins, DNA fragments or even cells.

From the electrochemical point of view, nanoparticle bioconjugates can be used as electrochemical labels in various biosensing systems. The nanoparticle excellent electroactivity (for example AunPs and heavy metal QDs) allows the use of electrochemical techniques for their detection, reaching low limits of detection and consequently low concentrations of target biomolecules can be detected.

The nanoparticles, due to their high surface ratio can also be used as direct electron transfer enhancers for certain protein/enzyme redox centers that are usually embedded in the protein corona that hinders or eliminate completely their electrochemistry. Several reports that study redox-proteins electrochemistry, found that immobilizing these proteins on nanoparticles would induce the catalytic redox reactions in which they are usually involved, without the need of any other mediator and without losing the protein spatial configuration.

3.1. Carbon nanomaterials in electrocatalytic sensing of biomarkers

Carbon is one of the most widely-used material in electroanalysis and electrocatalysis [25,26] and several carbon based materials, such as fullerenes, graphene based materials and carbon nanotubes (CNTs), are reported as excellent electrode materials for electroanalysis and electrocatalysis.

In this last years the reported works, using graphene based materials in biosensing applications, undergone an exponential growth. Graphene, as the basic building block for graphitic materials of all other dimensionalities (0D fullerenes, 1D nanotubes, and 3D graphite)[27], was reported to show ability for direct electrochemistry of enzyme, electrocatalytic activity toward small biomolecules (hydrogen peroxide, NADH, dopamine, etc.), and graphene based enzyme biosensors were also reported in Graphene-based DNA sensing and environmental analysis. The majority of these works employed reduced graphene oxide derivate as electrode modifying nanomaterial.

In recent works [28] controlled the functional groups of nanoplatelets of graphite oxide and determined that the edge-plane-like sites of the electrode were the electroactive sites which help to increase the current response and the peak shift between uric acid and ascorbic acid.

Graphene was also incorporated in nanocomposites in order to combine its unique properties with the properties of other nanomaterials. Yue et al.[29] developed a sensing platform for the detection of nitrite with a composite film made of graphene nanoplatelet and heme protein. They found that single-layer graphene nanoplatelet provides a biocompatible microenvironment for protein immobilization with suitable electron transfer characteristics. Fan et al. prepared a TiO2-graphene nanocomposite by hydrolysis and in situ hydrothermal treatment. They modified a GC electrode surface with this composite and obtained a significant improvement in the electrocatalytic activity toward adenine and guanine.[30]

Other carbon-based materials have also been used in nanocomposites in order to couple their unique features with the selectivity and catalytic ability of other materials.

Carbon nanotubes also show excellent performance in biosensors (Ahammad, Lee, & Rahman, 2009; Vairavapandian, Vichchulada, & Lay, 2008) and their electrocatalytic activity has been systematically studied [34] [50 – 55, 61] Komathi et al.69 demonstrated the nanomolar detection of dopamine through the use of a new nanocomposite made up of MWCNTs, a grafted silica network, and gold nanoparticles.

Several works report the use of electrodes modified with C60 to generate reproducible electrocatalytic responses for certain biomarkers. [35] Tan, Bond and co-workers ([35]) reported the electrochemical oxidation of L-cysteine in aqueous solution at C60 modified Glassy carbon electrode. Detection strategies for L-cysteine are widely sought since the molecule is an important biomarker for a variety of diseases ([36]). In this pioneer work, C60 was easily immobilized onto the electrode surface, and without any pre-treatment step, the modified electrode was able to promote a reduction of the potential-peak of cysteine oxidation from 550mV (at a bare electrode) to 450mV. This reduction in cysteine overpotential coupled with an increment in the voltammetric peak magnitude was reported to be due to the presence of C60 which acted as a mediator, providing alternative reaction sites for electron transfer processes. Goyal et al. [37] reported the electrocatalytic detection of uric acid following the work pioneered by Tan. Uric acid is a human metabolic product that can be found in biofluids such as human serum, blood, urine, etc. Its unusual high levels can indicate several diseases like for example diabetes and gout, whereas abnormally low concentrations can indicate copper toxicity,

Fanconi's disease Wilson's disease, between others. They reported that the uric acid and ascorbic acid overlapping voltammetric responses, obtained with a bare glassy carbon electrode, could be resolved in two well-defined peaks when using/employing C60 supported on glassy carbon electrode. The obtained peaks had a potential difference of ca. 150mV with detection limits as low as 0.12mM, in addition they declared their method to be superior to former reports due the elimination of the electrode pre-treatment and post measure cleaning steps. Furthermore the C60 modified electrodes were easy to prepare and showed good stability, which make them attractive for other electroanalytical assays.

3.2. Metal nanoparticles in electrocatalytic sensing of biomarkers

Metal nanoparticles can be directly detected owing to their own redox properties (of the element atoms they are formed by) or indirectly using their electrocatalytic effect toward reactions of other species.

Gold nanoparticles can also be used as amplifying platforms for enzyme and other protein labels (hemoglobin), working as high surface ratio carriers, and by this way promote the catalytic electrochemical detection of target biomolecules. Similarly to carbon nanomaterials, AuNPs were reported to promote the electron transfer between the electrode and the catalytic groups that are usually embedded in the protein/enzyme core.

Gold NPs (AuNPs) and silver NPs (AgNPs) are of particular interest in immunosensors and DNA sensors due to their advantageous properties, such as hydrophilicity, standard fabrication methods, excellent biocompatibility, unique characteristics in the conjugation with biological recognition elements, and multiplex capacity for signal transducer. Therefore, a large number of published methods use Au- or AgNPs in DNA [16, 17, 18] protein [19] and even cell [20] electrochemical detection besides optical detections like ICP-MS [21], or they even use an ELISA enhancer [22].

Based on the selective catalysis of AuNPs, selective electrochemical analysis could also be achieved as, for example, in the dopamine electrochemical detection in presence of ascorbic acid. In this case, AuNPs can be used as selective catalysts since their presence induces the decreasing of ascorbic acid overpotential and the effective separation of the oxidation potentials of ascorbic acid and dopamine [13]. The catalytic effect of AuNPs in the electrochemical detection of S-nitosothiols was studied by Jia et al. [38] (RSNOs) play key roles in human health and disease, but improved quantifying techniques to be applied in blood and other biological fluids. In this work an electrochemical assay to determine RSNOs was developed based on the efficient catalysis of gold nanoparticles for RSNO

decomposition. The approach displayed high sensitivity for RSNOs with a low detection limit to 5.08×10^{-11} M and was free from interference of some endogenous substances such as NO_2^-, NO_3^- and GSH co-existing in blood serum. In addition this approach is potentially useful to evaluate RSNOs levels in various biological fluids via varying gold nanoparticles concentration.

PtNPs in conjugation with carbon nanotubes (CNTs) and glutaraldehyde, PtNPs also allowed the development of a carbon-based electrode as a sensor for glucose, in a similar system as one of the reported H_2O_2 sensors [13].

Regarding its application in DNA sensors, Polsky et al. [10] used nucleic acid functionalized PtNPs as catalytic labels to amplify the electrochemical detection of both DNA hybridization and aptamer/protein recognition. The assay was based on the catalytic effect of the PtNPs on the reduction of H_2O_2 to H_2O, using gold slides as electrodes. The amperometric measurement of the electrocatalyzed reduction of H_2O_2, detected DNA with a LOD of 1×10^{-11} M.

Palladium belongs to the platinum group of metals, and, due to its similar features in terms of electrocatalytic activity toward numerous redox reactions, it has been used in electrode modification processes in several electrochemical sensors [33]. Palladium NPs (PdNPs) were applied in several electrochemical biosensors. For instance, a glucose biosensor based on codeposition of PdNPs and glucose oxidase onto carbon electrodes [34], encapsulated channels for protein biosensing and the reduction of H2O2 [35], and a DNA-template preparation of PdNPs onto ITO for H2O2 reduction and ascorbic acid oxidation, has been reported [33].

3.3. Protein detection using electrocalytic-sensing systems

Between the several biomarkers with interest for medical diagnostics, proteins represent a significant group since they can be associated with many diseases, manifested through their malfunction or increased/decreased expression by human organs, tissues or cells. Therefore their detection and quantification stands out as an important tool for screening, early diagnostics, prognostics and also to monitor the outcomes of therapies. [3]

The most used methods for the detection of protein biomarkers are enzyme-linked immunosorbent assay (ELISA), western blot assays, immuno-precipitation, immunoblotting techniques and immunofluorescence. ELISA assays is the most usual assay employed in protein sensing for diagnostics, it relies in the sandwich-type immunoassays that have high specificity and sensitivity because of the use of a couple of match antibodies [3]. But besides being time-consuming and labor-intensive, requiring highly qualified

personnel, this and other traditional protein detection methods fail to achieve the very low limits of detection that are required for several biomarkers (like certain cancer biomarker). More cost-effective methods requiring simple/user-friendly instrumentation that can provide an adequate sensitivity and accuracy would be ideal for point-of- care diagnosis. For this reason, there is a high demand for simple, fast, efficient and user-friendly alternative methods for the detection of protein markers.

The recent development of immunoassay techniques aims in most cases at decreasing analysis times, improving assay sensitivity, simplification and automation of the assay procedures. [39] Among other types of immunosensors, electrochemical immunosensors are very attractive tools and have gained considerable interest. [40] Unlike spectroscopic-based techniques, electrochemical methods are not affected by sample turbidity and fluorescing compounds commonly found in biological samples. Furthermore, the required instruments are relatively simple and can be miniaturized with very low power requirements.[41]

Immunosensors, usually used for quantitative determination of protein biomarkers, are important analytical tools based on the detection of the binding event between antibody and antigen. Finding antibodies for specific protein biomarker is not always easy and this represents a drawback of the traditional immunoassays. Therefore other synthetic biomolecules, such as aptamers, have been synthetized and studied to achieve their inclusion in protein detection assays. Several elucidating reviews can be found, that cover all the steps between the synthesis and final application in biosensor systems. [42–44]

Aptamers are synthetic single stranded DNA or RNA molecules that fold up into 3D structures with high affinity for their target molecules (for example proteins, and cell receptor molecules) that retain their binding properties after immobilization. Since they are synthetized for a specific portion of a protein, they can be used as bio-recognition elements in several types of protein biosensors, and in particular for the detection of small proteins. A label-free bioelectronic detection of aptamer-thrombin interaction, based on electrochemical impedance spectroscopy (EIS) technique was reported by Kara et al. [45] Multiwall carbon nanotubes (MWCNTs) composite was used as modifier of screen-printed carbon electrodes (SPCEs), and the aptamer was then immobilized on the modified electrode through covalent attachment. The binding of thrombin was then monitored by EIS in the presence of $[Fe(CN)6]^{3-/4-}$ redox pair. The MWCNT modified electrodes showed improved characteristics when compared to the bare ones. This study exemplifies an alternative electrochemical biosensor for the detection of other proteins. Even though most of the reported aptamers were applied for the detection of

standards and not human serum proteins, a recent work compared the performance of an aptamer-based biosensor with an equivalent antibody-based biosensor. [46] They used QCM sensor system for the detection of immunoglobulin E (IgE) in human serum to test both bio-receptors and although both operated in the same protein range, the aptamer-based achieved a lower limit of detection. The aptamers were equivalent or superior to antibodies in terms of specificity and sensitivity, and could support regeneration after ligand binding and recycling of the biosensor with little loss of sensitivity.

Aptamers can also be conjugated to nanoparticles and used for a variety of applications. As for example two specific aptamers conjugated to silica-coated magnetic and fluorophore-doped silica nanoparticles for magnetic extraction and fluorescent labeling allows to detect and extract targeted cells in a variety of matrixes [47]. This work illustrates the overall enhanced sensitivity and selectivity of the two-particle assay using an innovative multiple aptamer approach, signifying a critical feature in the advancement of this technique.

Yang's group [21] developed an ultrasensitive and simple electrochemical method for the fabrication of a sandwich-type heterogeneous electrochemical immunosensors using mouse IgG or PSA antigen as target. Fig.2 shows a typical fabrication procedure of DNA-free electrochemical immunosensor. An IgG layer was formed on an ITO electrode via a stepwise assembly process (Fig. 2). First, partially ferrocenyl tethered dendrimer (Fc-D) was covalently immobilized to the ITO electrode onto the phosphonate self-assembled monolayer. Some of the unreacted amines of Fc-D were modified with biotin groups to allow the specific binding of streptavidin. Afterward, biotinylated antibodies were immobilized to the streptavidin-modified ITO electrode. An IgG-nanocatalyst conjugate was also prepared via direct adsorption of IgG onto AuNPs. This conjugate and the immunosensing layer sandwiched the target protein. Signal amplification was achieved by catalytic reduction of p-nitrophenol to p-aminophenol using gold nanocatalyst labels and the chemical reduction of p- quinone imine by NaBH4. This novel DNA-free method could attain a very low detection limit (1 fg mL^{-1}).

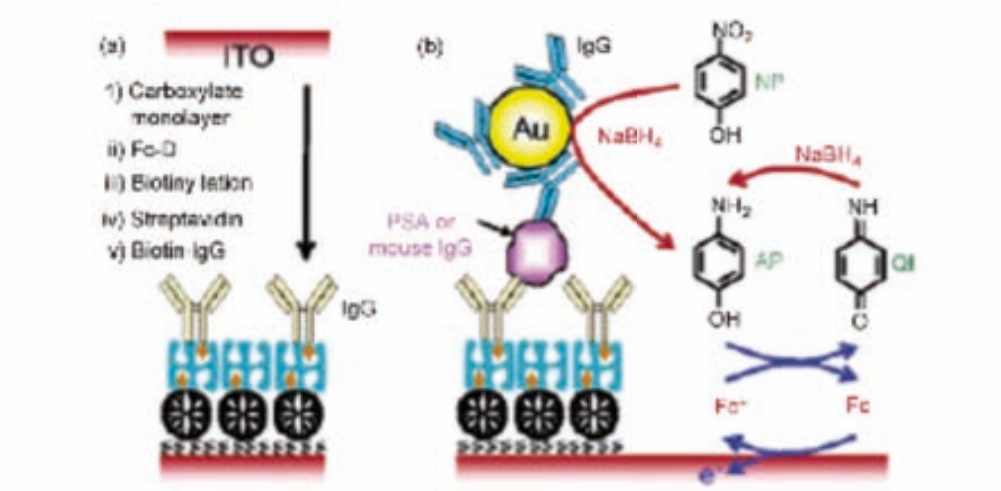

Figure 2(a) Schematic representation of the preparation of an immunosensing layer. (b) Schematic view of electrochemical detection of mouse IgG or prostate specific antigen.

As aforementioned, nanoparticles can act as electrocatalytic labels for several reactions involving other species in solution. Inspired by the last explained example that uses a gold nanoparticle conjugated to an antibody

Cancer diagnostic is one of the main application areas of biomarkers. Cancer biomarkers include proteins overexpressed in blood and serum (Fig. 3) or at the surface of cancer cells (Fig.4), and their low levels at the initial stages of the disease are most important for an early intervention in the cancer progression. Therefore there is a high demand of fast and sensitive detection systems that can overcome the existent limitations.

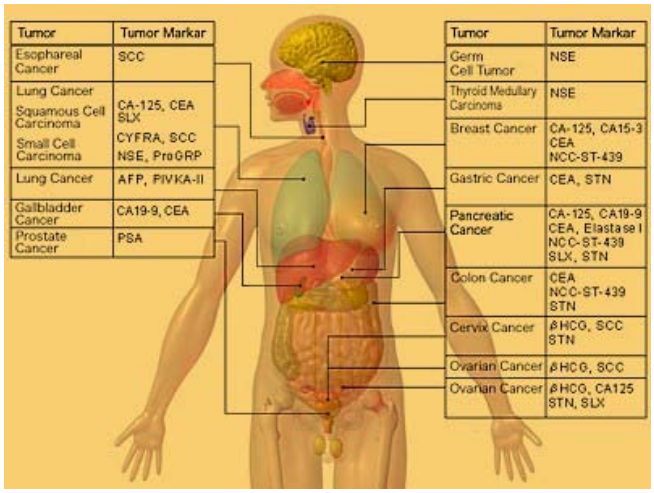

Figure 3. Schematic representation of several tumor markers and their tumor origin.

A simple and sensitive label-free electrochemical immunoassay electrode for detection of carcinoembryonic antigen (CEA) was developed by Yao's group. [48] CEA antibody (anti-CEA) was covalently attached on glutathione monolayer-modified AuNPs and the resulting anti-CEA-AuNPs bioconjugates were immobilized on Au electrode by electro-copolymerization with o-

aminophenol (OAP). Electrochemical impedance spectroscopy studies demonstrated that the formation of CEA antibody–antigen complexes increased the electron-transfer resistance of $[Fe(CN)6]^{3-/4-}$ redox pair at the poly-OAP/anti-CEA-AuNPs/Au electrode. The immunosensor could detect the CEA with a detection limit of 0.1 ng mL^{-1} and a linear range of 0.5–20 ng mL^{-1}. The use of anti-CEA/AuNP bioconjugates and poly-OAP film could enhance the sensitivity and anti-nonspecific binding of the resulting immunoassay electrode.

3.4. Cancer cell detection using electrocatalytic sensing systems

Cancer cells express several proteins, receptors or specific enzymes, which can be used as targets in their detection, isolation and quantification. In consequence, cancer cells could in theory be detected by the electrocatalytic sensing techniques developed for the sensing of proteins.

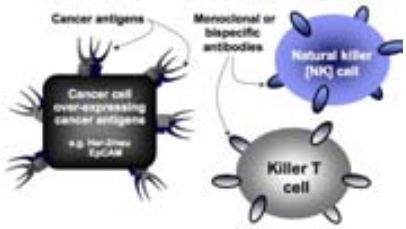

Figure 4. Schematic representation of the antigens expression at the surface of cancer cells.

Numerous optical detection methods were developed using nanomaterial optical probes for the detection of various cancer cell models, but few works describe the use of nanoparticle labels for their electrochemical detection.

Several groups based their electrochemical cytosensors on the recognition of surface carbohydrates and glycopeptides, and incorporated nanomaterials to enhance the detection. Din et al. developed a label-free strategy for facile electrochemical analysis of dynamic glycan expression on living cells. They used carbon nanohorns to efficiently immobilize lectin for the construction of a recognition interface and enhancing the accessibility of cell surface glycan motifs. [49] Other electrochemical cytosensor was designed based on the specific recognition of mannosyl on a cell surface to concanavalin A (ConA) and the signal amplification of gold nanoparticles (AuNPs). By sandwiching a cancer cell between a gold electrode modified with ConA and the AuNPs/ConA loaded with 6-ferrocenylhexanethiol (Fc), the electrochemical cytosensor was established. The cell number and the amount of cell surface mannose moieties were quantified by cyclic voltammetry (CV) analysis of the Fc loaded on the surface of the AuNPs. Since a single AuNP could carry

hundreds of Fc, a significant amplification for the detection of target cell was obtained. They used K562 leukemic cells as model, and observed that the electrochemical response was proportional to the cell concentration in the range from 1.0×10^{2} to 1.0×10^{7} cells mL^{-1} showing very high sensitivity. [50]

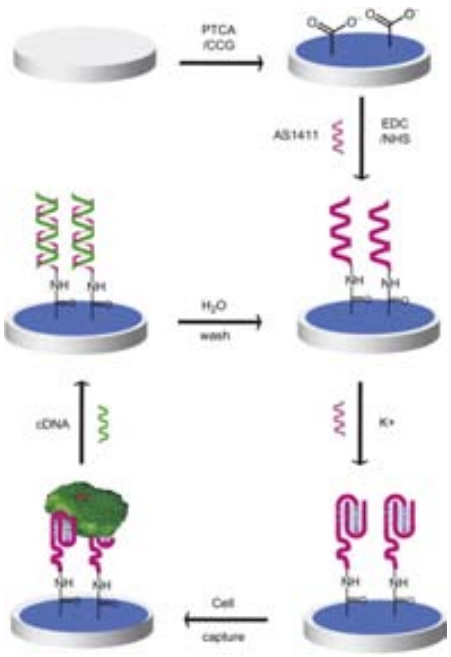

Figure 5. Schematic representation of the reusable aptamer/graphene-based aptasensor. The sensor is constructed based on graphene-modified electrode and the first clinical trials II used aptamer, AS1411. AS1411 and its complementary DNA are used as a nanoscale anchorage substrate to capture/release cells.

Feng et al. reported an electrochemical label-free sensor for cancer cell detection using the first clinical trial II used aptamer AS1411 and functionalized grapheme (Fig. 5). By taking advantages of the aptamer high binding affinity and specificity to the overexpressed nucleolin on the cancer cell surface, the developed electrochemical aptasensor could distinguish cancer cells and normal ones and detect as low as one thousand cells. This sensor could also be regenerated and reused. This work is a good example of label-free cancer cell detection based on aptamer and graphene-modified electrode. The authors claim that this graphene/aptamer-based design can be adaptable for detection of protein, small molecules, and nucleic acid targets by using different aptamer's DNA sequences. [51]

Other groups based their cytosensors on the recognition of membrane protein receptor supposed to be specific for the particular cancer type under investigation.

Li et al. proposed a sensitive electrochemical immunoassay to detect breast cancer cells by simultaneously measuring two co-expressing tumor markers, human mucin-1 and carcinoembryonic antigen (CEA) on the surface of the

cancer cells, which could efficiently improve the accuracy of the detection as well as facilitate the classification of the cancer cells. The experimental results revealed that a proper electrochemical response could only be observed under the condition that both of the tumor markers were identified on the surface of the tumor cells. With this method, breast cancer cell MCF-7 could be easily distinguished from other kinds of cells, such as acute leukemia cells CCRF-CEM and normal cells islet beta cells. Moreover, the prepared cytosensor could specially monitor breast cancer cell MCF-7 in a wide range from 10^4 to 10^7 cell mL^{-1} with fine reproduction and low detection limit, which may have great potential in clinical applications.[52]

Other group [53] reported a single nanotube field effect transistor array, functionalized with IGF1R-specific and Her2-specific antibodies, which exhibits highly sensitive and selective sensing of live, intact MCF7 and BT474 human breast cancer cells in human blood. Single or small bundle of nanotube devices that were functionalized with IGF1R-specific or Her2-specific antibodies showed 60% decreases in conductivity upon interaction with BT474 or MCF7 breast cancer cells in two μl drops of blood. Control experiments produced a less than 5% decrease in electrical conductivity, illustrating the high sensitivity for whole cell binding by these single nanotube-antibody devices. They suggest that the free energy change, due to multiple simultaneous cell-antibody binding events, exerted stress along the nanotube surface, decreasing its electrical conductivity due to an increase in band gap. They reported this achievement as a nanoscale oncometer with single cell sensitivity with a diameter 1000 times smaller than a cancer cell that functions in a drop of fresh blood.

Circulating Tumor Cells (CTCs) are blood-travelling cells that detach from a main tumor or from metastasis. CTCs quantification is under intensive research for examining cancer metastasis, predicting patient prognosis, and monitoring the therapeutic outcomes of cancer. [1–5] Although extremely rare, CTCs detection/quantification in physiological fluids represents a potential alternative to the actual invasive biopsies and subsequent proteomic and functional genetic analysis.[6,7]

Therefore their discrimination from normal blood cells offers a high potential in tumor diagnosis.[4,8] Established techniques for CTC identification include labeling cells with antibodies (immunocytometry) or detecting the expression of tumor markers by reverse-transcriptase polymerase chain reaction (RT-PCR).[9] Recently, several works that employ nanomaterials for optical detection of CTCs were reported.

Conclusion and future perspectives

The application of NPs as catalysts in biomarker detection systems is related to the decrease of overpotentials of many important redox species including also the catalyzed reduction of other metallic ions used in labeling-based protein sensing.

Although the most exploited materials in catalysis are the metals from platinum group, with the introduction of nanotechnology and the increasing interest for biosensing applications, gold NPs, due to their facile conjugation with biological molecules, besides other advantages, seem to be the most used metal nanoparticles. Their applications as either electrocatalytic labels or modifiers of protein related transducers are bringing important advantages in terms of sensitivity and detection limits in addition to other advantages.

The employment of carbon based nanomaterials like grapheme oxide underwent an intensive progress in the last few years. Their ability to electrocatalyze different electrochemical reactions together with a better control on the synthesis and its electrochemical properties, promises an exponential growth of new reported applications in the biosensing field.

Cancer cell detection could also profit from the use of electrocatalytic nanomaterials, to improve the current limitations in terms of sensitivity and simplicity of the assay. Since the cancer cells express specific proteins or carbohydrates at their plasma membrane, in theory the electrocatalytic properties of NPs used in protein-biomarker detection could also be extended to cell analysis. Interesting new strategies for the electrochemical detection of cancer cells, could be much appreciated due to the excellent characteristics of these biosensing techniques that include fast and sensitive responses, easy to use equipment, handling of low volume of samples, portability and the possibility to be integrated in fluidic devices, so as to achieve point-of-care detection instruments.

For this reason, the cancer detection is one of the objects of study in the following chapters of this thesis. For example the hydrogen catalysis reaction induced by AuNPs applied for protein detection (chapter 3) was also studied for cancer cells detection. A new strategy that comprises the capturing of CTCs, from among other cells, and includes also their fast labeling/detection, by means of fast and easy-to-use electrochemical systems, is supposed to be ideal for point-of-care diagnostics and therefore was also developed (chapter4).

So as to conclude, the conjugation of NPs with electrochemical sensing systems promises large evolution in actual electroanalysis methods and is

expected to bring more advances in the biomarker detection for diagnostics. However, even though some of the developed electrocatalytic nanoparticle based sensing systems have shown high sensitivity and selectivity, their implementation in clinical analysis still needs a rigorous testing and control period so as to really evaluate these advantages in comparison to classical assays in terms of reproducibility, stability and cost while being applied for real sample analysis. Further developments including the development of simple electrochemical devices (i.e. pocket size such as glucosimeter) or fluidic integrated devices are necessary for future entrance in real sample diagnostics in terms of point-of-care biosensors.

References

[1] A. Merkoçi, *Biosenssing Using Nanomaterials*, John Wiley & Sons, Inc., Hoboken, NJ, USA, **2009**.

[2] A. Merkoçi, *The FEBS journal* **2007**, *274*, 310-6.

[3] A. de la Escosura-Muñiz, A. Merkoçi, *Expert Opinions Medical Diagn*. **2010**, *4*, 21-37.

[4] A. De La Escosura-Muñiz, C. Sánchez-Espinel, B. Díaz-Freitas, A. González-Fernández, M. Maltez-da Costa, A. Merkoçi, *Analytical Chemistry* **2009**, *81*, 10268-10274.

[5] A. T. Bell, *Science (New York, N.Y.)* **2003**, *299*, 1688-91.

[6] G. Ertl, H. Knözinger, F. Schüth, J. Weitkamp, *Handbook of Heterogeneous Catalysis*, Wiley-vch Verlag, **1997**.

[7] J. Das, H. Yang, *The Journal of Physical Chemistry C* **2009**, *113*, 6093-6099.

[8] S. Liu, H. Ju, *Electroanalysis* **2003**, *15*, 1488-1493.

[9] L. Agüí, J. Manso, P. Yáñez-Sedeño, J. M. Pingarrón, *Sensors and Actuators B: Chemical* **2006**, *113*, 272-280.

[10] Q. Xu, C. Mao, N.-N. Liu, J.-J. Zhu, J. Sheng, *Biosensors & bioelectronics* **2006**, *22*, 768-73.

[11] X.-L. Luo, J.-J. Xu, Y. Du, H.-Y. Chen, *Analytical biochemistry* **2004**, *334*, 284-9.

[12] J. Jia, B. Wang, A. Wu, G. Cheng, Z. Li, S. Dong, *Analytical Chemistry* **2002**, *74*, 2217-2223.

[13] T. Hoshi, N. Sagae, K. Daikuhara, K. Takahara, J.-ichi Anzai, *Materials Science and Engineering: C* **2007**, *27*, 890-894.

[14] W. Yang, J. Wang, S. Zhao, Y. Sun, C. Sun, *Electrochemistry Communications* **2006**, *8*, 665-672.

[15] B. K. Jena, C. R. Raj, *Journal of Physical Chemistry C* **2007**, *111*, 6228-6232.

[16] M. T. Castañeda, S. Alegret, a. Merkoçi, *Electroanalysis* **2007**, *19*, 743-753.

[17] A. D. L. Escosura-Muñiz, A. Ambrosi, A. Merkoçi, *Trends in Analytical Chemistrys in Analytical Chemistry* **2008**, *27*, 568-584.

[18] C. M. Welch, R. G. Compton, *Analytical and bioanalytical chemistry* **2006**, *384*, 601-619.

[19] F. W. Campbell, R. G. Compton, *Analytical and Bioanalytical Chemistry* **2010**, *396*, 241-259.

[20] R. Polsky, R. Gill, L. Kaganovsky, I. Willner, *Analytical chemistry* **2006**, *78*, 2268-71.

[21] J. Das, M. A. Aziz, H. Yang, *Journal of the American Chemical Society* **2006**, *128*, 16022-3.

[22] S. Naylor, *Expert Reviews, Molecular diagnostics* **2003**, *3*, 525-529.

[23] Y.-E. Choi, J.-W. Kwak, J. W. Park, *Sensors (Basel, Switzerland)* **2010**, *10*, 428-55.

[24] R. Frank, R. Hargreaves, *Nat Rev Drug Discov* **2003**, *2*, 566-580.

[25] Y. Shao, J. Wang, H. Wu, J. Liu, I. Aksay, Y. Lin, *Electroanalysis* **2010**, *22*, 1027-1036.

[26] B. S. Sherigara, W. Kutner, D. Souza, *Electroanalysis* **2003**.

[27] A K. Geim, K. S. Novoselov, *Nature materials* **2007**, *6*, 183-91.

[28] J.-L. Chang, K.-H. Chang, C.-C. Hu, W.-L. Cheng, J.-M. Zen, *Electrochemistry Communications* **2010**, *12*, 596-599.

[29] R. Yue, Q. Lu, Y. Zhou, *Biosensors & bioelectronics* **2011**, *26*, 4436-41.

[30] Y. Fan, K.-J. Huang, D.-J. Niu, C.-P. Yang, Q.-S. Jing, *Electrochimica Acta* **2011**, *56*, 4685-4690.

[31] a. J. S. Ahammad, J.-J. Lee, M. A. Rahman, *Sensors* **2009**, *9*, 2289-2319.

[32] B. Pérez-López, A. Merkoçi, *Advanced Functional Materials* **2011**, *21*, 255-260.

[33] D. Vairavapandian, P. Vichchulada, M. D. Lay, *Analytica chimica acta* **2008**, *626*, 119-29.

[34] C. E. Banks, T. J. Davies, G. G. Wildgoose, R. G. Compton, *Chemical communications (Cambridge, England)* **2005**, 829-41.

[35] W. T. Tan, A. M. Bond, S. W. Ngooi, E. B. Lim, J. K. Goh, *Analytica chimica acta* **2003**, *491*, 181.

[36] O. Nekrassova, N. S. Lawrence, R. G. Compton, *Talanta* **2003**, *60*, 1085.

[37] R. N. Goyal, V. K. Gupta, A. Sangal, N. Bachheti, *Electroanalysis* **2005**, *17*, 2217.

[38] H. Jia, X. Han, Z. Li, Q. Tian, Y. Miao, Xiaoxiang, Du, Libo, Liu, *Talanta* **2011**, *85*, 1871-1875.

[39] A. L. Ghindilis, P. Atanasov, M. Wilkins, E. Wilkins, *Biosensors and Bioelectronics* **1998**, *13*, 113-131.

[40] J. Lin, H. Ju, *Biosensors & bioelectronics* **2005**, *20*, 1461-70.

[41] M. S. Wilson, *Analytical chemistry* **2005**, *77*, 1496-502.

[42] J. A Phillips, D. Lopez-Colon, Z. Zhu, Y. Xu, W. Tan, *Analytica chimica acta* **2008**, *621*, 101-8.

[43] O. a Sadik, A. O. Aluoch, A. Zhou, *Biosensors & bioelectronics* **2009**, *24*, 2749-65.

[44] S. Guo, S. Dong, *TrAC Trends in Analytical Chemistry* **2009**, *28*, 96-109.

[45] P. Kara, A. De La Escosura-Muñiz, M. Maltez-da Costa, M. Guix, M. Ozsoz, A. Merkoçi, *Biosensors and Bioelectronics* **2010**, *26*, 1715-1718.

[46] C. Yao, T. Zhu, Y. Qi, Y. Zhao, H. Xia, W. Fu, *Sensors (Basel, Switzerland)* **2010**, *10*, 5859-71.

[47] C. D. Medley, S. Bamrungsap, W. Tan, J. E. Smith, *Analytical chemistry* **2011**, *83*, 727-34.

[48] H. Tang, J. Chen, L. Nie, Y. Kuang, S. Yao, *Biosensors & bioelectronics* **2007**, *22*, 1061-7.

[49] L. Ding, W. Cheng, X. Wang, Y. Xue, J. Lei, Y. Yin, H. Ju, *Chemical communications (Cambridge, England)* **2009**, 7161-3.

[50] C. Ding, S. Qian, Z. Wang, B. Qu, *Analytical biochemistry* **2011**, *414*, 84-7.

[51] L. Feng, Y. Chen, J. Ren, X. Qu, *Biomaterials* **2011**, *32*, 2930-7.

[52] T. Li, Q. Fan, T. Liu, X. Zhu, J. Zhao, G. Li, *Biosensors & bioelectronics* **2010**, *25*, 2686-9.

[53] N. Shao, E. Wickstrom, B. Panchapakesan, *Nanotechnology* **2008**, *19*, 465101.

This thesis is divided in 7 chapters. A brief explanation of each chapter is giving in the following part.

Chapter 1, titled “General Introduction”, is an introductory chapter that comprises two parts. The first is the thesis overview that briefly describes each of the seven chapters in which the thesis manuscript is divided. The second part is a review on the state-of-the art of the sensing technologies based on electrocatalytic nanomaterials. The review focuses the application of nanomaterials for biomarker electrochemical detection in general, with more detail on protein and cancer cell detection. The DNA detection is not addressed in this chapter, even though DNA sequences can be considered biomarkers when a genetic disorder is implicit. Nevertheless a book chapter, written owing to the book editor invitation, is discussed in chapter 5.

(The introductory review is in preparation for its subsequent submission).

Chapter 2, “Objectives”, introduces the objectives that motivated and guided this work.

Chapter 3, “Electrocatalytic nanoparticles for protein detection”, describes the development of two electrocatalytic methods, based on gold nanoparticles. The first one is the electrocatalytic deposition of silver onto AuNPs and the second one the electrocatalyzed hydrogen evolution reaction (HER). The application of both methods on electrochemical immunoassays for HIgG detection (as a model protein), the application of the second for the quantificatiozn of Hepatitis-B antibodies in real human samples are also described.

Chapter 4, “Electrocatalytic gold nanoparticles for cell detection”, describes the application of AuNP based HER, explained in the preceding chapter, to the detection of cancer cells using different approaches. The first approach shows the detection of adhered cancer cells and the second one the detection of circulating tumor cells

Chapter 5 , “Additional works”, comprises two parts. The first part briefly describes the state-of-the-art of the nanoparticle-induced catalysis for electrochemical DNA biosensors. The second describes an additional work

concerning the application of CNTs composites for the electrochemical detection of thrombin spiked in human serum.

Finally, in ***Chapter 6***, “Conclusions and future perspectives”, the general conclusions are presented, as also as the future perspectives on the application of the work described in the previous chapters. In ***Chapter 7***, are displayed the publications and manuscripts that resulted from this thesis research (as explained in the Preface).

Chapter 2

Objectives

Chapter 2

Objectives

The main objective of this thesis is to develop novel and improved electrochemical sensing systems for biomarker detection, exploiting the electrocatalytic effects of nanomaterials in general and nanoparticles particularly.

Detailed objectives

1. **Synthesis and characterization of gold nanoparticles.**
   Synthesis of gold nanoparticles, using a bottom-up approach, to obtain stable colloidal suspensions. Characterization of the synthetized nanoparticles by transmission electronic microscopy (TEM), scanning electronic microscopy (SEM), UV-Vis absorption spectroscopy as well as electrochemical methods so as to identify their future applications in electrochemical sensing and biosensing. Alternative characterization of nanoparticles by zeta-potential determination, and ICP-MS is also employed.

2. **Biofunctionalization of gold nanoparticles.**
   Functionalization of gold nanoparticles with biomolecules, like antibodies or other proteins, to obtain nano-bioconjugates capable of being used as labels in the electrochemical detection of proteins and cells, with interest in clinical diagnostics. Evaluate the biofunctionalization of nanoparticles in respect to their stability and proper recognition of the target biomolecule, using

3. **Develop electrochemical immunoassays using gold nano-bioconjugates as labels, and magnetic microparticles as immobilization surfaces.**
   Study the use of magnetic-microparticles suspensions as immobilization surfaces in a sandwich-like immunoassay using gold nanoparticle bioconjugates as electrochemical labels. Functionalize the microparticles with the protein used as capture agent, and apply the obtained conjugate to the immunoassay improving the incubation and cleaning steps. Evaluate the improvement in the overall assay by electrochemical analysis, microscopy techniques and UV-Vis absorption spectroscopy.

4. **Study the electrocatalytic effect of gold nanoparticles in other reactions with interest in electrochemical sensing applications**

    4.1. Study the silver electrodeposition over gold nanoparticle bioconjugates used as detection labels in a magnetoimmunoassay. Evaluate the improvement of this method in the detection of a model protein.

    4.2. Study the electrocatalytic effect of gold nanoparticles in the hydrogen evolution reaction (HER) and use it to quantify gold nanoparticles. Apply the nanoparticle quantification method to a magnetoimmunoassay were gold nanoparticle bioconjugates are used as detection labels for a model protein.

    4.3. Apply the gold nanoparticle quantification, based on HER electrocatalysis, to a magnetoimmunoassay in order to detect the presence of anti-Hepatitis B antibodies in the blood-serum of patients and verify their immunization against Hepatitis B virus.

5. **Develop electrochemical cell detection assays using gold nano-bioconjugates as labels**

    5.1. Study the application of the gold nanoparticle quantification, based on HER electrocatalysis, to a cancer cell detection assay in order to obtain a rapid method for quantification of cancer cells grown onto the carbon electrode surface.

    5.2. Evaluate the application of the gold nanoparticle quantification, based on HER electrocatalysis, to detect circulating tumor cells (CTC), using adenocarcinoma cells in suspension as a model target.

    5.3. Study the use of magnetic-microparticles suspensions, functionalized with specific antibodies, as immobilization surfaces for the cell capture. Use gold nanoparticle bioconjugates as electrochemical labels and apply the gold nanoparticle quantification, based on HER electrocatalysis, to evaluate the CTCs detection Evaluate the improvement of this method in the detection of adenocarcinoma cells in suspension.

RESULTS AND DISCUSSION

Chapter 3

Electrocatalytic nanoparticles for protein detection

3.1. Introduction

Catalysis is considered as the central field of nanoscience and nanotechnology (Grunes et al., 2003). Interest in catalysis induced by metal nanoparticles (NPs) is increasing dramatically in the last years. The use of NPs in catalysis appeared in the 19th century with photography (use of gold and silver NPs) and the decomposition of hydrogen peroxide (use of PtNPs) (Bradley, 1994). In 1970, Parravano and co-workers (Cha et al., 1970) described the catalytic effect of AuNPs on oxygen-atom transfer between CO and CO2. Usually, these NP catalysts are prepared from a metal salt, a reducing agent and a stabilizer. Since these first works, NPs have been widely used for their catalytic properties in organic synthesis, for example, in hydrogenation and C-C coupling reactions Reetz et al., 2004), and the heterogeneous oxidation of CO (Lang et al., 2004) on AuNPs.

On the other hand, immunoassays are currently the predominant analytical technique for the quantitative determination of a broad variety of analytes in clinical, medical, biotechnological, and environmental significance. Recently, the use of metal nanoparticles, mainly gold nanoparticles (AuNPs) as labels for different biorecognition and biosensing processes has received wide attention, due to the unique electronic, optical, and catalytic properties (Wang et al, 2002a; Wang et al., 2003a; Wang et al., 2003c; Liu et al., 2006; Kim et al., 2006; Daniel et al., 2004; Fritzsche et al., 2003; Seydack, 2005). Electrochemical detection is ideally suited for these nanoparticle-based bioassays (Katz et al., 2004; Merkoçi et al., 2005; Merkoçi, 2007) owning to unique advantages related to NPs: rapidity, simplicity, inexpensive instrumentation and field-portability. The use of nanoparticles for multiplex analysis of DNA (Wang et al., 2003b) as well as proteins (Liu et al., 2004) have been also demonstrated showing a great potential of NP applications in DNA and protein studies. A summary of the most relevant works using AuNPs as label for bioassays along with some relevant results in terms of detection limit (DL) and precision is shown in table 1.

The use of colloidal gold as electrochemical label for voltammetric monitoring of protein interactions was pioneered in 1995 by González-García and Costa-García (González-García et al., 1995), although the first metalloimmunoassay based on a colloidal gold label was not reported until 2000 by Dequaire et al. (Dequaire et al. 2000). Despite the inherent high sensitivity of the stripping metal analysis (Piras et al., 2005) different strategies have been proposed to improve the sensitivity of these metalloimmunoassays.

Another protein detection alternative was reported by our group (Ambrosi et al., 2007). It is based on a versatile gold-labeled detection system using either spectrophotometric or electrochemical method. In this assay a double codified label (DC-AuNP) based of AuNP conjugated to an HRP-labeled anti-human IgG antibody, and antibodies modified with HRP enzyme are used to detect human IgG as a model protein. A substantial sensitivity enhancement can be achieved, for example, by using the AuNPs as catalytic labels for further amplification steps.

Although an ultrasensitive electrochemical detection immunosensor has been reported recently using the catalytic reduction of p-nitrophenol by AuNP-labels (Das et al., 2006), most common strategy uses the catalytic deposition of gold (Liao et al., 2005) and especially of silver onto AuNPs to improve the sensitivity.

In most cases, the silver enhancement relies on the chemical reduction, mainly using hydroquinone, of silver ions (Karin et al., 2006; Guo et al., 2005; Chu et al., 2005; Chu et al., 2005) to silver metal onto the surface of the AuNPs followed by anodic-stripping electrochemical measurement. However, this procedure is time consuming and its sensitivity is compromised by nonspecific silver depositions onto the transducing surface.

In 2000, Costa-García and co-workers (Hernández-Santos et al., 2000a,b) reported a novel electrochemical methodology to quantify colloidal gold adsorbed onto a carbon paste electrode based on the electrocatalytic silver deposition. This strategy has been exploited by the same group for a very sensitive immunoassay (De la Escosura-Muñiz et al., 2006) and DNA hybridization detection (De la Escosura-Muñiz et al., 2007) but using a gold (I) complex (aurothiomalate) (De la Escosura-Muñiz et al., 2004) as electroactive label, instead of colloidal gold. Besides the lower time consuming, the silver electrodeposition process shows very interesting advantages over the chemical deposition protocol reported before, since silver only deposits on the AuNPs. This fact results in a high signal-to-background ratio by reducing the nonspecific silver depositions of the chemical procedure.

The electrocatalytic silver deposition on AuNPs has been recently applied in a DNA hybridization assay (Lee et al., 2004; Lee et al., 2005), but till now, to the best of our knowledge, the utilization of this amplification procedure for electrochemical immunoassay detection with AuNP label has not yet been reported.

On the other hand, magnetic particles have been widely used as platforms in biosensing, and the silver chemical deposition approached to improve the

sensitivity of the assays (Wang et al., 2001b; Wang et al., 2002b). The magneto based electrochemical biosensors present improved properties in terms of sensitivity and selectivity, due to the preconcentration of the analyte, the separation from the matrix of the sample and the immobilization / collection on the transducer surface, achieved using magnetic fields. However, till now, the utilization of the amplification procedure based on the silver electrodeposition for the electrochemical detection of AuNPs used as labels in magnetobioassays has not yet been reported.

The use of nanoparticles for multiplex analysis of DNA (Wang et al., 2003b) as well as proteins (Liu et al., 2004) have been also demonstrated showing a great potential of NP applications in DNA and protein studies. A summary of the most relevant works using AuNPs as label for bioassays along with some relevant results in terms of detection limit (DL) and precision is shown in table

Table 1. Summary of the most relevant works using AuNPs as labels for DNA sensors and immunosensors.

	Electrode	Electrochemical technique	Electrochemical detection	Analyte	DL	Precision	Ref
DNA sensors	SPCE	PSA	Direct	19-base oligo	5 ng/50 μL	RSD 12 %	Wang et al. 2001a
	CPE	SWV	Direct	21-base oligo	2.17 pM	-	Kerman et al., 2004
	SPCE	Chronopotentiometric stripping analysis	Direct (polymeric beads loaded with multiple gold nanoparticles)	19- base-pair oligo	300 aM	-	Kawde et al. 2004
	SPMBE	ASV	Autocatalytic reductive deposition of (AuIII) on gold nanoparticle	35 base-pair human cytomegalovirus nucleic acid target	600 aM	-	Dequaire et al. 2006
	Au microarrays	Capacitance	Silver enhancement	27 base-pair oligo	50 nM	-	Park et al., 2002
	GCE	DPV	Silver enhacement	32-base oligo	50 pM	-	Cai et al., 2002
	ITO chip	PSA	Silver enhancement	PCR amplicons	2×10^{-12} M	RSD 8%	Cai et al., 2004
	ITO	PSA	Silver enhancement	PCR amplicons		-	Li et al., 2004
Immuno sensors	SPCE	ASV	Direct	IgG	3×10^{-12} M	-	Dequaire et al., 2000
	GECE	DPV	Direct	IgG	65 pg/mL	RSD 3%	Ambrosi et al., 2007
	GCE	ASV	Silver enhancement	IgG	6×10^{-12} M	-	Chu et al., 2005
	GCE	ASV	Silver enhancement	*S. japonicum* antibody	3.0 ng/mL	-	Chu et al., 2005
	Ag-ISE	Potentiometry	Silver enhancement	IgG	12.50 pmol/50 μL	RSD 4%	Karin et al., 2006

SPMBE: Screen-printed microband electrode; SPCE: Screen-printed carbon electrode; GCE: Glassy carbon electrode; Ag-ISE: Silver ion selective electrode; CPE: Carbon paste electrode; GECE: Graphite epoxy composite; ITO: Indium tin oxide; DPV: Differential pulse voltammetry; PSA:Potentiometric stripping analysis; ASV: Anodic stripping voltammetry; SWV: Square wave voltammetr

REFERENCES

Ambrosi, A., Castañeda, M.T., Killard, A.J., Smith M.R, Alegret, S., Merkoçi, A. 2007. Anal. Chem. 79, 5232-5240.

Bradley, J.S. 1994 .Clusters and Colloids chapter 6, pp 459.

Cai, H., Wang, Y., He, P., Fang, Y. 2002. Anal. Chim. Acta 469, 165-172.

Cai, H., Shang, C., Hsing, I.M. 2004. Anal. Chim. Acta 523, 61-68.

Cespedes, F., Martinez-Fabregas, E., Bartroli, J., Alegret, S. 1993. Anal. Chim. Acta 273, 409-417.

Cha, D.Y., Parravano, G. 1970. J. Catal. 18, 320-238.

Chu, X., Fu, X., Chen, K., Shen, G.L, Yu, R.Q. 2005. Biosens. Bioelectron. 20, 1805–1812.

Daniel, M.C., Astruc, D. 2004. Chem. Rev. 104, 293-346.

Das, J., Abdul-Aziz, M., Yang, H.A. 2006. J. Am. Chem. Soc. 128, 16022-16023.

De la Escosura-Muñiz, A., González-García, M.B., Costa-García, A. 2004. Electroanal., 16, 1561-1568.

De la Escosura-Muñiz, A., González-García, M.B., Costa-García, A. 2006. Sens. Act. B, 114, 473–481.

De la Escosura-Muñiz, A., González-García, M.B., Costa-García, A. 2007 Biosens. Bioelectron. 22, 1048–1054.

Dequaire, M., Degrand, C., Limoges, B. 2000. Anal. Chem. 72, 5521-5528.

Dequaire, M.R., Limoges, B., Brossier, P. 2006. Analyst 131, 923-929.

Fritzsche, W., Taton, T.A. 2003. Nanotech. 14, R63-R73.

González-García, M.B., Costa-García, A. 1995. Bioelectrochem. Bioenerg. 38, 389-395.

Grunes, J., Zhu, J., Somorjai, G.A. 2003. Chem. Commun. 18, 2257-2260.

Guo, H., He, N., Ge, S., Yang, D., Zhang, J. 2005. Talanta 68, 61–66.

Gupta, S., Huda, S., Kilpatrick, P.K., Velev, O.D. 2007. Anal. Chem. 79, 3810-3820.

Hernández-Santos, D., González-García, M.B., Costa- García, A. 2000a. Electroanal. 12, 1461-1466.

Hernández-Santos, D., González-García, M.B., Costa- García, A. 2000b. Electrochim. Acta 46, 607-615.

Karin, Y., Torres C., Dai, Z., Rubinova, N., Xiang, Y., Pretsch, E., Wang, J., Bakker, Y. 2006. J. Am. Chem. Soc. 128, 13676-13677.

Katz E., Willner, I., Wang, J. 2004. Electroanal. 16, 19-44.

Kawde, A.N., Wang, J. 2004. Electroanal. 16, 101-107.

Kerman, K., Morita, Y., Takamura, Y., Ozsoz, M., Tamiya, E. 2004. Anal. Chim. Acta, 510, 169-174.

Kim, J.H, Seo, K.S., Wang, J. 2006. IEEE Sensors Journal 6, 248-253.

Lang, H.F., Maldonado, S.,.Stevenson, K.J,.Chandler, B.D. 2004. J. Am. Chem. Soc. 126, 12949-12956.

Lee, T.M.H, Cai, H., Hsing, I.M. 2004. Electroanal. 16, 1628-1631.

Lee, T.M.H., Cai, H., Hsing, I.M., Analyst 2005. 130, 364-369.

Li, L.L., Cai, H.,. Lee, T.M.H., Barford, J., Hsing, I.M. 2004. Electroanal. 16, 81-87.

Liao, K.T., Huang, H.J. 2005. Anal. Chim. Acta 538, 159–164.

Liu, G., Wang, J., Kim, J., Rasul–Jan, M., Collins, G.E. 2004. Anal. Chem. 76, 7126-7130.

Liu, G., Wu, H., Wang, J., Lin, Y. 2006. Small 2, 1139 – 1143.

Merkoçi, A., Aldavert, M., Marín, S., Alegret, S. 2005. Trends Anal. Chem. 24, 341-349.

Merkoçi, A. 2007. FEBS Journal 274, 310-316.

Park, S.J., Taton, T.A, Mirkin, C.A. 2002. Science 295, 1503-1506.

Piras, L., Reho, S. 2005. Sen. Act. B 111, 450–454.

Reetz, M.T., Schulenburg, H., López, M., Spliethoff, B., Tesche, B. 2004. Chimia 58, 896-899.

Santandreu, M., Cespedes, F., Alegret, S., Martinez-Fabregas, E. 1997. Anal. Chem. 69, 2080-2085.

Seydack, M. 2005. Biosens. Bioelectron. 20, 2454–2469.

Turkevich, J., Stevenson, P., Hillier, J. 1951. Discuss. Faraday Soc. 11, 55-75.

Wang, J., Xu, D., Kawde, A.N., Polsky, R. 2001a. Anal. Chem. 73, 5576-5581.

Wang, J., Polsky, R., Xu, D. 2001b. Langmuir 17, 5739-5741.

Wang, J., Liu, G., Polsky, R., Merkoçi, A. 2002a. Electrochem. Comm. 4, 722–726.

Wang, J., Xu, D., Polsky, R. 2002b. J. Am. Chem. Soc. 124, 4208-4209.

Wang, J.,. Liu, G, Merkoçi, A. 2003a. Anal. Chim. Acta 482, 149–155.

Wang, J., Liu, G., Merkoçi, A. 2003b. J. Am. Chem. Soc. 125, 3214-3215.

Wang, M., Sun, C, Wang, L., Ji, X., Bai, Y., Li, T., Li, J. 2003c. J. Pharm. Biom. Anal. 33, 1117-1125.

3.2. Electrocatalytic deposition of silver onto AuNPs applied to magneto immunoassays

In this work, an electrocatalytic silver-enhanced metalloimmunoassay using AuNPs as labels and microparamagnetic beads (MB) as platforms for the immunological interaction is developed for model proteins, in order to achieve very low detection limits with interest for further applications in several fields.

3.2.1. Catalytic effect of AuNPs on the silver electro-deposition.

The silver enhancement method, based on the catalytic effect of AuNPs on the chemical reduction of silver ions, has been widely used to improve the detection limits of several metalloimmunoassays. In these assays (Karin et al., 2006; Guo et al., 2005; Chu et al., 2005) the silver ions are chemically reduced onto the electrode surface in the presence of AuNPs connected to the studied bioconjugates, without the possibility to discriminate between AuNP or electrode surface. Furthermore, these methods are time consuming and two different mediums are needed in order to obtain the analytical signal: the silver/chemical reduction medium to ensure the silver deposition and the electrolytic medium necessary to the silver-stripping step.

However, in this work, for the first time, the selective electro-catalytic reduction of silver ions on AuNPs is clarified, and the advantages of using MBs as bioreaction platforms combined with the electrocatalytic method are used to design a novel sensing device.

The principle of the electrocatalytic method is resumed in figure 1A. Cyclic voltammograms, obtained by scanning from +0.30 V to –1.20 V in aqueous 1.0 M NH_3 / 2.0 x 10^{-4} M $AgNO_3$, for an electrode without (a) and with (b) AuNPs previously adsorbed during 15 minutes are shown. It can be observed that the half-wave potential of the silver reduction process is lowered when AuNPs are previously deposited on the electrode surface. Under these conditions, there is a difference (ΔE) of 200 mV between the half-wave potential of the silver reduction process on the electrode surface without (a) and with (b) AuNPs are adsorbed on the electrode surface (b). The amount of the catalytic current related to silver reduction increases with the amount of AuNPs adsorbed on the electrode surface (results not shown).

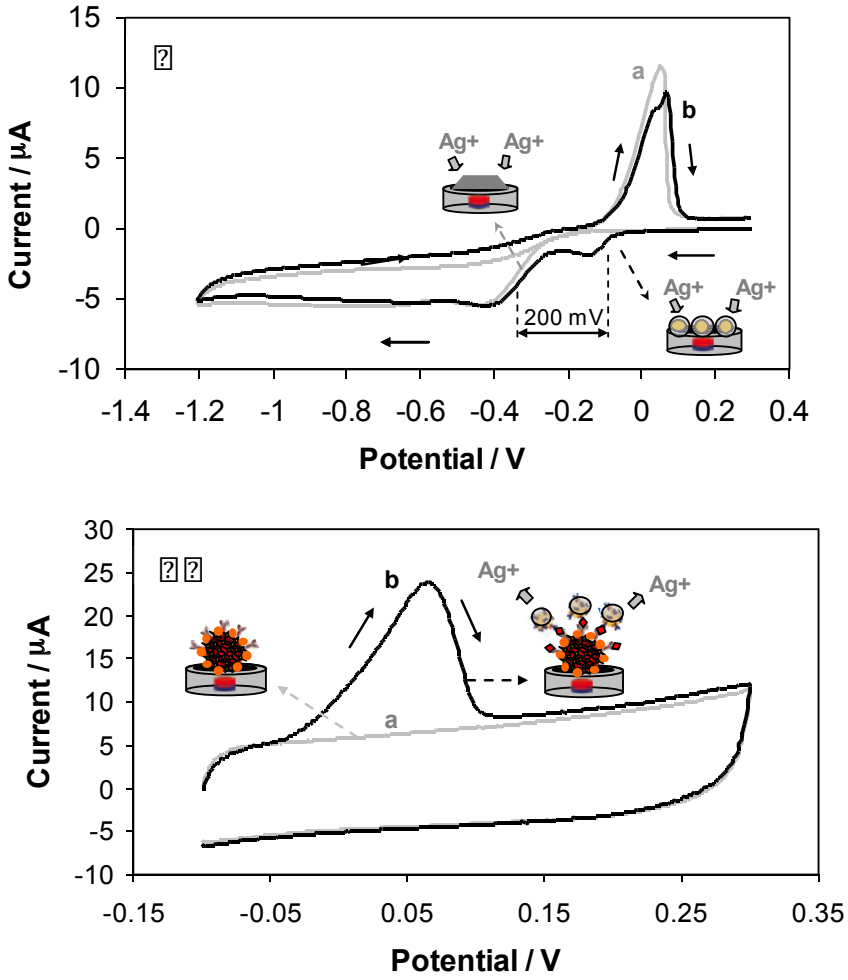

Fig. 1. (A) Cyclic voltammograms, scanned from +0.30 V to –1.20 V in aqueous 1.0 M NH3-2.0 x 10^{-4} M AgNO3, for an electrode without deposited AuNPs (a-curve) and for an electrode where previously AuNPs have been deposited from the synthesis solution for 15 minutes (b-curve). (B) Cyclic voltammograms recorded in aqueous 1.0 M NH3-2.0 x 10^{-4} M AgNO3, from -0.12 V to +0.30 V for the sandwich type assay described in experimental section, with an human IgG concentration of 5.0 x 10^{-7} µg/mL (b-curve) and with the same concentration of the non specific antigen (goat IgG - blank assay-a-curve). Silver deposition potential: -0.12 V; silver deposition time: 60 seconds; scan rate: 50 mV/s.

Taking this fundamental behavior into account, a novel analytical procedure for the sensitive detection of AuNPs is designed. It consists in choosing an adequate deposition potential, i.e. -0.12 V, at which the direct electro-reduction of silver ions, during a determined time, would take place on the AuNPs surface instead of the bare electrode surface. At the beginning of the process, the electrocatalytical reduction of silver ions onto the AuNPs surface occurs and once a silver layer is already formed more silver ions are going to be reduced due to a self-enhancement deposition. The electrocatalytic process is effective due to the large surface area of AuNPs allowing an easy

diffusion and reduction of the silver ions. The proposed mechanism is the following:

In a first step, while applying a potential of -0.12 V during 60 s, the silver from the ammonia complex, are reduced to a metallic silver layer onto the AuNPs surface:

$$\xrightarrow{\text{AuNPs, E= -0.12 V}}$$

$$Ag(NH_3)_2+ + 1\ e^- \rightarrow Ag(\text{deposited on AuNPs}) + 2\ NH_3$$

In a second step an anodic potential scan is performed (from -0.12 V to +0.30 V) in the same medium, during which the re-oxidation of silver at +0.10 V is recorded:

$$\xrightarrow{\text{E(-0.12 V to +0.30 V)}}$$

$$Ag(\text{deposited onto AuNPs}) + 2\ NH_3 \rightarrow Ag(NH_3)2 + 1\ e^-$$

The amount of silver electrodeposited at the controlled potential (corresponding to deposition onto AuNPs surface only) is proportional to the adsorbed AuNPs. Consequently the re-oxidation peak at +0.10 V produces a current which is proportional to the AuNPs quantity. The obtained re-oxidation peak constitutes thus the analytical signal, used later on for the AuNPs and consequently the protein quantification.

3.2.2. Sandwich type immunocomplex

The preparation of the sandwich type immunocomplex was carried out following a previously optimized procedure (Ambrosi et al., 2007), but introducing slight changes in order to minimize the unspecific absorptions that interfere the sensitive electrocatalytic detection. The analytical procedure is schemed in figure 2 (for detailed experimental conditions, see Publication 5 in Chapter 7).

The use of blocking agents so that any portion of the MB surface which does not contain the primary antibody is "blocked" thereby preventing non-specific binding with the analyte of interest (protein) is crucial. The obtained values of the analytical signals are highly dependent on the blocking quality. Following the previously reported procedure, based on the direct electrochemical detection of AuNP, the blank samples signal (the samples without the antigen or with a non-specific antigen) were very high (data not shown).

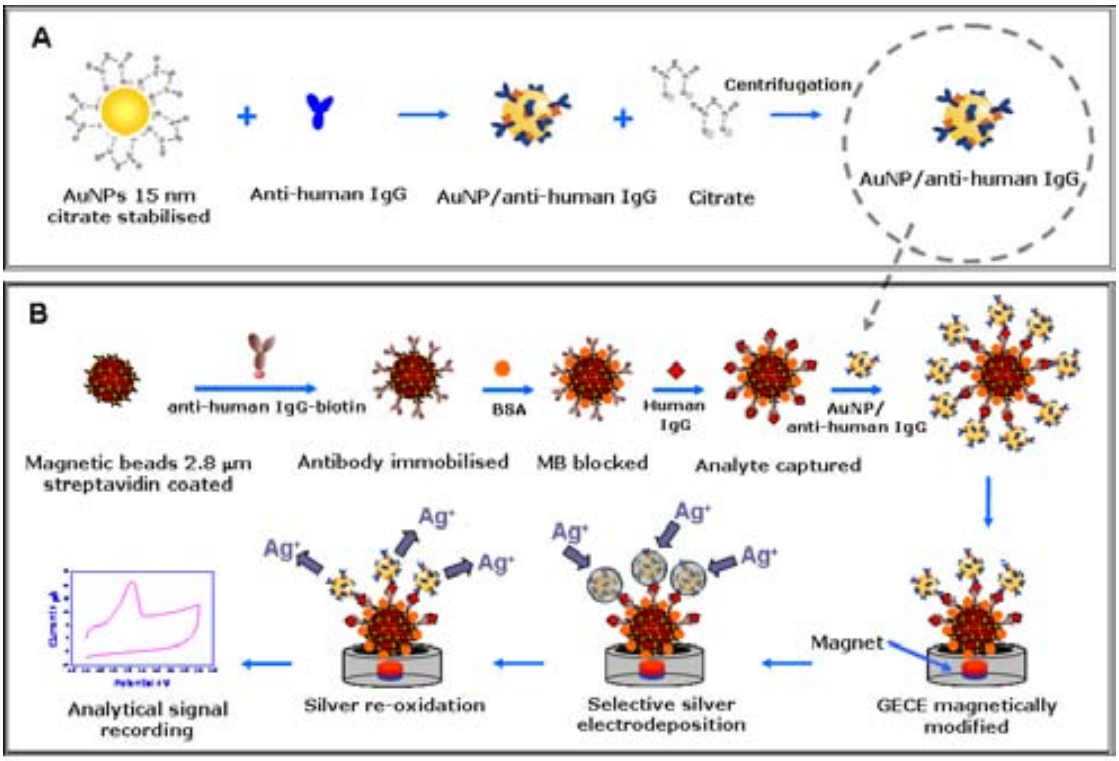

Fig. 2. Schematic (not in scale) of: (A) AuNP conjugation with anti-human IgG; (B) Analytical procedure for the sandwich type assay and the obtaining of the analytical signal based on the catalytic effect of AuNPs on the silver electrodeposition. Procedure detailed in experimental section.

The resulted unspecific adsorptions could be due to some factors. For a given concentration of the blocking agent the unspecific adsorptions will depend on the time interval used to perform such a step. By increasing the time interval of the blocking step (from 30 to 60 minutes and using PBS-BSA 5% as blocking agent) in the sandwich assay we could ensure a better coverage of the free bounding sites onto the MB surface avoiding by this way the unspecific adsorptions. Another important factor that affects the unspecific adsorptions is the washing step that aims at removing the unbound species avoiding by this way possible signals coming from AuNPs not related to the required antigen. Stirring instead of gentle washing brought significant decrease of unspecific adsorptions too. TEM images of the sandwich assay before and after the mentioned improvement corroborated also in understanding the phenomena related to these non-desired adsorptions (see Publication 4, Supplementary Info. to more information).

Clear evidences of the successful immunological reaction in a condition of the absence of unspecific adsorptions are the transmission electron micrographs (TEM) images shown in figure 3.

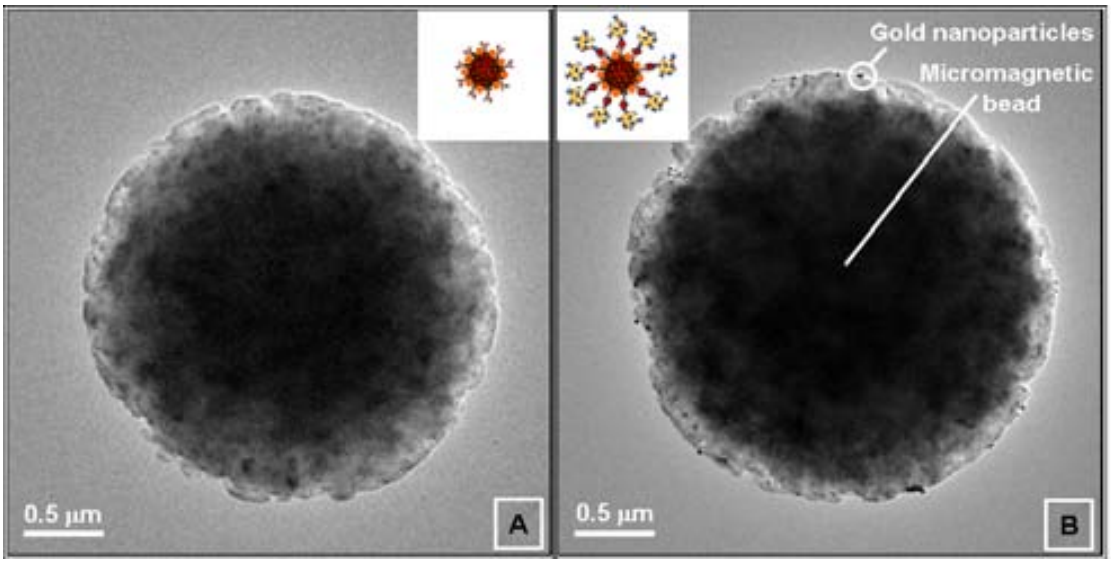

Fig. 3. Transmission electron micrographs (TEM) images of the MBs after the sandwich type assay detailed in experimental section. Assay carried out with 1.0 x 10-3 µg/ml of the non specific antigen (goat IgG) (blank assay-A-) and assay performed with 1.0 x 10-3 µg/ml of the specific antigen (human IgG) (B).

When the assay is carried out in the presence of the non-specific antigen (goat IgG - Figure 2A) only MBs are observed with a very low amount of AuNPs non specifically bonded. However, if the assay is performed with the specific antigen (human IgG - Figure 2B), a high quantity of AuNPs is observed around the MBs, which indicates that the immunological reaction has taken place.

Thus, following the analytical procedure described in experimental section the selective silver deposition onto the AuNPs surface is achieved. The potential and the time of the silver electro-deposition have been previously optimized (see figure S2 in the supplementary material). The application of a -0.12 V potential during 60 s resulted the best as a compromise between the higher sensitivity and analysis time.

Typical analytical signals obtained for the sandwich type assay performed with a human IgG concentration of 5.0 x 10^{-7} µg/mL (a) and for the blank assay performed with the same concentration of goat IgG (b) are shown at figure 3B.

The electrocatalytic deposition of silver ions onto the surface of the magnetic electrode versus the applied potential used for silver deposition is studied also by scanning electron microscopy (SEM). Figure 4 shows SEM images of the MB deposited onto the magnetic electrode surface, after performing silver

electro-deposition at different deposition potentials (-0.10, -0.12 and -0.20 V) during 1 minute.

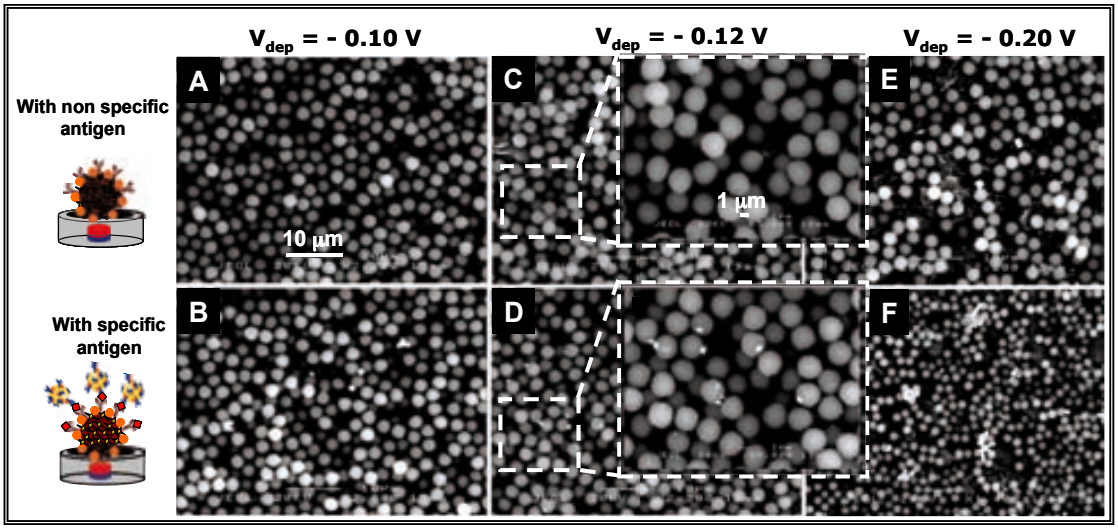

Fig. 4. Scanning electron microscopy (SEM) images of the MB deposited on the electrode surface, after the silver electro-deposition in aqueous 1.0 M NH3-2.0x10-4 M AgNO3, at -0.10 V (A,B,) -0.12 (C,D) and -0.20 V (E,F) during 1 minute, for the sandwich type assay performed as described in experimental section, with the non specific antigen (goat IgG -blank assays-A,C,E) and for the specific antigen (human IgG) at concentration of 1.0 x 10-3 µg/mL (B,D,F).

The upper images of Figure 4 (A,C,E) correspond to the sandwich type assays performed with the non specific antigen (goat IgG - blank assays). The lower part images (B,D,F) correspond to the assays with an specific antigen (human IgG) concentration of 1.0·10-3 µg/mL. It can be observed that at a deposition potential of -0.10 V, (A) no silver crystals are formed in the absence of the specific antigen while low amounts of silver crystals (white structures in the B image) are observed with the assay performed with the specific antigen. This means that the silver deposition has scarcely occurred to the AuNPs anchored onto the MB through the immunological reaction. (B). The formation of these silver crystals is much more evident when the same assay (with specific antigen) is performed at deposition potential of -0.12 V (D) where a bigger amount of MB appear to be covered with silver crystals – the same phenomena not observed for the blank assay (C). The obtained image is clear evidence that the used potential have been adequate for the silver deposition onto the AuNPs attached to the MB through the immunological reaction. The Energy Dispersive X-Ray (EDX) analysis (provided by SEM instrument) is also performed and the results are in agreement with the SEM images. The EDX results confirm the presence of gold and silver only in the assay performed with the specific antigen (see figure S3 in the supplementary material of Publication 4). By using more

negative deposition potentials (i.e. -0.20 V) the deposition of silver takes place in a high extent also on the electrode surface as it was expected (E). This phenomenon can be appreciated by bigger cluster like white silver crystals that may be associated not only with silver deposited onto the AuNPs but also onto the surface of the magnetic electrode. This potential (-0.20 V) is not adequate to quantify the specific antigen due to false positive results that can be generated. The -0.12 V have been used in our experiments as the optimal deposition potential that can not even discriminate between the assays and the blank but also be able to do protein quantification at a very low detection limit.

Similar silver structures formed onto AuNPs have been earlier after chemical silver (I) reduction for a DNA array-based assay (Park et al., 2002) or an immunoassay (Gupta et al., 2007) but this is the first time that such potential controlled silver deposition induced by the electrocatalytical effect of AuNP are being evidenced. Moreover the relation between the current produced by the oxidation of the selectively deposited silver layer and the quantity of AuNP is demonstrated as see in the following part.

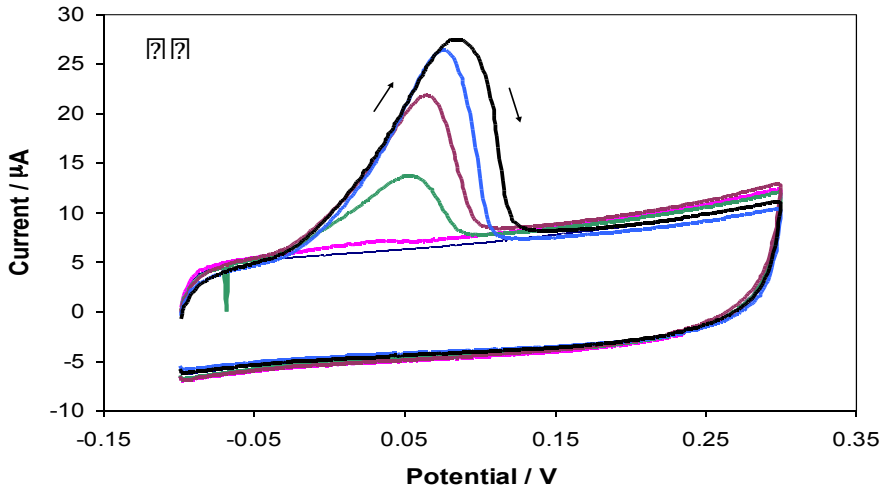

Fig. 5. (A) Cyclic voltammograms recorded in aqueous 1.0 M NH3-2.0 x 10-4 M AgNO3, from -0.12 V to +0.30 V, for the sandwich type assay described in experimental section with 1.0 x 10-6 µg/mL of the non specific antigen (goat IgG -thin line) and for increasing specific antigen (human IgG) concentrations: 5.0 x 10-8, 1.0 x 10-7, 5.0 x 10-7, 7.5 x 10-7 and 1.0 x 10-6 µg/mL. Silver electro-deposition potential: -0.12 V; silver deposition time: 60 seconds; scan rate: 50 mV/s.

In figure 5A are shown cyclic voltammograms for different concentrations of human IgG following the procedure explained in experimental section. Figure 5B represents the corresponding peak heights used as analytical signals,. As observed in this figure a good linear relationship for the concentrations of

human IgG, in the range from 5.0 x 10-8 to 7.5 x 10-7 µg/mL, with a correlation coefficient of 0.9969, according to the following equation:

ip (µA) = 21.436 [human IgG] (µg/mL) + 3.750 (n = 3) is obtained.

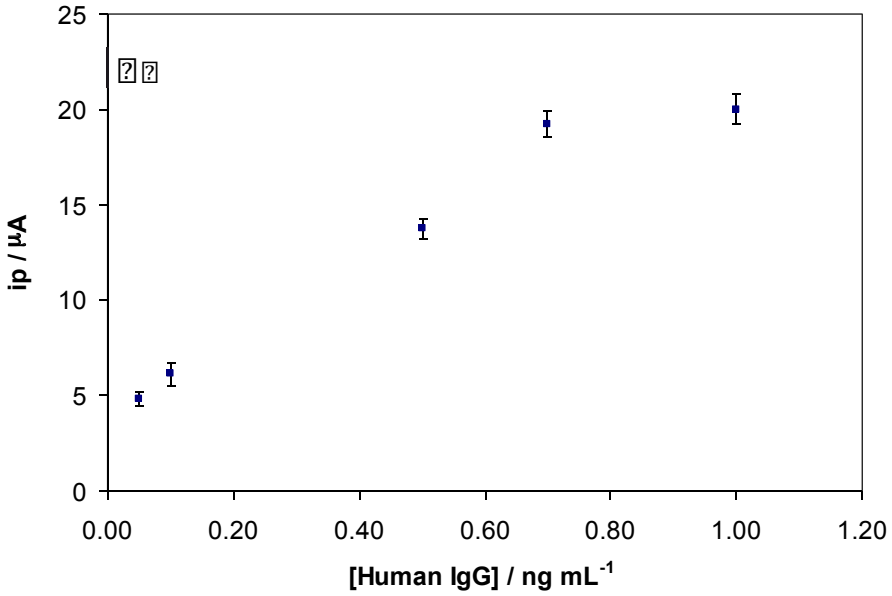

Fig. 5 (B) The corresponding relationship between the different concentrations of the human IgG and the obtained peak currents used as analytical signals.

The limit of detection (calculated as the concentration corresponding to three times the standard deviation of the estimate) of the antigen was 23 fg ofhuman IgG for mL of sample. The reproducibility of the method shows a RSD around 4%, obtained for a series of 3 repetitive immunoreactions for 5.0 x 10-7 µg human IgG / mL.

These results indicate that with the silver enhancement method can be detected 1000 times lower concentrations of antigen than with the direct differential pulse voltammetry (DPV) gold detection as done previously in our group.

3.3. Electrochemical quantification of AuNPs based on the electrocatalyzed HER and its application to magneto immunoassays

The catalytic ability of gold nanoparticles (AuNPs) toward the formation of H2 in the electrocatalyzed Hydrogen Evolution Reaction (HER) is thoroughly studied, using screen-printed carbon electrodes (SPCEs) as electrotransducers. The AuNPs on the surface of the SPCE, provide free electroactive sites to the protons present in the acidic medium that are catalytically reduced to hydrogen by applying an adequate potential, with a resulting increment in the reaction rate of the HER measured here by the generated catalytic current. This catalytic current is related with the concentration of AuNPs in the sample and allows their quantification. Finally, this electrocatalytic method is applied for the first time, in the detection of AuNPs as labels in a magnetoimmunosandwich assay using SPCEs as electrotransducers for the determination of HIgG as a model protein.

Nanoparticles in general have special surface characteristics for their use in catalytic processes,[2,3] mainly due to the proportion of atoms at the surface of small nanoparticles that can be much higher then in the bulk state and results in a high surface to volume ratio. Interesting works were made with platinum nanoparticles (PtNPs) functionalized with nucleic acids that act as electrocatalytic labels for the amplified electrochemical detection of DNA hybridization and aptamer/protein recognition that resulted in sensitivity limits of 10pM, in DNA detection, and 1nM in the aptamer/thrombin detection system. [4]

In the wide range of nanomaterials, gold nanoparticles (AuNPs) grab a lot of attention once they have been applied in innumerous studies. [5,6,7] Bulk gold is considered an inert material towards redox processes [8] due to the repulsion between the filled d-states of gold and molecular orbitals of molecules like O_2 or H_2, but small AuNPs show a different behaviour [9,10] since contain a large number of coordinative unsaturated atoms in edge positions. The quantum effects related with shape and size of AuNPs originated by d band electrons of the surface which are shifted towards the Fermi-level, promote the ability to interact in electrocatalytic reactions. All these features allow the occurrence of adsorption phenomena with catalytic properties,[11] and places AuNPs in the palette of materials with potential interest to be used in electrocatalyzed reactions.[12,13] Furthermore they exhibit good biological compatibility and excellent conductivity that highlights

them for biosensor applications. Examples of interesting approaches using AuNPs are the works developed by Yang *et al.* [5] where they are used as DNA labels with electrocatalytic properties achieving detection limits in the fM order. Our group has also reported the use of AuNPs for further silver catalytic electrodeposition and applied this reaction for enhanced detection of proteins. [14]

In this work we make use of the advantageous characteristics of screen-printed carbon electrodes (SPCEs) in terms of low cost, miniaturization possibilities, low sample consuming and wide working potential range in the Hydrogen Evolution Reaction (HER) in presence of AuNPs. In addition we combined all the mentioned advantages with the relative high hydrogen overpotential [15] and low background currents for the detection of AuNPs using SPCEs. This is based on the electroactive properties of AuNPs to catalyze HER in acidic media, which is measured by recording the current generated in the simple and efficient chronoamperometric mode.

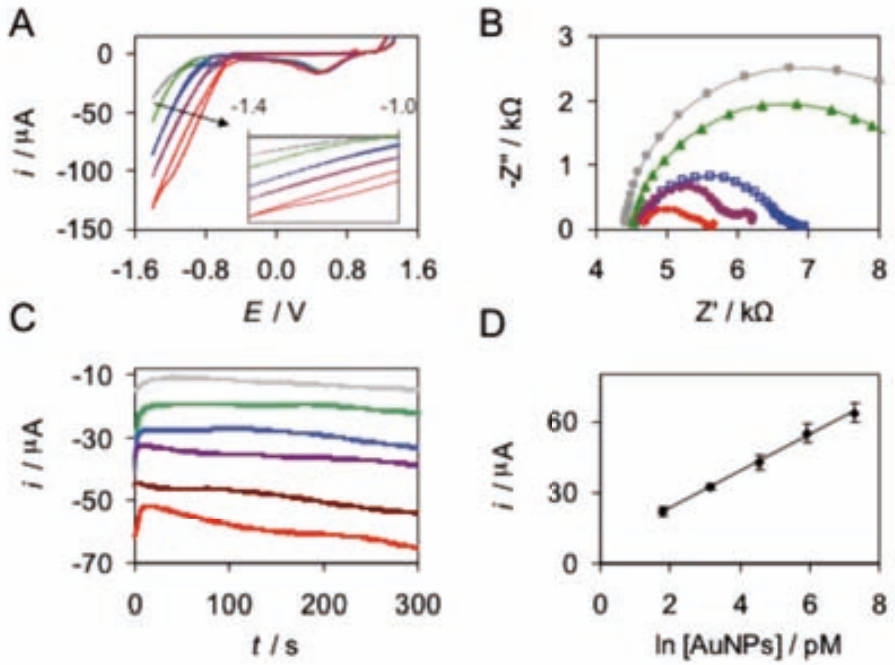

Fig.1. A: CV performed with increasing concentration of AuNPs. Upper curve corresponds to the background signal followed by 1.48, 23.5, 93.8, 1500pM of AuNPs solution from top to bottom; B: Electrochemical Impedance Spectroscopy plots of different electrodes with increasing concentrations of AuNPs solutions from top to bottom as described in 1.A; C: Chronoamperograms recorded in 1M HCl solution (upper line) and for AuNPs ranging from 5.85pM to 1.5nM (top to bottom); D: Calibration plot obtained by plotting the absolute value of the currents at 200s with logarithm of AuNPs concentration.

The electrocatalytic effect of AuNPs deposited onto SPCEs, to the HER (in acidic medium) is shown in fig.1A, where cyclic voltammograms in 1M HCl are

presented. The background CV (upper curve) shows that the proton reduction starts at approximately -0.8V vs. Ag/AgCl when no AuNPs are present, and undergoes a positive shift up to 500mV in a proportional relation with the concentration of AuNPs in solution. A similar behaviour was previously observed for bulk gold. [17] Moreover, a higher current is obtained for potentials lower than -1.00V at higher concentrations of AuNPs. The oxygen reduction onto SPCEs surface is neglected in this work once it occurs at potentials lower than -1.40V and therefore will not affect the background signals.

To better evaluate the catalytic reaction the active surface of the working electrode in absence and presence of adsorbed AuNPs was characterized by electrochemical impedance spectroscopy (EIS) that can give further information on the impedance changes of the electrode surface. Fig.1B displays EIS plots from several AuNPs concentrations, showing the decrease in resistance when increasing the AuNPs concentration (ranging from 1.48 to 1500pM, from top to bottom). This is due to the fact that AuNPs behave as free electroactive adsorption sites that enhance the electron transfer in the system resulting in a lower semi-circle diameter, which means a decrease of the charge, transfer resistance at electrode surface.

From the voltammetric studies (fig.1A), it can be concluded that by applying an adequate reductive potential (within the potential window (PW) from -1.0 to -1.4V) the protons in the acidic medium are catalytically reduced to hydrogen in presence of AuNPs and this reduction can be chronoamperometrically measured (fig. 1C). The absolute value of the cathodic current generated at a fixed time can be considered as the analytical signal and related with the amount of AuNPs present in the sample.

The different parameters affecting the analytical signal obtained by the chronoamperometric mode, such as the acidic medium and the electroreduction potential were optimised (data not shown). From several acidic solutions studied it was found that 1M HCl displayed a better performance and the optimum electroreduction potential was -1.00V. Regarding the fixed time to measure the current chosen as analytical signal, it was found a compromise between the time of analysis and signal to noise ratio at 200 seconds.

Furthermore, it was found that a previous oxidation of the AuNPs at +1.35 V was important for obtaining the best electrocatalytic effect on the HER in the further reductive step. During the application of this potential, some gold atoms in the outer layers of AuNPs surface are transformed into Au(III) ions. These ions could also exert a catalytic effect on hydrogen evolution [18]

together with the significant number of AuNPs still remaining after the oxidation. In order to clarify this, Scanning Electrochemical Microscopy (SEM) images of SPCEs with deposited AuNPs (from 1.5nM solution in 1M HCl) were obtained after the different steps of the chronoamperometry procedure. In fig.2 these images are shown together with a scheme of the processes occurring on the electrode surface. It can be observed that the AuNPs remain on the surface of the SPCE after the application of the oxidation potential (b), and after a complete chronoamperogram was performed (c). AuNPs were observed to be distributed all over carbon working electrode area, with a certain aggregation in high rugosity areas like it was expected.

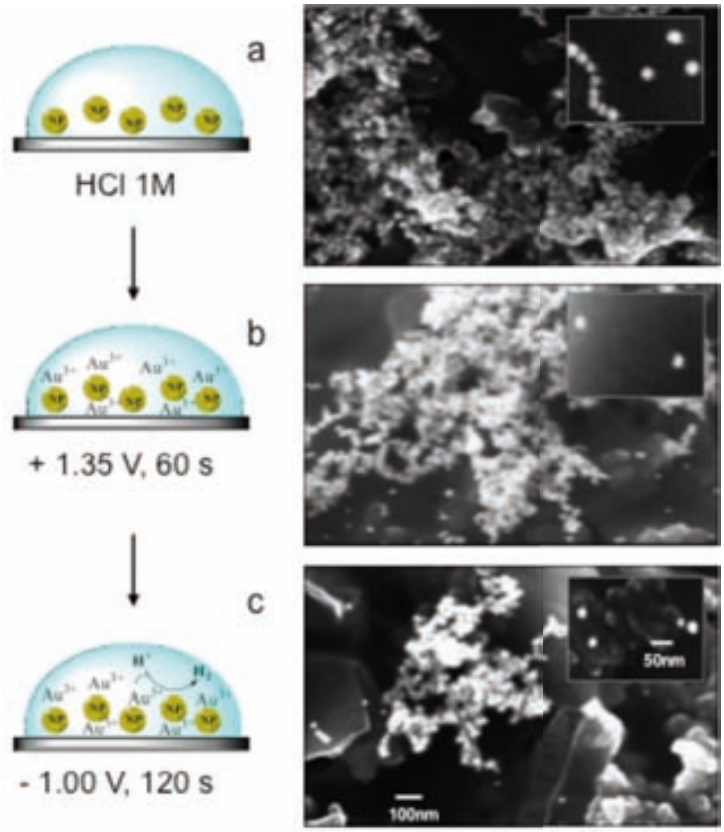

Figure 3.A: Scheme of the magnetosandwich immunoassay steps and electrochemical detection of the obtained sandwich. B: Relation between the analytical signal and the logarithm of HIgG concentration.

After optimizing the experimental procedure, a series of chronoamperograms for AuNPs solutions in a similar concentration range as in the CV curves of figure1A, were registered under the optimal conditions (figure 1C). The absolute value of the current at 200s (analytical signal) was plotted versus the logarithm of AuNPs concentration (figure 1D), resulting in a linear relationship in the range between 4.8pM and 1.5nM according to the following equation:

$$i_{(mA)} = 7.71 \times \ln[AuNPs]_{(pM)} + 8.19, \quad r = 0.999, \; n = 3$$

A detection limit for AuNPs of 1.03pM (calculated as the concentration corresponding to three times the standard deviation of the estimate) and a RSD of 5% for three repetitive measurements of 5.88pM AuNPs were obtained.

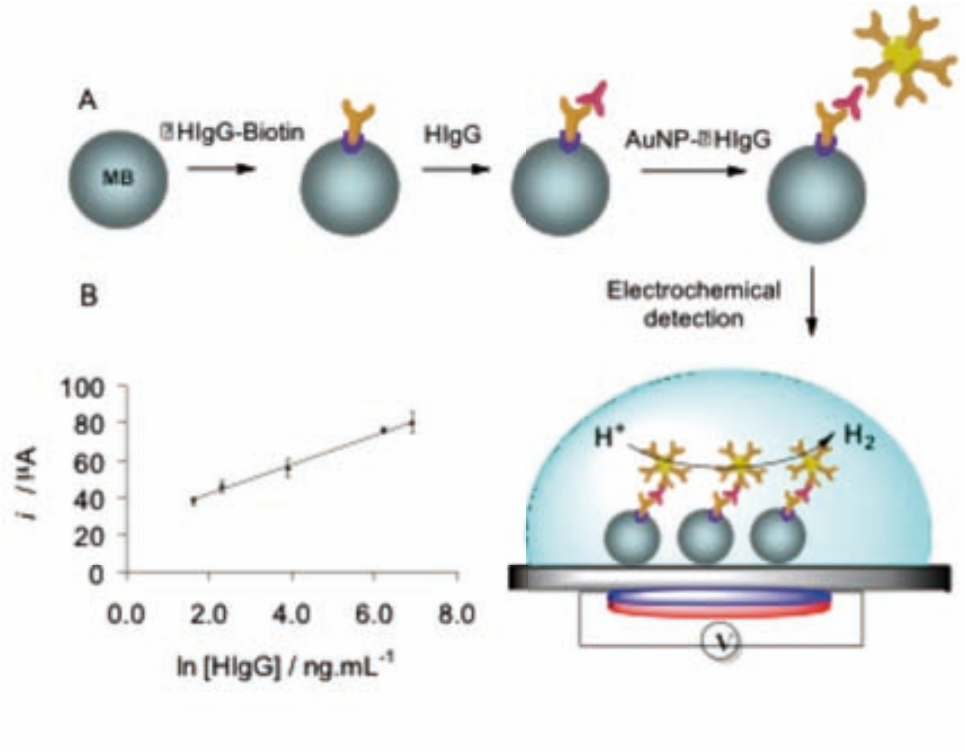

Figure 3.A: Scheme of the magnetosandwich immunoassay steps and electrochemical detection of the obtained sandwich. B: Relation between the analytical signal and the logarithm of HIgG concentration.

Finally, the advantageous properties of this catalytic method were approached for protein detection (HIgG as model analyte) in a magnetoimmunoassay. This system also takes advantage from the magnetic beads properties used here as platforms, in terms of low matrix effects and sample preconcentration when they are applied in protein analysis. Fig.3A displays a scheme of the overall experimental procedure and fig.3B shows the relation between the analytical signal and the concentration of HIgG in the range between 5 and 1000 ng mL^{-1}. A linear relationship was obtained by plotting the current values versus the logarithm of the HIgG concentration according to the following equation:

$$i_{(mA)} = 7.84 \times \ln [HIgG]_{(ng/mL)} + 26.4 \text{ , } r = 0.998, n = 3$$

The limit of detection was 1.45 ng.mL^{-1} of HIgG (calculated as the concentration corresponding to three times the standard deviation of the estimate). The reproducibility of the method shows a RSD around 3%,

obtained for 3 repetitive assays for 50 ng mL^{-1} of target. The selectivity of the assay was demonstrated performing a blank assay using a non specific protein.

REFERENCES

[1] A Merkoçi, M. Aldavert, S. Marín, S. Alegret, TrAC 24 (2005) 341-349; A. Merkoçi, FEBS Journal 274 (2007) 310–316.

[2] A. Abad, A. Corma, H. García, Chem. Eur. J. 14 (2008) 212-222.

[3] H.L. Jiang, T. Umegaki, T. Akita, X.B. Zhang, M. Haruta, Q. Xu, Chem Eur. J. 16 (2010) 3132-3137.

[4] R. Polsky, R. Gill, L. Kaganovsky, I. Willner, Anal. Chem. 78 (2006) 2268-2271.

[5] J. Das, H. Yang, J. Phys. Chem. C 113 (2009) 6093-6099.

[6] A. De la Escosura-Muñiz, A. Ambrosi, A. Merkoçi, TrAC 27 (2008) 568-584.

[7] A. Ambrosi, M.T. Castañeda, A.J. Killard, M.R. Smyth, A. Merkoçi, Anal.Chem. 79 (2007) 5232-5240.

[8] B. Hammer, J.K. Nørskov, Nature 376 (1995) 238-240.

[9] SR. Belding, E.J.F. Dickinson, R.G. Compton, J. Phys. Chem. C 113 (2009), 11149-11156

[10] K.Z. Brainina, L.G. Galperin, A.L. Galperin, J Solid State Electrochem. 14 (2010) 981-988.

[11] M. Haruta, N. Yamada, T. Kobayashi, S. Iijima, J. Catal. 115 (1989) 301-309.

[12] W. Chen, S. Chen, Angew. Chem. Int. Ed. 48 (2009) 4386-4389.

[13] B. E. Hayden, D.Pletcher, J. P. Suchsland, Angew. Chem. 119 (2007) 3600-3602.

[14] A. De la Escosura-Muñiz, M. Maltez-da Costa, A. Merkoçi, Biosens. Bioelectron. 24 (2009) 2475-2482.

[15] L.A. Kibler, Chem. Phys. Chem. 7 (2006) 985-991.

[16] J. Turkevich, P. Stevenson, J. Hillier, Discuss. Faraday Soc. 11 (1951) 55-75.

[17] J. Perez, E.R. Gonzalez, H.M. Villullas, J. Phys. Chem. B 102 (1998) 10931-10935.

[18] M. Díaz-González, A. de la Escosura-Muñiz, M. González-García, A. Costa-García, Biosens. Bioelectron. 23 (2008) 1340-1346.

3.4. Detection of anti-Hepatitis-B antibodies in human serum using AuNPs based electrocatalysis.

Viral hepatitis due to hepatitis B virus is a major public health problem all over the world. Hepatitis B is a complex virus, which replicates primarily in the liver, causing inflammation and damage, but it can also be found in other infected organs and in lymphocytes. For this reason, the hepatitis B vaccine is strongly recommended for healthcare workers, people who live with someone with hepatitis B, and others at higher risk. In many countries, hepatitis B vaccine is inoculated to all infants and it is also recommended to previously unvaccinated adolescents.

The external surface of this virus is composed of a viral envelope protein also called hepatitis B surface antigen (HBsAg). Previously infected and vaccinated people show normally high levels of IgG antibodies against this antigen (α-HBsAg IgG). The presence or absence of these antibodies in human serum is useful to determine the need for vaccination (if α-HBsAg IgG antibodies are absent), to check the immune response in patients which has suffered hepatitis B, the evolution of chronic HB carrier patients and also the immunity of vaccinated people [McMahon et al., 2005].

Current methods for the detection of α-HBsAg IgG antibodies such as Enzyme-Linked Immunosorbent Assay (ELISA) and Microparticle Enzyme Immunoassay (MEIA) are time-consuming, and require advanced instrumentation. Hence, alternative cost-effective methods that employ simple/user-friendly instrumentation and are able to provide adequate sensitivity and accuracy would be ideal for this kind of analysis. In this context, biosensor technology coupled with the use of nanoparticles (NPs) tags offers benefits compared to traditional methods in terms of time of analysis, sensitivity and simplicity. From the variety of NPs, gold nanoparticles (AuNPs) have gained attention in the last years due to the unique structural, electronic, magnetic, optical, and catalytic properties which have made them a very attractive material for biosensor systems and bioassays.

Sensitive electrochemical DNA sensors [Pumera et al., 2005; Castañeda et al., 2007; Marín et al., 2009], immunosensors [Ambrosi et al., 2007; De la Escosura-Muñiz et al., 2009a] and other bioassays have recently been developed by our group and others [De la Escosura-Muñiz et al., 2008] using AuNPs or other NPs as labels and providing direct detection without prior chemical dissolution. In some of these bioassays, magnetic beads (MBs) are used as platforms of the bioreactions, providing important advantages: i) the analyte is preconcentrated on the surface of the MBs, ii) applying a magnetic

field, the complex MB-analyte can be separated from the matrix of the sample, minimizing matrix effects and improving the selectivity of the assay.

Furthermore, we have recently reported a novel cell sensor based on a new electrotransducing platform (screen-printed carbon electrodes-SPCEs-) where the cells are cultured and then recognized by specific antibodies [Díaz et al., 2009] labeled with AuNPs [De la Escosura-Muñiz et al., 2009b]. These AuNPs are chronoamperometrically detected approaching their catalytic properties on the hydrogen evolution, avoiding their chemical dissolution.

Here we present a novel magnetosandwich assay based on AuNPs tags for the capturing of α-HBsAg IgG antibodies in human sera of patients previously exposure to hepatitis B (either for infection, reinfection or for vaccination) and final chronoamperometric detection approaching the catalytic properties of AuNPs on the hydrogen evolution reaction. The α-HBsAg IgG antibodies concentration in the sera samples has been previously calculated by a standard method (MEIA), finding that the sensitivity of the electrochemical biosensor is high enough so as to detect the HB responders.

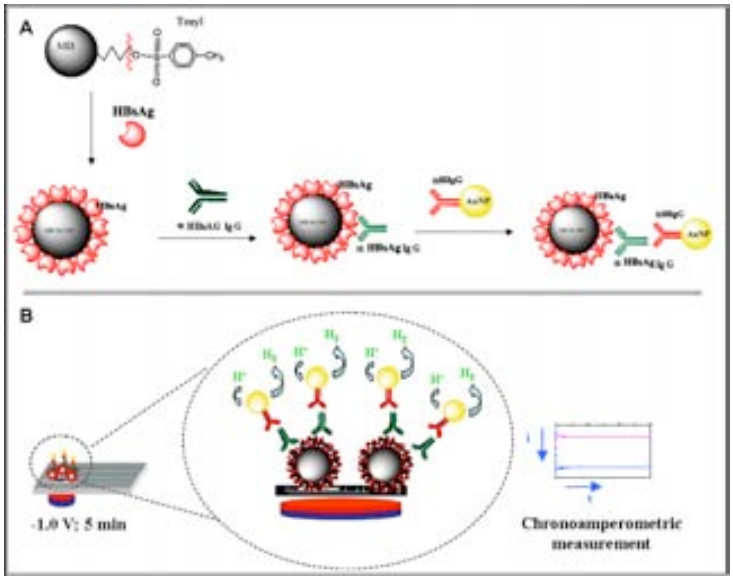

Fig. 1. (A) Scheme of the experimental procedure performed. HBsAg captured on the surface of magnetic beads, incubation with human serum containing α-HBsAg IgG antibodies and recognition with AuNPs conjugated with goat anti-human IgG antibodies. **(B)** Scheme of the electrochemical detection procedure based on the electrocatalytic hydrogen generation.

The experimental procedure for capturing the α-HBsAg IgG antibodies from human sera and the further signaling with AuNPs tags is schematized in Figure 1. MBs modified with tosyl groups are used as platforms of the bioreactions, allowing to preconcentrate the sample and also to avoid unspecific adsorptions on the surface of the electrotransducer. The used MBs

can easily be conjugated with molecules that have amino- or carboxi- groups, by nucleofilic substitution reaction. Approaching this property, hepatitis B surface antigens (HBsAg) are immobilized onto the surface of the MBs, ensuring in this way an active surface (MB/HBsAg) for capturing α-HBsAg IgG antibodies, whose unspecific adsorption on the tosylactivated MBs is avoided by a blocking step using BSA. When adding the sera samples, the α-HBsAg IgG analyte recognize the specific antigens forming the MB/HBsAg/α-HBsAg IgG complex. After a washing step, the α-HBsAg IgG antibodies selectively attached onto MB/HBsAg are captured by goat polyclonal antibodies anti-Human IgG (HIgG) previously conjugated with AuNPs. This secondary immunoreaction gives rise to the formation of the final complex (MB/HBsAg/α-HBsAg IgG/AuNPs/α–HIgG), where the quantity of AuNPs is proportional to the concentration of α-HBsAg IgG antibodies in the sample.

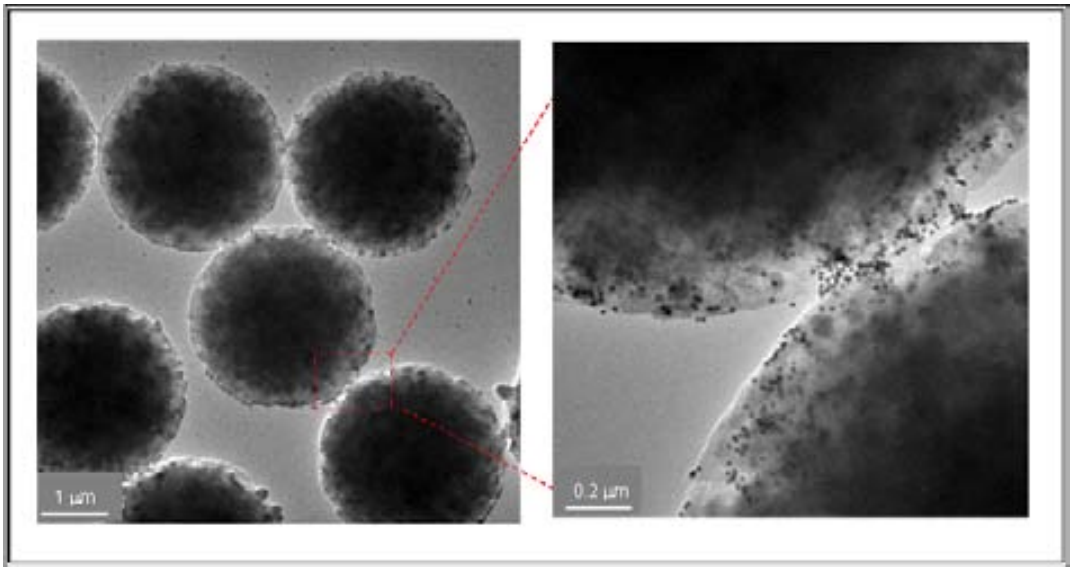

Fig. 2. TEM images of the MB/HBsAg/α-HBsAg IgG/AuNPs/α–HIgG complex formed following the experimental procedure detailed in *section 2* for a serum containing 132 mIU/mL of α-HBsAg IgG **(left)** and detail of the region between two MBs, where the AuNPs (small black points) are observed **(right)**.

Figure 2 shows TEM image of MB/HBsAg/α-HBsAg IgG/AuNPs/α–HIgG formed following the reported procedure. AuNPs (small black points) covering the surface of the MBs (big spheres) can be observed demonstrating the specifity of the assay. The results obtained by TEM images were followed by electrochemical measurements. A 25 µL sample of the magnetosandwich complex placed onto the surface of the SPCE electrotransducer was detected through measuring of the AuNPs catalytic properties on the hydrogen evolution [Chikae et al., 2006; De la Escosura-Muñiz et al., 2009b] at an adequate potential (usually -1.0 V) in an acidic medium. This catalytic effect has also been observed for platinum and palladium nanoparticles [Meier et al., 2004]. Nevertheless the use of AuNPs as here reported are more suitable

for biosensing purposes, due to their simple synthesis, narrow size distribution, biocompatibility, and easy bioconjugation.

It was also found that a previous oxidation of the AuNPs at +1.35 V was necessary for obtaining the best electrocatalytic effect on the hydrogen evolution in the further reductive step (data not shown). During the application of this potential, some gold atoms in the outer layers of AuNPs surface are transformed into Au (III) ions. These ions could also exert a catalytic effect on hydrogen evolution [Díaz-González et al., 2008] together with the significant number of AuNPs still remaining after the oxidation step. After that, the catalytic current generated by the reduction of the hydrogen ions is chronoamperometrically recorded and related to the quantity of the α-HBsAg IgG antibodies. The electroreduction potential has been previously optimized (in the range -0.80 V to -1.20 V) and as a compromise between signal intensity and reproducibility a potential value of -1.00 V was found as optimal.

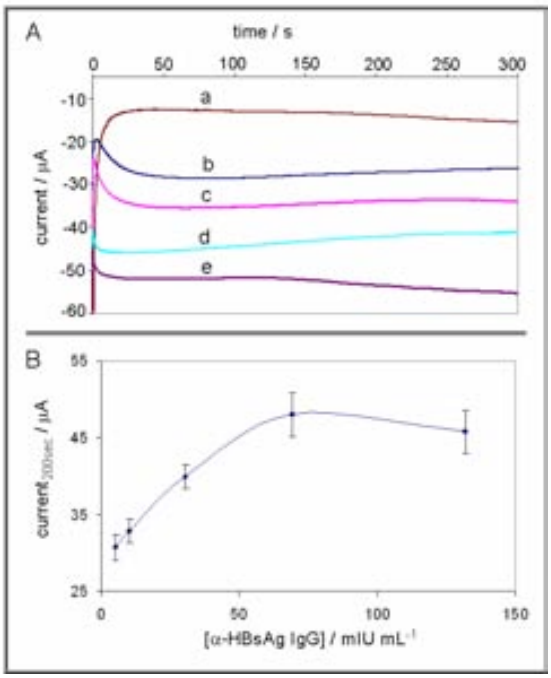

Fig. 3. (A) Chronoamperograms recorded in 1M HCl by applying a potential of -1.00 V for 5 min, for a magnetosandwich performed in a non immune control serum (blank curve, **a**) and magnetosandwichs performed for sera containing increasing concentrations of α-HBsAg IgG antibodies: 5 (**b**), 10.1 (**c**), 30.5 (**d**) and 69.2 (**e**) mIU/mL. **(B)** Effect of the α-HBsAg IgG antibodies concentration on the analytical signal.

In Figure 3A are shown the chronoamperograms recorded following the procedure detailed in methods section, for magnetosandwich assays performed in a non immune serum as control (a) and for assays performed in sera containing 5 (b), 10.1 (c), 30.5 (d), 69.2 (e) and 132 (f) mIU/mL of α-HBsAg IgG antibodies. As it can be observed, the cathodic catalytic current

increases when increasing the concentration of antibodies in the samples, as it was expected. The curve presented in Figure 3B shows that there is a good linear relationship (correlation coefficient of 0.991) between the α-HBsAg IgG antibodies and the absolute value of the current registered at 200 seconds (analytical signal) in the range of 5-69.2 mIU/mL, according to the equation:

current (μA) = 0.265 [α-HBsAg IgG (mIU/mL)] + 30.27 (n = 3) [1]

The limit of detection (calculated as the concentration of α-HBsAg IgG antibodies corresponding to 3 times the standard deviation of the estimate) was 3 mIU/mL. Since it is considered that vaccine responders show ≥ 10 mIU/mL (McMahon et al. 2005) our test is enough to guarantee the detection of those levels. The reproducibility of the method shows a relative standard deviation (RSD) of 5%, obtained for a series of three repetitive assay reactions for a serum sample containing 10.1 mIU/mL of α-HBsAg IgG antibodies.

Finally, a human serum sample with an unknown concentration of α-HBsAg IgG antibodies was electrochemically analyzed. Following the explained experimental procedure, a value of the analytical signal of 36.8 ± 1.5 μA (n=3) was obtained. From the equation [1], a concentration of 24.6 ± 5.7 mIU/mL in the serum sample was estimated. This sample was also analyzed by the MEIA method, obtaining a value of 23.1 ± 1.6 mIU/mL. These results show a deviation of 6.5% between both methods, being this accuracy good enough to guarantee that the electrochemical method is a valid alternative to check the levels of α-HBsAg IgG antibodies in human serum. This accuracy value was also corroborated performing an approximation to the statistical paired sample T-test (see supporting information).

The performance of the developed electrochemical biosensor is similar to the achieved in recently reported biosensors for the detection of α-HBsAg IgG in human sera based on optical [Moreno-Bondi et al., 2006; Qi et al., 2009] or piezoelectric [Lee et al., 2009] measurements in terms of sensitivity and reproducibility of the assays. Although the linear range of the electrochemical biosensor is shorter than the reported in these works (serial dilutions of the samples can solve this drawback) we should consider advantageous characteristics in terms of cost, simplicity and time of analysis that make the presented electrochemical biosensor a promising alternative for future point of care analysis.

REFERENCES

Ambrosi, A., Castañeda, M.T., Killard, A.J., Smyth, M.R., Alegret, S., Merkoçi, A. 2007. Anal. Chem. 79, 5232–5240.

Castañeda, M. T., Merkoçi, A., Pumera, M., Alegret, S. 2007 Biosens. Bioelectron. 22, 1961–1967.

Chikae, M., Idegami, K., Kerman, K., Nagatani, N., Ishikawa, M., Takamura, Y., Tamiya, E. 2006. Electrochem. Commun. 8, 1375–1380.

De la Escosura-Muñiz, A., Ambrosi, A., Merkoçi, A. 2008. Trends Anal. Chem. 27, 568–584.

De la Escosura-Muñiz, A., Maltez-da Costa, M., Merkoçi, A. 2009a. Biosens. Bioelectron. 24, 2475–2482.

De la Escosura-Muñiz, A., Sánchez-Espinel, A., Díaz-Freitas, B. González-Fernández, A., Maltez-da Costa, M., Merkoçi, A. 2009b. Anal. Chem. 81, 10268–10274.

Díaz, B., Sanjuan I., Gambón F., Loureiro, C., Magadán, S. and González-Fernández, A. 2009. Cancer Immunol. Immunother. 58, 351-360.

Díaz-González, M., de la Escosura-Muñiz, A., González-García, M., Costa-García, A. 2008. Biosens. Bioelectron, 23, 1340-1346.

Lee, H.J., Namkoong, K., Cho, E.C., Ko, C., Park, J.C., Lee, S.S. 2009. Biosens. Bioelectron. 24, 3120-3125.

Marín, S., Merkoçi, A. 2009. Nanotechnology, 20, 055101.

McMahon, B.J., Bruden, D.L., Petersen, K.M., Bulkow, L.R., Parkinson, A.J., Nainan, O., Khristova, M., Zanis, C., Peters, H., Margolis, H.S. 2005. Annals of Internal Medicine, 142, 333-341.

Meier, J., Schiøtz, J., Liu, P., Nørskov, J.K., Stimming, U. 2004. Chem. Phys. Lett. 390, 440–444.

Moreno-Bondi, M.C., Taitt, C.R., Shriver-Lake, L.C., Ligler, F.S. 2006. Biosens. Bioelectron. 21, 1880-1886.

Pumera, M., Castañeda, M.T., Pividori, M.I., Eritja, R., Merkoçi, A., Alegret, S. 2005. Langmuir, 21, 9625-9629.

Qi, C., Zhu, W., Niu, Y., Zhang, H.G., Zhu, G.Y., Meng, Y.H., Chen, S., Jin, G. 2009. Journal of Viral Hepatitis, 16, 822-832.

Turkevich, J., Stevenson, P., Hillier, J. 1951. Discuss. Faraday Soc. 11, 55– 75.

3.4. Conclusions

Electrochemical deposition of silver onto AuNPs applied to magneto immunoassays

In this work, for the first time, the selective electrocatalytic reduction of silver ions onto the surface of AuNPs is clarified. This catalytic property is combined with the use of microparamagnetic beads as platform for the immobilization of biological molecules, and advantages used to design a novel sensing device. The electrochemical measurement accompanied by scanning electron microscopy images reveal the silver electrocatalysis enhancement by the presence of nanoparticles anchored to the electrode surface through specific antigen-antibody interactions.

In the sensing device, AuNP as label is used to detect human IgG as a model protein and the excess/non-linked reagents of the immunological reactions are separated using a magnetic platform, allowing the electrochemical signal coming from AuNP to be measured, and thus the presence or absence of protein be determined. The magnetic separation step significantly reduces background signal and gives the system distinct advantages for alternative detection modes of antigens. Finally, the sensible electrochemical detection of the AuNPs is achieved, based on their catalytic effect on the electro-reduction of silver ions.

Several problems inherent to the silver electrocatalysis method are resolved by using the magnetic beads as platforms of the bioassays: (i) The selectivity inherent to the use of magnetic beads avoids unspecific adsorptions of AuNPs on the electrode surface, that could give rise to unspecific silver electrodeposition due to the high sensitivity of the amplification method and (ii)

The developed electrocatalytic method allows to achieve low levels of AuNPs, so very low protein detection limits, up to 23 fg / mL, are obtained., that are 1000 times lower in comparison to the method based on the direct detection of AuNPs. The novel detection mode allows the obtaining of a novel immunosensor with low protein detection limits, with special interest for further applications in clinical analysis, food quality and safety as well as other industrial applications.

This system establishes a general detection methodology that can be applied to a variety of immunosystems and DNA detection systems, including lab-on-a-chip technology. Currently, this methodology is being applied in our lab for the detection of low concentrations of proteins with clinical interest in real samples.

Electrochemical quantification of AuNPs based on the electrocatalyzed HER and its application to magneto immunoassays

The catalytic ability of gold nanoparticles (AuNPs) toward the formation of H2 in the electrocatalyzed Hydrogen Evolution Reaction (HER) is thoroughly studied, using screen-printed carbon electrodes (SPCEs) as electrotransducers. The AuNPs on the surface of the SPCE, provide free electroactive sites to the protons present in the acidic medium that are catalytically reduced to hydrogen by applying an adequate potential, with a resulting increment in the reaction rate of the HER measured here by the generated catalytic current. This catalytic current is related with the concentration of AuNPs in the sample and allows their quantification. Finally, this electrocatalytic method is applied for the first time, in the detection of AuNPs as labels in a magnetoimmunosandwich assay using SPCEs as electrotransducers, allowing the determination of human IgG at levels of 1 ng/mL.

In conclusion we show here that AuNPs constitute a very good electrocatalytic system for the HER in acidic medium by providing free electroactive hydrogen adsorption sites towards the formation of molecular hydrogen. Based on this system an optimised AuNPs indirect quantification method, taking advantage of the chronoamperometric mode, is developed.

The catalytic properties of AuNPs were also approached for a model protein (Human-IgG) detection in a magnetoimmunoassay that decreases the distance between the electrode and the electrocatalytic label enhancing the electron tunnelling and consequently the catalytic signal used for biodetection. The advantages of the electrocatalytic detection method together with the use of MBs as platforms of the bioreactions and the use of SPCEs as electrotransducers will open the way to efficient, portable, low-cost and easy-to-use devices for point-of care use for several application with interest not only for clinical analysis but for environmental as well as safety and security.

Detection of anti-Hepatitis-B antibodies in human serum using AuNPs based electrocatalysis

A sandwich immunoassay using magnetic beads as bioreaction platforms and AuNPs as electroactive labels for the electrochemical detection of human IgG antibodies anti-Hepatitis B surface antigen (HBsAg), is here presented as an alternative to the standard methods used in hospitals for the detection of human antibodies directed against HBsAg (such as ELISA or MEIA).

The reported assay takes advantage of the properties of the magnetic beads used as platforms of the immunoreactions and the AuNPs used as electrocatalytic labels. The final detection of these AuNPs tags is performed in a rapid and simple way approaching their catalytic properties towards the hydrogen ions electroredection in an acidic medium without previous nanoparticle dissolution.

The developed biosensor allows the detection of 3 mIU of α-HBsAg IgG antibodies in human serum, being sensitive enough to guarantee the detection of up to 10 mIU which is the lower limit for HBs Ag responders.

The obtained results are a good promise toward the development of a fully integrated biosensing set-up. The results were compared with those obtained with the MEIA method, showing a deviation of 6.5 %.

The developed technology based on this detection mode would be simple to use, low cost and integrated into a portable instrumentation that may allow its application even at doctor-office. The sample volumes required can be lower than those used in the traditional methods. This may lead to several other applications with interest for clinical control.

From all this, it can be concluded that the reported biosensor is a valid alternative to the standard methods for the detection of α-HBsAg IgG antibodies in human serum, in a more rapid, simple and cheap way.

Chapter 4

Electrocatalytic nanoparticles for cell detection

4.1. Introduction

Early detection of cancer is widely acknowledged as the crucial key for an early and successful treatment. The detection of tumor cells is an increasingly important issue that has received wide attention in recent years mainly due to two reasons: i) new methods are allowing the identification of metastatic tumor cells (for example, in peripheral blood), with special relevance both for the evolution of the disease and for the response of the patient to therapeutic treatments, and ii) diagnosis based on cell detection is, thanks to the use of monoclonal antibodies, more sensitive and specific than that based on traditional methods.

Detecting multiple biomarkers and circulating cells in human body fluids is a particularly crucial task for the diagnosis and prognosis of complex diseases, such as cancer and metabolic disorders[i]. An early and accurate diagnosis is the key to an effective and ultimately successful treatment of cancer, but requires new sensitive methods for detection. Many current methods for routine detection of tumor cells are time-consuming (e.g., immunohistochemistry), expensive, or require advanced instrumentation (e.g., flow cytometry). Hence, alternative cost-effective methods employing simple/user-friendly instrumentation, able to provide adequate sensitivity and accuracy, would be ideal for point-of-care diagnosis. Therefore, in recent years, there have been some attempts at cell analysis using optical based biosensors. In addition to optical biosensors, sensitive electrochemical DNA sensors immunosensors other bioassays, have all been recently developed by our group and others, using nanoparticles (NPs) as labels, and providing direct detection without prior chemical dissolution.

Here, we present the design and application of a novel cell sensor inspired by the immunosensors reported in the previous chapter. A nanoparticle-based electrocatalytic method, that allows rapid and consecutive detection/identification of cells is presented in the next two sections. Detection is based on the reaction of cell surface proteins with specific antibodies conjugated to gold nanoparticles (AuNPs). Use of the catalytic properties of the AuNPs on hydrogen formation from hydrogen ions, makes it possible to quantify the nanoparticles, and in turn, to quantify the corresponding attached cancer cells. This catalytic effect has also been observed for other nanoparticles, but AuNPs are more suitable for biosensing purposes, because of their simple synthesis, narrow size distribution, biocompatibility and easy bioconjugation.

4.2. Detection of leukemic cells using AuNPs based electrocatalysis

As an example of a novel biosensor, we report here an electrocatalytic device for the specific identification of tumor cells, which quantifies gold nanoparticles (AuNPs) coupled with an electrotransducing platform/sensor. Proliferation and adherence of tumor cells are achieved onto the electrotransducer / detector which consists of a mass-produced screen-printed carbon electrode (SPCE).

Detection is based on the reaction of cell surface proteins with specific antibodies conjugated to gold nanoparticles (AuNPs). Use of the catalytic properties of the AuNPs on hydrogen formation from hydrogen ion, makes it possible to quantify the nanoparticles, and in turn, to quantify the corresponding attached cancer cells. The catalytic current generated by the reduction of the hydrogen ions is chronoamperometrically recorded and related to the quantity of the cells of interest.

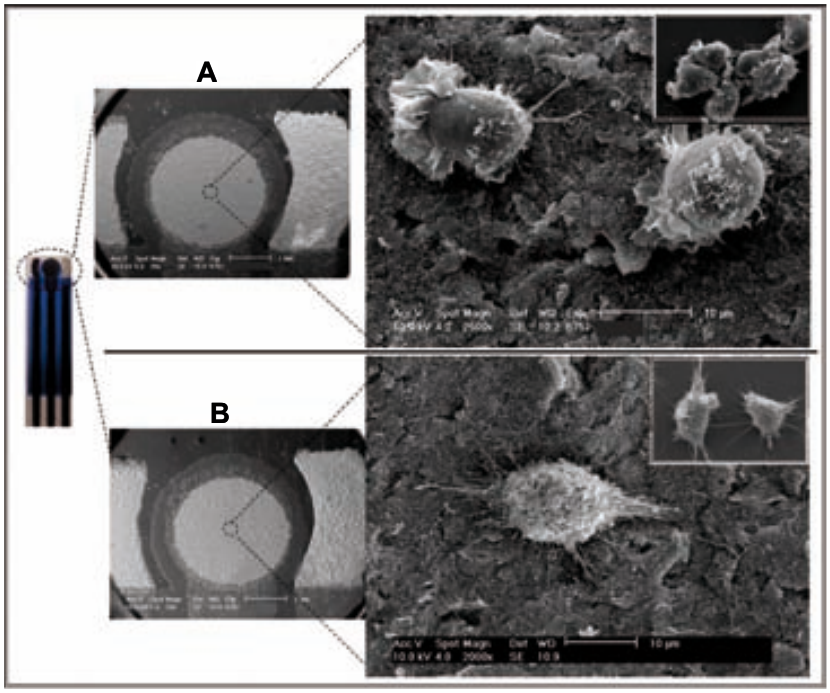

Figure 1. SEM images of the electrotransducer (SPCE) (left) with its three surfaces and details of the HMy2 (A) and PC-3 (B) cell lines on the carbon working electrode (right). Inset images correspond to cell growth on the plastic area of the SPCEs.

Two adherent human tumor cells (HMy2 and PC-3) that differ in the expression of surface HLA-DR molecules were used. HMy2 (a B-cell line) presents surface HLA-DR molecules, whereas PC-3 (a tumoral prostate cell

line) is negative to this marker; they were used as target cells and 'blank /control assay' cells, respectively. The growth of both cell lines on SPCEs was compared with that in flasks – the routine environment used in cell culture. Cell growth was allowed to take place on the surface of the working electrode. Figure 1 shows SEM images of both cell lines attached to the working electrode of the SPCEs. Both types of cells were able to grow on the carbon surface and, most interestingly, they showed similar morphological features to those cells growing on the plastic surface (inset images).

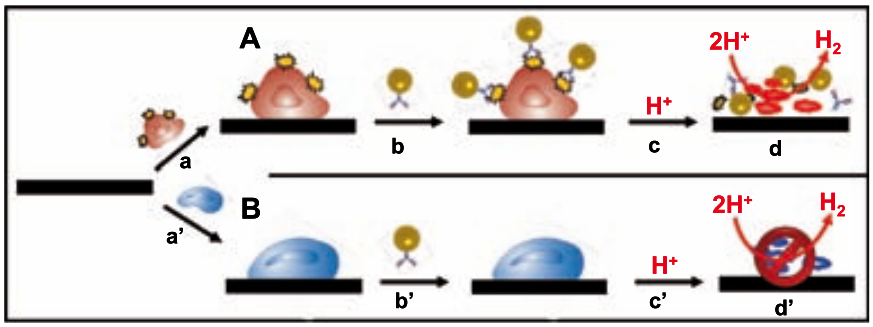

Figure2 A tumoral cell line (HMy2) (A) expressing surface HLA-DR molecules is compared to a cell line that is negative to this marker (PC-3) (B). Cells were attached onto the surface of the electrodes (a,a'), incubated with AuNPs/aDR (b,b'), an acidic solution was added (c,c') and the hydrogen generation was electrochemically measured (d,d').

Figure 2 shows the cell assay used to specifically identify tumoral cells starting from the SPCE electrotransducer. Both types of cell, HMy2 (Scheme 1A) and PC-3 (Scheme 1B) were initially introduced onto the surface of the SPCEs and allowed to grow (a,a'), prior to incubation with antibody modified AuNPs (b,b'). Finally, analysis by electrocatalytic detection based on hydrogen ion reduction (d,d') was carried out. Taking advantage of the catalytic properties of AuNPs on hydrogen evolution, antibodies conjugated with AuNPs were used to discriminate positive or negative cells for one specific marker.

The presence of HLA-DR proteins on the surface of HMy2 cells was compared with PC-3 cells used as "blank". Two different antibodies were used for this purpose: a commercial anti-DR mAb (αDR) and a homemade BH1 mAb, both able to recognize HLA-DR class II molecules. For the commercial one, αDR antibodies were directly labeled with AuNPs, whereas for the homemade BH1 antibody, a second step was necessary using AuNPs conjugated to secondary antibodies (αIgM). Another homemade antibody (32.4 mAb) that recognizes both types of cells was used as positive control.

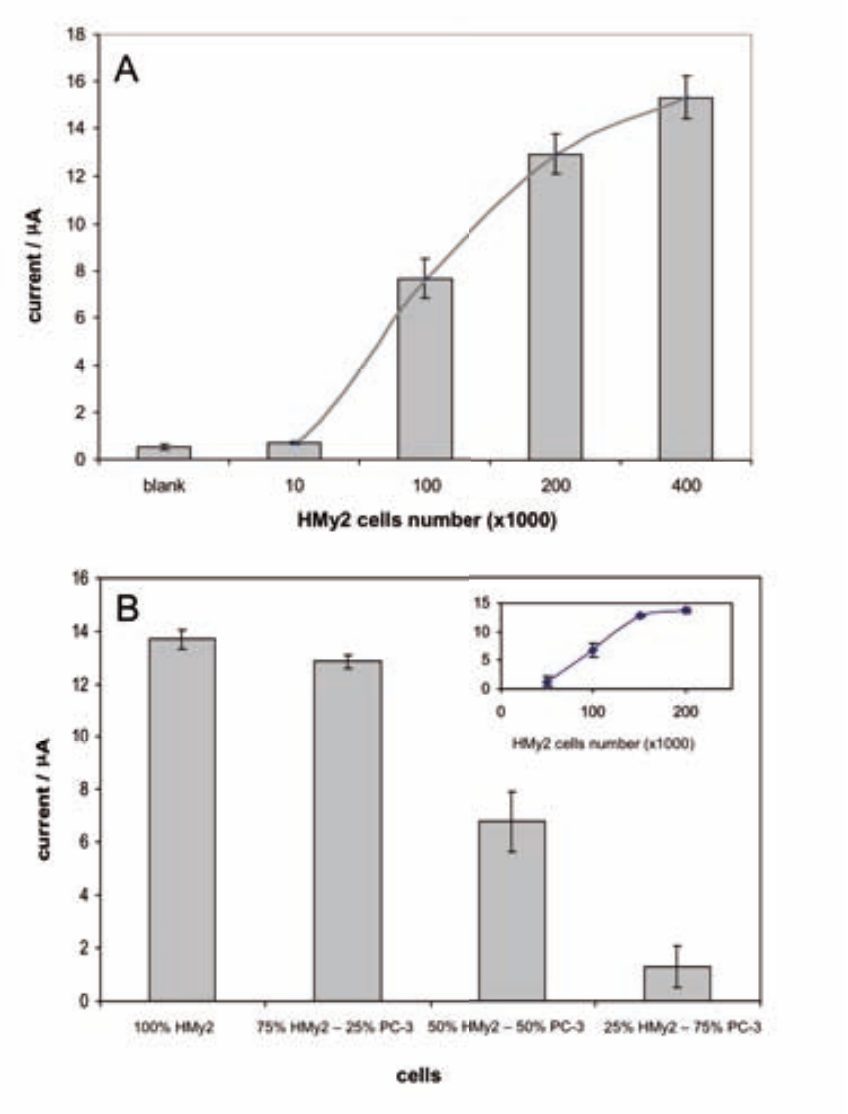

Figure 3. (A) Effect of the number of HMy2 cells on the electrocatalytical signals, after incubation with AuNPs/aDR. (B) Electrocatalytical signals obtained with HMy2 cells, after incubation with AuNPs/aDR in the presence of PC-3 cells at different HMy2/PC-3 ratios (the first bar "100% HMy2" corresponds to 200,000 HMy2 cells, while the last bar "25% HMy2 – 75%PC-3" corresponds to 50,000 HMy2 cells and 150,000 PC-3 cells).

After adding 50 µl of a 1M HCl solution, when a negative potential of -1.00 V was applied, the hydrogen ions of the medium were reduced to hydrogen, and this reduction was catalyzed by the AuNPs attached through the immunological reaction. The current produced was measured. The electrochemical response in the presence of AuNPs/αDR antibodies was positive in HMy2 (DR+ cells), but not, as expected, in PC-3 (DR- cells) (Supporting Information Figure S3A). This response was greatly increased by the use of secondary antibodies, as was observed for the BH1 mAb followed by AuNPs/αIgM. For the control antibody (32.4 mAb), the electrochemical signals suggested that the PC-3 cells had grown on the SPCEs and that

recognition took place to a higher extent for these cells than for the HMy2 cell line.

These results concur with those for both cell lines in the immunofluorescence analysis by flow cytometry (Supporting Information Figure S3B). The figure shows that, while HMy2 cells are positive to both the commercial αDR and the BH1 mAbs, PC-3 cells are negative to these antibodies. The same result was found for the positive control undertaken with the antibody 32.4, which recognizes both types of cells by immunofluorescence, but has a higher intensity of recognition for PC-3 cells.

To minimize analysis time, the commercial aDR mAb was chosen for the quantification studies, even though the BH1 mAb had a higher response. Different quantities of HMy2 cells, ranging from 10,000 to 400,000, were incubated on the SPCEs and, subsequently, recognized by the AuNPs/ aDR. Figure 3A shows the effect of the number of cells on the electrocatalytical signal. An increase can be seen in the value of the analytical signal obtained, which is correlated to the amount of HMy2 cells cultured. Although, due to the scale, no major differences can be appreciated in Figure 3A, a difference of around 170 nA was observed between control cells (blank) and 10,000 cells. The inset curve shows that there is a very good linear relationship between both parameters in the range of 10,000 to 200,000 cells, with a correlation coefficient of 0.9955, according to the following equation:

current (mA) = 0.0641 [cells number/1000] + 0.497 (mA) (n=3)

The limit of detection (calculated as the concentration of cells corresponding to three times the standard deviation of the estimate) was 4,000 cells in 700 ml of sample. The reproducibility of the method shows an RSD of 7%, obtained for a series of 3 repetitive assay reactions for 100,000 cells.

In addition, the ability of the method to discriminate HMy2 in the presence of PC-3 cells was also demonstrated. Figure 3B shows the values of the analytical signal after incubation with AuNPs/aDR for mixtures of HMy2 and PC-3 cells at different ratios (100% corresponds to 200,000 cells). The presence of PC-3 cells does not significantly affect the analytical signal coming from the recognition of HMy2 cells and, once again, a good correlation was obtained for the signal detected, and for the amount of positive cells on the electrode. This could pave the way for future applications to discriminate, for example, tumor cells in tissues or blood, as well as biopsies, where at least 4,000 cells express a specific marker on their surface.

Further technological improvements, such as reducing the size of the working electrode, could lead to a reduction in the volume of the sample required for analysis, thereby allowing the detection of even lower quantities of cells. In addition, amplification strategies could be implemented; for example, micro/nanoparticles could be simultaneously used as labels and carriers of AuNPs, making it possible to obtain an enhanced catalytic effect (more than one AuNP per antibody would be used) that would produce improved sensitivities and detection limits.

The developed methodology could be extended for the discrimination/detection of several types of cells (tumoral, inflammatory) expressing proteins on their surface, by using specific monoclonal antibodies directed at these targets. For example, the methodology could be applied for the diagnosis of metastasis. Metastatic tumor cells can express specific membrane proteins different to those in the healthy surrounding tissue, where they colonize. It could also be used for those primary tumors, where tumor cells exhibit specific tumor markers, or overexpress others than those that are normally absent, or have very low expression in healthy tissues. The breast cancer receptor (BCR) could possibly fall into this category, as it appears at low levels in healthy cells, but is overexpressed in some types of breast cancer. With a positive response, the identification of tumor cells could be very useful for an early treatment of the patient with monoclonal antibodies specifically targeted against this cancer receptor.

4.3. Detection of circulating tumor cells using AuNPs based electrocatalysis

Circulating Tumor Cells (CTCs) are traveling cells that detach from a main tumor or from metastasis. CTCs quantification is under intensive research for examining cancer dissemination, predicting patient prognosis, and monitoring the therapeutic outcomes of cancer [1–3]. Although CTCs are extremely rare, their detection/quantification in physiological fluids represents a potential alternative to the actual invasive biopsies and subsequent proteomic and functional genetic analysis [4,5]. In fact, isolation of CTCs from peripheral blood, as a 'liquid biopsy', is expected to be able to complement conventional tissue biopsies of metastatic tumors for therapy guidance [1,6]. A particularly important aspect of a 'liquid biopsy' is that it is safe and can be performed frequently, because repeated invasive procedures may be responsible for limited sample accessibility [7]. Established techniques for CTC identification include labeling cells with tagged antibodies (immunocytometry) and subsequent examination by fluorescence analysis or detecting the expression of tumor markers by reverse-transcriptase polymerase chain reaction (RT-PCR)[8]. However, the required previous isolation of CTCs from the human fluids is limited to complex analytic approaches that often result in a low yield and purity [9,10].

Cancer cells overexpress specific proteins at their plasma membrane which are often used as targets in CTCs sensing methodologies using the information available for the different types of cancer cells [11]. An example of these target proteins is the Epithelial Cell Adhesion Molecule (EpCAM), a 30-40 kDa type I glycosylated membrane protein expressed at low levels in a variety of human epithelial tissues and overexpressed in most solid carcinomas [12]. Decades of studies have revealed the roles of EpCAM in tumorigenesis and it has been identified to be a cancer stem cell marker in a number of solid cancers, such as in colorectal adenocarcinomas, where it is found in more than 98% of them, and its expression is inversely related to the prognosis[13,14]. Another example of a tumor associated protein is the Carcinoembryonic antigen (CEA), a 180-200 kDa highly glycosylated cell surface glycoprotein which overexpression was originally thought to be specific for human colon adenocarcinomas. Nowadays it is known to be associated with other tumors, and the large variations of serum CEA levels and CEA expression by disseminated tumor cells have been strongly correlated with the tumor size, its state of differentiation, the degree of invasiveness and the extent of metastatic spread[14,15].

The objective of this work is to develop a rapid electrochemical biosensing strategy for CTCs quantification using antibody-functionalized gold nanoparticles (AuNPs) as labels and magnetic beads (MBs) as capture platforms in liquid suspensions. AuNPs have shown to be excellent labels in both optical (e.g. ELISA) and electrochemical (e.g. differential pulse voltammetric) detection of DNA[16] or proteins[17,18]. The use of the electrocatalytic properties of the AuNPs on hydrogen formation from hydrogen ions (Hydrogen Evolution Reaction, HER) also enables an enhanced quantification of nanoparticles[19] allowing their application in immnuoassays as explained in the previous chapter.

Since human fluid samples are complex and contain a variety of cells and metabolites, the fast detection of CTCs becomes quite a difficult task. To get through this obstacle, several attempts of filtration, pre-concentration or other purification steps are actually being reported by researchers that work in this field and each of them has advantages and drawbacks [22,23]. The only FDA (U.S. Food and Drug Administration) approved method for the detection of CTCs is the Cell Search System® that first enriches the tumor cells immunomagnetically by means of ferrofluidic nanoparticles conjugated to EpCAM and then, after immunomagnetic capture and enrichment, allows the identification and enumeration of CTCs using fluorescent staining [24,25]. When sample processing is complete, images are presented to the user in a gallery format for final cell classification. Because this is an expensive, time consuming and complex analysis, our objective is to design and evaluate an electrochemical detection system based on the electrocatalytic properties of the AuNPs, in combination with the use of superparamagnetic microparticles (MBs) modified with anti-EpCAM as a cell capture agent (Fig. 1a). The integration of both systems, the capture with MBs and the labeling with electrocatalytic AuNPs, should provide a selective and sensitive method for the detection and quantification of CTCs in liquid suspensions.

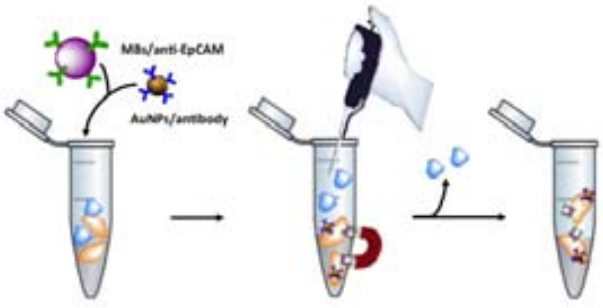

Figure 1a. Overall scheme of Caco2 cells capture by MBs-anti-EpCAM and simultaneous labeling with AuNPs/specific antibodies in the presence of control cells;

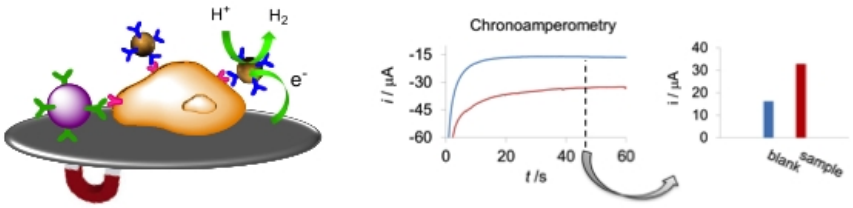

Figure 1b. Detection of labeled Caco2 cells through the Hydrogen Evolution Reaction (HER) electrocatalyzed by the AuNP labels. Right: Chronoamperograms registered in 1M HCl, during the HER applying a constant voltage of -1.0V, for AuNP labeled CaCo2 cells (3.5 x104 - red curve) and for the blank (PBS/BSA - blue curve). Right: Comparison of the corresponding analytical signals (absolute value of the current registered at 50 seconds).

The human colon adenocarcinoma cell line Caco2, was chosen as a model CTC. Similarly to other adenocarcinomas, colon adenocarcinoma cells, show a strong expression of EpCAM (close to 100%)[12] and for this reason this glycoprotein was used as the capture target. In relation to AuNPs labeling, we explored two different protein targets: EpCAM and CEA, both expressed by Caco2 cells. Two separate electrochemical detections were performed, each one using a different antibody conjugated to AuNPs, in order to choose the one that achieves a better electrochemical response in terms of both sensitivity and selectivity.

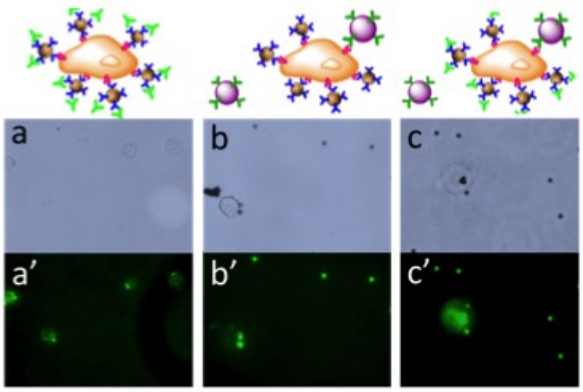

Figure 2. Figure 2 IFluorescence microscopy characterization. (a-c) Microscopy imaging of Caco2 cells in bright field (a, b, c), and fluorescence modes (a', b', c'). (a, a') Cells in suspension labeled with AuNPs/rabbit-anti-EpCAM and sequential labeling with FITC-conjugated secondary anti-rabbit antibody; (b, b') cells captured with MBs/mouse-anti-EpCAM and simultaneous labeling with AuNPs/rabbit-anti-EpCAM showing the autofluorescence of MBs; (c, c') cells in the same conditions as in b after sequential labeling with FITC-conjugated secondary anti-rabbit antibody.

Evaluation of the interaction between Caco2 cells and electrochemical labels

To assess the effectiveness of AuNPs/antibody-conjugate labels, their specific interaction with Caco2 cells in suspension was evaluated. With this aim, fluorescence microscopy imaging of cell samples before and after incubation with biofunctionalized AuNPs, using a fluorescent tagged secondary antibody, was performed. The free anti-EpCAM antibody proved to have high affinity for EpCAM at Caco2 surface (data not shown), but it was necessary to verify that after conjugation with AuNPs the antibody maintains its ability to recognize the target protein. The resulting fluorescence at the cell membrane (Fig. 2) confirmed the specific biorecognition of the Caco2 cells by the AuNPs/anti-EpCAM. This fact was also evidenced by flow cytometry analysis of the cell samples. Flow cytometry is well suited to check the affinity of different antibodies to several cell proteins and, by using the proper controls, it can also be used to quantify both labeled and unlabeled cells. Using the same protocol for sample preparation as for optical microscopy, Caco2 samples were analyzed (Fig. 3). When the cells were labeled with AuNPs/rabbit-anti-EpCAM-conjugate, followed by a fluorescent secondary anti-rabbit antibody, a strong increase in cell fluorescence was observed (Fig. 3a). Several controls were performed for both methods. Caco2 cells were incubated with rabbit-anti-EpCAM antibody both free and conjugated to AuNPs. Controls were also performed with AuNPs/anti-EpCAM without fluorescent-tagged secondary antibody (Supplementary Fig. 2a), and with AuNPs conjugated to another rabbit polyclonal anti-EpCAM antibody which proved to be non-specific to Caco2 cells (Supplementary Fig. 2b).

Optimization of Caco2 cells magnetic capture and labeling

For the magnetic capture of Caco2, we first used 4.5 μm MBs conjugated to a monoclonal anti-EpCAM antibody. Although 4.5 *μ*m MBs are generally used for cell applications, due to their large size and high magnetic mobility, our experiments with anti-EpCAM functionalized 4.5 *μ*m MBs resulted in discrepancies both in flow cytometry analysis and electrochemical detection. After MBs and AuNPs incubation, Caco2 cells seemed damaged and/or agglomerated when analyzed by fluorescence microscopy and flow cytometry (Supplementary Fig. 3 and 4). This damage may be due to the large size of these MBs, which promotes higher flow-induced shear stress during the cleaning steps performed with stirring[27,28] . Since CTCs are reported to be vulnerable cells which viability is easily compromised after capture[6], we tested smaller MBs (tosylactivated 2.8μm) that are recommended for extremely

fragile cells, due to their smaller size and lower magnetophoretic mobility, and can reduce the possibility of interference between the nearest particles[29]. These are uniform polystirene beads (with a magnetic core), coated with a polyurethane layer modified with sulphonyl ester groups, that can subsquently react covalently with proteins or other ligands containing amino or sulfhydryl groups. MBs were functionalized with a monoclonal anti-EpCAM antibody previously tested by flow cytometry analysis. The electrochemical measurements and the cytometry analyses were in agreement: these MBs can capture the cells without perceived damage (Fig. 3b and 3c) and allow for better electrochemical results.

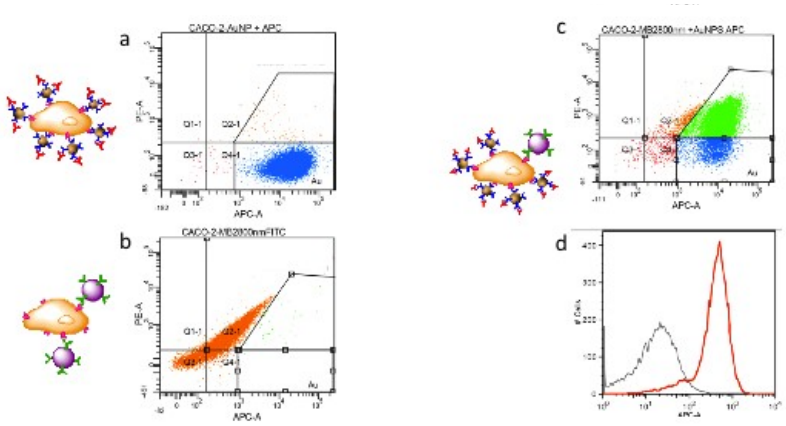

Figure 3. Figure 3 I Flow Cytometry analysis performed after 30 minute incubations, as described in the methods section. After appropriate forward and sideward scatter gating, the Caco2 cells were evaluated using PE-A and APC-A signals. (a) Representative dot plots of Caco2 cells labeled with AuNPs/anti-EpCAM ; (b) Caco2 cells captured by MBs/anti-EpCAM; (c) Caco2 cells captured with MBs/anti-EpCAM and simultaneously labeled with AuNPs/anti-EpCAM. (d) Representative histogram count of Caco2 cells captured with MBs/anti-EpCAM, unlabeled (black) vs. labeled (red) with AuNPs/anti-EpCAM using the APC-conjugated secondary antibody.

We also performed optimization of the ratio MBs/cell, as well as the cell incubation sequence with both MBs/anti-EpCAM and AuNPs/anti-EpCAM conjugates to improve the AuNPs electrochemical signal. The ratio between MB and AuNPs/anti-EpCAM used in the detection assay is very important, because MBs/anti-EpCAM quantity should be minimized to allow the maximum labeling by AuNPs/anti-EpCAM conjugate that will in turn give the detection signal. Regarding the incubation sequence with conjugates, if a separate incubation is performed using MBs/anti-EpCAM in the first place, the EpCAM at the cell surface could be “blocked” for the further labeling with AuNPs/anti-EpCAM, resulting in a loss of AuNPs electrochemical signal. In the case that a simultaneous incubation is performed, both MBs and AuNPs conjugates would compete for the same protein and consequently, the

aforementioned blocking effect could also occur. To test this, several ratios of MBs/AuNPs conjugates (1:1, 2:1, 4:1 and 14:1 MBs/cell), using two incubation protocols (MBs/anti-EpCAM and AuNPs/anti-EpCAM simultaneous and separate incubations) were evaluated. Flow cytometry results (Supplementary Fig. 5) showed that a high MB/cell ratio is associated not only to more cell damage/death (cells are exposed to a higher magnetic attraction) but also to a higher number of cells without the MBs/anti-EpCAM. Therefore, it seems that an excess of MBs/anti-EpCAM (14:1 MBs/cell) is not favorable to the detection, and the best results were achieved with a 2:1 MBs/cell ratio. It is also important to clarify that when MBs/anti-EpCAM were not used (only AuNPs/anti-EpCAM labeling) the flow cytometry analysis reported 98% of AuNPs/anti-EpCAM-labeled cells with a low value of dead cells. This result was obtained for cells incubated with a large excess of AuNPs/anti-EpCAM (3nM AuNPs) (Supplementary Fig. 6a), which leads to the conclusion that, contrary to MBs/anti-EpCAM, an excess of AuNPs/anti-EpCAM does not affect cell integrity, probably due to their smaller size. Finally, concerning the incubation sequence, we chose the simultaneous one as the optimal in order to obtain a fast capture/labeling of cells with both conjugates (Supplementary Fig. 6b). Moreover, when using the 2:1 MBs/cell ratio the flow cytometry analysis did not indicate major differences between the two tested incubations.

Evaluation of Caco2 cell capture and labeling in the presence of control cells

The accurate study of the Caco2 cell-biofunctionalized AuNP interaction is very important to elucidate the specifity and selectivity of the sensing system presented here. The use of scanning electron microscopy (SEM) is a well known characterization technique for cells with relative large dimensions. However, its application in the case of cells interaction with small nanometer sized materials in liquid suspension is not an easy task. Cells often lack the requirements of structure stability and electron conductivity necessary for high magnification SEM images, and it is usually necessary to cover all the sample with a nano/micro layer of conductive material. This metallization process will mask the small nanoparticles attached to the cell surface. Therefore, we adapted a SEM sample preparation protocol to fulfill two requirements: the cells should always be kept in suspension, so that the characterization is done in exactly the same conditions than the electrochemical detection, and no sample coating should be performed, to avoid the masking of AuNPs/anti-EpCAM that should be present at the cell surface. Accordingly, cell samples were kept in suspension while treated with glutaraldehyde fixative with subsequent dehydration solutions, and finally resuspended in

hexamethyldisilazane (HMDS) solution prior to the drop-deposition onto a silicon dioxide wafer. No metal-oxides were used and the critical-point drying procedure was not performed nor the final metallization step. HMDS is generally used in photolitography techniques, as an adhesion promoter between silicon dioxide films and the photoresist. However, in the present method, HMDS is used as a substitute of the critical-point, as it is reported to be a time-saving alternative without introducing additional artefacts in SEM images.[30,31] We processed samples in which Caco2 cells were incubated in the presence or absence of AuNPs/anti-EpCAM conjugate.

With the optimized SEM preparation protocol and the Field Emission-SEM (FE-SEM) precise technical settings, we obtained high quality images (Fig. 4a). At high magnification we could see the detail of the plasma membrane and using the Backscattered Electrons mode (BSE) we could discriminate the small AuNPs attached onto the Caco2 cell membrane through the immunoreaction (Fig. 4b). Since heavy elements backscatter electrons more strongly than light elements, they appear brighter in the obtained image, thus enhancing the contrast between objects of different chemical compositions. In addition, as we did not use metal-oxides during the fixation of cells, the only metal-origin element in the samples should be the gold from the AuNPs used as labels. When the same procedure was performed for monocytes (Fig. 4c **and d**), no AuNPs were observed, demonstrating the specificity of the AuNPs anti-EpCAM.

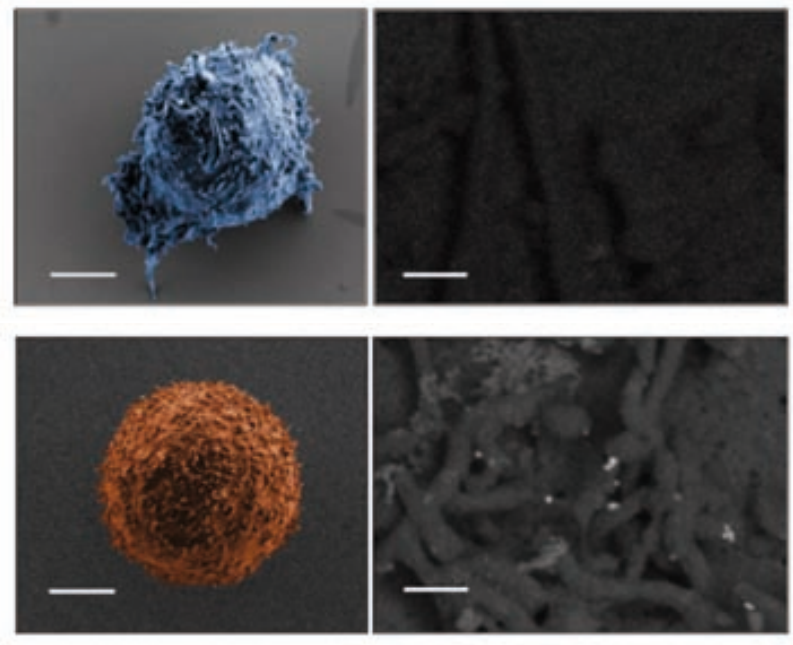

Figure4. Figure 4 | Scanning electron microscopy. (a) SEM image (false colored with Corel Paint Shop Pro) of Caco2 cell incubated with AuNPs/anti-EpCAM conjugates; (b) Higher magnification image, using backscattered electrons mode, showing

AuNPs distributed along the cell plasma membrane. (c) SEM image (false colored with Corel Paint Shop Pro) of control cell (THP-1); (d) Higher magnification image of THP-1 cell in backscattered electrons mode. Scale bars, 3 mm (a and c) and 200 nm (b-d).

We processed other samples in which Caco2 cells were mixed with the THP-1 control cells in a 70% Caco2 and 30% THP-1 proportion, and then incubated with MBs/anti-EpCAM with and without labeling of AuNPs/anti-EpCAM. As expected, no monocytes were found in the SEM sample (Fig. 5) since they were supposed to be removed during the magnetic separation steps. At higher magnification, using the BSE mode (Fig. 5c and d), the presence of AuNPs/anti-EpCAM dispersed onto the Caco2 surface could be observed. Several membrane protrusions were also observed in all the SEM images when MBs/anti-EpCAM were used as capture conjugates (Fig. 5b). These are finger like structures that epithelial cells can develop in cell-matrix adherent processes [32–34] and in which Ep-CAM can also be involved [34,35]. It is important to note that this protusions are enhanced when MBs are used (Supplementary Fig. 8), whereas in the samples of Caco2 and Caco2- labelled only with AuNPs/anti-EpCAM (Supplementary Fig. 7) the cell structure seems well confined. Although this evidence is not directly related to the assay performance, we believe these effects may be related to the different sizes of MBs and AuNPs, being MBs aproximately 1.4 x10^3 times larger.

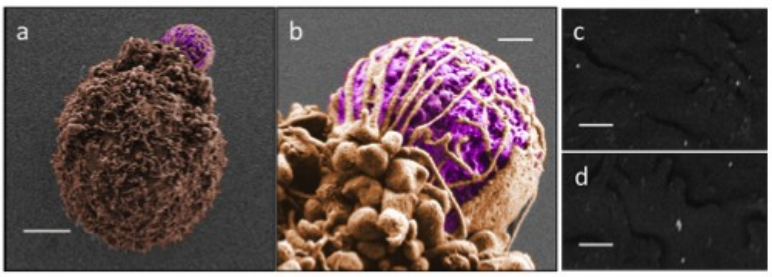

Figure 5. Figure 5 l Scanning electron microscopy. (a-d) Caco2 cells captured with MB/anti-EpCAM and simultaneously labeled with AuNPs/anti-EpCAM, in presence of THP-1 cells.(a, b) SEM images (false colored with Corel Paint Shop Pro) of a Caco2 cell captured by MBs/anti-EpCAM. (c, d) Higher magnification backscattered images of the Caco2 cell surface showing AuNPs distributed along the cell plasma membrane. Scale bars, 3 mm (a), 400 nm (b) and 200 nm (c, d).

Electrochemical detection of Caco2 cells

The full-optimized process was used for the electrochemical detection of Caco2 cells in presence of monocytes (THP-1), other circulating cells which could interfere in real blood samples. The use of the electrocatalytic properties of the AuNPs on hydrogen formation from hydrogen ions (HER) makes it possible to quantify the AuNPs and, in turn, to quantify the corresponding labelled cancer cells (through the proteins to which these are connected)[19]. Chronoamperometric plotting of the analytical signal is much simpler, from signal acquisition point of view, than the stripping analysis or differential pulse voltammetry described in previous works[16,17]. To evaluate the selectivity of the assays, Caco2 cells were mixed with the THP-1 control cells in different proportions, and then incubated with both MB/anti-EpCAM and AuNPs/anti-EpCAM in a one-step incubation. After magnetic separation and cleaning steps, the samples were analyzed following the electrocatalytic method explained. Samples with 100%, 70%, 50% and 20% of Caco2 cells (Fig. 6a) were tested (100% corresponds to 5 $x10^4$ cells), achieving a limit of detection (LOD) of 8.34 $x10^3$ Caco2 cells, with a correlation coefficient (R) of 0.91 and a linear range from 1 $x10^4$ to 5 $x10^4$ cells with Relative Standard Deviation (RSD) = 4.92% for 5 $x10^4$ cells. LOD was determined by extrapolating the concentration at blank signal plus 3 s.d. of the blank. The results proved that this method is selective for Caco2 cells. However, the achieved limit of detection is not enough to guarantee the application of the method. This is probably due to the aforementioned competition between antibody-modified MBs and AuNPs for the EpCAM protein. Furthermore, EpCAM is considered a general marker for a large variety of epithelial cells, so the selection of a more specific target was required to improve both the specificity and the sensitivity of the assay. Concretely, the CEA protein was chosen as it is reported to be strongly associated with the invasiveness of cancer cells, and it is known to be overexpressed by colon adenocarcinoma cells[14,15]. The AuNPs were biofunctionalized with a mouse anti-CEA and used as electrochemical labels. The incubation of Caco2 cells with the AuNPs/anti-CEA was done simultaneously with the capturing by MBs/anti-EpCAM followed by the electrocatalytic detection. The electrochemical analysis of Caco2 cells (**Fig. 6c**) resulted in a LOD of 1.6 $x10^2$ cells with R= 0.993, in a linear range from 1 $x10^3$ to 3.5 $x10^4$ cells. LOD was determined by extrapolating the concentration at blank signal plus 3 s.d. of the blank. The RSD = 5.6 % for 5 $x10^4$ cells, evidences a very good reproducibility of the results if we take into consideration that the number of nanoparticles attached to the cells due to the interaction between the antibody and CEA depends primarily on the number and distribution of the antigen molecule over the surface, which may vary from

cell to cell and from batch to batch[36]. The results obtained using AuNPs/anti-CEA as the detection labels were much better, in terms of LOD, than those with AuNPs/anti-EpCAM.

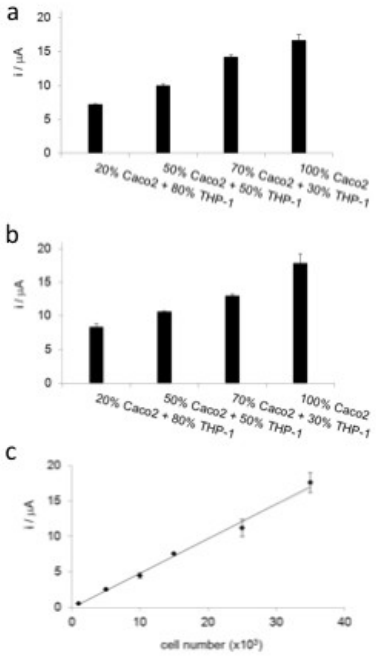

Figure 6.

When changing the AuNPs-conjugate antibody to anti-CEA the goal was to have better specificity in the detection without losing the sensitivity. Consequently, the AuNPs/anti-CEA was also tested for the electrochemical detection of Caco2 cells in the presence of THP-1 control cells (Fig. 6b). Caco2 cells were mixed with THP-1 in different proportions (100, 70, 50, 20% of Caco2 cells; 100% corresponds to 5 $x10^4$ cells) and then incubated with both MB/anti-EpCAM and AuNPs/anti-CEA in a one-step incubation. After magnetic separation and cleaning steps, samples were analysed by the same electrochemical procedure previously mentioned. The statistical analysis reported a LOD of 2.2 $x10^2$ Caco2 cells, with a correlation coefficient of 0.968 in a linear range from 1 $x10^4$ to 5 $x10^4$ cells with RSD = 6.3% for 5 $x10^4$ cells. This value is quite similar to that obtained in the absence of THP-1, evidencing the high selectivity obtained thanks to the CEA recognition together with the magnetic separation/purification.

Conclusions

The use of nanoparticles as labeling agents in immunoassays results in an improvement of sensitivity over the traditional enzyme or dye based assays[37]. Nanometer-sized particles such as metal and iron-oxide nanoparticles display optical, electrochemical, magnetic or structural properties that the materials in molecular or bulk state do not have. When these particles are conjugated with specific antibodies they can target tumor-expressed proteins with high affinity and specificity. For example, AuNPs of 20 nm diameter have large surface areas that promote a good conjugation to antibodies and provide a fast interaction with nanometer sized antigens at the cell surface. The labeled tumor cells can then be detected and quantified through the appropriate methods for AuNPs detection, which can be optical, electric or electrochemical. From the several methods available, the electrochemical routes hold several advantages related to the gold nanoparticles specific characteristics, such as their own redox properties and excellent electroactivity towards other reactions. Exploiting the latest, advantages can be taken from the electrocatalytic effect that AuNPs have over several reactions, which exclude the need for contact between the electrode surface and the nanoparticle[37], and is suitable when detecting particles used as labels for relatively large dimensions such as the tumor cells.

The electrochemical detection of metal nanoparticles in general, and AuNPs in particular, can be accomplished using simple and portable apparatus that do not require large volume samples, time-consuming steps or high skilled users if thinking on point of care applications. After optimization, the detection can be seen as a semi-automated technique that could be integrated in small lab-on-a-chip platforms with the additional improvements related to the required volumes and time of analysis inherent to these systems[38].

The developed CTC detection technology includes several parameter optimizations as for example the size of the magnetic particles, their functionalization with antibodies, or the specificity of the antibody used to functionalize the AuNPs labels, including other protocol related parameters (e.g. incubation times) and the respective parameters related to the characterization by microscopy (optical and electronic) and flow cytometry.

Using the technical advances in electron microscopy to better characterize the cell-nano and -microparticle interactions, we processed samples in which Caco2 cells were mixed with THP-1 control cells (other circulating cells which could interfere in real blood samples) and were then incubated with AuNPs/anti-EpCAM and MB/anti-EpCAM conjugates. Using the Backscattered Electrons mode (BSE) mode we confirmed the presence of

AuNPs/anti-EpCAM all around the Caco2 cell surface, whereas no monocytes were present in the sample. These observations proved that the capture and labeling with anti-EpCAM-functionalized particles is selective for Caco2 cells and thus a specific detection of target cells in the presence of other circulating cells can be achieved.

The full-optimized process was used for the electrochemical detection of Caco2 cells in the presence of THP-1. Although the results proved that the method was selective for Caco2 cells, the achieved limit of detection was not enough to guarantee the application of the method. The fact that the capture and detection labels were oriented to the same target protein, could hinder our detection due to the possible blocking effect that MBs could exert over the small AuNPs. For this reason, we believed that the detection could be improved using a different antibody in the detection conjugated label, specific to other protein in the cell plasma membrane. To pursuit this goal, other antigens/proteins that are also present at Caco2 cells surface, and assumed to be relevant in the study/quantification of CTCs, were also considered. Since EpCAM is a general marker for a large variety of epithelial cells, another more specific detection using CEA as the target for the AuNPs-conjugate label was performed. We obtained better LOD values, in the absence and presence of other control cells, that are nearer the desirable for a valuable CTCs detection. One of the possible explanations for the better results achieved, is the fact that CEA is a much bigger protein than EpCAM (180kDa vs. 40kDa). Even though both CEA and EpCAM are transmembrane proteins, the first one presents a larger extracelular domain, more similar in size to the antibody (150kDa). Even though the anti-CEA Fab fragment size, which is mainly responsible for the antigen recognition, has an equivalent size to the Fab' from anti-EpCAM, the possible steric effects related to the antigen size[39,40] can help to elucidate why a better signal is obtained when using CEA as target at the cell membrane. The electrochemical detection and the characterization results demonstrate that this method is selective for Caco2 cells, and that the electrochemical signal is not affected by the presence of other circulating cells. So we conclude that the achieved detection through the AuNPs/anti-CEA is more selective for the target tumor cells and can exclude the false positive results related to the EpCAM marker.

We envision the application of the presented method to the quantification of CTCs in real human samples where besides cells (cancerous and non-cancerous ones), also proteins and metabolites are present. Although the anti-CEA antibody is not specific for CTCs (in fact, it can also recognize the CEA that is frequently found in the serum of patients with several types of

cancer), its combination with MBs/anti-EpCAM provides a selective capture and labeling of cells that express both antigens. This principle can also be adapted for other cancer cells by redesigning both micro- and nano-conjugates with the appropriate antibodies. Furthermore, the potential incorporation of the presented method for isolation, labeling and sensitive electrochemical detection/quantification of Caco2 cells in lab-on-a-chip systems[3,41] could contribute to the desired standardization of CTCs detection technologies.

References

1. Pantel, K. & Alix-Panabières, C. Circulating tumour cells in cancer patients: challenges and perspectives. *Trends in molecular medicine* **16**, 398-406 (2010).
2. Bednarz-Knoll, N., Alix-Panabières, C. & Pantel, K. Clinical relevance and biology of circulating tumor cells. *Breast cancer research : BCR* **13**, 228 (2011).
3. Nagrath, S. *et al.* Isolation of rare circulating tumour cells in cancer patients by microchip technology. *Nature* **450**, 1235-9 (2007).
4. Taback, B. *et al.* Detection of occult metastatic breast cancer cells in blood by a multimolecular marker assay: correlation with clinical stage of disease. *Cancer research* **61**, 8845-50 (2001).
5. Wang, S. *et al.* Three-dimensional nanostructured substrates toward efficient capture of circulating tumor cells. *Angewandte Chemie (International ed. in English)* **48**, 8970-3 (2009).
6. den Toonder, J. Circulating tumor cells: the Grand Challenge. *Lab on a chip* **11**, 375-7 (2011).
7. Allard, W.J. *et al.* Tumor cells circulate in the peripheral blood of all major carcinomas but not in healthy subjects or patients with nonmalignant diseases. *Clinical cancer research : an official journal of the American Association for Cancer Research* **10**, 6897-904 (2004).
8. Li, K., Zhan, R., Feng, S.-S. & Liu, B. Conjugated polymer loaded nanospheres with surface functionalization for simultaneous discrimination of different live cancer cells under single wavelength excitation. *Analytical Chemistry* **83**, 2125-2132 (2011).
9. Zieglschmid, V., Hollmann, C. & Böcher, O. Detection of disseminated tumor cells in peripheral blood. *Critical reviews in clinical laboratory sciences* **42**, 155-96 (2005).
10. Nagrath, S. *et al.* Isolation of rare circulating tumour cells in cancer patients by microchip technology. *Nature* **450**, 1235-9 (2007).
11. Perfézou, M., Turner, A. & Merkoçi, A. Cancer detection using nanoparticle-based sensors. *Chemical Society reviews* (2011).doi:10.1039/c1cs15134g

12. Went, P.T.H. *et al.* Frequent EpCam Protein Expression in Human Carcinomas. *Human Pathology* **35**, 122-128 (2004).

13. Patriarca, C., Macchi, R.M., Marschner, A.K. & Mellstedt, H. Epithelial cell adhesion molecule expression (CD326) in cancer: A short review. *Cancer treatment reviews* (2011).doi:10.1016/j.ctrv.2011.04.002

14. Belov, L., Zhou, J. & Christopherson, R.I. *Cell surface markers in colorectal cancer prognosis. International journal of molecular sciences* **12**, 78-113 (2010).

15. Shi, Z.R., Tsao, D. & Kim, Y.S. Subcellular Distribution , Synthesis , and Release of Carcinoembryonic Antigen in Cultured Human Colon Adenocarcinoma Cell Lines Subcellular Distribution , Synthesis , and Release of Carcinoembryonic. *Cancer Research* **43**, 4045-4049 (1983).

16. Pumera, M. *et al.* Magnetically trigged direct electrochemical detection of DNA hybridization using Au67 quantum dot as electrical tracer. *Langmuir : the ACS journal of surfaces and colloids* **21**, 9625-9 (2005).

17. Ambrosi, A. *et al.* Double-codified gold nanolabels for enhanced immunoanalysis. *Analytical chemistry* **79**, 5232-40 (2007).

18. Ambrosi, A., Airò, F. & Merkoçi, A. Enhanced gold nanoparticle based ELISA for a breast cancer biomarker. *Analytical chemistry* **82**, 1151-6 (2010).

19. Maltez-da Costa, M., De La Escosura-Muñiz, A. & Merkoçi, A., Electrochemical quantification of gold nanoparticles based on their catalytic properties toward hydrogen formation: Application in magnetoimmunoassays. *Electrochemistry Communications* **12**, 1501-1504 (2010).

20. De La Escosura-Muñiz, A. *et al.* Gold nanoparticle-based electrochemical magnetoimmunosensor for rapid detection of anti-hepatitis B virus antibodies in human serum. *Biosensors and Bioelectronics* **26**, 1710-1714 (2010).

21. De La Escosura-Muñiz, A. *et al.* Rapid identification and quantification of tumor cells using an electrocatalytic method based on gold nanoparticles. *Analytical Chemistry* **81**, 10268-10274 (2009).

22. Sergeant, G., Penninckx, F. & Topal, B. Quantitative RT-PCR detection of colorectal tumor cells in peripheral blood--a systematic review. *The Journal of surgical research* **150**, 144-52 (2008).

23. Riethdorf, S., Wikman, H. & Pantel, K. Review: Biological relevance of disseminated tumor cells in cancer patients. *International journal of cancer. Journal international du cancer* **123**, 1991-2006 (2008).

24. Cohen, S.J. *et al.* Isolation and characterization of circulating tumor cells in patients with metastatic colorectal cancer. *Clinical colorectal cancer* **6**, 125-32 (2006).

25. Riethdorf, S. *et al.* Detection of circulating tumor cells in peripheral blood of patients with metastatic breast cancer: a validation study of the CellSearch system. *Clinical cancer research : an official journal of the American Association for Cancer Research* **13**, 920-8 (2007).

26. Turkevich, J., Stevenson, P.C. & Hillier, J. The formation of colloidal gold. **57**, 670-673 (1953).

27. Zborowski, M. & Chalmers, J.J. Magnetic Cell Separation. *Laboratory Techniques in Biochemistry and Molecular Biology* (2008).

28. Mccloskey, K.E., Chalmers, J.J. & Zborowski, M. Magnetic Cell Separation : Characterization of Magnetophoretic Mobility to enrich or deplete cells of interest from a heterogeneous. *Society* **75**, 6868-6874 (2003).

29. Varadan, V., Chen, L. & Xie, J. *Nanomedicine : design and applications of magnetic nanomaterials, nanosensors and nanosystems*. *The FASEB Journal* (Wiley: 2008).doi:10.1002/9780470715611

30. Nation, L. A new method using hexamethyldisilazane for preparation of soft insect tissues for scanning electron microscopy. *Stain Technology* **58**, 347-351 (1983).

31. Bray, D.F., Bagu, J. & Koegler, P. Comparison of hexamethyldisilazane (HMDS), Peldri II, and critical-point drying methods for scanning electron microscopy of biological specimens. *Microscopy Research and Technique* **26**, 489-495 (1993).

32. Guillemot, J.C. *et al.* Ep-CAM transfection in thymic epithelial cell lines triggers the formation of dynamic actin-rich protrusions involved in the organization of epithelial cell layers. *Histochemistry and cell biology* **116**, 371-8 (2001).

33. Gupton, S.L. & Gertler, F.B. Filopodia: The Fingers That Do the Walking. *Science Signaling* re 5 (2007).doi:10.1126/stke.4002007re5

34. Trzpis, M., McLaughlin, P.M.J., de Leij, L.M.F.H. & Harmsen, M.C. Epithelial cell adhesion molecule: more than a carcinoma marker and adhesion molecule. *The American journal of pathology* **171**, 386-95 (2007).

35. Baeuerle, P. a & Gires, O. EpCAM (CD326) finding its role in cancer. *British journal of cancer* **96**, 417-23 (2007).

36. Loureiro, J. *et al.* Magnetoresistive chip cytometer. *Lab on a chip* **11**, 2255-61 (2011).

37. De La Escosura-Muñiz, A. & Merkoçi, A. Electrochemical detection of proteins using nanoparticles: applications to diagnostics. *Expert Opinion on Medical Diagnostics* **4**, 21-37 (2010).

38. Whitesides, G.M. The origins and the future of microfluidics. *Nature* **442**, 368-73 (2006).

39. Hlavacek, W.S., Posner, R.G. & Perelson, a S. Steric effects on multivalent ligand-receptor binding: exclusion of ligand sites by bound cell surface receptors. *Biophysical journal* **76**, 3031-43 (1999).

40. Bongini, L. *et al.* A dynamical study of antibody-antigen encounter reactions. *Physical biology* **4**, 172-80 (2007).

41. El-Ali, J., Sorger, P.K. & Jensen, K.F. Cells on chips. *Nature* **442**, 403-11 (2006)

Chapter 5

Additional works

5.1 Carbon nanotube based platform for electrochemical detection of thrombin

5.2. Nanoparticle-induced catalysis for electrochemical DNA biosensors

5.1. Carbon nanotube based platform for electrochemical detection of thrombin.

A label-free bioelectronic detection of aptamer–thrombin interaction based on electrochemical impedance spectrometry (EIS) technique was reported as the result of this work. Multiwalled carbon nanotubes (MWCNTs) were used as modifiers of screen-printed carbon electrotransducers (SPCEs), showing improved characteris- tics compared to the bare SPCEs. 5′ amino linked aptamer sequence was immobilized onto the modified SPCEs and then the binding of thrombin to aptamer sequence was monitored by EIS transduction of the Rct in the presence of 5 mM $[Fe(CN)6]^{3-/4-}$, obtaining a detection limit of 105 pM. This study represents an alternative electrochemical biosensor for the detection of proteins with interest for future applications.

Aptamers hold great promise for rapid and sensitive protein detections and for developing protein arrays (Mukhopadhyay, 2005). These synthetic nucleic acid sequences act as antibodies in binding proteins owing to their relative ease of isolation and modification, holding a high affinity and high stability (Jayesna, 1999; Hansen et al., 2006).

In the last years, there has been a great interest for developing aptasensors. Different transduction techniques such as optical (McCauley et al., 2003; Zhang et al., 2009; Pavlov et al., 2005), atomic force microscopic (Basnar et al., 2006), electrochemical (Radi et al., 2005; Zayats et al., 2006; Suprun et al., 2008) and piezo- electrical (Pavlov et al., 2004) have been reported. Aptamer based biosensors have a great promise in protein biosensing due to their high sensitivity, selectivity, simple instrumentation, portability and cost effectiveness (Minunni et al., 2005; Baker et al., 2006).

It is well known that the sequence-specific single-stranded DNA oligonucleotide 5′ -GGTTGGTGTGGTTGG-3′ (thrombin aptamer) acts as thrombin inhibitor. This thrombin aptamer binds to the anion-binding exo-site and inhibits thrombin ' s function by competing with exo-site binding substrates fibrinogen and the platelet thrombin receptor (Paborsky et al., 1993). This highly specific aptamer/thrombin binding interaction has been extensively approached to develop different biosensors for thrombin, as summarized in Table S1 at the supplementary material. Furthermore, the selectivity of thrombin aptasensors has been demonstrated to be excellent

against possible interfering substances such as human serum albumin (HSA) or lysozymes (Hu et al., 2009; Ding et al., 2010) present in human serum.

In recent studies, electrochemical impedance spectrometric transduction of aptamer based protein analysis has shown a great prospect for label-free detections (Bogomolava et al., 2009). Electrochemical impedance spectroscopy (EIS) has been proven as one of the most powerful analytical tools for diagnostic analysis based on interfacial investigation capability. EIS measures the response of an electrochemical system to an applied oscillating potential as 59 a function of the frequency. Impedimetric techniques have been developed to characterize the fabricated biosensors and to monitor the catalytic reactions of biomolecules such as enzymes, proteins, nucleic acids, whole cells, antibodies (Steichen et al., 2007; Steichen and Herman, 2005).

Effect of the MWCNTs on the impedimetric signal

A label-free Impedimetric aptasensor system has been developed for the direct detection of human anti-thrombin as model protein, using MWCNT modified SCPE as electrochemical transducers. 5′ amino linked aptamer sequence is immobilized onto the MWCNT modified SPCE surface via the carbodiimide chemistry and finally the thrombin detection was accomplished by EIS transduction of aptamer–protein interaction. A general scheme of the experimental procedure is shown in Fig. 1A.

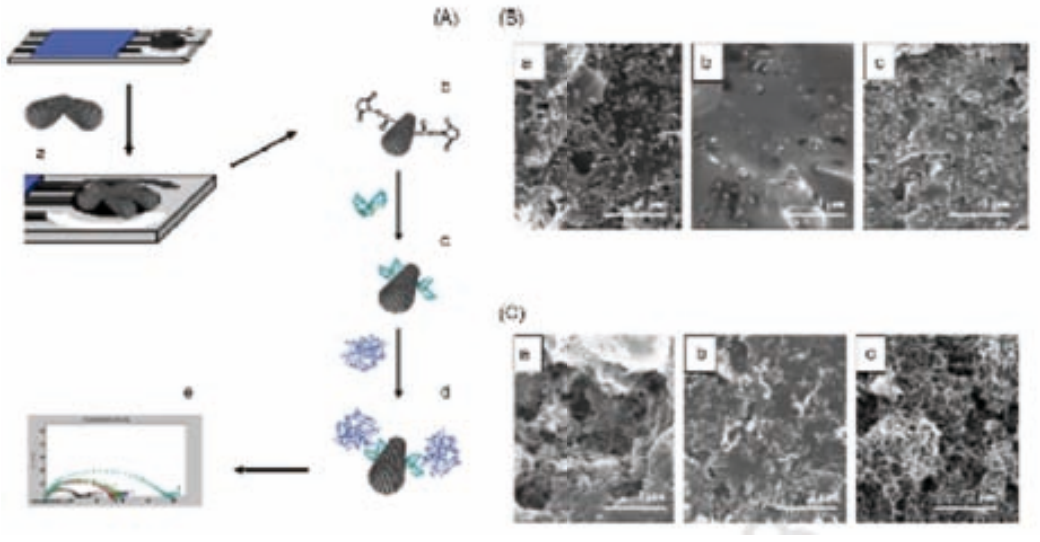

Fig. 1. (A) Schematic representation of the experimental procedure followed for the obtaining of analytical signal: (a) MWCNTs modification; (b) surface modification with covalent agents; (c) aptamer binding; (d) anti-thrombin interaction; (e) EIS detection. (B) SEM images of the working surface area of bare SPCES after electrochemical pretreatment (a), after aptamer immobilization (b) and after its interaction with thrombin (c). (C) SEM images of the working surface of MWCNT modified SPCEs

after the same modifications detailed in (B).

MWCNTs are used as modifiers of the SPCE electrotransducer surface because of their notable charge-transfer capability between heterogeneous phases. Furthermore, they modify the electrode surface providing higher rugosity with an increased active surface to further aptamer immobilization. In addition to this, aptamers can self assemble in carbon nanotubes by stacking interactions between the nucleic acid bases and the carbon nanotube walls (Zelada-Guillén et al., 2009) or they can be anchored to the carboxylic groups of oxidized nanotubes by chemical reactions. The changes in the morphology of the working electrode surface of the SPCE after the CNTs and aptamers immobilizations are evidenced in the SEM images shown in Fig. 1B, C. Furthermore by applying an electrochemical pretreatment in order to oxidize the MWCNTs carboxylic groups are generated. These are necessary for the further aptamer immobilization through the carbodiimide interaction and represent another advantage of MWCNTs. In Fig. S3 (see supplementary material) are summarized the analytical signals obtained for bare SPCEs electrodes after the sequential biomodifications (without aptamer, with aptamer and with aptamer + thrombin) (a) and also the effect of the previous SPCEs modification with MWCNTs electrochemically pretreated (b) and non pretreated (c). As it was expected, the impedimetric signal increases when increasing the SPCEs modification and this effect is enhanced when electrochemically pretreated MWCNTs are previously immobilized onto the SPCE surface.

The selectivity of the sensor was tested doing different reference assays, using tyrosinase as negative control. The effect of the direct adsorption of both thrombin and tyrosinase on the MWCNT modified SPCE was also evaluated. A significant increase in the Rct values was observed from both proteins due to bounding at the sensing surface via carbodiimide chemistry, being this increase of the same magnitude in both cases. This assay demonstrates that the direct adsorption of both proteins on the MWCNTs surface takes place in a similar magnitude, so further differences in the aptamer-based signals will be due to the specific interaction and not to non-specific adsorptions. After that, the aptasensor was evaluated. When only the aptamer is immobilized onto the surface of the MWCNTs modified SPCE, an increase in the Rct values is also observed, considered as the reference value. In addition, if the specific reaction with the anti-thrombin is performed, a high increase (of about 15 kOhm) in the Rct value is registered. However, when the assay is carried out with the tyrosinase, no changes are observed from the reference value, demonstrating the selectivity of the assay.

The effect of anti-trombin concentration on the analytical signal (Rct) for the thrombin sensitive detection was evaluated. The resulting limit of detection was 105pM, with a reproducibility (RSD) of 7.5% and a good linear correlation factor (0.99).

Conclusions

An impedimetric aptasensor for direct detection of human alpha thrombin at multiwalled carbon nanotube modified enhanced surfaces is developed. The selectivity of aptasensor was evaluated by using the EIS response differences between aptamer–thrombin and aptamer–tyrosinase interaction. The thrombin detection limit of 105 pM shows that the designed aptasensor is capable to perform a label-free and sensitive detection. Considering also advantages related to low-cost, fast and reliable electrochemical detection mode applied in this methodology different other aptamer sequences for other proteins are expected to be used in the future. The extension and application of the developed technique to other analytes and fields should be a mater of further investigations related also to a better understanding and improvements of the aptamer immobilization quality onto the carbon nanotube modified electrodes.

5.2. Nanoparticle-induced catalysis for electrochemical DNA biosensors

The full chapter is shown in the chapter 7, Publication 4. This book chapter was written due to the editor, Prof. Mehmet Ozsoz, invitation.

In this chapter the use of nanoparticles (NPs) in catalytic electrochemical analysis of DNA as a new detection strategy reported in recent years is revised. The subjects covered here include labelling with nanoparticles and its subsequent signal enhancement employed for DNA hybridization detection. Direct sensing of nanoparticle labels as well as indirect detection routes through electrochemical sensing of label-catalyzed reactions has been reported. Nanofabrication of platforms used for the detection of DNA through electrochemical signal amplification were be also revised. Some recent examples of interesting nanoparticle induced catalytic methodologies applied for proteins detection using electrochemical biosensors are also given because of their potential interest in future applications in DNA detection.

The main conclusions obtained are as follows.

The induced catalysis by NPs is showing special interest in the DNA biosensing technology. The application of NPs as catalysts in DNA detection systems is related to the decrease of overpotentials of many important redox species including also the catalysed reduction of other metallic ions used in labelling based hybridization sensing. Although the most exploited materials in catalysis are the metals from platinum group, with the introduction of nanotechnology and the increasing interest for biosensing applications, gold nanoparticles, due to their facile conjugation with biological molecules, besides other advantages, are showing to be the most used. Their applications as either electrocatalytic labels or modifiers of DNA related transducers are bringing important advantages in terms of sensitivity and detection limits in addition to other advantages.

AgNPs are not so commonly used as AuNPs but nevertheless their catalytic properties in electrochemical detection have also been exploited. For instance they were reported as promoters for electron transfer between the graphite electrode and hemoglobin in a NO sensor system where they also act as a base to attach the hemoglobin onto a pyrolytic graphite electrode while preserving the hemoglobin natural conformation and therefore its reactivity.[46] With respect to the application of silver catalytic properties on DNA

hybridization detection, the published works refer mostly its use in combination with AuNPs by means of chemical or electrochemical silver deposition onto them. [29]

The catalytic properties of NPs used in protein detection can also be extended to DNA analysis. For example the selective electrocatalytic reduction of silver ions onto the surface of AuNP reported by our group and applied for proteins detection can be extended to DNA analysis too. [47] The hydrogen catalysis reaction induced by AuNPs [48] and applied even for cancer cells detection [20] is expected to bring advantages for DNA detection as well.

The reported studies suggest that the use of NPs as catalysts in electroanalysis in general and particularly in DNA sensing is not confined to metal NPs only. The conjugation of NPs with electrochemical sensing systems promises large evolution in actual electroanalysis methods and is expected to bring more advantages in DNA sensing overall in the development of free PCR DNA detection besides other applications that may include microfluidics and lateral flow detection devices. Their successful application in DNA detection in real samples would require a significant improvement of cost-efficiency of NP based detection system in general and those based on NP induced electrocatalysis particularly.

Chapter 6

General Conclusions and Future Perspectives

The main objective of this thesis is to develop novel and improved electrochemical sensing systems for biomarker detection, exploiting the electrocatalytic effects of nanomaterials in general and nanoparticles particularly.

The conclusions can be detailed as follows:

Synthesis and characterization of gold nanoparticles.

Synthesis of gold nanoparticles, using a bottom-up approach, to obtain stable colloidal suspensions. Characterization of the synthetized nanoparticles by transmission electronic microscopy (TEM), scanning electronic microscopy (SEM), UV-Vis absorption spectroscopy as well as electrochemical methods so as to identify the applications in electrochemical sensing and biosensing. Alternative characterization of nanoparticles by zeta-potential determination, and ICP-MS were also employed.

Biofunctionalization of gold nanoparticles.

Functionalization of gold nanoparticles with biomolecules, like antibodies or other proteins, to obtain nano-bioconjugates capable of being used as labels in the electrochemical detection of proteins and cells, with interest in clinical diagnostics. Evaluation of the biofunctionalization of nanoparticles in respect to their stability and proper recognition of the target biomolecule, using

Development of electrochemical immunoassays using gold nano-bioconjugates as labels, and magnetic microparticles as immobilization surfaces.

Utilization of magnetic-microparticles suspensions as immobilization surfaces in a sandwich-like immunoassay with gold nanoparticle bioconjugates as electrochemical labels. Functionalization of the microparticles with the protein used as capture agent, and application of the obtained conjugate to the immunoassay improving the incubation and cleaning steps.

Evaluation of electrocatalytic effect of gold nanoparticles in other reactions with interest in electrochemical sensing applications

Evaluation the silver electrodeposition over gold nanoparticle bioconjugates used as detection labels in a magnetoimmunoassay. Evaluate the improvement of this method in the detection of a model protein.

Evaluation the electrocatalytic effect of gold nanoparticles in the hydrogen evolution reaction (HER) and use it to quantify gold nanoparticles. Apply the nanoparticle quantification method to a magnetoimmunoassay were gold nanoparticle bioconjugates are used as detection labels for a model protein.

Application of the gold nanoparticle quantification, based on HER electrocatalysis, to a magnetoimmunoassay, to detect the presence of anti-Hepatitis B antibodies in the blood-serum of patients and verify their immunization against Hepatitis B virus.

6. **Development electrochemical cell detection assays using gold nano-bioconjugates as labels**

Study the application of the gold nanoparticle quantification, based on HER electrocatalysis, to a cancer cell detection assay in order to obtain a rapid method for quantification of cancer cells grown onto the carbon electrode surface.

Evaluate the application of the gold nanoparticle quantification, based on HER electrocatalysis, to detect circulating tumor cells (CTC), using adenocarcinoma cells in suspension as a model target.

Study the use of magnetic-microparticles suspensions, functionalized with specific antibodies, as immobilization surfaces for the cell capture. Use gold nanoparticle bioconjugates as electrochemical labels and apply the gold nanoparticle quantification, based on HER electrocatalysis, to

evaluate the CTCs detection Evaluate the improvement of this method in the detection of adenocarcinoma cells in suspension.

The catalytic ability of gold nanoparticles (AuNPs) toward the electrocatyltic deposition of silver, and to the formation of H2 in the electrocatalyzed Hydrogen Evolution Reaction (HER) was thoroughly studied, using screen-printed carbon electrodes (SPCEs) as electrotransducers. The AuNPs provide free electroactive sites to the protons present in the acidic medium, that are catalytically reduced to hydrogen by applying an adequate potential, with a resulting increment in the reaction rate of the HER measured here by the generated catalytic current. This catalytic current allows for the quantification of AuNPs.

This electrocatalytic methods were applied for the first time, in the detection of AuNPs as labels in a magnetoimmunosandwich assay using SPCEs as electrotransducers, obtaining a sensitive detection system.

Future perspectives

Given the increased use of various metallic nanoparticles, we envisage possible further applications of these smart nanobiocatalytic particles for other diagnostic purposes. The simultaneous detection of several kinds of cells (e.g. to perform blood tests, detection of inflammatory or tumoral cells in biopsies or fluids) could be carried out, including multiplexed screening of cells, proteins and even DNA.

The conjugation of NPs with electrochemical sensing systems promises large evolution in actual electroanalysis methods and is expected to bring more advances in the biomarker detection for diagnostics.

However, even though some of the developed electrocatalytic nanoparticle based sensing systems have shown high sensitivity and selectivity, their implementation in clinical analysis still needs a rigorous testing and control period so as to really evaluate these advantages in comparison to classical assays in terms of reproducibility, stability and cost while being applied for real sample analysis. Further developments including the development of simple electrochemical devices (i.e. pocket size such as glucosimeter) or fluidic integrated devices are necessary for future entrance in real sample diagnostics in terms of point-of-care biosensors.

Chapter 7

Publications

7.1. Publications accepted by the UAB PhD commission

Publication 1. "Electrochemical quantification of gold nanoparticles based on their catalytic properties toward hydrogen formation: application in magneto immunoassays" M. Maltez-da Costa, A. de la Escosura-Muñiz, A. Merkoçi *Electrochemistry Communications* **2010**, 12, 1501-1504

Publication 2. "Gold nanoparticle-based electrochemical magneto-immunosensor for rapid detection of anti-hepatitis B virus antibodies in human serum" A. de la Escosura-Muñiz, M. Maltez-da Costa, C. Sánchez-Espinel, B. Díaz-Freitas, J. Fernández-Suarez, A. González-Fernández, A. Merkoçi, *Biosensors and Bioelectronics* **2010**, 26, 1710-1714.

Publication 3. "Nanoparticle-induced catalysis for electrochemical DNA biosensors" book chapter from "Electrochemical DNA Biosensors" M. Maltez-da Costa, A. de la Escosura-Muñiz, A. Merkoçi, edited by Mehmet Ozsoz (Pan Stanford Publishing, i*n press*, **2012**)

Publication 4. "Aptamers based electrochemical biosensor for protein detection using carbon nanotubes platforms" P. Kara, A. de la Escosura-Muñiz, M. Maltez-da Costa, M. Guix, M. Ozsoz, A. Merkoçi, *Biosensors and Bioelectronics*, **2010**, 26, 1715-1718.

Electrochemical quantification of gold nanoparticles based on their catalytic properties toward hydrogen formation: Application in magnetoimmunoassays

M. Maltez-da Costa, A. Escosura Muñiz, A. Merkoçi

Electrochemistry Communications

2010, 12, 1501-1504

Electrochemistry Communications 12 (2010) 1501–1504

Contents lists available at ScienceDirect

Electrochemistry Communications

journal homepage: www.elsevier.com/locate/elecom

Electrochemical quantification of gold nanoparticles based on their catalytic properties toward hydrogen formation: Application in magnetoimmunoassays

Marisa Maltez-da Costa [a], Alfredo de la Escosura-Muñiz [a,b], Arben Merkoçi [a,c,*]

[a] Nanobioelectronics & Biosensors Group, Institut Català de Nanotecnologia, CIN2 (ICN-CSIC), Campus UAB, Barcelona, Spain
[b] Instituto de Nanociencia de Aragón, Universidad de Zaragoza, Zaragoza, Spain
[c] ICREA, Barcelona, Spain

ARTICLE INFO

Article history:
Received 4 August 2010
Received in revised form 17 August 2010
Accepted 17 August 2010
Available online 25 August 2010

Keywords:
Gold nanoparticles
Electrocatalytic hydrogen formation
Screen-printed carbon electrodes
Chronoamperometry
Magnetoimmunoassay
Human IgG

ABSTRACT

The catalytic ability of gold nanoparticles (AuNPs) toward the formation of H_2 in the electrocatalyzed Hydrogen Evolution Reaction (HER) is thoroughly studied, using screen-printed carbon electrodes (SPCEs) as electrotransducers. The AuNPs on the surface of the SPCE, provide free electroactive sites to the protons present in the acidic medium that are catalytically reduced to hydrogen by applying an adequate potential, with a resulting increment in the reaction rate of the HER measured here by the generated catalytic current. This catalytic current is related with the concentration of AuNPs in the sample and allows their quantification. Finally, this electrocatalytic method is applied for the first time, in the detection of AuNPs as labels in a magnetoimmunosandwich assay using SPCEs as electrotransducers, allowing the determination of human IgG at levels of 1 ng/mL.

1. Introduction

In the last decade metal nanoparticles have been extensively investigated with the aim to enhance the sensitivity of detection techniques and sensing platforms. [1] Nanoparticles in general have special surface characteristics for their use in catalytic processes, [2,3] mainly due to the proportion of atoms at the surface of small nanoparticles that can be much higher than in the bulk state and results in a high surface to volume ratio. Interesting works were made with platinum nanoparticles (PtNPs) functionalized with nucleic acids that act as electrocatalytic labels for the amplified electrochemical detection of DNA hybridization and aptamer/protein recognition that resulted in sensitivity limits of 10 pM, in DNA detection, and 1 nM in the aptamer/thrombin detection system. [4]

In the wide range of nanomaterials, gold nanoparticles (AuNPs) grab a lot of attention once they have been applied in innumerous studies. [5–7] Bulk gold is considered an inert material towards redox processes [8] due to the repulsion between the filled d-states of gold and molecular orbitals of molecules like O_2 or H_2, but small AuNPs show a different behaviour [9,10] since contain a large number of coordinative unsaturated atoms in edge positions. The quantum effects related with shape and size of AuNPs originated by d band electrons of the surface which are shifted towards the Fermi-level, promote the ability to interact in electrocatalytic reactions. All these features allow the occurrence of adsorption phenomena with catalytic properties, [11] and places AuNPs in the palette of materials with potential interest to be used in electrocatalyzed reactions. [12,13] Furthermore they exhibit good biological compatibility and excellent conductivity that highlights them for biosensor applications. Examples of interesting approaches using AuNPs are the works developed by Yang et al. [5] where they are used as DNA labels with electrocatalytic properties achieving detection limits in the fM order. Our group has also reported the use of AuNPs for further silver catalytic electrodeposition and applied this reaction for enhanced detection of proteins. [14]

In this work we make use of the advantageous characteristics of screen-printed carbon electrodes (SPCEs) in terms of low cost, miniaturization possibilities, low sample consuming and wide working potential range in the Hydrogen Evolution Reaction (HER) in presence of AuNPs. In addition we combined all the mentioned advantages with the relative high hydrogen overpotential [15] and low background currents for the detection of AuNPs using SPCEs. This is based on the electroactive properties of AuNPs to catalyze HER in acidic media which is measured by recording the current generated in the simple and efficient chronoamperometric mode.

* Corresponding author. Institut Català de Nanotecnologia, ETSE-Edifici Q 2ª planta, Campus UAB, 08193 Bellaterra, Barcelona, Spain. Tel.: +34 935868014; fax: +34 935868020.
E-mail address: arben.merkoci.icn@uab.es (A. Merkoçi).

1388-2481/$ – see front matter © 2010 Elsevier B.V. All rights reserved.
doi:10.1016/j.elecom.2010.08.018

2. Experimental

2.1. Reagents and equipment

Streptavidin-coated magnetic-beads (MBs) 2.8 μm sized were purchased from Dynal Biotech (M-280, Invitrogen, Spain). Biotinylated anti-human IgG (αHIgG-B, B1140, developed in goat), human IgG from human serum (HIgG, I4506), anti-human IgG (αHIgG, I1886, developed in goat), and IgG from goat serum (GIgG, I5256), were purchased from Sigma-Aldrich (Spain).

Home made screen-printed carbon electrotransducers (SPCEs) consisted of three electrodes: carbon working, silver reference and carbon counter electrodes in a single polyester strip of 29 mm × 6.7 mm. The working electrode diameter was 3 mm.

2.2. Preparation/modification of the gold nanoparticles and the magnetosandwich

The 20-nm AuNPs were synthesized adapting the method pioneered by Turkevich et al. [16]. The conjugation of AuNPs to αHIgG and their further incorporation in the magnetosandwich immunoassay using magnetic beads (MBs) were performed following the methodology previously reported by our group [7,14]. Briefly, MBs modified with streptavidin were used to immobilise specific antibodies modified with biotin (αHIgG-B). After the capture of the HIgG in the sample, the sandwich was formed with secondary specific antibodies conjugated with AuNPs (AuNPs-αHIgG). Control assays were performed using GIgG instead of HIgG.

2.3. Electrochemical experiments

Electrochemical experiments were carried out at room temperature, using a PGSTAT100 (Echo Chemie, The Netherlands) potentiostat/galvanostat. Each electrochemical measurement was performed by dropping 50 μL of AuNPs/HCl solution (different concentrations) freshly prepared onto the SPCE so the possible aggregation of the AuNPs in this medium is not observed. This drop is kept over the working area due to the hydrophobicity of the insulator layer covering the SPCEs. Background signals were recorded following the same electrochemical procedure but using an aliquot of 1 M HCl.

Cyclic voltammetry (CV) was carried out from + 1.35 V to –1.40 V at 50 mV s^{-1} and chronoamperometry was performed at a fixed potential during a determined time.

Electrochemical impedance spectroscopy (EIS) measurements were performed holding the electrode at a potential of −1.00 V, with signal amplitude of 10 mV and the measurement frequency ranged from 0.01 Hz to 10,000 Hz.

For the magnetosandwich immunoassay, 50 μL of the sandwich/HCl solution were placed on the SPCE surface before the measurement.

3. Results and discussion

The electrocatalytic effect of AuNPs deposited onto SPCEs to the HER (in acidic medium) is shown in Fig. 1A, where cyclic voltammograms in 1 M HCl are presented. The background CV (upper curve) shows that the proton reduction starts at approximately −0.80 V vs. Ag/AgCl when no AuNPs are present, and undergoes a positive shift up to 500 mV in a proportional relation with the concentration of AuNPs in solution. A similar behaviour was previously observed for bulk gold. [17] Moreover, a higher current is obtained for potentials lower than −1.00 V at higher concentrations of AuNPs. The oxygen reduction onto SPCEs surface is neglected in this work once it occurs at potentials lower than −1.40 V and therefore will not affect the background signals.

To better evaluate the catalytic reaction, the active surface of the working electrode in absence and presence of adsorbed AuNPs was characterized by electrochemical impedance spectroscopy (EIS), that can give further information on the impedance changes of the electrode surface. Fig. 1B displays EIS plots from several AuNPs concentrations, showing the decrease in resistance when increasing the AuNPs concentration (ranging from 1.48 to 1500 pM, from top to bottom). This is due to the fact that AuNPs behave as free electroactive

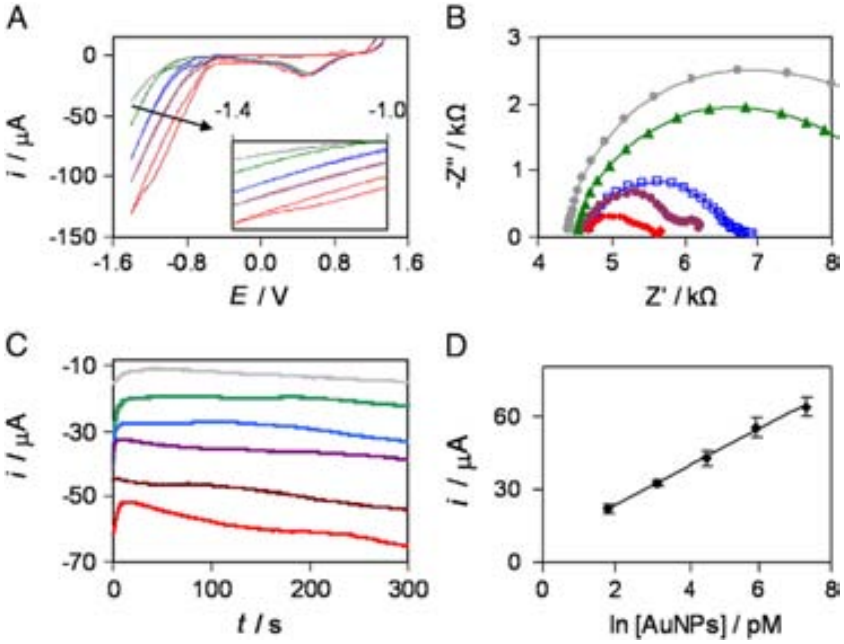

Fig. 1. A: CV performed with increasing concentration of AuNPs. Upper curve corresponds to the background signal followed by 1.48, 23.5, 93.8, and 1500 pM of AuNPs solution from top to bottom; B: Electrochemical Impedance Spectroscopy plots of different electrodes with increasing concentrations of AuNPs in 1 M HCl from top to bottom as described in 1.A; C: Chronoamperograms recorded in 1 M HCl solution (upper line) and for increasing concentrations of AuNPs in 1 M HCl ranging from 5.85 pM to 1.5 nM (top to bottom); D: Calibration plot obtained by plotting the absolute value of the currents at 200 s with logarithm of AuNPs concentration.

adsorption sites that enhance the electron transfer in the system resulting in a lower semi-circle diameter which means a decrease of the charge transfer resistance at electrode surface.

From the voltammetric studies (Fig. 1A), it can be concluded that by applying an adequate reductive potential (within the potential window (PW) from −1.00 to −1.40 V) the protons in the acidic medium are catalytically reduced to hydrogen in presence of AuNPs and this reduction can be chronoamperometrically measured (Fig. 1C). The absolute value of the cathodic current generated at a fixed time can be considered as the analytical signal and related with the amount of AuNPs present in the sample.

The different parameters affecting the analytical signal obtained by the chronoamperometric mode, such as the acidic medium and the electroreduction potential were optimised (data not shown). From several acidic solutions studied it was found that 1 M HCl displayed a better performance and the optimum electroreduction potential was −1.00 V. Regarding the fixed time to measure the current chosen as analytical signal, it was found a compromise between the time of analysis and signal to noise ratio at 200 s.

Furthermore, it was found that a previous oxidation of the AuNPs at +1.35 V was important for obtaining the best electrocatalytic effect on the HER in the further reductive step. During the application of this potential, some gold atoms in the outer layers of AuNPs surface are transformed into Au(III) ions. These ions could also exert a catalytic effect on hydrogen evolution [18] together with the significant number of AuNPs still remaining after the oxidation. In order to clarify this, Scanning Electrochemical Microscopy (SEM) images of SPCEs with deposited AuNPs (from 1.5 nM solution in 1 M HCl) were obtained after the different steps of the chronoamperometric procedure. In Fig. 2 these images are shown together with a scheme of the processes occurring on the electrode surface. It can be observed that the AuNPs remain on the surface of the SPCE after the application of the oxidation potential (B), and after a complete chronoamperogram was performed (C). AuNPs were observed to be distributed all over carbon working electrode area, with a certain aggregation in high rugosity areas like it was expected.

After optimizing the experimental procedure, a series of chronoamperograms for AuNPs solutions in a similar concentration range as in the CV curves of Fig. 1A, were registered under the optimal conditions (Fig. 1C). The absolute value of the current at 200 s (analytical signal) was plotted vs. the logarithm of AuNPs concentration (Fig. 1D), resulting in a linear relationship in the range between 4.8 pM and 1.5 nM according to the following equation:

$$i_{(\mu A)} = 7.71 \times \ln[\text{AuNPs}]_{(\text{pM})} + 8.19,\ r = 0.999,\ n = 3$$

A detection limit for AuNPs of 1.03 pM (calculated as the concentration corresponding to three times the standard deviation of the estimate) and a RSD of 5% for three repetitive measurements of 5.88 pM AuNPs were obtained.

Finally, the advantageous properties of this catalytic method were approached for protein detection (HIgG as model analyte) in a

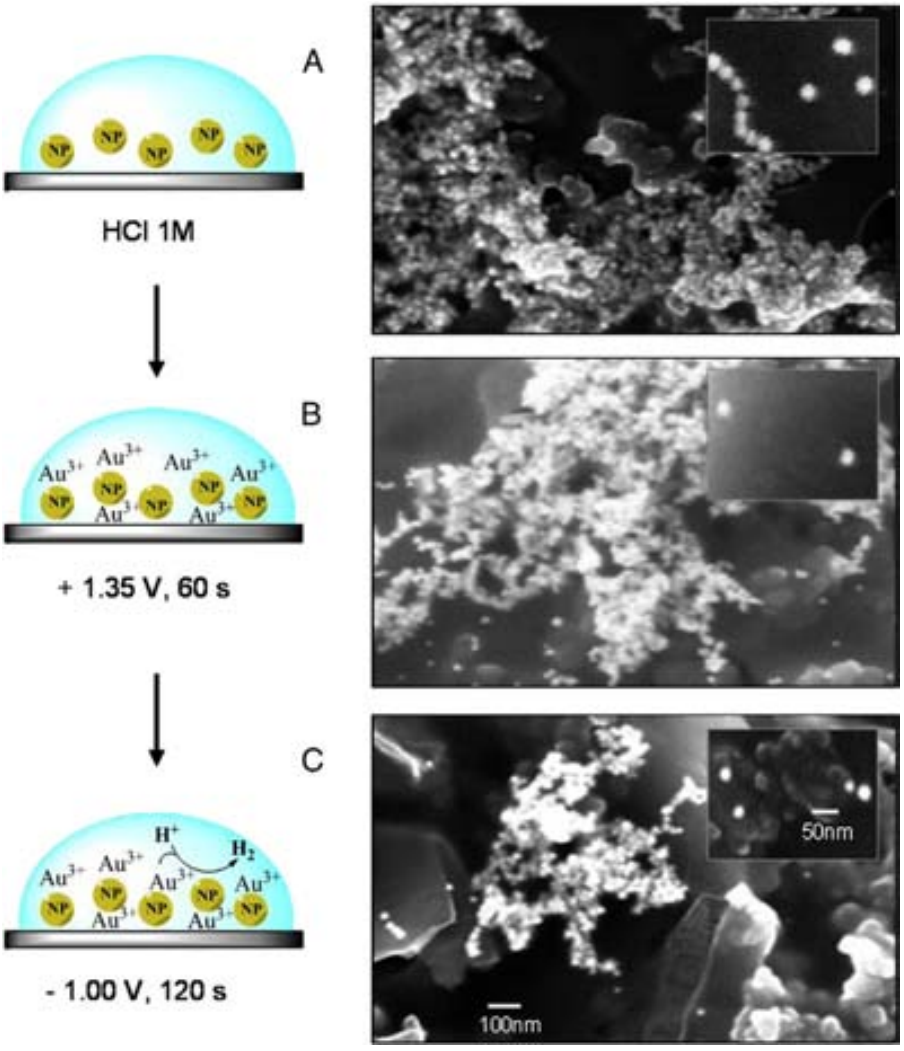

Fig. 2. Scheme of electrochemical HER induced by AuNPs (left) and SEM images taken after each electrochemical step (right). Experimental conditions as explained in the text.

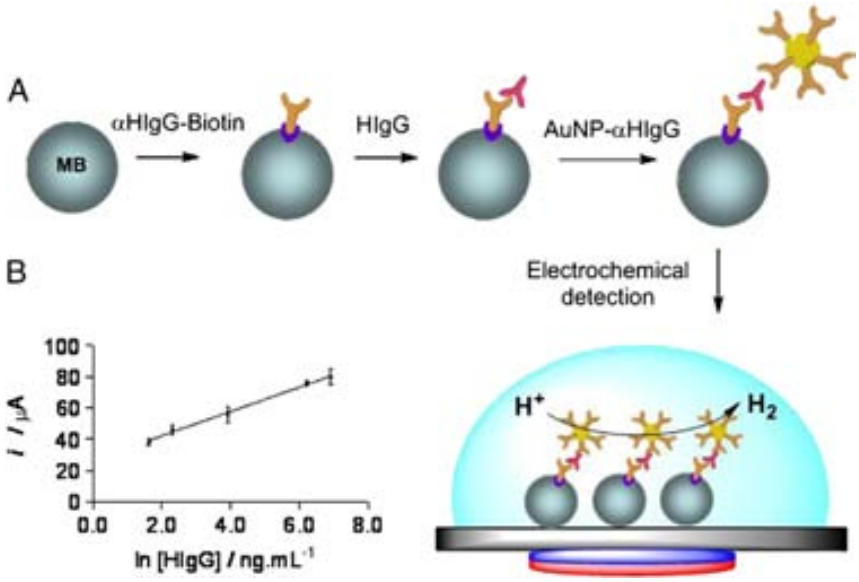

Fig. 3. A: Scheme of the magnetosandwich immunoassay steps and electrochemical detection of the obtained sandwich. B: Relation between the analytical signal and the logarithm of HIgG concentration.

magnetoimmunoassay. This system also takes advantage from the magnetic beads properties used here as platforms, in terms of low matrix effects and sample preconcentration when they are applied in protein analysis. Fig. 3A displays a scheme of the overall experimental procedure and Fig. 3B shows the relation between the analytical signal and the concentration of HIgG in the range between 5 and 1000 ng mL^{-1}. A linear relationship was obtained by plotting the current values vs. the logarithm of the HIgG concentration according to the following equation:

$$i_{(\mu A)} = 7.84 \times \ln[\mathrm{HIgG}]_{(\mathrm{ng/mL})} + 26.4, r = 0.998, n = 3$$

The limit of detection was 1.45 ng mL^{-1} of HIgG (calculated as the concentration corresponding to three times the standard deviation of the estimate). The reproducibility of the method shows a RSD around 3%, obtained for 3 repetitive assays for 50 ng mL^{-1} of target. The selectivity of the assay was demonstrated performing a blank assay using a non specific protein (GIgG instead of HIgG) (data not shown).

4. Conclusions

In conclusion we show here that AuNPs constitute a very good electrocatalytic system for the HER in acidic medium by providing free electroactive hydrogen adsorption sites towards the formation of molecular hydrogen. Based on this system an optimised AuNPs indirect quantification method, taking advantage of the chronoamperometric mode, is developed. The catalytic properties of AuNPs were also approached for a model protein (Human IgG) detection in a magnetoimmunoassay that decreases the distance between the electrode and the electrocatalytic label enhancing the electron tunnelling and consequently the catalytic signal used for biodetection. The advantages of the electrocatalytic detection method together with the use of MBs as platforms of the bioreactions and the use of SPCEs as electrotransducers will open the way to efficient, portable, low-cost and easy-to-use devices for point-of-care use for several applications with interest not only for clinical analysis but also for environmental analysis as well as safety and security control.

Acknowledgments

We acknowledge funding from the MEC (Madrid) for the projects MAT2008-03079/NAN, CSD2006-00012 “NANOBIOMED” (Consolider-Ingenio 2010) and the *Juan de la Cierva* scholarship (A. de la Escosura-Muñiz).

References

[1] A. Merkoçi, M. Aldavert, S. Marín, S. Alegret, TrAC 24 (2005) 341–349; A. Merkoçi, FEBS J. 274 (2007) 310–316.
[2] A. Abad, A. Corma, H. García, Chem. Eur. J. 14 (2008) 212–222.
[3] H.L. Jiang, T. Umegaki, T. Akita, X.B. Zhang, M. Haruta, Q. Xu, Chem. Eur. J. 16 (2010) 3132–3137.
[4] R. Polsky, R. Gill, L. Kaganovsky, I. Willner, Anal. Chem. 78 (2006) 2268–2271.
[5] J. Das, H. Yang, J. Phys. Chem. C 113 (2009) 6093–6099.
[6] A. De la Escosura-Muñiz, A. Ambrosi, A. Merkoçi, TrAC 27 (2008) 568–584.
[7] A. Ambrosi, M.T. Castañeda, A.J. Killard, M.R. Smyth, A. Merkoçi, Anal. Chem. 79 (2007) 5232–5240.
[8] B. Hammer, J.K. Nørskov, Nature 376 (1995) 238–240.
[9] S.R. Belding, E.J.F. Dickinson, R.G. Compton, J. Phys. Chem. 113 (2009) 11149–11156.
[10] K.Z. Brainina, L.G. Galperin, A.L. Galperin, J. Solid State Electrochem. 14 (2010) 981–988.
[11] M. Haruta, N. Yamada, T. Kobayashi, S. Iijima, J. Catal. 115 (1989) 301–309.
[12] W. Chen, S. Chen, Angew. Chem. Int. Ed. 48 (2009) 4386–4389.
[13] B.E. Hayden, D. Pletcher, J.P. Suchsland, Angew. Chem. 119 (2007) 3600–3602.
[14] A. de la Escosura-Muñiz, M. Maltez-da Costa, A. Merkoçi, Biosens. Bioelectron. 24 (2009) 2475–2482.
[15] L.A. Kibler, Chem. Phys. Chem. 7 (2006) 985–991.
[16] J. Turkevich, P. Stevenson, J. Hillier, Discuss. Faraday Soc. 11 (1951) 55–75.
[17] J. Perez, E.R. Gonzalez, H.M. Villullas, J. Phys. Chem. B 102 (1998) 10931–10935.
[18] M. Díaz-González, A. de la Escosura-Muñiz, M. González-García, A. Costa-García, Biosens. Bioelectron. 23 (2008) 1340–1346.

Gold nanoparticle-based electrochemical magnetoimmunosensor for rapid detection of anti-hepatitis B virus antibodies in human serum

A. de la Escosura Muñiz, **M. Maltez-da Costa**, C. Sánchez-Espinel, B. Díaz-Freitas, J. Fernández-Suarez, A. González-Fernández, A. Merkoçi

Biosensors and Bioelectronics

2010, 26, 1710–1714

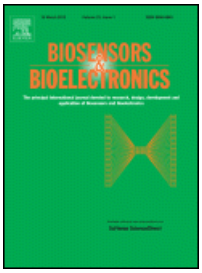

Biosensors and Bioelectronics 26 (2010) 1710–1714

Contents lists available at ScienceDirect

Biosensors and Bioelectronics

journal homepage: www.elsevier.com/locate/bios

Short communication

Gold nanoparticle-based electrochemical magnetoimmunosensor for rapid detection of anti-hepatitis B virus antibodies in human serum

Alfredo de la Escosura-Muñiz[a,b], Marisa Maltez-da Costa[a], Christian Sánchez-Espinel[c], Belén Díaz-Freitas[c], Jonathan Fernández-Suarez[d], África González-Fernández[c], Arben Merkoçi[a,e,*]

[a] Nanobioelectronics & Biosensors Group, Institut Català de Nanotecnologia, CIN2 (ICN-CSIC), Campus UAB, Barcelona, Spain
[b] Instituto de Nanociencia de Aragón, Universidad de Zaragoza, Zaragoza, Spain
[c] Immunology, Biomedical Research Center (CINBIO), University of Vigo, Campus Lagoas Marcosende, Vigo, Pontevedra, Spain
[d] Microbiology Service, Hospital Meixoeiro, Complejo Hospitalario Universitario de Vigo (CHUVI) Vigo, Pontevedra, Spain
[e] ICREA, Barcelona, Spain

ARTICLE INFO

Article history:
Received 14 April 2010
Received in revised form 5 July 2010
Accepted 19 July 2010
Available online 17 August 2010

Keywords:
Hepatitis B
Gold nanoparticles
Immunosensor
Magnetosandwich immunoassay
Screen-printed electrodes
Hydrogen evolution electrocatalysis

ABSTRACT

A sandwich immunoassay using magnetic beads as bioreaction platforms and AuNPs as electroactive labels for the electrochemical detection of human IgG antibodies anti-Hepatitis B surface antigen (HBsAg), is here presented as an alternative to the standard methods used in hospitals for the detection of human antibodies directed against HBsAg (such as ELISA or MEIA). The electrochemical detection of AuNPs is carried out approaching their catalytic properties towards the hydrogen evolution in an acidic medium, without previous nanoparticle dissolution. The obtained results are a good promise toward the development of a fully integrated biosensing set-up. The developed technology based on this detection mode would be simple to use, low cost and integrated into a portable instrumentation that may allow its application even at doctor-office. The sample volumes required can be lower than those used in the traditional methods. This may lead to several other applications with interest for clinical control.

1. Introduction

Viral hepatitis due to hepatitis B (HB) virus is a major public health problem all over the world. Hepatitis B is a complex virus, which replicates primarily in the liver, causing inflammation and damage, but it can also be found in other infected organs and in lymphocytes. For this reason, the hepatitis B vaccine is strongly recommended for healthcare workers, people who live with someone with hepatitis B, and others at higher risk. In many countries, hepatitis B vaccine is inoculated to all infants and it is also recommended to previously unvaccinated adolescents.

The external surface of this virus is composed of a viral envelope protein also called hepatitis B surface antigen (HBsAg). Previously infected and vaccinated people show normally high levels of IgG antibodies against this antigen (α-HBsAg IgG). The presence or absence of these antibodies in human serum is useful to determine the need for vaccination (if α-HBsAg IgG antibodies are absent), to check the immune response in patients which has suffered hepatitis B, the evolution of chronic HB carrier patients and also the immunity of vaccinated people [McMahon et al., 2005].

Current methods for the detection of α-HBsAg IgG antibodies such as Enzyme-Linked Immunosorbent Assay (ELISA) and Microparticle Enzyme Immunoassay (MEIA) are time-consuming, and require advanced instrumentation. Hence, alternative cost-effective methods that employ simple/user-friendly instrumentation and are able to provide adequate sensitivity and accuracy would be ideal for this kind of analysis. In this context, biosensor technology coupled with the use of nanoparticles (NPs) tags offers benefits compared to traditional methods in terms of time of analysis, sensitivity and simplicity. From the variety of NPs, gold nanoparticles (AuNPs) have gained attention in the last years due to the unique structural, electronic, magnetic, optical, and catalytic properties which have made them a very attractive material for biosensor systems and bioassays.

Sensitive electrochemical DNA sensors [Pumera et al., 2005; Castañeda et al., 2007; Marín and Merkoçi, 2009], immunosensors [Ambrosi et al., 2007; De la Escosura-Muñiz et al., 2009a] and other bioassays have recently been developed by our group and others [De la Escosura-Muñiz et al., 2008] using AuNPs or other NPs as labels and providing direct detection without prior chemical dis-

* Corresponding author at: Institut Català de Nanotecnologia, ETSE-Edifici Q 2ª planta, Campus UAB, 08193 Bellaterra, Barcelona, Spain.
Tel.: +34 935868014; fax: +34 935868020.
E-mail address: arben.merkoci.icn@uab.es (A. Merkoçi).

0956-5663/$ – see front matter © 2010 Elsevier B.V. All rights reserved.
doi:10.1016/j.bios.2010.07.069

solution. In some of these bioassays, magnetic beads (MBs) are used as platforms of the bioreactions, providing important advantages: i) the analyte is preconcentrated on the surface of the MBs, ii) applying a magnetic field, the complex MB–analyte can be separated from the matrix of the sample, minimizing matrix effects and improving the selectivity of the assay.

Furthermore, we have recently reported a novel cell sensor based on a new electrotransducing platform (screen-printed carbon electrodes, SPCEs) where the cells are cultured and then recognized by specific antibodies [Díaz et al., 2009] labeled with AuNPs [De la Escosura-Muñiz et al., 2009b]. These AuNPs are chronoamperometrically detected approaching their catalytic properties on the hydrogen evolution, avoiding their chemical dissolution.

Here we present a novel magnetosandwich assay based on AuNPs tags for the capturing of α-HBsAg IgG antibodies in human sera of patients previously exposed to hepatitis B (either for infection, reinfection or for vaccination) and final chronoamperometric detection approaching the catalytic properties of AuNPs on the hydrogen evolution reaction. The α-HBsAg IgG antibodies concentration in the sera samples has been previously calculated by a standard method (MEIA), finding that the sensitivity of the electrochemical biosensor is high enough so as to detect the HB responders.

2. Experimental

2.1. Apparatus and electrodes

The electrochemical transducers used were homemade screen-printed carbon electrodes (SPCEs), consisting of three electrodes: working electrode, reference electrode and counter electrode in a single strip fabricated with a semi-automatic screen-printing machine DEK248 (DEK International, Switzerland). The reagents used for this process were: Autostat HT5 polyester sheet (McDermid Autotype, UK), Electrodag 423SS carbon ink, Electrodag 6037SS silver/silver chloride ink and Minico 7000 Blue insulating ink (Acheson Industries, The Netherlands). (See the detailed SPCE fabrication procedure and pictures of the obtained sensors in the supplementary material, Fig. S1.)

The electrochemical experiments where performed with a μAutolab II (Echo Chemie, The Netherlands) potentiostat/galvanostat connected to a PC and controlled by Autolab GPES software. All measurements were carried out at room temperature, with a working volume of 50 μL, which was enough to cover the three electrodes contained in the home made SPCEs used as electrotransducers connected to the potentiostat by a homemade edge connector module.

A Transmission Electron Microscope (TEM) Jeol JEM-2011 (Jeol Ltd., Japan) was used to characterize the gold nanoparticles and the magnetosandwich complexes.

2.2. Reagents and solutions

Tosylactivated Magnetic Beads 2.8 μm sized were purchased from Dynal Biotech (M-280, Invitrogen, Spain). Recombinant hepatitis B surface Antigen (HBsAg) subtype adw2 was produced by Shanta Biotechnics Limited (Hyderabad, India) (stock solution 1130 μg/mL). Serum samples were obtained from previously HB infected, reinfected or vaccinated patients from Hospital Meixoeiro, Complejo Hospitalario Universitario de Vigo (CHUVI, Spain). Goat antibodies directed against human IgG antibodies (αHIgG antibodies), hydrogen tetrachloroaurate (III) trihydrate ($HAuCl_4 \cdot 3H_2O$, 99.9%) and trisodium citrate ($Na_3C_6H_5O_7 \cdot 2H_2O$) were purchased from Sigma–Aldrich (Spain). Unless otherwise stated, all buffer reagents and other inorganic chemicals were supplied by Sigma, Aldrich or Fluka (Spain). All chemicals were used as received and all aqueous solutions were prepared in double-distilled water. The borate buffer solution (BB) was prepared with 0.1 M boric acid and adjusted to pH 9.2 with NaOH 5 M. Phosphate buffer solution (PBS) was composed of 0.1 M phosphate buffered saline pH 7.4. Blocking buffer solution consisted in a PBS pH 7.4 solution with 0.5% (w/v) bovine serum albumin (BSA). The washing buffer (WB) consisted in PBS, pH 7.4, solution with 0.05% Tween 20. Analytical grade HCl (Merck, Spain) was prepared with ultra-pure water.

2.3. Methods

2.3.1. Preparation and modification of gold nanoparticles

The 20-nm gold nanoparticles (AuNPs) were synthesized by reducing tetrachloroauric acid with trisodium citrate, a method pioneered by Turkevich [Turkevich et al., 1951] (see the experimental procedure for AuNP synthesis and TEM images in the supplementary material, Fig. S2). The conjugation of AuNPs to goat polyclonal antibodies anti-human IgG (α-HIgG) was performed according to the following procedure, previously optimized by our group [Ambrosi et al., 2007]: 1.5 mL of 3 nM AuNPs colloidal solution was mixed with 100 μL of 100 μg/mL of antibody solution and incubated at 25 °C for 20 min. Subsequently, a blocking step with 100 μL of 1 mg/mL BSA, incubating at 25 °C for 20 min was undertaken. Finally, a centrifugation at 14,000 rpm for 20 min was carried out, and α-HIgG/AuNPs conjugate was reconstituted in PBS-Tween (0.05%) solution.

2.3.2. Magnetosandwich assay using gold nanoparticle labels

The magnetosandwich assay was performed following a methodology previously optimized in our group [De la Escosura-Muñiz et al., 2009a], with some variations. Briefly, 2.5 μL stock solution of washed tosylactivated magnetic beads were incubated at 37 °C under gentle stirring, with 12.5 μL HBsAg in BB pH 9.2 solution, during 45 min in a TS-100 ThermoShaker. The MB immobilized antigen matrix was then separated from solution by magnetic separation, and resuspended in blocking buffer (PBS–BSA 5%) to block any remaining active surface of MBs. The blocking step was performed at 25 °C for 60 min under gentle stirring. After washing with PBS-tween, incubation with 25 μL of human serum (serum of post infected patients) was performed at 25 °C during 30 min under gentle stirring. A non-immune serum was used as a control for this assay. The resulting immunocomplex was magnetically separated from serum matrix and washed with PBS-tween and PBS solutions. The last incubation step, with the AuNPs/α-HIgG conjugate previously prepared, was performed under the same conditions as the last incubation with subsequently washing steps, resulting in the complete magnetoimmunosandwich that was ready to be analyzed.

2.3.3. Electrocatalytic detection

Quantitative analyses were carried out taking advantage of the chronoamperometric mode. Chronoamperograms were obtained by placing a mixture of 25 μL of 2 M HCl and 25 μL of the magnetosandwich (performed for sera containing different α-HBsAg IgG concentrations) solution onto the surface of the electrodes and, subsequently, holding the working electrode at a potential of +1.35 V for 1 min and then applying a negative potential of −1.00 V for 5 min, recording the cathodic current generated. The absolute value of the current registered at 200 s was chosen as analytical signal. A new electrode was employed for each measurement. The concentration of α-HBsAg IgG antibodies in each serum sample was previously evaluated by MEIA using an AxSYM Analyzer System from Abbot Diagnostics (USA). The system was previously calibrated using AxSYM AUSAB (hepatitis B surface antigen; recombinant; subtypes ad and ay) standard calibrators in the

range between 0 and 1000 mIU/mL (concentration standardized against the World Health Organization Reference Standard).

3. Results and discussion

The experimental procedure for capturing the α-HBsAg IgG antibodies from human sera and the further signaling with AuNPs tags is schematized in Fig. 1. MBs modified with tosyl groups are used as platforms of the bioreactions, allowing to preconcentrate the sample and also to avoid unspecific adsorptions on the surface of the electrotransducer. The used MBs can easily be conjugated with molecules that have amino- or carboxi- groups, by nucleofilic substitution reaction. Approaching this property, hepatitis B surface antigens (HBsAg) are immobilized onto the surface of the MBs, ensuring in this way an active surface (MB/HBsAg) for capturing α-HBsAg IgG antibodies, whose unspecific adsorption on the MBs is avoided by a blocking step using BSA. When adding the sera samples, the α-HBsAg IgG analyte recognize the specific antigens forming the MB/HBsAg/α-HBsAg IgG complex. After a washing step, the α-HBsAg IgG antibodies selectively attached onto MB/HBsAg are captured by goat polyclonal antibodies anti-Human IgG (α-HIgG antibodies) previously conjugated with AuNPs. This secondary immunoreaction gives rise to the formation of the final complex (MB/HBsAg/α-HBsAg IgG/α-HIgG/AuNPs), where the quantity of AuNPs is proportional to the concentration of α-HBsAg IgG antibodies in the sample. Fig. 2 shows TEM image of MB/HBsAg/α-HBsAg IgG/α-HIgG/AuNPs formed following the reported procedure. AuNPs (small black points) covering the surface of the MBs (big spheres) can be observed demonstrating the specificity of the assay. The results obtained by TEM images were followed by electrochemical measurements. A 25 μL sample of the magnetosandwich complex placed onto the surface of the SPCE electrotransducer was detected through measuring the AuNPs catalytic properties on the hydrogen evolution [Chikae et al., 2006; De la Escosura-Muñiz et al., 2009b] at an adequate potential (usually −1.00 V) in an acidic medium. This catalytic effect has also been observed for platinum and palladium nanoparticles [Meier et al., 2004]. Nevertheless the use of AuNPs as here reported is more suitable for biosensing purposes, due to their simple synthesis, narrow size distribution, biocompatibility, and easy bioconjugation. It was also found that a previous oxidation of the AuNPs at +1.35 V was necessary for obtaining the best electrocatalytic effect on the hydrogen evolution in the further reductive step (data not shown). During the application of this potential, some gold atoms in the outer layers of AuNPs surface are transformed into Au (III) ions. These ions could also exert a catalytic effect on hydrogen evolution [Díaz-González et al., 2008] together with the significant number of AuNPs still remaining after the oxidation step. After that, the catalytic current generated by the reduction of the hydrogen ions is chronoamperometrically recorded and related to the quantity of the α-HBsAg IgG antibodies. The electroreduction potential has been previously optimized (in the range −0.80 V to −1.20 V) and as a compromise between signal intensity and reproducibility a potential value of −1.00 V was found as optimal. In Fig. 3A are shown the chronoamperograms recorded following the procedure detailed in methods Section 2.3.3, for magnetosandwich assays performed in a non immune serum as control (a) and for assays performed in sera containing 5 (b), 10.1 (c), 30.5 (d), 69.2 (e) mIU/mL of α-HBsAg IgG antibodies. As it can be observed, the cathodic catalytic current increases when increasing the concentration of antibodies in the samples, as it was expected. The curve presented in Fig. 3B shows that there is a good linear relationship (correlation coefficient of 0.991) between the α-HBsAg IgG antibodies and the absolute value of the current registered at 200 s (analytical signal) in the range of 5–69.2 mIU/mL, according to the equation:

$$\text{current}\,(\mu\text{A}) = 0.265[\alpha\text{-HBsAg IgG}\,(\text{mIU/mL})] + 30.27\,(n = 3) \quad (1)$$

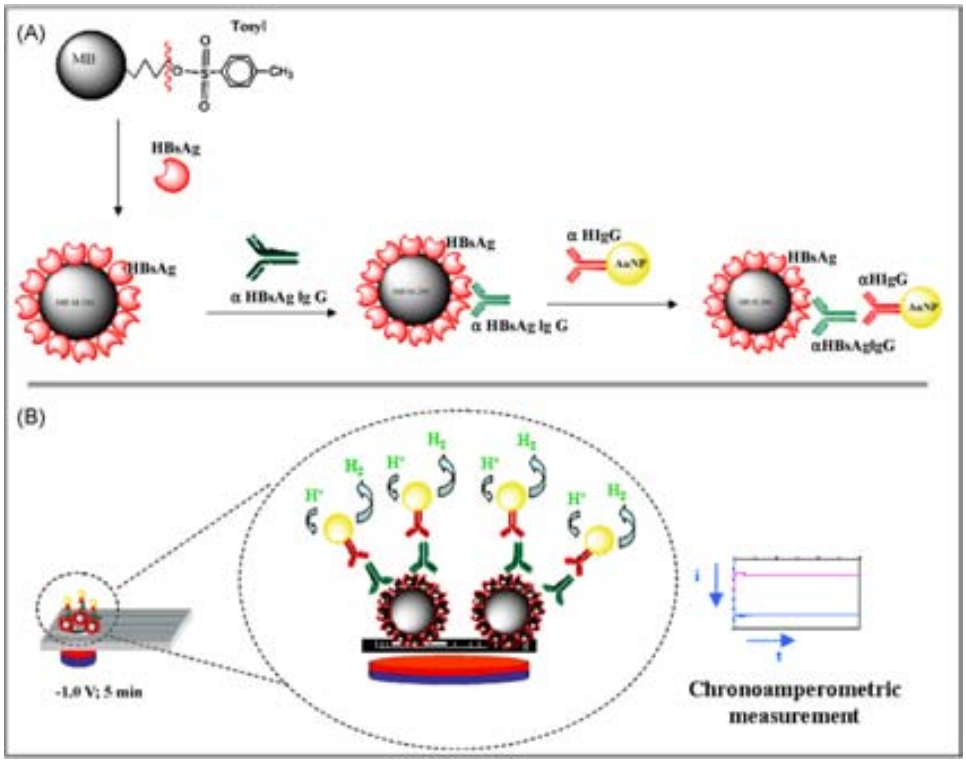

Fig. 1. (A) Scheme of the experimental procedure performed. HBsAg captured on the surface of magnetic beads, incubation with human serum containing α-HBsAg IgG antibodies and recognition with AuNPs conjugated with goat α-human IgG antibodies. (B) Scheme of the electrochemical detection procedure based on the electrocatalytic hydrogen generation.

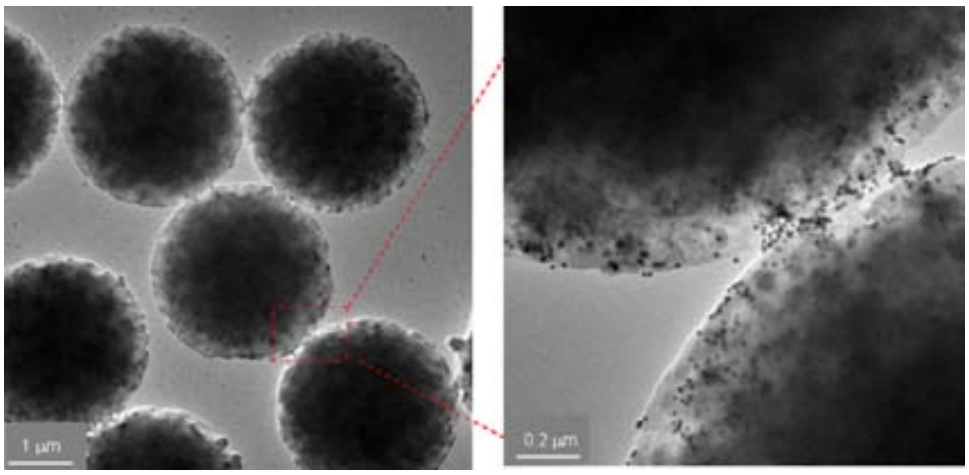

Fig. 2. TEM images of the MB/HBsAg/α-HBsAg IgG/α-HIgG/AuNPs complex formed following the experimental procedure detailed in Section 2.3.2 for a serum containing 132 mIU/mL of α-HBsAg IgG (left) and detail of the region between two MBs, where the AuNPs (small black points) are observed (right).

The limit of detection (calculated as the concentration of α-HBsAg IgG antibodies corresponding to 3 times the standard deviation of the estimate) was 3 mIU/mL. Since it is considered that vaccine responders show ≥10 mIU/mL (McMahon et al., 2005) our test is enough to guarantee the detection of those levels. The reproducibility of the method shows a relative standard deviation (RSD) of 5%, obtained for a series of three repetitive assay reactions for a serum sample containing 10.1 mIU/mL of α-HBsAg IgG antibodies.

Finally, a human serum sample with an unknown concentration of α-HBsAg IgG antibodies was electrochemically analyzed. Following the explained experimental procedure, a value of the analytical signal of 36.8 ± 1.5 μA (n = 3) was obtained. From Eq. (1), a concentration of 24.6 ± 5.7 mIU/mL in the serum sample was estimated. This sample was also analyzed by the MEIA method, obtaining a value of 23.1 ± 1.6 mIU/mL. These results show a deviation of 6.5% between both methods, being this accuracy good enough to guarantee that the electrochemical method is a valid alternative to check the levels of α-HBsAg IgG antibodies in human serum. This accuracy value was also corroborated performing an approximation to the statistical paired sample T-test (see supplementary material).

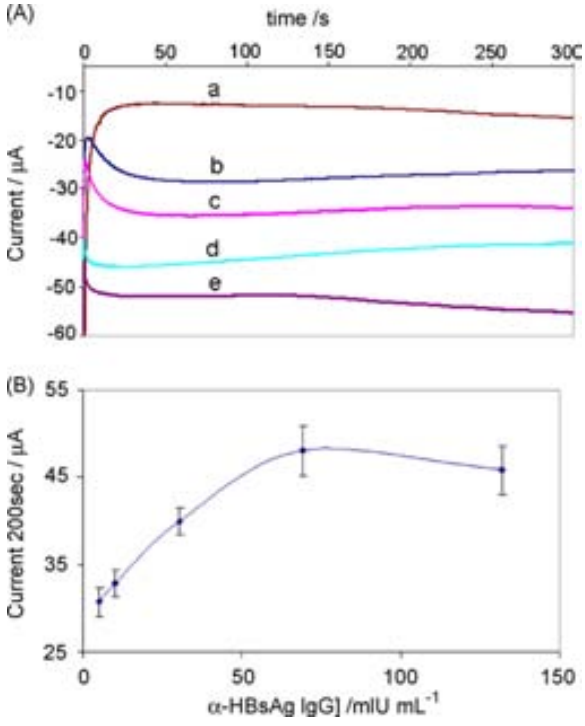

Fig. 3. (A) Chronoamperograms recorded in 1 M HCl by applying a potential of −1.00 V for 5 min, for a magnetosandwich performed in a non immune control serum (blank curve, a) and magnetosandwichs performed for sera containing increasing concentrations of α-HBsAg IgG antibodies: 5 (b), 10.1 (c), 30.5 (d) and 69.2 (e) mIU/mL. (B) Effect of the α-HBsAg IgG antibodies concentration on the analytical signal.

The performance of the developed electrochemical biosensor is similar to the achieved in recently reported biosensors for the detection of α-HBsAg IgG in human sera using optical [Moreno-Bondi et al., 2006; Qi et al., 2009] or piezoelectric [Lee et al., 2009] measurements in terms of sensitivity and reproducibility of the assays. Although the linear range of the electrochemical biosensor is shorter than the reported in these works (serial dilutions of the samples can solve this drawback) we should consider advantageous characteristics in terms of cost, simplicity and time of analysis that make the presented electrochemical biosensor a promising alternative for future point of care analysis.

4. Conclusions

A novel magnetosandwich assay based biosensor based on AuNPs labels has been developed and applied for the detection of antibodies anti-hepatitis B surface antigen (α-HBsAg) in human serum. The reported assay takes advantage of the properties of the magnetic beads used as platforms of the immunoreactions and the AuNPs used as electrocatalytic labels. The final detection of these AuNPs tags is performed in a rapid and simple way approaching their catalytic properties towards the hydrogen ions electroreduction in an acidic medium. The developed biosensor allows the detection of 3 mIU/mL of α-HBsAg IgG antibodies in human serum, being sensitive enough to guarantee the detection of up to 10 mIU/mL which is the lower limit for HBs Ag responders. The results were compared with those obtained with the MEIA method, showing a deviation of 6.5%. From all this, it can be concluded that the reported biosensor is a valid alternative to the standard methods for the detection of α-HBsAg IgG antibodies in human serum, in a more rapid, simple and cheap way.

Acknowledgments

We acknowledge funding from the MEC (Madrid) for the projects MAT2008-03079/NAN and CSD2006-00012

"NANOBIOMED" (Consolider-Ingenio 2010) and the Juan de la Cierva scholarship (A. de la Escosura-Muñiz), and from SUDOE-FEDER (Immunonet-SOE1/P1/E014) and Xunta de Galicia (INBIOMED, 2009/63).

Appendix A. Supplementary data

Supplementary data associated with this article can be found, in the online version, at doi:10.1016/j.bios.2010.07.069.

References

Ambrosi, A., Castañeda, M.T., Killard, A.J., Smyth, M.R., Alegret, S., Merkoçi, A., 2007. Anal. Chem. 79, 5232–5240.
Castañeda, M.T., Merkoçi, A., Pumera, M., Alegret, S., 2007. Biosens. Bioelectron. 22, 1961–1967.
Chikae, M., Idegami, K., Kerman, K., Nagatani, N., Ishikawa, M., Takamura, Y., Tamiya, E., 2006. Electrochem. Commun. 8, 1375–1380.
De la Escosura-Muñiz, A., Ambrosi, A., Merkoçi, A., 2008. Trends Anal. Chem. 27, 568–584.
De la Escosura-Muñiz, A., Maltez-da Costa, M., Merkoçi, A., 2009a. Biosens. Bioelectron. 24, 2475–2482.
De la Escosura-Muñiz, A., Sánchez-Espinel, A., Díaz-Freitas, B., González-Fernández, A., Maltez-da Costa, M., Merkoçi, A., 2009b. Anal. Chem. 81, 10268–10274.
Díaz, B., Sanjuan, I., Gambón, F., Loureiro, C., Magadán, S., González-Fernández, A., 2009. Cancer Immunol. Immunother. 58, 351–360.
Díaz-González, M., de la Escosura-Muñiz, A., González-García, M., Costa-García, A., 2008. Biosens. Bioelectron. 23, 1340–1346.
Lee, H.J., Namkoong, K., Cho, E.C., Ko, C., Park, J.C., Lee, S.S., 2009. Biosens. Bioelectron. 24, 3120–3125.
Marín, S., Merkoçi, A., 2009. Nanotechnology 20, 055101.
McMahon, B.J., Bruden, D.L., Petersen, K.M., Bulkow, L.R., Parkinson, A.J., Nainan, O., Khristova, M., Zanis, C., Peters, H., Margolis, H.S., 2005. Ann. Intern. Med. 142, 333–341.
Meier, J., Schiøtz, J., Liu, P., Nørskov, J.K., Stimming, U., 2004. Chem. Phys. Lett. 390, 440–444.
Moreno-Bondi, M.C., Taitt, C.R., Shriver-Lake, L.C., Ligler, F.S., 2006. Biosens. Bioelectron. 21, 1880–1886.
Pumera, M., Castañeda, M.T., Pividori, M.I., Eritja, R., Merkoçi, A., Alegret, S., 2005. Langmuir 21, 9625–9629.
Qi, C., Zhu, W., Niu, Y., Zhang, H.G., Zhu, G.Y., Meng, Y.H., Chen, S., Jin, G., 2009. J. Viral Hepat. 16, 822–832.
Turkevich, J., Stevenson, P., Hillier, J., 1951. Discuss. Faraday Soc. 11, 55–75.

Nanoparticle induced catalysis for electrochemical DNA biosensors

M. Maltez-da Costa, A. de la Escosura-Muniz, A. Merkoçi

Electrochemical DNA Biosensors, edited by Mehmet Ozsoz

2012, chapter 5, 141-162

Chapter 5

Nanoparticle-Induced Catalysis for Electrochemical DNA Biosensors

Marisa Maltez-da Costa,[a] Alfredo de la Escosura-Muñiz,[a] and Arben Merkoçi[a,b]

[a] *Nanobioelectronics & Biosensors Group, Institut Català de Nanotecnologia, CIN2 (ICN-CSIC), Esfera Universitat Autònoma de Barcelona, Bellaterra, Barcelona, Spain*
[b] *ICREA, Barcelona, Spain*
arben.merkoci.icn@uab.es

In this chapter, the use of nanoparticles (NPs) in catalytic electrochemical analysis of DNA as a new detection strategy reported in recent years is revised. The topics covered here include labeling with nanoparticles and their subsequent signal enhancement employed for DNA hybridization detection. Direct sensing of nanoparticle labels as well as indirect detection routes through electrochemical sensing of label-catalyzed reactions have been reported. Nanofabrication of platforms used for the detection of DNA through electrochemical signal amplification has also been revised. Some recent examples of interesting nanoparticle-induced catalytic methodologies applied for protein detection using electrochemical biosensors are also given, because of their potential interest in future applications in DNA detection.

Electrochemical DNA Biosensors
Edited by Mehmet Ozsoz

www.panstanford.com

5.1 Introduction

Various nanomaterials, including carbon nanotubes, nanoparticles, nanomagnetic beads, and nanocomposites, are being used to develop highly sensitive and robust biosensors and biosensing systems [1] with a special emphasis on the development of electrochemical-based (bio)sensors [2, 3] due to their simplicity and cost efficiency.

One of the main requirements for a good performance of a biosensor is the high sensitivity of the response. This is of great importance when, for example, it is required to use the biosensor in clinical diagnostics for the detection of low levels of clinical biomarkers in human fluids [4], because in most cases the biomarker to be detected is present in very low concentrations. The need for biosensing systems that can detect these markers with high sensitivity without loss of selectivity, that is, low detection limits with high reliability and superior reproducibility, is becoming an important challenge.

The amplified detection of biorecognition events and specifically of DNA hybridization events stands out of the biosensing field, because it is one of the most important objectives of the current bioanalytical chemistry. In this context, approaching the catalytic properties of some (bio)materials appears to be a promising way to enhance the sensitivity of the bioassays.

Catalysts are materials that change the rate of chemical reactions without being consumed in the process. Because of their huge economical contribution, by lowering the costs of several processes, they are actually one of most wanted materials and can be found in manufacturing processes, fuel cells, combustion devices, pollution control systems, food processing, and sensor systems. Catalysts are generally prepared from transition metals, most of them from the platinum group, but this fact still represents a high cost due to the material expensiveness, and thus a reduction in used amounts would be appreciated [5, 6].

The coupling of enzymes as biocatalytic amplifying labels is a generated paradigm in developing bioelectronic sensing devices. The biocatalytic generation of a redox product upon binding of the label to the recognition event, the incorporation of redox

mediators into DNA assemblies that activate bioelectrocatalytic transformations, or the use of enzyme labels that yield an insoluble product on electrode surfaces has been extensively used to amplify biorecognition events. Due to the several problems associated with these techniques and the fast development in nanotechnology, nanoparticle-assisted signal enhancement for DNA biosensors has been greatly developed in the last decade [7, 8, 9, 10, 11].

In electrochemical sensors, electrocatalytic procedures can be approached in two ways, either by using an electrode that have highly or moderately electrocatalytic properties, or by exploiting a significant change in the electrocatalytic activity of an electrode during the detection process. Gold and platinum are commonly employed as highly electrocatalytic electrodes. Although these electrodes allow fast electron-transfer kinetics for most electroactive species, their background currents are high and fluctuate with the applied potential, which may make difficult to obtain the high signal-to-background ratios, required to achieve low detection limits. In recent years, moderately electrocatalytic electrodes have been used to obtain high signal-to-background ratios. Such electrodes can be obtained by modifying a poorly electrocatalytic electrode with a low coverage of a highly electrocatalytic material. For example, indium-tin oxide (ITO) electrodes modified with a partial monolayer of ferrocene, carbon nanotubes, or gold nanoparticles (Au-NPs) have been employed [7, 11].

The actual knowledge concerning the special properties of NPs arises from the numerous studies related to the effects of changes in shape and size on the general properties of materials. From the electroanalysis point of view the major features resulting from these studies are enhancement of mass transport, high catalytic activity, high effective surface area, and control over local microenvironment at the electrode surface [8, 12, 13, 14].

The development of nanotechnology during the last decades has led scientists to fabricate and analyze catalysts at the nanoscale. These nanostructured materials are usually high-surface-area metals or semiconductors in the form of NPs with excellent catalytic properties due to the high ratio of surface atoms with free valences to the cluster of total atoms. The catalysis takes place on the active surface sites of metal clusters in a similar mechanism as the

conventional heterogeneous catalysis [12] and in general, this is a process that occurs at the molecular or atomic level independent of the catalyst dimensions [6, 14]. There is a considerable amount of research articles and interesting reviews in what concerns to the study of nanoparticle-catalyzed reactions, but the application of these reactions in electrochemical analysis is not so well documented.

Employing NPs in electroanalysis can induce more sensitive and selective sensors as well as more cost-effective and portable systems. Their application as catalysts in electroanalytical systems can decrease overpotentials of many important redox species, inducing discrimination between different electroactive analytes, and also allowing the occurrence and reversibility of some redox reactions, which are irreversible at common modified electrodes [15]. The catalytic effect can be explained through the enhancement of electron transfer between the electrode surface and the species in solution, by enhancement of mass transport or also by the NPs' high surface energy that allows the preferred adsorption of some species that by this way suffer a change in their overpotentials (Fig. 5.1).

The most exploited materials in catalysis are the metals from platinum group, but with the introduction of nanotechnology some other elements that in bulk state did not attract a lot of attention, either due to their lack of reactivity toward some analytes or due to their high costs in production, are now emerging.

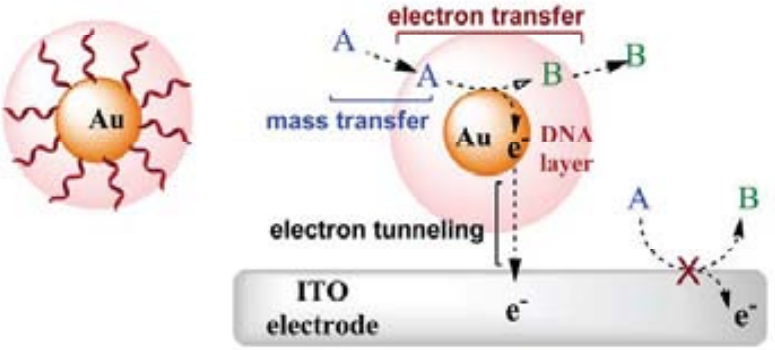

Figure 5.1. Schematic illustration of the processes that affect the electrocatalytic oxidation by Au-NP when functionalized with DNA strands (adapted from Ref. 7 with permission).

5.2 Catalysis Induced by Gold Nanoparticles

Gold nanoparticles (Au-NPs) and silver nanoparticles (Ag-NPs) are of particular interest in DNA sensors and immunosensors due to their advantageous properties, such as hydrophilicity, standard fabrication methods, excellent biocompatibility, unique characteristics in the conjugation with biological recognition elements, and multiplex capacity for signal transducer. Therefore, a large number of published methods use Au- or Ag-NPs in DNA [16, 17, 18] protein [19] and even cell [20] electrochemical detection besides optical detections like ICP-MS [21] or their use as ELISA enhancer [22].

Metallic gold was thought to be very stable and useless for some catalytic systems, but by the reduction of size to the nanoscale range, gold has been proved to be a very reactive element and it has been extensively used in sensing and biosensing systems as a catalyst for some interesting electroanalytical applications. For instance, a sensitive NO sensor was developed through the modification of a platinum microelectrode by Au-NPs in which they catalyze the electrochemical oxidation of NO with an overpotential decrease of about 250 mV [15]. An SO_2 gas sensor was also developed using Au-NPs to catalyze the electrochemical oxidation of SO_2 when the gas diffuses through the pores of the working electrode [23].

Based on the selective catalysis of Au-NPs, selective electrochemical analysis could also be achieved as, for example, in the dopamine electrochemical detection in presence of ascorbic acid. In this case, Au-NPs can be used as selective catalysts since their presence induces the decreasing of ascorbic acid overpotential and the effective separation of the oxidation potentials of ascorbic acid and dopamine [13].

5.2.1 *Electrocatalytic Activity of Gold Nanoparticle Labels on Silver Deposition*

Wang *et al.* [24] first reported a DNA hybridization detection method based on the precipitation of silver on Au-NP tags and subsequent electrochemical stripping detection of the dissolved silver. The assay employed a sandwich-like protocol with streptavidin–Au-NPs labeling the biotinylated-breast cancer gene (BRCA1) sequences.

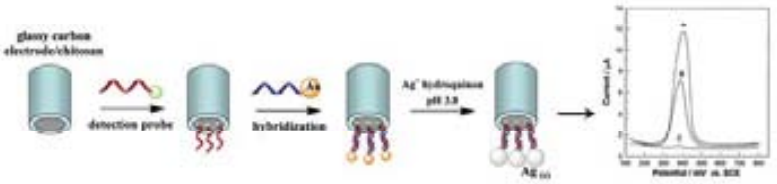

Figure 5.2. Schematic diagram of the silver chemical deposition on Au-NP labels applied for the electrochemical detection of DNA hybridization. Voltammograms correspond to DPV responses of the Au-NP–labeled oligonucleotide probes in presence of (A) complementary, (B) single-base mismatch, and (C) non-complementary oligonucleotides (adapted from Ref. 25 with permission).

After the silver precipitation on the gold, the silver was dissolved and detected at a disposable thick film carbon electrode using potentiometric stripping. This method coupled the inherent signal amplification of nanoparticle-promoted silver precipitation and the stripping metal analysis with effective discrimination against non-hybridized DNA. Cai *et al.* [25] reported a similar assay based on the silver deposition onto Au-NP–labeled oligonucleotides and subsequent electrochemical detection of Ag ions anchored onto Au-NPs connected to hybrids through differential pulse voltammetry using a glassy carbon electrode (Fig. 5.2). With this assay they obtained a detection limit of 50 pM of complementary oligonucleotides.

Later on, Lee *et al.* [26] reported the electrocatalytic effect of Au-NPs on silver electrodeposition upon ITO-based electrodes (Fig. 5.3), in absence of pre-oxidation steps, and its successful application to the DNA hybridization detection obtaining a signal-to-noise ratio of 20 that presented a great improvement in relation to their previous works under similar conditions.

5.2.2 *Electrocatalytic Activity of Gold Nanoparticle Labels on Other Reactions*

The specific binding of highly electrocatalytic labels to a biosensing layer immobilized on poor electrocatalytic electrode enhances the electrocatalytic current signal. If these labels are arranged in a low coverage level, the induced change in background current will be small which results in a large change in signal along with

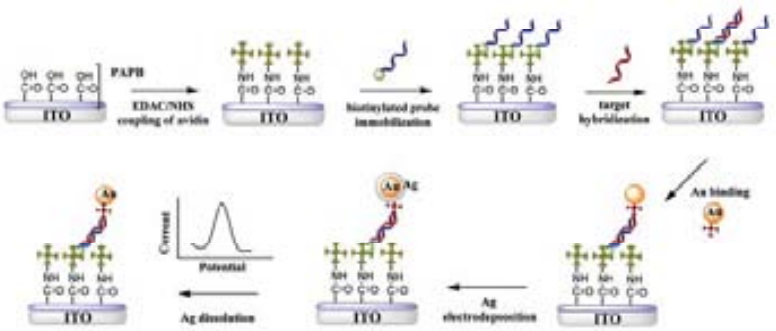

Figure 5.3. Schematic representation of the electrocatalytic effect of Au-NPs on silver electrodeposition on ITO-based electrodes applied for the DNA hybridization detection (adapted from Ref. 26 with permission).

low backgrounds, that is, possibility to achieve very low detection limits. However, the conjugation of the electrocatalytic labels with biomolecules may decrease their electrocatalytic activity, and a long distance between the electrode and the labels may also produce an undesired slow electron tunneling between them, even if the label exhibits a high electrocatalytic activity itself. To overcome these problems, it is possible to enhance the electrocatalytic activity of labels by electrochemical, thermal, or chemical treatment. Thermal and electrochemical treatments may damage the sensing layers during the detection process, since, respectively, high temperatures and extreme applied potentials are often necessary. But mild chemical treatments can be a desirable option [11].

When Au-NP labels are present near an electrode they can act as (electro)catalytic agents. However if the electrocatalytic reaction is not reproducible, which jeopardizes the achievement of low detection limits, the electrocatalytic reaction should be minimized and the electrochemical signal should arise only from the catalytic reaction [7]. The latest can be done by limiting the electron transfer between nanoparticles and the electrode through the use of nonconductive spacers like other particles, organic monolayers, etc. [11, 27, 28].

Selvaraju *et al.* [11] reported the use of Au-NPs as catalytic labels to achieve ultrasensitive DNA detection via fast catalytic reactions involved in p-nitrophenol reduction in presence of $NaBH_4$. In order

to minimize the electrocatalytic oxidation of $NaBH_4$ by Au-NPs they used magnetic beads as capture probe immobilization platforms that acted also as spacers between Au-NPs and the ferrocene-modified ITO electrode, achieving this effect only when the density of Au-NPs at magnetic beads surface is low. The Au-NPs used as labels, were modified with a monolayer of DNA detection probe, without a significant loss in catalytic activity of Au-NPs for signal amplification. By the conjugation of all the mentioned techniques they achieved good signal amplification with low background current and a detection limit of 1fM for DNA target with good target discrimination.

Recently, Yang's group [7] reported a novel strategy for Au-NP–based signal enhancement by the improvement of electrocatalytic activity of labels. The DNA layer on the Au-NPs does not significantly limit the mass transfer of small molecules and ions such as p-hydroquinone and Ag^+, or inhibits the catalytic reduction of p-nitrophenol. However, the distance between the electrocatalytic Au-NP label and the ITO electrode is too long and the enhancement by electrochemical treatment requires extremely applied potentials. To overcome this problem, this same group applied a simple chemical treatment of Au-NPs by using $NaBH_4$ instead of electrochemical treatment (Fig. 5.4). The results showed that $NaBH_4$ treatment could significantly enhance electrocatalytic activity of DNA-conjugated Au-NPs toward the hydrazine current on the ITO electrodes, without damaging the biosensing layers. This result, in combination with the electrode modification with Au-NPs, allowed a high signal current

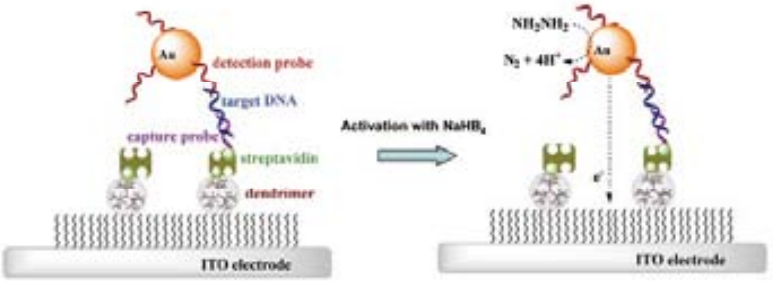

Figure 5.4. Schematic view of electrochemical DNA detection using the enhanced electrocatalytic activity of Au-NP labels toward hydrazine (NH_2NH_2) reduction on ITO electrodes (adapted from Ref. 7 with permission).

whereas the low intrinsic electrocatalytic activity of ITO electrodes minimized the background current. With this method, 1fM of target DNA in an electrochemical DNA sensor was detected without the need of target or enzymatic signal amplification [29].

5.2.3 *Electrocatalytic Activity of Gold Nanoparticles Used as Modifiers of Electrotransducer Surfaces*

Another application of metal nanoparticles in electrochemical detection of DNA is their incorporation with composites used as electrode surface modifiers. Even though these modified electrodes can show higher background signals than the unmodified electrodes, the incorporation of Au-NPs can be used to promote selective immobilization spots to well-oriented DNA detection probes.

Liu *et al.* [9] have recently reported the application of composites of Au-NPs and multi-walled carbon nanotubes (Au-NPs/MWCNT) for enhancing the electrochemical detection of DNA hybridization. Au-NPs were deposited onto the surface of MWCNTs by one-step reaction and then a thiolated-DNA probe was immobilized onto the Au-NPs/MWCNTs–modified glassy carbon electrode (GCE) through the strong gold–sulfur linkage, which could control the molecular orientation of probe DNA. On the basis of DNA detection it was found that the Au-NP/MWCNT composites could highly improve the sensitivity of DNA biosensor due to their enhanced conductivity and increased effective surface area. Furthermore, it was revealed that selectivity and reproducibility of the DNA sensor were also excellent. which resulted in a significant platform for the hybridization detection of DNA.

5.3 Catalysis Induced by Platinum and Palladium Nanoparticles

5.3.1 *Electrocatalytic Activity of Platinum Nanoparticle Labels*

Despite the high cost of this metal in the bulk state, the subsequent saving that reducing the metal size implies placed platinum nanoparticles (Pt-NPs) in the centre of attention of scientists due to their ability to be used as catalyst for many industrial processes [13].

Pt-NPs are used as catalysts for electrochemical hydrogen peroxide (H_2O_2) detection, where they act as modifiers of the electrode surface and electrocatalyze the oxidation of H_2O_2 observed by a lower oxidation peak potential when compared with the bulk platinum electrode [30]. As the H_2O_2 is a product of many enzymatic reactions, this electrode has a vast potential application as an electrochemical biosensor for many substances [15].

Pt-NPs have also been used as catalysts in gas sensors like nitric oxide (NO) sensor making use of the electrocatalytic effect in the oxidation of this specie [31]. In conjugation with carbon nanotubes (CNTs) and glutaraldehyde, Pt-NPs also allowed the development of a carbon-based electrode as a sensor for glucose, in a similar system as one of the reported H_2O_2 sensors [13].

Regarding its application in DNA sensors, Polsky *et al.* [10] used nucleic acid functionalized Pt-NPs as catalytic labels to amplify the electrochemical detection of both DNA hybridization and aptamer/protein recognition. The assay was based on the catalytic effect of the Pt-NPs on the reduction of H_2O_2 to H_2O, using gold slides as electrodes. The amperometric measurement of the electrocatalyzed reduction of H_2O_2 detected DNA with a LOD of 1×10^{-11} M.

N. Zhu *et al.* [32] reported in 2005 the use of Pt-NPs combined with nafion-solubilized MWCNTs as electrode-surface modifiers for fabricating sensitivity-enhanced electrochemical DNA biosensor. The hybridization events were monitored by DPV measurements of the intercalated daunomycin (Fig. 5.5). Due to the ability of MWCNTs to promote electron-transfer reactions and the high

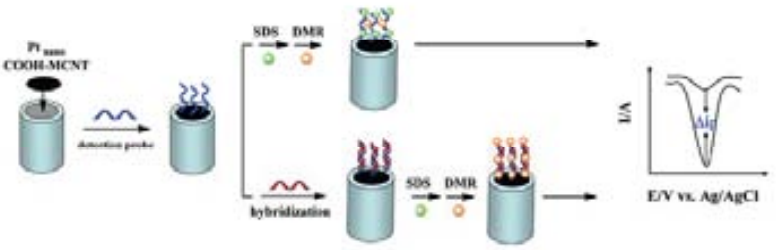

Figure 5.5. Schematic representation of the electrochemical detection of DNA hybridization based on Pt-NPs combined with MWCNTs (adapted from Ref. 32 with permission).

Chapter 5

Nanoparticle-Induced Catalysis for Electrochemical DNA Biosensors

Marisa Maltez-da Costa,[a] Alfredo de la Escosura-Muñiz,[a] and Arben Merkoçi[a,b]

[a] *Nanobioelectronics & Biosensors Group, Institut Català de Nanotecnologia, CIN2 (ICN-CSIC), Esfera Universitat Autònoma de Barcelona, Bellaterra, Barcelona, Spain*
[b] *ICREA, Barcelona, Spain*
arben.merkoci.icn@uab.es

In this chapter, the use of nanoparticles (NPs) in catalytic electrochemical analysis of DNA as a new detection strategy reported in recent years is revised. The topics covered here include labeling with nanoparticles and their subsequent signal enhancement employed for DNA hybridization detection. Direct sensing of nanoparticle labels as well as indirect detection routes through electrochemical sensing of label-catalyzed reactions have been reported. Nanofabrication of platforms used for the detection of DNA through electrochemical signal amplification has also been revised. Some recent examples of interesting nanoparticle-induced catalytic methodologies applied for protein detection using electrochemical biosensors are also given, because of their potential interest in future applications in DNA detection.

Electrochemical DNA Biosensors
Edited by Mehmet Ozsoz

www.panstanford.com

5.1 Introduction

Various nanomaterials, including carbon nanotubes, nanoparticles, nanomagnetic beads, and nanocomposites, are being used to develop highly sensitive and robust biosensors and biosensing systems [1] with a special emphasis on the development of electrochemical-based (bio)sensors [2, 3] due to their simplicity and cost efficiency.

One of the main requirements for a good performance of a biosensor is the high sensitivity of the response. This is of great importance when, for example, it is required to use the biosensor in clinical diagnostics for the detection of low levels of clinical biomarkers in human fluids [4], because in most cases the biomarker to be detected is present in very low concentrations. The need for biosensing systems that can detect these markers with high sensitivity without loss of selectivity, that is, low detection limits with high reliability and superior reproducibility, is becoming an important challenge.

The amplified detection of biorecognition events and specifically of DNA hybridization events stands out of the biosensing field, because it is one of the most important objectives of the current bioanalytical chemistry. In this context, approaching the catalytic properties of some (bio)materials appears to be a promising way to enhance the sensitivity of the bioassays.

Catalysts are materials that change the rate of chemical reactions without being consumed in the process. Because of their huge economical contribution, by lowering the costs of several processes, they are actually one of most wanted materials and can be found in manufacturing processes, fuel cells, combustion devices, pollution control systems, food processing, and sensor systems. Catalysts are generally prepared from transition metals, most of them from the platinum group, but this fact still represents a high cost due to the material expensiveness, and thus a reduction in used amounts would be appreciated [5, 6].

The coupling of enzymes as biocatalytic amplifying labels is a generated paradigm in developing bioelectronic sensing devices. The biocatalytic generation of a redox product upon binding of the label to the recognition event, the incorporation of redox

mediators into DNA assemblies that activate bioelectrocatalytic transformations, or the use of enzyme labels that yield an insoluble product on electrode surfaces has been extensively used to amplify biorecognition events. Due to the several problems associated with these techniques and the fast development in nanotechnology, nanoparticle-assisted signal enhancement for DNA biosensors has been greatly developed in the last decade [7, 8, 9, 10, 11].

In electrochemical sensors, electrocatalytic procedures can be approached in two ways, either by using an electrode that have highly or moderately electrocatalytic properties, or by exploiting a significant change in the electrocatalytic activity of an electrode during the detection process. Gold and platinum are commonly employed as highly electrocatalytic electrodes. Although these electrodes allow fast electron-transfer kinetics for most electroactive species, their background currents are high and fluctuate with the applied potential, which may make difficult to obtain the high signal-to-background ratios, required to achieve low detection limits. In recent years, moderately electrocatalytic electrodes have been used to obtain high signal-to-background ratios. Such electrodes can be obtained by modifying a poorly electrocatalytic electrode with a low coverage of a highly electrocatalytic material. For example, indium-tin oxide (ITO) electrodes modified with a partial monolayer of ferrocene, carbon nanotubes, or gold nanoparticles (Au-NPs) have been employed [7, 11].

The actual knowledge concerning the special properties of NPs arises from the numerous studies related to the effects of changes in shape and size on the general properties of materials. From the electroanalysis point of view the major features resulting from these studies are enhancement of mass transport, high catalytic activity, high effective surface area, and control over local microenvironment at the electrode surface [8, 12, 13, 14].

The development of nanotechnology during the last decades has led scientists to fabricate and analyze catalysts at the nanoscale. These nanostructured materials are usually high-surface-area metals or semiconductors in the form of NPs with excellent catalytic properties due to the high ratio of surface atoms with free valences to the cluster of total atoms. The catalysis takes place on the active surface sites of metal clusters in a similar mechanism as the

conventional heterogeneous catalysis [12] and in general, this is a process that occurs at the molecular or atomic level independent of the catalyst dimensions [6, 14]. There is a considerable amount of research articles and interesting reviews in what concerns to the study of nanoparticle-catalyzed reactions, but the application of these reactions in electrochemical analysis is not so well documented.

Employing NPs in electroanalysis can induce more sensitive and selective sensors as well as more cost-effective and portable systems. Their application as catalysts in electroanalytical systems can decrease overpotentials of many important redox species, inducing discrimination between different electroactive analytes, and also allowing the occurrence and reversibility of some redox reactions, which are irreversible at common modified electrodes [15]. The catalytic effect can be explained through the enhancement of electron transfer between the electrode surface and the species in solution, by enhancement of mass transport or also by the NPs' high surface energy that allows the preferred adsorption of some species that by this way suffer a change in their overpotentials (Fig. 5.1).

The most exploited materials in catalysis are the metals from platinum group, but with the introduction of nanotechnology some other elements that in bulk state did not attract a lot of attention, either due to their lack of reactivity toward some analytes or due to their high costs in production, are now emerging.

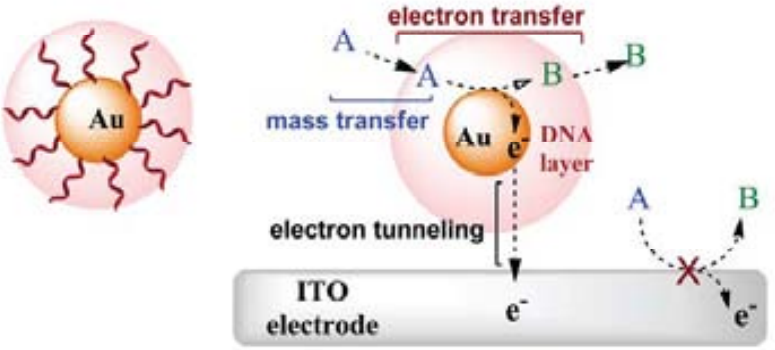

Figure 5.1. Schematic illustration of the processes that affect the electrocatalytic oxidation by Au-NP when functionalized with DNA strands (adapted from Ref. 7 with permission).

5.2 Catalysis Induced by Gold Nanoparticles

Gold nanoparticles (Au-NPs) and silver nanoparticles (Ag-NPs) are of particular interest in DNA sensors and immunosensors due to their advantageous properties, such as hydrophilicity, standard fabrication methods, excellent biocompatibility, unique characteristics in the conjugation with biological recognition elements, and multiplex capacity for signal transducer. Therefore, a large number of published methods use Au- or Ag-NPs in DNA [16, 17, 18] protein [19] and even cell [20] electrochemical detection besides optical detections like ICP-MS [21] or their use as ELISA enhancer [22].

Metallic gold was thought to be very stable and useless for some catalytic systems, but by the reduction of size to the nanoscale range, gold has been proved to be a very reactive element and it has been extensively used in sensing and biosensing systems as a catalyst for some interesting electroanalytical applications. For instance, a sensitive NO sensor was developed through the modification of a platinum microelectrode by Au-NPs in which they catalyze the electrochemical oxidation of NO with an overpotential decrease of about 250 mV [15]. An SO_2 gas sensor was also developed using Au-NPs to catalyze the electrochemical oxidation of SO_2 when the gas diffuses through the pores of the working electrode [23].

Based on the selective catalysis of Au-NPs, selective electrochemical analysis could also be achieved as, for example, in the dopamine electrochemical detection in presence of ascorbic acid. In this case, Au-NPs can be used as selective catalysts since their presence induces the decreasing of ascorbic acid overpotential and the effective separation of the oxidation potentials of ascorbic acid and dopamine [13].

5.2.1 *Electrocatalytic Activity of Gold Nanoparticle Labels on Silver Deposition*

Wang *et al.* [24] first reported a DNA hybridization detection method based on the precipitation of silver on Au-NP tags and subsequent electrochemical stripping detection of the dissolved silver. The assay employed a sandwich-like protocol with streptavidin–Au-NPs labeling the biotinylated-breast cancer gene (BRCA1) sequences.

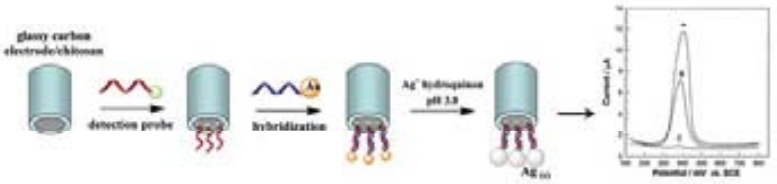

Figure 5.2. Schematic diagram of the silver chemical deposition on Au-NP labels applied for the electrochemical detection of DNA hybridization. Voltammograms correspond to DPV responses of the Au-NP–labeled oligonucleotide probes in presence of (A) complementary, (B) single-base mismatch, and (C) non-complementary oligonucleotides (adapted from Ref. 25 with permission).

After the silver precipitation on the gold, the silver was dissolved and detected at a disposable thick film carbon electrode using potentiometric stripping. This method coupled the inherent signal amplification of nanoparticle-promoted silver precipitation and the stripping metal analysis with effective discrimination against non-hybridized DNA. Cai *et al.* [25] reported a similar assay based on the silver deposition onto Au-NP–labeled oligonucleotides and subsequent electrochemical detection of Ag ions anchored onto Au-NPs connected to hybrids through differential pulse voltammetry using a glassy carbon electrode (Fig. 5.2). With this assay they obtained a detection limit of 50 pM of complementary oligonucleotides.

Later on, Lee *et al.* [26] reported the electrocatalytic effect of Au-NPs on silver electrodeposition upon ITO-based electrodes (Fig. 5.3), in absence of pre-oxidation steps, and its successful application to the DNA hybridization detection obtaining a signal-to-noise ratio of 20 that presented a great improvement in relation to their previous works under similar conditions.

5.2.2 *Electrocatalytic Activity of Gold Nanoparticle Labels on Other Reactions*

The specific binding of highly electrocatalytic labels to a biosensing layer immobilized on poor electrocatalytic electrode enhances the electrocatalytic current signal. If these labels are arranged in a low coverage level, the induced change in background current will be small which results in a large change in signal along with

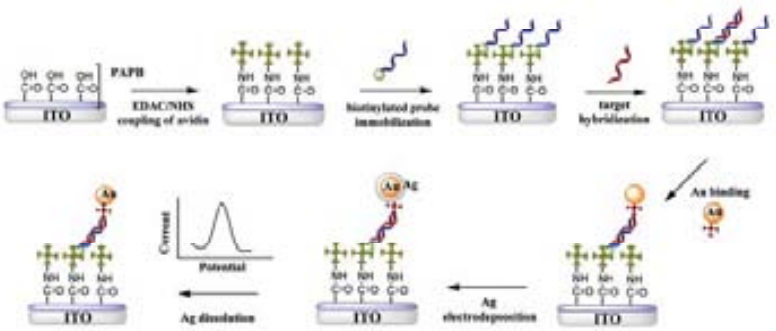

Figure 5.3. Schematic representation of the electrocatalytic effect of Au-NPs on silver electrodeposition on ITO-based electrodes applied for the DNA hybridization detection (adapted from Ref. 26 with permission).

low backgrounds, that is, possibility to achieve very low detection limits. However, the conjugation of the electrocatalytic labels with biomolecules may decrease their electrocatalytic activity, and a long distance between the electrode and the labels may also produce an undesired slow electron tunneling between them, even if the label exhibits a high electrocatalytic activity itself. To overcome these problems, it is possible to enhance the electrocatalytic activity of labels by electrochemical, thermal, or chemical treatment. Thermal and electrochemical treatments may damage the sensing layers during the detection process, since, respectively, high temperatures and extreme applied potentials are often necessary. But mild chemical treatments can be a desirable option [11].

When Au-NP labels are present near an electrode they can act as (electro)catalytic agents. However if the electrocatalytic reaction is not reproducible, which jeopardizes the achievement of low detection limits, the electrocatalytic reaction should be minimized and the electrochemical signal should arise only from the catalytic reaction [7]. The latest can be done by limiting the electron transfer between nanoparticles and the electrode through the use of nonconductive spacers like other particles, organic monolayers, etc. [11, 27, 28].

Selvaraju *et al.* [11] reported the use of Au-NPs as catalytic labels to achieve ultrasensitive DNA detection via fast catalytic reactions involved in p-nitrophenol reduction in presence of $NaBH_4$. In order

to minimize the electrocatalytic oxidation of $NaBH_4$ by Au-NPs they used magnetic beads as capture probe immobilization platforms that acted also as spacers between Au-NPs and the ferrocene-modified ITO electrode, achieving this effect only when the density of Au-NPs at magnetic beads surface is low. The Au-NPs used as labels, were modified with a monolayer of DNA detection probe, without a significant loss in catalytic activity of Au-NPs for signal amplification. By the conjugation of all the mentioned techniques they achieved good signal amplification with low background current and a detection limit of 1fM for DNA target with good target discrimination.

Recently, Yang's group [7] reported a novel strategy for Au-NP–based signal enhancement by the improvement of electrocatalytic activity of labels. The DNA layer on the Au-NPs does not significantly limit the mass transfer of small molecules and ions such as p-hydroquinone and Ag^+, or inhibits the catalytic reduction of p-nitrophenol. However, the distance between the electrocatalytic Au-NP label and the ITO electrode is too long and the enhancement by electrochemical treatment requires extremely applied potentials. To overcome this problem, this same group applied a simple chemical treatment of Au-NPs by using $NaBH_4$ instead of electrochemical treatment (Fig. 5.4). The results showed that $NaBH_4$ treatment could significantly enhance electrocatalytic activity of DNA-conjugated Au-NPs toward the hydrazine current on the ITO electrodes, without damaging the biosensing layers. This result, in combination with the electrode modification with Au-NPs, allowed a high signal current

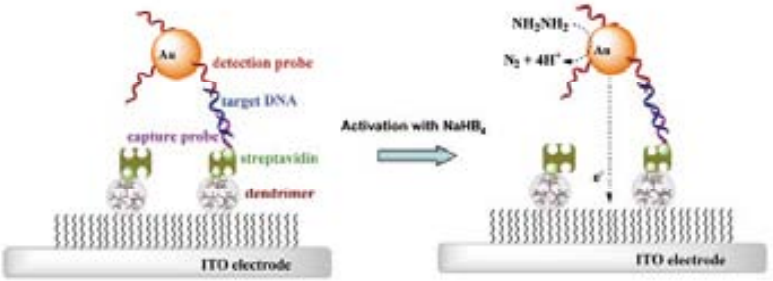

Figure 5.4. Schematic view of electrochemical DNA detection using the enhanced electrocatalytic activity of Au-NP labels toward hydrazine (NH_2NH_2) reduction on ITO electrodes (adapted from Ref. 7 with permission).

whereas the low intrinsic electrocatalytic activity of ITO electrodes minimized the background current. With this method, 1fM of target DNA in an electrochemical DNA sensor was detected without the need of target or enzymatic signal amplification [29].

5.2.3 *Electrocatalytic Activity of Gold Nanoparticles Used as Modifiers of Electrotransducer Surfaces*

Another application of metal nanoparticles in electrochemical detection of DNA is their incorporation with composites used as electrode surface modifiers. Even though these modified electrodes can show higher background signals than the unmodified electrodes, the incorporation of Au-NPs can be used to promote selective immobilization spots to well-oriented DNA detection probes.

Liu *et al.* [9] have recently reported the application of composites of Au-NPs and multi-walled carbon nanotubes (Au-NPs/MWCNT) for enhancing the electrochemical detection of DNA hybridization. Au-NPs were deposited onto the surface of MWCNTs by one-step reaction and then a thiolated-DNA probe was immobilized onto the Au-NPs/MWCNTs–modified glassy carbon electrode (GCE) through the strong gold–sulfur linkage, which could control the molecular orientation of probe DNA. On the basis of DNA detection it was found that the Au-NP/MWCNT composites could highly improve the sensitivity of DNA biosensor due to their enhanced conductivity and increased effective surface area. Furthermore, it was revealed that selectivity and reproducibility of the DNA sensor were also excellent. which resulted in a significant platform for the hybridization detection of DNA.

5.3 Catalysis Induced by Platinum and Palladium Nanoparticles

5.3.1 *Electrocatalytic Activity of Platinum Nanoparticle Labels*

Despite the high cost of this metal in the bulk state, the subsequent saving that reducing the metal size implies placed platinum nanoparticles (Pt-NPs) in the centre of attention of scientists due to their ability to be used as catalyst for many industrial processes [13].

Pt-NPs are used as catalysts for electrochemical hydrogen peroxide (H_2O_2) detection, where they act as modifiers of the electrode surface and electrocatalyze the oxidation of H_2O_2 observed by a lower oxidation peak potential when compared with the bulk platinum electrode [30]. As the H_2O_2 is a product of many enzymatic reactions, this electrode has a vast potential application as an electrochemical biosensor for many substances [15].

Pt-NPs have also been used as catalysts in gas sensors like nitric oxide (NO) sensor making use of the electrocatalytic effect in the oxidation of this specie [31]. In conjugation with carbon nanotubes (CNTs) and glutaraldehyde, Pt-NPs also allowed the development of a carbon-based electrode as a sensor for glucose, in a similar system as one of the reported H_2O_2 sensors [13].

Regarding its application in DNA sensors, Polsky *et al.* [10] used nucleic acid functionalized Pt-NPs as catalytic labels to amplify the electrochemical detection of both DNA hybridization and aptamer/protein recognition. The assay was based on the catalytic effect of the Pt-NPs on the reduction of H_2O_2 to H_2O, using gold slides as electrodes. The amperometric measurement of the electrocatalyzed reduction of H_2O_2 detected DNA with a LOD of 1×10^{-11} M.

N. Zhu *et al.* [32] reported in 2005 the use of Pt-NPs combined with nafion-solubilized MWCNTs as electrode-surface modifiers for fabricating sensitivity-enhanced electrochemical DNA biosensor. The hybridization events were monitored by DPV measurements of the intercalated daunomycin (Fig. 5.5). Due to the ability of MWCNTs to promote electron-transfer reactions and the high

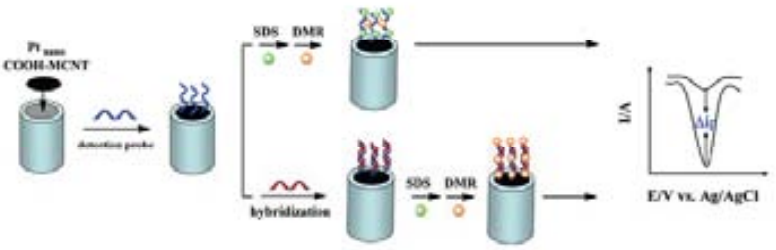

Figure 5.5. Schematic representation of the electrochemical detection of DNA hybridization based on Pt-NPs combined with MWCNTs (adapted from Ref. 32 with permission).

catalytic activities of Pt-NPs for chemical reactions, the sensitivity was remarkably improved achieving a detection limit of 0.1 pM of target DNA. The results showed that this DNA hybridization biosensor responded more sensitively to target DNA than those based on Pt-NPs or MWCNTs only.

5.3.2 *Electrocatalytic Activity of Palladium Nanoparticle Labels*

Palladium belongs to the platinum group of metals, and, due to its similar features in terms of electrocatalytic alctivity toward numerous redox reactions, it has been used in electrode modification processes in several electrochemical sensors [33]. Palladium nanoparticles (Pd-NPs) were applied in several electrochemical biosensors. For instance, a glucose biosensor based on codeposition of Pd-NPs and glucose oxidase onto carbon electrodes [34], encapsulated channels for protein biosensing and the reduction of H_2O_2 [35], and a DNA-template preparation of Pd-NPs onto ITO for H_2O_2 reduction and ascorbic acid oxidation, has been reported [33].

In the work reported by Chang *et al.* [36], Pd-NPs in combination with MWCNTs were used to fabricate an electrochemical DNA biosensor with enhanced sensitivity. Methylene blue (MB) was used as hybridization indicator and a method with high sensitivity and effective electrochemical discrimination against complementary DNA, by coupling the large surface area and effective electron transfer of MB redox from MWCNTs and the catalysis of the MB redox reaction by Pd-NPs, was achieved. The Pd-NPs/MWCNTs significantly increased the DNA hybridization signal to push down the detection limits and facilitate potential manipulation of the modified glassy carbon electrode. The LOD obtained was 0.12 pM for target DNA. The catalytic activity of Pd-NPs employed in this work is related to their ability to adsorb/release the involved hydrogen atoms promoting the electronic transfer during the MB redox reaction.

An ultrasensitive DNA sensor using the rapid enhancement and electrocatalytic activity of DNA-conjugated Pd-NPs on $NaBH_4$ hydrolysis was reported by Yang's group [37]. After a previous

catalytic activities of Pt-NPs for chemical reactions, the sensitivity was remarkably improved achieving a detection limit of 0.1 pM of target DNA. The results showed that this DNA hybridization biosensor responded more sensitively to target DNA than those based on Pt-NPs or MWCNTs only.

5.3.2 *Electrocatalytic Activity of Palladium Nanoparticle Labels*

Palladium belongs to the platinum group of metals, and, due to its similar features in terms of electrocatalytic alctivity toward numerous redox reactions, it has been used in electrode modification processes in several electrochemical sensors [33]. Palladium nanoparticles (Pd-NPs) were applied in several electrochemical biosensors. For instance, a glucose biosensor based on codeposition of Pd-NPs and glucose oxidase onto carbon electrodes [34], encapsulated channels for protein biosensing and the reduction of H_2O_2 [35], and a DNA-template preparation of Pd-NPs onto ITO for H_2O_2 reduction and ascorbic acid oxidation, has been reported [33].

In the work reported by Chang *et al.* [36], Pd-NPs in combination with MWCNTs were used to fabricate an electrochemical DNA biosensor with enhanced sensitivity. Methylene blue (MB) was used as hybridization indicator and a method with high sensitivity and effective electrochemical discrimination against complementary DNA, by coupling the large surface area and effective electron transfer of MB redox from MWCNTs and the catalysis of the MB redox reaction by Pd-NPs, was achieved. The Pd-NPs/MWCNTs significantly increased the DNA hybridization signal to push down the detection limits and facilitate potential manipulation of the modified glassy carbon electrode. The LOD obtained was 0.12 pM for target DNA. The catalytic activity of Pd-NPs employed in this work is related to their ability to adsorb/release the involved hydrogen atoms promoting the electronic transfer during the MB redox reaction.

An ultrasensitive DNA sensor using the rapid enhancement and electrocatalytic activity of DNA-conjugated Pd-NPs on $NaBH_4$ hydrolysis was reported by Yang's group [37]. After a previous

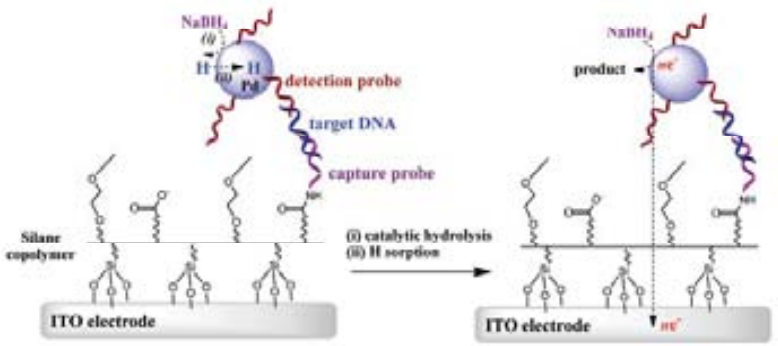

Figure 5.6. Schematic representation of the electrochemical DNA detection using the catalytic and electrocatalytic oxidation of $NaBH_4$ on Pd-NP labels onto ITO electrodes and the rapid enhancement of electrocatalytic activity of DNA-conjugated Pd-NPs (adapted from Ref. 37 with permission).

similar work with Au-NPs as electrocatalytic labels [11], they recently reported Pd-NPs, activated by $NaBH_4$, as ideal electrocatalytic labels for DNA detection (Fig. 5.6) that work even at high pH levels with reduced incubation time. The high pH is necessary in order to avoid the self-hydrolysis of $NaBH_4$ at lower values, even though the catalytic hydrolysis of $NaBH_4$ can be slower at this pH. The resulting sensor achieved an LOD of 10 aM (BRCA1 associated gene sequence) with a detection range of 10 orders of magnitude, using an ITO electrode as substrate and following the hybridization process by linear sweep voltammetry. The rapid enhancement comes from the fast catalytic hydrolysis of $NaHB_4$ onto Pd-NPs' surfaces and subsequent fast hydrogen sorption into Pd-NPs. The electrocatalytic activity of DNA-conjugated Pd-NPs allows high currents for the electro-oxidation within the potential windows.

5.4 Catalysis Induced by Other Nanoparticles

5.4.1 *Electrocatalytic Activity of Titanium Dioxide Nanoparticle Labels*

Metal oxides are emerging as important materials because of their versatile properties such as high-temperature superconductivity,

ferroelectricity, ferromagnetism, piezoelectricity, and semiconductivity [38].

Recently, nanostructured TiO_2 particle (TiO_2-NP) preparation and their applications in photovoltaic studies, photocatalysis, and environmental studies have attracted much attention mostly in the emerging sensor technology based on nanoparticles and nanocomposites with chemical and biological molecules [33]. In protein-based biosensors the efficient electrical communication between redox proteins and solid electrode surfaces is still an important request, and many methods have been tried in order to obtain direct electrochemical responses of proteins embedded in surface modifier films. An example for the latter is the work presented by Zhou *et al.* [39] where the photovoltaic effect of TiO_2-NPs, induced by ultraviolet light, can greatly improve the catalytic activity of hemoglobin as a peroxidase with increased sensitivity when compared to the catalytic reactions in the dark, which indicates a possible method to tune the properties of proteins for development of photocontrolled protein-based biosensors. The method claims an enhancement in the catalytic activity of hemoglobin, by a specific interaction with 35 nm TiO_2-NP, toward the H_2O_2 reduction. This catalytic effect was not observed by other comparative experiments with films containing nanostructured CdS or ZnO_2.

The advances in hybrid nanotechnology involving nucleic acids are mostly linked with sequence-specific nucleic acid interactions. TiO_2-oligonucleotide nanocomposites retain the intrinsic photocatalytic capacity of TiO_2 as well as the bioactivity of the oligonucleotide DNA; therefore, the developments in this area have been oriented toward cellular imaging and protein or DNA sensor microarrays [38].

Lo *et al.* [38] reported a nanocomposite biosensor for the amperometric detection of H_2O_2 based on thionin incorporated bilayer of DNA/nano-TiO_2 film-modified electrode. Furthermore, this system showed electrocatalytic activity toward the O_2 and H_2O_2 reduction in physiological conditions.

A nano-TiO_2 substrate in combination with Au-NP–modified DNA probe was used by Lu *et al.* [40] to develop a novel photoelectrochemical method for quantitative detection of the linear DNA hybridization. In the detection process schematized in

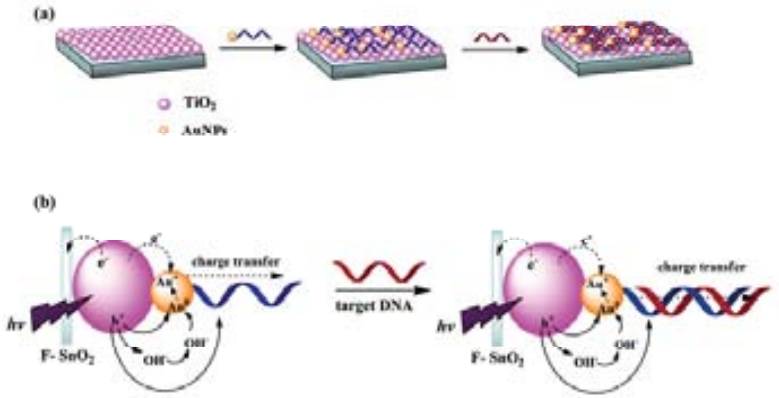

Figure 5.7. Schematic illustration of the fabrication of Au-DNA probe modified TiO_2 electrode and the detection of target DNA (A) and the photo-induced processes of electron-hole generation and charge transfer processes (B) (adapted from Ref. 40 with permission).

Fig. 5.7, the probe immobilization and the following hybridization induced the photocurrent change of the TiO_2 electrode that was enhanced with the Au-NP–DNA probe immobilization, and then gradually decreased with increasing the concentration of the target DNA. They could effectively discriminate the hybridization from un-hybridization processes, and potentiate this system as a biosensor to study a wide variety of biological processes.

A very recent work from Hu *et al.* [41] proposes a direct electrochemical detection procedure for DNA hybridization using the electrochemical signal changes of conductive poly(m-amino-benzenosulfonic) acid (PABSA)/TiO_2 nanosheet membranes, which were electropolymerized by pulse potentiostatic method (see scheme in Fig. 5.8). The polymerization efficiency is greatly improved by the use of TiO_2-NPs, and their combination with PABSA resulted in a highly conductive composite membrane with unique and novel nanosheet morphology (80 nm thick ramified membrane) that provides more activation sites and enhances the surface electron-transfer rate. Furthermore these nanosheets presented good redox activity and electroconductivity even in neutral environment (PBS solution of pH 7.0), and the DNA probes could be easily covalently immobilized, so that the hybridization

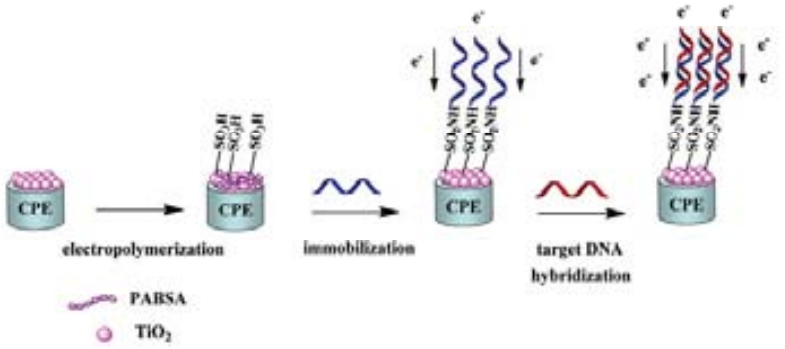

Figure 5.8. Schematic representation of the immobilization and hybridization of DNA on the PABSA/TiO_2 nanosheets (adapted from Ref. 41 with permission).

event could be monitored through impedance measurements. The LOD obtained was 1.7 pM of target probe (CaMV35S gene sequence) with a RSD of 4.91% (for 1.0 μM of target DNA) and the biosensor selectivity was tested with non-complementary and double-base mismatched sequences. Since this hybridization detection does not require labeling of the oligonucleotide probe or target prior to the assay, this procedure results in an advantageous method in terms of simplicity, non-invasiveness, and low costs.

5.4.2 *Electrocatalytic Activity of Osmium Oxide Nanoparticle Labels*

Isoniazid-capped 25 nm osmium oxide nanoparticles (OsO_2-NPs) were reported by Gao and Yang [42] as successfully electrocatalytic tags in a microRNA ultrasensitive detection system, schematized in Fig. 5.9. The assay employs an ITO electrode with immobilized capture probes (antisense to microRNAs for testing) and after hybridization with periodate-treated microRNAs, the OsO_2-NP tags are brought to the electrode through a condensation reaction between isoniazid molecules, grafted onto the nanoparticles and the 3'-end dialdehydes of the microRNA in a hydrazine PBS buffer. The readout oxidation potential of hydrazine was directly correlated to the concentration of the hybridized microRNA and the assay

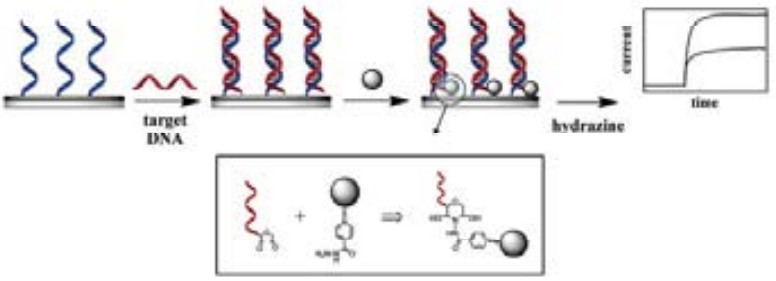

Figure 5.9. Schematic illustration of miRNA assay using electrocatalytic OsO_2-NPs (adapted from Ref. 42 with permission).

reported a linear relationship between current and concentration from 0.3 to 200 pM microRNA with a measureable signal reported for as low as 80 fM microRNA in 2.5 mL droplets following 60 min hybridization. Successful attempts were made in the microRNA expression analysis of HeLa cells.

Additionally the assay can easily distinguish between a single base mismatch, with a signal detected for fully matched microRNA, and less than 25% signal reported for mismatched microRNA. These results are comparable to the previous electrochemical microRNA detection by this group [43], and offer many of the same advantages over more conventional methods, such as PCR-based and Northern blot techniques. The use of OsO_2-NPs in preference to the electrocatalytic moieties presented previously by this group offers additional advantages for the electrocatalytic quantification of microRNA. These advantages include control over the choice of the capping groups on the nanoparticle, which simplifies their ligation to the microRNA and the improved catalytic effect on the oxidation of the hydrazine that results in improved signal. However, the authors do not address the efficiency and reliability of the conjugation of the nanoparticle tags to the microRNA [43].

5.4.3 *Electrocatalytic Activity of Other Nanoparticles*

Other non-metal particles have also been described as possible catalysts in electroanalytical systems [13, 33]. For example, copper oxide nanoparticles (CuO-NPs) of 5 nm size were mixed with

graphite powder and used as catalysts for the electrochemical detection of amikacin antibiotic oxidation, achieving a 40 times higher current than with a bulk CuO-modified carbon paste electrode [15]. Cu_2O hollow spheres (150–220 nm sized spherical aggregations of small Cu_2O-NPs) were applied by Zhu *et al.* [44] in electrochemical DNA sensing using a carbon paste electrode and MB as the hybridization indicator. They make use of these particles as enhancers to the ssDNA probe immobilization on the electrode surface to obtain a sensitive detection of Hepatitis B virus DNA sequences by differential pulse voltammetry.

More recently, Prussian blue nanoparticles (PB-NPs) were found to catalyze the electrochemical reduction of H_2O_2 when immobilized in the form of layers on ITO electrodes [14]. The application of PB-NPs as catalytic labels for highly sensitive detection of DNA hybridization was also reported based on their catalytic effect toward H_2O_2 when embedded in polystyrene spheres and loaded onto a gold-disk electrode [45].

Iron and iron oxide nanoparticles (Fe and Fe_3O_4-NPs) also present catalytic properties in electroanalysis. Fe-NPs were described as efficient and selective catalysts in the electrochemical detection of H_2O_2 in the presence of O_2 by facilitating the electron transfer between adsorbates and the glassy carbon electrode surface. Fe_3O_4-NPs were used to modify a crystalline gold electrode for the electrochemical detection of dopamine. They showed good catalytic activity by lowering the dopamine oxidation overpotential, allowing the dopamine and ascorbic acid peaks to become separated and resolvable and with even lower detection limits than the Au-NP system referred above [13].

5.5 Conclusions

The induced catalysis by NPs is showing special interest in the DNA biosensing technology. The application of NPs as catalysts in DNA detection systems is related to the decrease of overpotentials of the involved redox species including also the catalyzed reduction of other metallic ions used in labeling-based hybridization sensing. Although the most exploited materials in catalysis are the metals

from platinum group, with the introduction of nanotechnology and the increasing interest for biosensing applications, gold nanoparticles, due to their facile conjugation with biological molecules, besides other advantages, are being shown to be the most used. Their applications as either electrocatalytic labels or modifiers of DNA related transducers are bringing important advantages in terms of sensitivity and detection limits in addition to other advantages.

Ag-NPs are not so commonly used as Au-NPs but nevertheless their catalytic properties in electrochemical detection have also been exploited. For instance, they were reported as promoters for electron transfer between the graphite electrode and hemoglobin in a NO sensor system where they also act as a base to attach the hemoglobin onto a pyrolytic graphite electrode while preserving the hemoglobin natural conformation and therefore its reactivity [46]. With respect to the application of silver catalytic properties on DNA hybridization detection, the published works refer mostly to its use in combination with Au-NPs by means of chemical or electrochemical silver deposition onto them [29].

The catalytic properties of nanoparticles used in protein detection can also be extended to DNA analysis. For example, the selective electrocatalytic reduction of silver ions onto the surface of Au-NP reported by our group and applied for protein detection can be extended to DNA analysis too [47]. The hydrogen catalysis reaction induced by Au-NPs [48] and applied even for cancer cells detection [20] is expected to bring advantages for DNA detection as well.

The reported studies suggest that the use of nanoparticles as catalysts in electroanalysis in general, and particularly in DNA sensing is not confined to metal nanoparticles only. The conjugation of nanoparticles with electrochemical sensing systems promises large evolution in actual electroanalysis methods and is expected to bring more advantages in DNA sensing overall in the development of free PCR–DNA detection besides other applications that may include microfluidics and lateral flow detection devices. These works are under way at our and other laboratories. Their successful application in DNA detection in real samples would require a significant improvement of cost-efficiency of nanoparticle-based

detection systems, in general and those based on nanoparticle-induced electrocatalysis, in particular.

Acknowledgments

We acknowledge funding from the MEC (Madrid) for the projects MAT2008-03079/NAN, CSD2006-00012 "NANOBIOMED" (Consolider-Ingenio 2010) the E.U.'s support under FP7 contract number 246513 "NADINE" and the NATO Science for Peace and Security Programme's support under the project SfP 983807.

References

1. A. Merkoçi, *Biosensing using Nanomaterials,* John Wiley & Sons, Hoboken, New Jersey (2009).
2. A. Merkoçi (ed.), Nanobiomaterials in electroanalysis, *Electroanalysis* **19**, 739–741 (2007).
3. A. Merkoçi, Electrochemical biosensing with nanoparticles, *FEBS Journal* **274** 310–316 (2007).
4. A. de la Escosura-Muñiz and A. Merkoçi, Electrochemical detection of proteins using nanoparticles: applications to diagnostics, *Expert Opin. Med. Diagn.* **4**, 21–37 (2010).
5. A. T. Bell, The impact of nanoscience in heterogeneous catalysis, *Science* **299**, 1688–1691 (2003).
6. G. Ertl, H. Knözinger, and J. Weitkamp, *Handbook of Heterogeneous Catalysis,* Wiley-VCH, Weinheim (1997).
7. J. Das and H. Yang, Enhancement of electrocatalytic activity of DNA-conjugated gold nanoparticles and its application to DNA detection, *J. Phys. Chem. C* **113**, 6093–6099 (2009).
8. T. G. Drummond, M. G. Hill, and J. K. Barton, Electrochemical DNA sensors. *Nature Biotechnol.* **21**. 1192–1199 (2003).
9. J. Liu, J. Liu, L. Yang, X. Chen, M. Zhang, F. Meng, T. Luo, and M. Li, Nanomaterial assisted enhancement of hybridization for DNA biosensors: a review, *Sensors* **9**, 7343–7364 (2009).
10. R. Polsky, R. Gill, L. Kaganovsky, and I. Willner, Nucleic acid functionalized PtNPs: catalytic labels for the amplified electrochemical detection of biomolecules, *Anal. Chem.* **78**, 2268–2271 (2006).

11. T. Selvaraju, J. Das, K. Jo, K. Kwon, C. Huh, T. K. Kim, and H. Yang, Nanocatalyst based assay using DNA-conjugated Au nanoparticles for electrochemical DNA detection, *Langmuir* **24**, 9883–9888 (2008).
12. D. Hernández-Santos, M. B. González-García, and A. Costa-García, Metal-nanoparticles-based electroanalysis, *Electroanalysis* **14**(18), 1225–1235 (2002).
13. C. M. Welch and R. G. Compton. The use of nanoparticles in electroanalysis: a review, *Anal. Bioanal. Chem.* **384**, 601–619 (2006).
14. A. Wieckowski, E. R. Savinova, and C. G. Vayenas, *Catalysis and Electrocatalysis at Nanoparticles Surfaces*, Marcel Dekker, New York (2003).
15. X. Luo, A. Morrin, A. J. Killard, and M. R. Smyth, Applications of nanoparticles in electrochemical sensors and biosensors, *Electroanalysis* **18**, 319–326 (2006).
16. A. Merkoçi, M. Aldavert, S. Marín, and S. Alegret, New materials for electrochemical sensing V: nanoparticles for DNA labelling, *Trends Anal. Chem.* **24**, 341–349 (2005).
17. M. Pumera, M. T. Castañeda, M. I. Pividori, R. Eritja, A. Merkoçi, and S. Alegret, Magnetically triggered direct electrochemical detection of DNA hybridization based Au67 Quantum Dot—DNA—paramagnetic bead conjugate, *Langmuir* **21**, 9625–9629 (2005).
18. A. de la Escosura-Muñiz, A. Ambrosi, and A. Merkoçi, Electrochemical analysis with nanoparticle-based biosystems, *Trends Anal. Chem.* **27**(7), 568–584 (2008).
19. A. Ambrosi, M. T. Castañeda, A. J. Killard, M. R. Smyth, S. Alegret, and A. Merkoçi, Double-codified gold nanolabels for enhanced immunoanalysis, *Anal. Chem.* **79**, 5232–5240 (2007).
20. A. de la Escosura-Muñiz, C. Sánchez-Espinel, B. Díaz-Freitas, Á. González-Fernández, M. Maltez-da Costa, and A. Merkoçi, Rapid identification of tumour cells using a novel electrocatalytic method based in gold nanoparticles, *Anal. Chem.* **81**, 10268–10274 (2009).
21. A. Merkoçi, M. Aldavert, G. Tarrasón, R. Eritja, and S. Alegret, Toward an ICPMS-linked DNA assay based on gold nanoparticles immunoconnected through peptide sequences, *Anal. Chem.* **77**, 6500–6503 (2005).
22. A. Ambrosi, F. Airò, and A. Merkoçi, Enhanced gold nanoparticle based ELISA for breast cancer biomarker, *Anal. Chem.* **82**, 1151–1156 (2010).
23. F. Wang and S. Hu. Electrochemical sensors based on metal semiconductor nanoparticles, *Microchim. Acta.* **165**, 1–22 (2009).

24. I. Wang, R. Polsky, and D. Xu, Silver-enhanced colloidal electrochemical stripping detection of DNA hybridization, *Langmuir* **17**, 5739–5741 (2001).
25. H. Cai, Y. Wang, P. He, and Y. Fang, Electrochemical detection of DNA hybridization based on silver-enhanced gold nanoparticle label, *Anal. Chim. Acta.* **469**, 165–172 (2002).
26. T. Lee, H. Cai, and I. Hsing, Effects of gold nanoparticles and electrode surface properties on electrocatalytic silver deposition for electrochemical DNA hybridization detection, *The Analyst* **130**, 364–369 (2005).
27. Y. Li, J. T. Cox, and B. Zhang, Electrochemical responses and electrocatalysis at single Au nanoparticles, *J. Am. Chem. Soc.* **132**, 3047–3054 (2010).
28. X. Xiao, S. Pan, J. S. Jang, F. Fan, and A. Bard, Single nanoparticle Electrocatalysis: effect of monolayers on particle and electrode on electron transfer, *J. Phys. Chem. C.* **113**, 14978–14982 (2009).
29. J. Liu, L. Yang, X. Chen, M. Zhang, F. Meng, T. Luo, and M. Li, Nanomaterial-assisted signal enhancement of hybridization for DNA biosensors: a review, *Sensors* **9**, 7343–7364 (2009).
30. T. You, O. Niwa, M. Tomita, and S. Hirono, Characterization of platinum nanoparticle-embedded carbon film electrode and its detection of hydrogen peroxide, *Anal. Chem.* **75**, 2080–2085 (2003).
31. S. Wang and X. Lin. Electrodeposition of Pt-Fe(III) nanoparticle on glassy carbon electrode for electrochemical nitric oxide sensor, *Electrochim. Acta* **50**, 2887–2891 (2005).
32. N. Zhu, Z. Chang, P. He, and Y. Fang, Electrochemical DNA biosensors based on platinium NPs combined carbon nanotubes, *Anal. Chim. Acta* **545**, 21–26 (2005).
33. F. W. Campbell and R. G. Compton, The use of nanoparticles in electroanalysis: an updated review, *Anal. Bioanal. Chem.* **396**, 241–259 (2010).
34. S. H. Lim, J. Wei, J. Lin, Q. Li, and J. K. You, A glucose biosensor based on electrodeposition of Palladium nanoparticles and glucose oxidase onto Nafion-solubilized carbon nanotube electrode, *Biosens. Bioelectron.* 2341–2346 (2005).
35. Y. Liu, J. Zhang, W. Hou, and J. J. Zhu, A Pd/SBA-15 composite: synthesis, characterization and protein biosensing, *Nanotechnology* **19**, 135707 (2008).
36. Z. Chang, H. Fan, K. Zhao, M. Chen, P. He, and Y. Fang. Electrochemical DNA biosensors based on Palladium nanoparticles combined with carbon nanotubes, *Electroanalysis* **20**, 131–136 (2008).

37. I. Das, H. Kim, K. Jo, K. H. Park, S. Jon, K. Lee, and H. Yang, Fast catalytic and electrocatalytic oxidation of sodium borohydride on palladium nanoparticles and its application to ultrasensitive DNA detection, *Chem. Comm.* 6394–6395 (2009).

38. P. Lo, S. A. Kumar, and S. Chen, Amperometric determination of H_2O_2 at nano TiO_2/DNA/thionin nanocomposite modified electrode, *Colloids Interf., B: Biointerfaces* **66**, 266–273 (2008).

39. H. Zhou, X. Gan, J. Wang, X. Zhu, and G. Li, Hemoglobin based hydrogen peroxide biosensor tuned by the photovoltaic effect of nano titanium dioxide, *Anal. Chem.* **77**, 6102–6104 (2005).

40. W. Lu, Y. Jin, G. Wang, D. Chen, and J. H. Li, Enhanced photoelectrochemical method for linear DNA hybridization detection using Au-nanoparticle labelled DNA as probe onto titanium dioxide electrode, *Biosens. Bioelectron.* **23**,1534–1539 (2008).

41. Y. Hu, T. Yang, X. Wang, and K. Jiao, Highly sensitive indicator-free impedance sensing of DNA hybridization based on poly (m-aminobenzenosulfonic acid)/TiO2 nanosheetmembranes with pulse potentiostatic method preparation, *Chem. Eur. J.* **16**, 1992–1999 (2010).

42. Z. Gao and Z. Yang, Detection of microRNAs using electrocatalytic NPs tags. *Anal. Chem.* **78**, 1470–1477 (2006).

43. E. A. Hunt, A. M. Goulding, and S. K. Deo, Direct detection and quantification of microRNAs, *Anal. Biochem.* **387**, 1–12 (2009).

44. H. Zhu, J. Wang, and G. Xu, Fast synthesis of Cu_2O hollow microspheres and their application in DNA biosensor of Hepatitis B virus, *Crystal Growth and Design* **9**, 633–638 (2009).

45. S. Suwansa-ard, Y. Xiang, R. Bash, P. Thavarungkul, P. Kanatharana, and J. Wang, Prussian Blue dispersed sphere catalytic labels for amplified electronic detection of DNA, *Electroanalysis* **20**, 308–312 (2008).

46. X. Gan, T. Liu, X. Zhu, and G. Li, An electrochemical biosensor for Nitric Oxide based on silver nanoparticles and hemoglobin, *Anal. Sciences* **20**, 1271–1275 (2004).

47. A. de la Escosura-Muñiz, M. Maltez-da Costa, and A. Merkoçi, Controlling the electrochemical deposition of silver onto gold nanoparticles: reducing interferences and increasing the sensitivity of magnetoimmuno assays, *Biosen. Bioelectron.* **24**, 2475–2482 (2009).

48. M. Maltez-da Costa, A. de la Escosura-Muñiz, and A. Merkoçi, Electrochemical quantification of gold nanoparticles based on their catalytic properties on hydrogen formation: application in magneto immunoassays, *Electrochem. Commun.* **12**, 1501–1504 (2010).

Aptamer based electrochemical biosensor for protein detection using carbon nanotube platforms

P. Kara, A.
de la Escosura-Muniza **M. Maltez-da Costa**, M. Guix, M. Ozsoz, A. Merkoçi

Biosensors and Bioelectronics

2010, 26, 1715–1718

Biosensors and Bioelectronics 26 (2010) 1715–1718

Contents lists available at ScienceDirect

Biosensors and Bioelectronics

journal homepage: www.elsevier.com/locate/bios

Short communication

Aptamers based electrochemical biosensor for protein detection using carbon nanotubes platforms

Pinar Kara[a,b], Alfredo de la Escosura-Muñiz[a,c], Marisa Maltez-da Costa[a], Maria Guix[a], Mehmet Ozsoz[b], Arben Merkoçi[a,d,*]

[a] Nanobioelectronics & Biosensors Group, Institut Català de Nanotecnologia, CIN2 (ICN-CSIC), Campus UAB, Barcelona, Spain
[b] Ege University Faculty of Pharmacy, Analytical Chemistry Department, Turkey
[c] Instituto de Nanociencia de Aragón, Universidad de Zaragoza, Zaragoza, Spain
[d] ICREA, Barcelona, Spain

ARTICLE INFO

Article history:
Received 14 April 2010
Received in revised form 13 July 2010
Accepted 22 July 2010
Available online 30 July 2010

Keywords:
Aptamer
Aptasensor
Thrombin
Electrochemical impedance spectroscopy
Screen-printed electrodes
Carbon nanotubes

ABSTRACT

A label-free bioelectronic detection of aptamer–thrombin interaction based on electrochemical impedance spectroscopy (EIS) technique is reported. Multiwalled carbon nanotubes (MWCNTs) were used as modifiers of screen-printed carbon electrotransducers (SPCEs), showing improved characteristics compared to the bare SPCEs. 5′amino linked aptamer sequence was immobilized onto the modified SPCEs and then the binding of thrombin to aptamer sequence was monitored by EIS transduction of the resistance to charge transfer (Rct) in the presence of 5 mM $[Fe(CN)_6]^{3-/4-}$, obtaining a detection limit of 105 pM. This study represents an alternative electrochemical biosensor for the detection of proteins with interest for future applications.

1. Introduction

Aptamers hold great promise for rapid and sensitive protein detections and for developing protein arrays (Mukhopadhyay, 2005). These synthetic nucleic acid sequences act as antibodies in binding proteins owing to their relative ease of isolation and modification, holding a high affinity and high stability (Jayesna, 1999; Hansen et al., 2006).

In the last years, there has been a great interest for developing aptasensors. Different transduction techniques such as optical (McCauley et al., 2003; Zhang et al., 2009; Pavlov et al., 2005), atomic force microscopic (Basnar et al., 2006), electrochemical (Radi et al., 2005; Zayats et al., 2006; Suprun et al., 2008) and piezoelectrical (Pavlov et al., 2004) have been reported. Aptamer based biosensors have a great promise in protein biosensing due to their high sensitivity, selectivity, simple instrumentation, portability and cost effectiveness (Minunni et al., 2005; Baker et al., 2006).

It is well-known that the sequence-specific single-stranded DNA oligonucleotide 5′-GGTTGGTGTGGTTGG-3′ (thrombin aptamer) acts as thrombin inhibitor. This thrombin aptamer binds to the anion-binding exosite and inhibits thrombin's function by competing with exosite binding substrates fibrinogen and the platelet thrombin receptor (Paborsky et al., 1993). This highly specific aptamer/thrombin binding interaction has been extensively approached to develop different biosensors for thrombin, as summarized in Table S1 at the supplementary material. Furthermore, the selectivity of thrombin aptasensors has been demonstrated to be excellent against possible interfering substances such as human serum albumin (HSA) or lysozymes (Hu et al., 2009; Ding et al., 2010) present in human serum.

In recent studies, electrochemical impedance spectroscopic transduction of aptamer based protein analysis has shown a great prospect for label-free detections (Bogomolava et al., 2009). Electrochemical impedance spectroscopy (EIS) has been proven as one of the most powerful analytical tools for diagnostic analysis based on interfacial investigation capability. EIS measures the response of an electrochemical system to an applied oscillating potential as a function of the frequency. Impedimetric techniques have been developed to characterize the fabricated biosensors and to monitor the catalytic reactions of biomolecules such as enzymes, proteins, nucleic acids, whole cells and antibodies (Steichen et al., 2007; Steichen and Herman, 2005).

* Corresponding author at: Institut Català de Nanotecnologia, ETSE-Edifici Q 2ª planta, Campus UAB, 08193 Bellaterra, Barcelona, Spain. Tel.: +34 935868014; fax: +34 935868020.
E-mail address: arben.merkoci.icn@uab.es (A. Merkoçi).

0956-5663/$ – see front matter © 2010 Elsevier B.V. All rights reserved.
doi:10.1016/j.bios.2010.07.090

Herein we describe a label-free aptasensor design for direct protein analysis at multi walled carbon nanotube (MWCNT) enhanced disposable screen-printed carbon electrodes (SPCEs) surfaces. The offered detection limit shows that the designed thrombin aptasensor is sensitive enough, capable of performing label-free detection using a low-cost, fast and reliable electrochemical technique. In addition by using different aptamer sequences, different proteins could be detected using a similar detection system.

2. Experimental

2.1. Apparatus and electrodes

Electrochemical impedance spectroscopy (EIS) measurements were performed using AUTOLAB PGSTAT-30-FRA (Eco Chemie, The Netherlands).

The electrochemical transducers used were homemade screen-printed carbon electrodes, consisting of three electrodes: working electrode, reference electrode and counter electrode in a single strip fabricated with a semi-automatic screen-printing machine DEK248 (DEK International, Switzerland). The reagents used for this process were: Autostat HT5 polyester sheet (McDermid Autotype, UK), Electrodag 423SS carbon ink, Electrodag 6037SS silver/silver chloride ink and Minico 7000 Blue insulating ink (Acheson Industries, The Netherlands). (See the detailed procedure of the SPCEs fabrication as well as images of the sensors obtained, Fig. S1 in the supplementary material.)

Scanning electron microscopic images (SEM) of both SPCEs and MWCNT modified SPCEs were obtained using a Hitachi S-570 microscope (Hitachi Ltd., Japan).

2.2. Reagents and solutions

A 5′ amino modified DNA aptamer that is selective to human alpha thrombin was purchased from Alpha DNA (Canada). The aptamer sequence has the following base composition: 5′ NH_2-GGTTGGTGTGGTTGG-3′

Multiwalled carbon nanotube (MWCNT) powders (95% purity), human alpha thrombin (α-thrombin), human serum from human male AB plasma (HS), N-hydroxysulphosuccinimide (NHS), [N-(3-dimethylamino)propyl)]–N-ethylcarbodiimide (EDC), tri-Natrium citrate and tyrosinase from mushroom (lyophilized powder, >1000 unit/mg solid) were purchased from Sigma–Aldrich (Spain). Other chemicals were of analytical reagent grade and supplied Merck and Sigma (Spain). All chemicals were used as received, all aqueous solutions were prepared in double-distilled water and all experiments were performed at room temperature. Working solutions of α-thrombin were prepared in human serum.

2.3. Methods

2.3.1. Modification of screen-printed carbon electrodes with multi-walled carbon nanotubes

The working surface area of a bare SPCE was modified by depositing a 7 μl drop of MWCNT suspension (1 mg MWCNT/1 ml THF), followed by a drying process at room temperature for 24 h. The characterization process of the working electrode surface was performed by SEM to check if an homogeneous distribution of MWCNT over the surface was achieved. In order to have a conductive surface for SEM studies the electrodes were mounted on adhesive carbon films and then sputtered with gold following the standard sample preparation procedure.

2.3.2. Electrochemical activation

Both bare SPCEs and MWCNT modified SPCEs were electrochemically pretreated by applying an oxidative potential of +1.40 V during 2 min.

2.3.3. Aptamer-modified biosensing surface preparation

SPCEs surfaces were chemically modified by exposure to 50 mM phosphate buffer containing 5 mM EDC and 8 mM NHS used for free amino group coupling. After that, the thrombin sensitive aptamer was immobilized onto the modified SPCEs surfaces by immersing these in a 54.5 nM aptamer solution, in acetate buffer pH 4.8, for 1 h. After that, the modified electrodes were immersed in a 1% bovine serum albumine (BSA) solution during 1 h to prevent non-specific adsorptions.

2.3.4. Aptamer/thrombin complex formation

α-thrombin solution at a concentration of 1.95 nM is accumulated onto the aptamer-modified SPCEs by immersing during 1 h the sensors into a α-thrombin solution prepared in human serum. Blank assays were performed by following the same protocol but using tyrosinase instead of α-thrombin.

2.3.5. Electrochemical impedance spectroscopy based detection

50 μL of a 5 mM $[Fe(CN)_6]^{3-/4-}$ solution prepared in PBS 50 mM pH 7.4 were dropped on the working area of the SPCEs and a potential of +0.24 V was applied. A frequency range from 10 kHz to 50 mHz and an AC amplitude of 10 mV were fixed. The impedance data was fitted to an equivalent circuit, and the value of the resistance to charge transfer (Rct) was chosen as the analytical signal (see the detailed equivalent circuit to fit the frequency scans at Fig. S2 in the supplementary material). All the measurements were done in quintuplicate.

3. Results and discussion

3.1. Effect of the MWCNTs on the impedimetric signal

A label-free impedimetric aptasensor system has been developed for the direct detection of human α-thrombin as model protein, using MWCNT modified SPCE as electrochemical transducers. 5′ amino linked aptamer sequence is immobilized onto the MWCNT modified SPCE surface via the carbodiimide chemistry and finally the thrombin detection was accomplished by EIS transduction of aptamer–protein interaction. A general scheme of the experimental procedure is shown in Fig. 1A.

MWCNTs are used as modifiers of the SPCE electrotransducer surface because of their notable charge-transfer capability between heterogeneous phases. Furthermore, they modify the electrode surface providing higher rugosity with an increased active surface to further aptamer immobilization. In addition to this, aptamers can self assemble in carbon nanotubes by π–π stacking interactions between the nucleic acid bases and the carbon nanotubes walls (Zelada-Guillén et al., 2009) or they can be anchored to the carboxylic groups of oxidized nanotubes by chemical reactions. The changes in the morphology of the working electrode surface of the SPCE after the MWCNTs and aptamers immobilizations are evidenced in the SEM images shown in Fig. 1B, C. Furthermore in order to oxidize the MWCNTs and generate carboxylic groups an electrochemical pretreatment is applied. These are necessary for the further aptamer immobilization through the carbodiimide interaction and represent another advantage of MWCNTs. In Fig. S3 (see supplementary material) are summarized the analytical signals obtained for bare SPCEs electrodes after the sequential biomodifications (without aptamer, with aptamer and with aptamer + thrombin) (a) and also the effect of the previous SPCEs modification with MWCNTs electrochemically pretreated (b) and non pretreated (c). As it was expected, the impedimetric signal increases when increasing the SPCEs modification and this effect is enhanced when electrochemically pretreated MWCNTs are previously immobilized onto the SPCE surface.

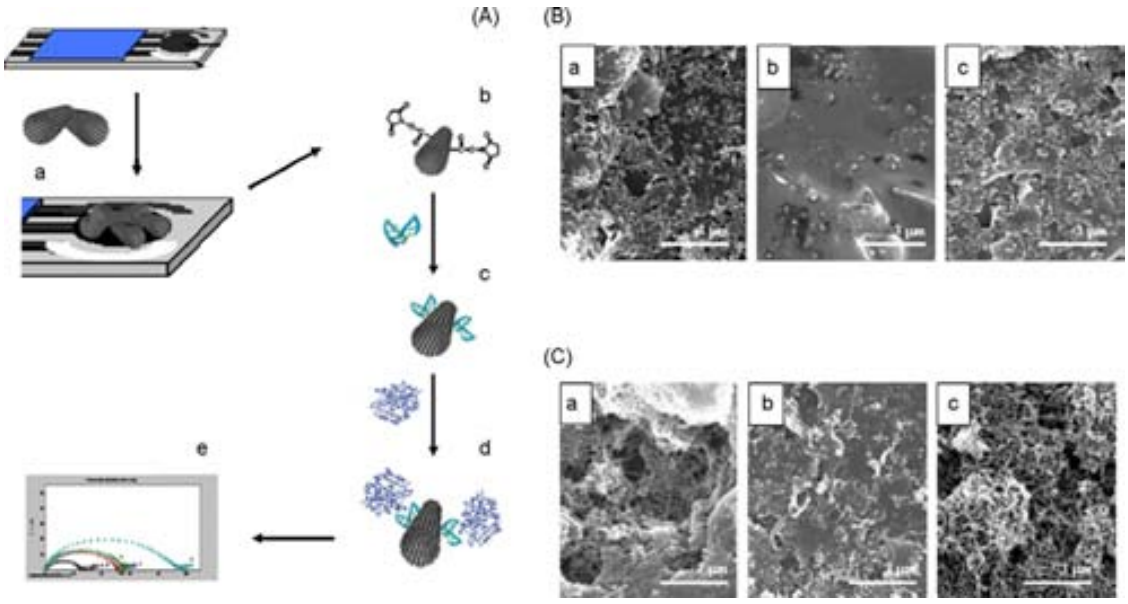

Fig. 1. (A) Schematic representation of the experimental procedure followed for the obtaining of the analytical signal: (a) MWCNTs modification of the SPCEs; (b) surface modification with covalent agents; (c) aptamer binding; (d) α-thrombin interaction; (e) EIS detection. (B) SEM images of the working surface area of bare SPCES after electrochemical pretreatment (a), after aptamer immobilization (b) and after its interaction with thrombin (c). (C) SEM images of the working surface area of MWCNT modified SPCEs after the same modifications detailed in (B). SEM resolution: 3 μm.

3.2. Selectivity of the impedimetric aptasensor

The selectivity of the sensor was tested doing different reference assays, using tyrosinase as negative control. The Rct values obtained for each assay are summarized in Fig. 2. First of all, the effect of the direct adsorption of both thrombin and tyrosinase on the MWCNT modified SPCE was evaluated. A significant increase in the Rct values was observed from both proteins due to bounding at the sensing surface via carbodiimide chemistry, being this increase of the same magnitude in both cases (b and c columns). This assay demonstrates that the direct adsorption of both proteins on the MWCNTs surface takes place in a similar magnitude, so further differences in the aptamer-based signals will be due to

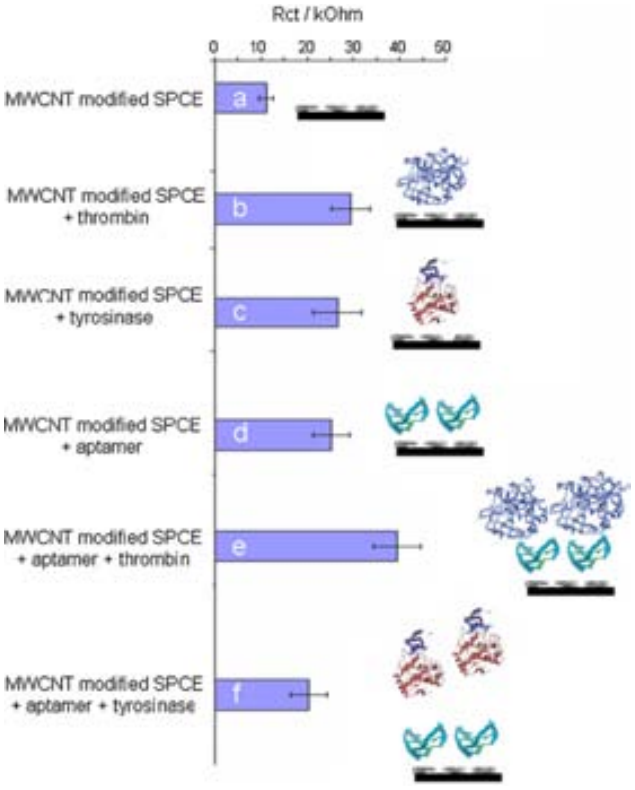

Fig. 2. Rct values obtained in 5 mM $[Fe(CN)_6]^{3-/4-}$ following the experimental procedure detailed in Section 2.3 for pretreated MWCNT modified SPCEs after performing different specificity assays.

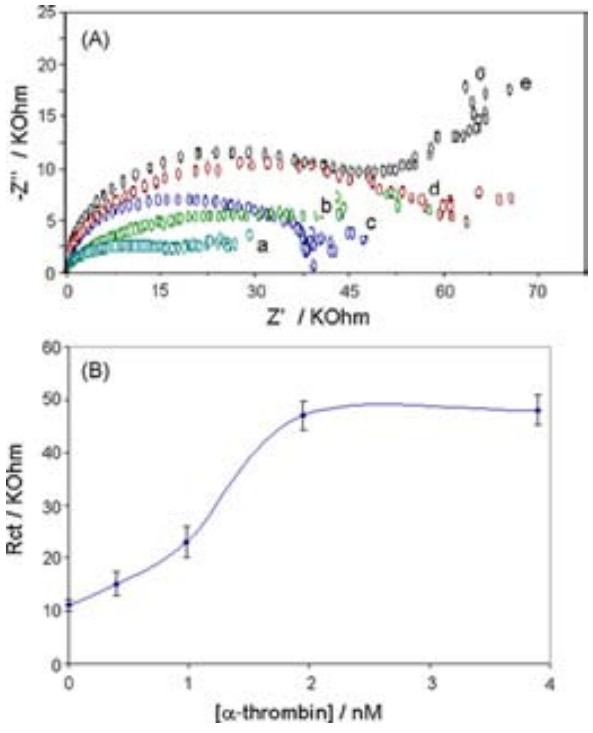

Fig. 3. (A) Impedance spectra obtained in 5 mM $[Fe(CN)_6]^{3-/4-}$ following the experimental procedure detailed in Section 2.3, using pretreated MWCNT modified SPCEs with immobilized aptamer for different α-thrombin concentrations: 0 nM (a), 0.39 nM (b), 0.98 nM (c), 1.95 nM (d) and 3.9 nM (e). (B) Corresponding relation between the α-thrombin concentrations and the Rct values (analytical signals).

the specific interaction and not to non-specific adsorptions. After that, the aptasensor was evaluated. When only the aptamer is immobilized onto the surface of the MWCNTs modified SPCE, an increase in the Rct values is also observed, considered as the reference value (d column). In addition, if the specific reaction with the α-thrombin is performed, a high increase (of about 15 kOhm) in the Rct value is registered (e column). However, when the assay is carried out with the tyrosinase, no changes are observed from the reference value, demonstrating the selectivity of the assay (f column).

3.3. α-thrombin quantification in human serum

Finally, the effect of the α-thrombin concentration on the analytical signal (Rct) for the thrombin sensitive aptamer-modified MWCNT SPCEs was evaluated. In Fig. 3A are shown the impedimetric spectra obtained for increased concentrations of α-thrombin from 0 to 3.9 nM. The curve presented in Fig. 3B shows that there is a good linear relationship (correlation coefficient of 0.99) between the α-thrombin concentration and the value of the analytical signal in the range of 0.39–1.95 nM, according to the equation:

$$\text{Rct (kOhm)} = 10.86\,[\alpha\text{-thrombin (nM)}] + 4.41\,(n = 5)$$

The limit of detection (calculated as the concentration of α-thrombin corresponding to 3 times the standard deviation of the estimate) was 105 pM. The reproducibility of the method shows a relative standard deviation (RSD) of 7.5%, obtained for a series of 5 repetitive assays performed for a 1.95 nM concentration of α-thrombin.

4. Conclusions

An impedimetric aptasensor for direct detection of human alpha thrombin at multiwalled carbon nanotube modified enhanced surfaces is developed. The selectivity of the aptasensor was evaluated by using the EIS response differences between aptamer–thrombin and aptamer–tyrosinase interaction. The thrombin detection limit of 105 pM shows that the designed aptasensor is capable to perform a label-free and sensitive detection. Considering also advantages related to low-cost, fast and reliable electrochemical detection mode applied in this methodology different other aptamer sequences for other proteins can be expected to be used in the future. The extension and application of the developed technique to other analytes and fields should be a matter of further investigations related also to a better understanding and improvements of the aptamer immobilization quality onto the carbon nanotube modified electrodes.

Acknowledgements

We acknowledge funding from the MEC (Madrid) for the projects MAT2008-03079/NAN, CSD2006-00012 “NANOBIOMED” (Consolider-Ingenio 2010) and the Juan de la Cierva scholarship (A. de la Escosura-Muñiz).

Appendix A. Supplementary data

Supplementary data associated with this article can be found, in the online version, at doi:10.1016/j.bios.2010.07.090.

References

Baker, B.R., Lai, R.Y., Wood, M.S., Doctor, E.H., Heeger, A.J., Plaxo, K.W., 2006. J. Am. Chem. Soc. 128, 3138–3139.
Basnar, B., Elnethan, R., Wilner, I., 2006. Anal. Chem. 78, 3638–3642.
Bogomolava, A., Komorova, E., Reber, K., Gerasimov, T., Yavuz, O., Bhatt, S., Aldissi, M., 2009. Anal. Chem. 81, 3944–3949.
Ding, C., Ge, Y., Lin, J.M., 2010. Biosens. Bioelectron. 25, 1290–1294.
Hansen, J.A., Wang, J., Kawde, A.N., Xiang, Y., Gothelf, K.V., Collins, G., 2006. J. Am. Chem. Soc. 128, 2228–2229.
Hu, J., Zheng, P.C., Jiang, J.H., Shen, G.L., Yu, R.Q., Liu, G.K., 2009. Anal. Chem. 81, 87–93.
Jayesna, S.D., 1999. Clin. Chem. 45, 1628–1650.
McCauley, T.G., Hamaguchi, N., Stanton, M., 2003. Anal. Biochem. 319, 244–250.
Minunni, M., Tombelli, S., Fonti, J., Spiriti, M., Mascini, M., Bogani, P., Buiatti, M., 2005. J. Am. Chem. Soc. 127, 7966–7967.
Mukhopadhyay, R., 2005. Anal. Chem. 77, 114A–118A.
Paborsky, L., McCurdy, S., Griffin, L., Toole, J., Leung, L., 1993. J. Biol. Chem. 268, 20808–20811.
Pavlov, V., Shlyahovsky, B., Willner, I., 2005. J. Am. Chem. Soc. 127, 6522–6523.
Pavlov, V., Xiau, Y., Shlyahovsky, B., Willner, I., 2004. J. Am. Chem. Soc. 126, 11768–11769.
Radi, A.E., Sanches, J.L.A., Baldrich, E., O'Sullivan, C.K., 2005. J. Am. Chem. Soc. 128, 117–124.
Steichen, M., Decrem, Y., Godfroid, E., Herman, C.B., 2007. Biosens. Bioelectron. 22, 2237–2243.
Steichen, M., Herman, C.B., 2005. Electrochem. Commun. 7, 416–420.
Suprun, E., Shumyantseva, V., Bulko, T., Rachmetova, S., Radko, S., Bodoev, N., Archakov, A., 2008. Biosens. Bioelectron. 24, 825–830.
Zayats, M., Huang, Y., Gill, R., Ma, C., Wilner, I., 2006. J. Am. Chem. Soc. 128, 13666–13667.
Zelada-Guillén, G.A., Riu, J., Düzgün, A., Rius, F.X., 2009. Angew. Chem. Int. Ed. 48, 7334–7337.
Zhang, Z., Yang, W., Wang, J., Yang, C., Yang, F., Yang, X., 2009. Talanta 78, 1240–1245.

7.2. ANNEX: Additional publications and manuscripts

Publication 5. "Controlling the electrochemical deposition of silver onto gold nanoparticles: reducing interferences and increasing the sensitivity of magnetoimmuno assays" A. de la Escosura-Muñiz, M. Maltez-da Costa, A. Merkoçi, *Biosensors and Bioelectronics* **2009**, 24, 2475-2482.

Publication 6. "Rapid identification and quantification of tumor cells using an electrocatalytic method based on gold nanoparticles" A. de la Escosura-Muñiz, C. Sánchez-Espinel, B. Díaz-Freitas, A. González-Fernández, M. Maltez-da Costa, A. Merkoçi, *Analytical Chemistry* **2009**, 81, 10268-10274.

Publication 7. "Detection of Circulating Tumor Cells Using Nanoparticles" M. Maltez-da Costa, A. de la Escosura-Muñiz, Carme Nogués, Leonard Barrios, Elena Ibáñez, A. Merkoçi, *submitted to Small* **2012.**

Publication 8. "Magnetic cell assay with electrocatalytic gold nanoparticles for rapid CTCs electrochemical detection" M. Maltez-da Costa, A. de la Escosura-Muñiz, Carme Nogués, Leonard Barrios, Elena Ibáñez, A. Merkoçi, *submitted to Nature Methods* **2012**.

Controlling the electrochemical deposition of silver onto gold nanoparticles: Reducing interferences and increasing sensitivity of magnetoimmuno assays

A. de la
Escosura-Muniz, **M. Maltez-da Costa**, A. Merkoçi

Biosensors and Bioelectronics

2009, 24, 2475–2482

Biosensors and Bioelectronics 24 (2009) 2475–2482

Contents lists available at ScienceDirect

Biosensors and Bioelectronics

journal homepage: www.elsevier.com/locate/bios

Controlling the electrochemical deposition of silver onto gold nanoparticles: Reducing interferences and increasing the sensitivity of magnetoimmuno assays

Alfredo de la Escosura-Muñiz[a,b], Marisa Maltez-da Costa[a], Arben Merkoçi[a,c,*]

[a] Nanobioelectronics & Biosensors Group, Institut Català de Nanotecnologia, Barcelona, Spain
[b] Instituto de Nanociencia de Aragón, Universidad de Zaragoza, Zaragoza, Spain
[c] ICREA, Barcelona, Spain

ARTICLE INFO

Article history:
Received 26 September 2008
Received in revised form 16 December 2008
Accepted 17 December 2008
Available online 25 December 2008

Keywords:
Silver electrocatalysis
Gold nanoparticles
Magnetic beads
Electrochemical biosensor
Immunoassay

ABSTRACT

An electrocatalytical method induced by gold nanoparticles in order to improve the sensitivity of the magnetoimmunosensing technology is reported. Microparamagnetic beads as primary antibodies immobilization platforms and gold nanoparticles modified with secondary antibodies as high sensitive electrocatalytical labels are used. A built-in magnet carbon electrode allows the collection/immobilization on its surface of the microparamagnetic beads with the immunological sandwich and gold nanoparticle catalysts attached onto. The developed magnetoimmunosensing technology allows the antigen detection with an enhanced sensitivity due to the catalytic effect of gold nanoparticles on the electroreduction of silver ions. The main parameters that affect the different steps of the developed assay are optimized so as to reach a high sensitive electrochemical detection of the protein. The low levels of gold nanoparticles detected with this method allow the obtaining of a novel immunosensor with low protein detection limits (up to 23 fg/mL), with special interest for further applications in clinical analysis, food quality and safety as well as other industrial applications.

1. Introduction

Catalysis is considered as the central field of nanoscience and nanotechnology (Grunes et al., 2003). Interest in catalysis induced by metal nanoparticles (NPs) is increasing dramatically in the last years. The use of NPs in catalysis appeared in the 19th century with photography (use of gold and silver NPs) and the decomposition of hydrogen peroxide (use of PtNPs) (Bradley, 1994). In 1970, Parravano and co-workers (Cha and Parravano, 1970) described the catalytic effect of AuNPs on oxygen-atom transfer between CO and CO_2. Usually, these NP catalysts are prepared from a metal salt, a reducing agent and a stabilizer. Since these first works, NPs have been widely used for their catalytic properties in organic synthesis, for example, in hydrogenation and C–C coupling reactions (Reetz et al., 2004), and the heterogeneous oxidation of CO (Lang et al., 2004) on AuNPs.

On the other hand, immunoassays are currently the predominant analytical technique for the quantitative determination of a broad variety of analytes in clinical, medical, biotechnological, and environmental significance. Recently, the use of metal nanoparticles, mainly gold nanoparticles (AuNPs) as labels for different biorecognition and biosensing processes has received wide attention, due to the unique electronic, optical, and catalytic properties (Wang et al., 2002a, 2003a,c; Liu et al., 2006; Kim et al., 2006; Daniel and Astruc, 2004; Fritzsche and Taton, 2003; Seydack, 2005). Electrochemical detection is ideally suited for these nanoparticle-based bioassays (Katz et al., 2004; Merkoçi et al., 2005; Merkoçi, 2007) owning to unique advantages related to NPs: rapidity, simplicity, inexpensive instrumentation and field-portability. The use of nanoparticles for multiplex analysis of DNA (Wang et al., 2003b) as well as proteins (Liu et al., 2004) has been also demonstrated showing a great potential of NP applications in DNA and protein studies. A summary of the most relevant works using AuNPs as label for bioassays along with some relevant results in terms of detection limit (DL) and precision is shown in Table 1. In addition, a review on the electrochemical biosystems based on nanoparticles has recently been reported (De la Escosura-Muñiz et al., 2008).

The use of colloidal gold as electrochemical label for voltammetric monitoring of protein interactions was pioneered in 1995 by González-García and Costa-García (1995), although the first metalloimmunoassay based on a colloidal gold label was not reported until 2000 by Dequaire et al. (2000). Despite the inherent high sensitivity of the stripping metal analysis (Piras and Reho, 2005) different strategies have been proposed to improve the sensitivity

* Corresponding author. Tel.: +34 935868014; fax: +34 935812379.
E-mail address: arben.merkoci.icn@uab.es (A. Merkoçi).

0956-5663/$ – see front matter © 2008 Elsevier B.V. All rights reserved.
doi:10.1016/j.bios.2008.12.028

Table 1
Summary of the most relevant works using AuNPs as labels for DNA sensors and immunosensors.

Biosensors	Electrode	Electrochemical technique	Electrochemical detection	Analyte	DL	Precision	Ref
DNA sensors	SPCE	PSA	Direct	19-Base oligo	5 ng/50 μL	RSD 12%	Wang et al. (2001a)
	CPE	SWV	Direct	21-Base oligo	2.17 pM	–	Kerman et al. (2004)
	SPCE	Chronopotentiometric stripping analysis	Direct (polymeric beads loaded with multiple gold nanoparticles)	19-Base-pair oligo	300 aM	–	Kawde and Wang (2004)
	SPMBE	ASV	Autocatalytic reductive deposition of Au(III) on gold nanoparticle	35-Base-pair human cytomegalovirus nucleic acid target	600 aM	–	Dequaire et al. (2006)
	Au microarrays	Capacitance	Silver enhancement	27-Base-pair oligo	50 nM	–	Park et al. (2002)
	GCE	DPV	Silver enhancement	32-Base oligo	50 pM	–	Cai et al. (2002)
	ITO chip	PSA	Silver enhancement	PCR amplicons	2×10^{-12} M	RSD 8%	Cai et al. (2004)
	ITO	PSA	Silver enhancement	PCR amplicons	–	–	Li et al. (2004)
Immunosensors	SPCE	ASV	Direct	IgG	3×10^{-12} M	–	Dequaire et al. (2000)
	GECE	DPV	Direct	IgG	65 pg/mL	RSD 3%	Ambrosi et al. (2007)
	GCE	ASV	Silver enhancement	IgG	6×10^{-12} M	–	Chu et al. (2005)
	GCE	ASV	Silver enhancement	*S. japonicum* antibody	3.0 ng/mL	–	Chu et al. (2005)
	Ag-ISE	Potentiometry	Silver enhancement	IgG	12.50 pmol/50 μL	RSD 4%	Karin et al. (2006)

SPMBE: screen-printed microband electrode; SPCE: screen-printed carbon electrode; GCE: glassy carbon electrode; Ag-ISE: silver ion selective electrode; CPE: carbon paste electrode; GECE: graphite epoxy composite electrode; ITO: indium tin oxide; DPV: differential pulse voltammetry; PSA: potentiometric stripping analysis; ASV: anodic stripping voltammetry; SWV: square wave voltammetry.

of these metalloimmunoassays. Another protein detection alternative was lastly reported by our group (Ambrosi et al., 2007). This is based on a versatile gold-labeled detection system based on either spectrophotometric or electrochemical method. In our procedure a double codified label (DC-AuNP) based on AuNP conjugated to an HRP-labeled anti-human IgG antibody, and antibodies modified with HRP enzyme is used to detect human IgG as a model protein.

A substantial sensitivity enhancement can be achieved, for example, by using the AuNPs as catalytic labels for further amplification steps. Although an ultrasensitive electrochemical immunosensor has been reported recently using the catalytic reduction of p-nitrophenol by AuNP-labels (Das et al., 2006), most common strategy uses the catalytic deposition of gold (Liao and Huang, 2005) and especially of silver onto AuNPs to improve the sensitivity.

In most cases, the silver enhancement relies on the chemical reduction, mainly using hydroquinone, of silver ions (Karin et al., 2006; Guo et al., 2005; Chu et al., 2005) to silver metal onto the surface of the AuNPs followed by anodic-stripping electrochemical measurement. However, this procedure is time consuming and its sensitivity is compromised by nonspecific silver depositions onto the transducing surface.

In 2000, Costa-García and co-workers (Hernández-Santos et al., 2000a,b) reported a novel electrochemical methodology to quantify colloidal gold adsorbed onto a carbon paste electrode based on the electrocatalytic silver deposition. This strategy has been exploited by the same group for a very sensitive immunoassay (De la Escosura-Muñiz et al., 2006) and DNA hybridization assay (De la Escosura-Muñiz et al., 2007) but using a gold(I) complex (aurothiomalte) as electroactive label instead of colloidal gold (De la Escosura-Muñiz et al., 2004). Besides the lower time consuming, the silver electrodeposition process shows very interesting advantages over the chemical deposition protocol reported before, since silver only deposits on the AuNPs. This fact results in a high signal-to-background ratio by reducing the nonspecific silver depositions of the chemical procedure.

The electrocatalytic silver deposition on AuNPs has been recently applied in a DNA hybridization assay (Lee et al., 2004, 2005), but till now, to the best of our knowledge, the utilization of this amplification procedure for electrochemical immunoassay detection with AuNP label has not yet been reported.

On the other hand, magnetic particles have been widely used as platforms in biosensing, and the silver chemical deposition approached to improve the sensitivity of the assays (Wang et al., 2001b, 2002b). The magneto based electrochemical biosensors present improved properties in terms of sensitivity and selectivity, due to the preconcentration of the analyte, the separation from the matrix of the sample and the immobilization/collection on the transducer surface, achieved using magnetic fields. However, till now, the utilization of the amplification procedure based on the silver electrodeposition for the electrochemical detection of AuNPs used as labels in magnetobioassays has not yet been reported.

In this work, an electrocatalytic silver-enhanced metalloimmunoassay using AuNPs as labels and microparamagnetic beads (MBs) as platforms for the immunological interaction is developed for model proteins, in order to achieve very low detection limits with interest for further applications in several fields.

2. Experimental

2.1. Apparatus and electrodes

Cyclic voltammetric experiments were performed with an electrochemical analyzer (CH Instrument, USA) connected to a PC. All measurements were carried out at room temperature in a 20 mL

cell (protected from light) with a three-electrode configuration. A graphite epoxy composite electrode with a magnet inside (GECE-M) was used as working electrode. It was prepared as described previously (Cespedes et al., 1993; Santandreu et al., 1997). Briefly, epoxy resin (Epotek H77A, Epoxy Technology, USA) and hardener (Epotek H77B) were mixed manually in the ratio 20:3 (w/w) using a spatula. When the resin and hardener were well mixed, the graphite powder (particle size 50 μm, BDH, UK) was added in the ratio 1:4 (w/w) and mixed for 30 min. The resulting paste was placed into a cylindrical PVC sleeve (6 mm i.d.) incorporating a neodymium magnet (diameter 3 mm, height 1.5 mm, Halde Gac Sdad, Spain, catalog number N35D315) into the body of graphite epoxy composite, 2 mm under the surface of the electrode. Electrical contact was completed using a copper disk connected to a copper wire. The conducting composite was cured at 40 °C for one week. Prior to use, the surface of the electrode was polished with abrasive paper and then with alumina paper (polishing strips 301044-001, Orion, Spain) and rinsed carefully with bidistilled water. An ultrasonic bath (JP Selecta, Spain) was used to clean the GECE-M surface. A platinum wire as counter electrode and an Ag/AgCl reference electrode were used in the three electrodes configuration. A Metrohm AG Herisau magnetic stirrer was used for the electrochemical pretreatments, the AuNPs oxidation, the silver electrodeposition and the cleaning step. A Transmission Electron Microscope (TEM) Jeol JEM-2011 (Jeol Ltd., Japan) was used to characterize the magnetic beads after the immunological assay. A Scanning Electron Microscope (SEM) Jeol JSM-6300 (Jeol Ltd., Japan) coupled to a Energy Dispersive X-Ray (EDX) Spectrophotometer ISIS 200 (Oxford Instruments, England) was used to characterize the magnetic beads after the silver electrodeposition.

2.2. Reagents and solutions

Streptavidin-coated Magnetic Beads (MBs) 2.8 μm sized were purchased from Dynal Biotech (M-280, Invitrogen, Spain). Biotin conjugate-goat anti-human IgG (Sigma B1140, developed in goat and gamma chain specific), human IgG from serum (Sigma I4506), goat IgG from serum (Sigma I5256), anti-human IgG (Sigma A8667, developed in goat, whole molecule), hydrogen tetrachloroaurate(III) trihydrate ($HAuCl_4{\cdot}3H_2O$, 99.9%), silver nitrate and trisodium citrate were purchased from Sigma–Aldrich Química, Spain. All buffer reagents and other inorganic chemicals were supplied by Sigma, Aldrich or Fluka (Sigma–Aldrich Química, Spain), unless otherwise stated. All chemicals were used as received and all aqueous solutions were prepared in doubly distillated water.

The phosphate buffer solution (PBS) consisted of 0.01 M phosphate buffered saline, 0.137 M NaCl, 0.003 M KCl (pH 7.4). Blocking buffer solution consisted of a PBS solution with added 5% (w/v) bovine serum albumin (pH 7.4). The binding and washing (B&W) buffer consisted of a PBS solution with added 0.05% (v/v) Tween 20 (pH 7.4). The measuring medium for the electrochemical measurements consisted of a 2.0×10^{-4} M silver nitrate solution in 1.0 M NH_3, prepared in ultra-pure water.

Analytical grade (Merck) NaCl, HCl, H_2SO_4, NH_3, KCN and NaOH were used. These solutions were prepared in ultra-pure water, except for KCN solutions, which were prepared in 0.1 M NaOH.

2.3. Methods

2.3.1. Synthesis of AuNPs and preparation of the conjugated AuNPs/anti-human IgG

AuNPs were synthesized by reducing tetrachloroauric acid with trisodium citrate, a method pioneered by Turkevich et al. (1951). Briefly, 200 mL of 0.01% $HAuCl_4$ solution were boiled with vigorous stirring. 5 mL of a 1% trisodium citrate solution were added quickly to the boiling solution. When the solution turned deep red, indicating the formation of AuNPs 15 nm sized, the solution was left stirring and cooling down.

The AuNPs loading with the antibody was performed according to the following procedure: 2 mL of AuNP suspension was mixed with 100 μL of 100 μg/mL anti-human IgG and incubated at 25 °C for 20 min. After that, a blocking step with 150 μL of 1 mg/mL BSA, incubating at 25 °C for 20 min was performed. Finally, a centrifugation at 14,000 rpm for 20 min was carried out, and then the AuNPs/anti-human IgG was reconstituted in H_2O milli-Q.

Previous works in our group (Ambrosi et al., 2007) have recorded TEM images in order to measure the size, and measured FFT (Fast Fourier Transform) of crystalline planes distances in order to verify the Au metallic structure. The characteristic absorbance peak of gold at 520 nm has been also observed by UV–vis spectrum.

2.3.2. Preparation of the sandwich type immunocomplex

The preparation of the MBs based sandwich type immunocomplex was performed following a method previously optimised in our group, with some improvements. Briefly, 150 μg (15 μL from the stock solution) of MBs was transferred into 0.5 mL Eppendorf tube. The MBs were washed twice with 150 μL of B&W buffer. The MBs were then resuspended in 108 μL of B&W buffer and 42 μL (from stock solution 0.36 mg/mL) of biotinylated anti-human IgG were added. The resulting MB and anti-human IgG) solution was incubated for 30 min at temperature 25 °C with gentle mixing in a TS-100 ThermoShaker. The formed MB/anti-human IgG were then separated from the incubation solution and washed 3 times with 150 μL of B&W buffer. The preparation process was followed by resuspending the MB/anti-human IgG in 150 μL of blocking buffer (PBS–BSA 5%) to block any remaining active surface of MBs and incubated at 25 °C for 60 min. After the washing steps with B&W buffer, the MB/anti-human IgG were incubated at 25 °C for 30 min with 150 μL of human IgG antigen (goat IgG for the blank assay) at different concentrations, forming by this way the immunocomplex MB/anti-human IgG/Human IgG. Finally, after the washing steps, the MB/anti-human IgG/Human IgG immunocomplex was incubated at 25 °C for 30 min with 150 μL of the previously synthesized AuNPs/anti-human-IgG complex. A scheme of this procedure is shown in Fig. 1.

2.3.3. Electrochemical detection based in the catalytic effect of AuNPs on the silver electrodeposition

The smoothed GECE-M surface was pre-treated before each assay by an electrochemical pre-treatment in 0.1 M HCl. The electrode was immersed in a 0.1 HCl M stirred solution and a potential of +1.25 V was applied for 2 min. After that, the electrode surface was washed with the B&W buffer.

This procedure has been optimized in a previous work for Au(I) complexes (De la Escosura-Muñiz et al., 2004). After the immunoassay protocol was performed, the electrode was immersed in a 0.1 M NaOH solution and held with stirring at +1.25 V for 2 min. Then, the electrode was transferred to a 0.1 M H_2SO_4 solution and held with stirring at +1.20 V for 2 min. After that, the electrode was rinsed with ultra-pure water and introduced in a stirred 1.0 M NH_3 solution containing silver nitrate at a fixed concentration (2.0×10^{-4} M) and held at a deposition potential of −0.12 V for 60 s. After that, cyclic voltammograms were scanned from deposition potential to +0.30 V at a scan rate of 50 mV/s, without stirring. Finally, in order to remove gold from the electrode surface, after each measurement, the GECE-M was immersed in another cell containing a 0.1 M KCN in 0.1 M NaOH (dangerous/hazard solution. This step is made in a fume cupboard) stirred solution for 2 min in open circuit.

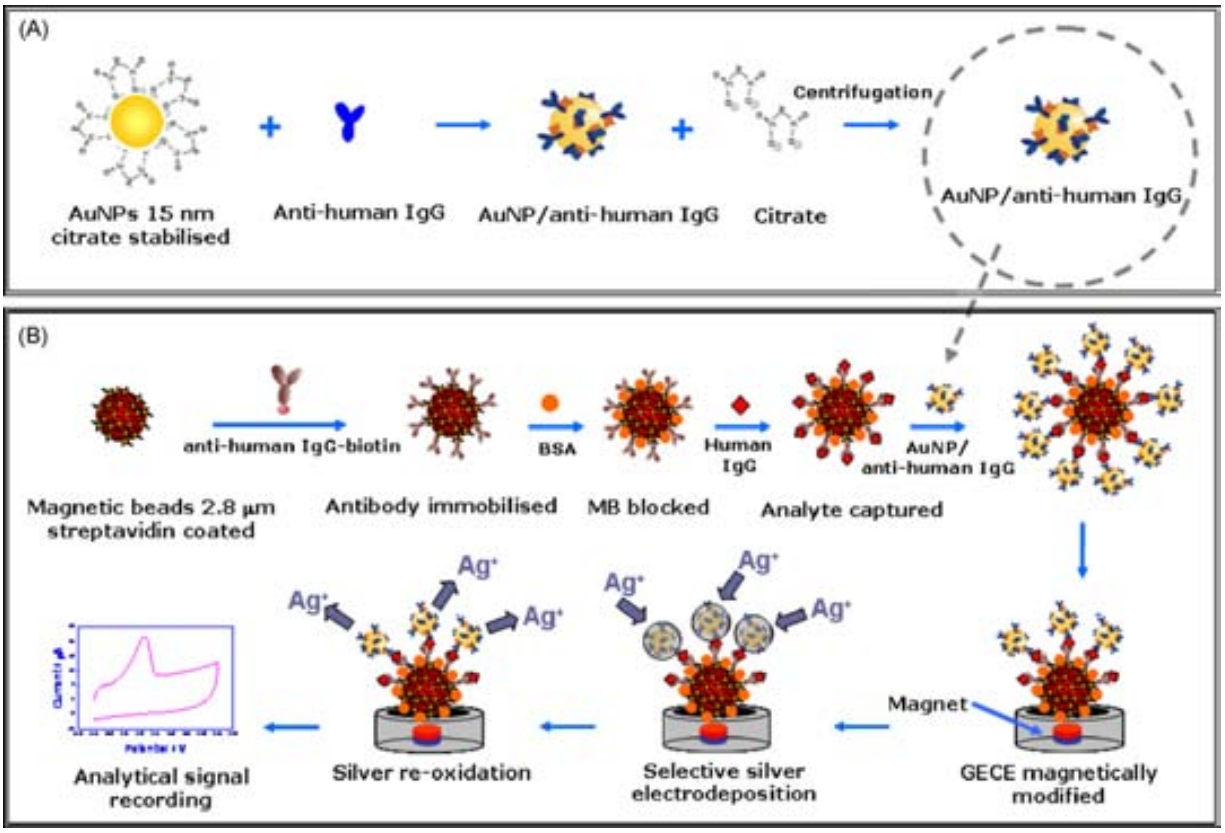

Fig. 1. Schematic (not in scale) of: (A) AuNP conjugation with anti-human IgG; (B) analytical procedure for the sandwich type assay and the obtaining of the analytical signal based on the catalytic effect of AuNPs on the silver electrodeposition. Procedure detailed in Section 2.

3. Results and discussion

3.1. Sandwich type immunocomplex

The preparation of the sandwich type immunocomplex was carried out following a previously optimized procedure (Ambrosi et al., 2007), but introducing slight changes in order to minimize the unspecific absorptions that interfere the sensitive electrocatalytic detection. The analytical procedure is described in Section 2 and schemed in Fig. 1.

The use of blocking agents so that any portion of the MB surface which does not contain the primary antibody is "blocked" thereby preventing nonspecific binding with the analyte of interest (protein) is crucial. The obtained values of the analytical signals are highly dependent on the blocking quality. Following the previously reported procedure, based on the direct electrochemical detection of AuNP, the blank samples signal (the samples without the antigen or with a nonspecific antigen) was very high (data not shown). The resulted unspecific adsorptions could be due to some factors. For a given concentration of the blocking agent the

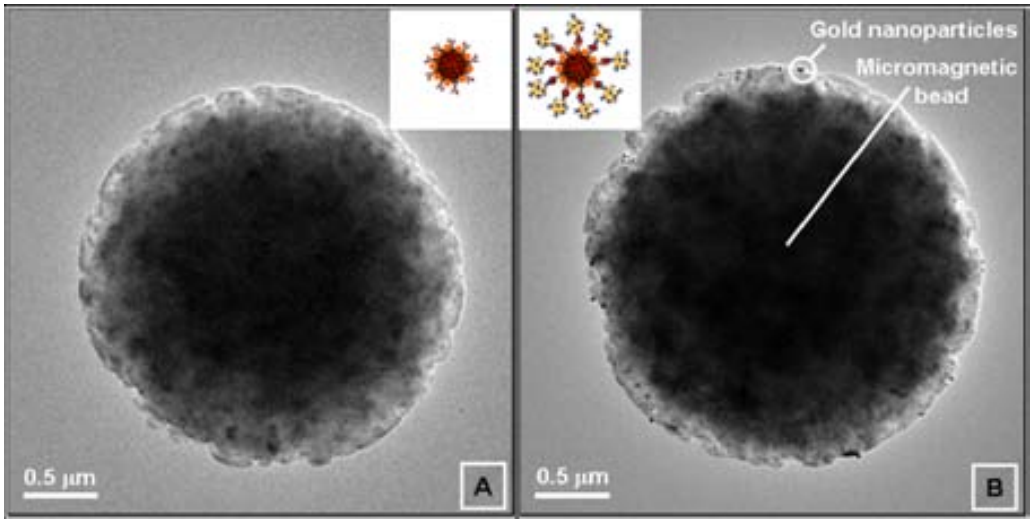

Fig. 2. Transmission electron micrographs (TEM) images of the MBs after the sandwich type assay detailed in Section 2. Assay carried out with 1.0×10^{-3} µg/mL of the nonspecific antigen (goat IgG) (blank assay—A) and assay performed with 1.0×10^{-3} µg/mL of the specific antigen (human IgG) (B).

unspecific adsorptions will depend on the time interval used to perform such a step. By increasing the time interval of the blocking step (from 30 to 60 min and using PBS–BSA 5% as blocking agent) in the sandwich assay we could ensure a better coverage of the free bounding sites onto the MB surface avoiding by this way the unspecific adsorptions. Another important factor that affects the unspecific adsorptions is the washing step that aims at removing the unbound species avoiding by this way possible signals coming from AuNPs not related to the required antigen. Stirring instead of gentle washing brought significant decrease of unspecific adsorptions too. TEM images of the sandwich assay before and after the mentioned improvement corroborated also in understanding the phenomena related to these non-desired adsorptions (see Fig. S1 in the *Supplementary Material*).

Clear evidences of the successful immunological reaction in a condition of the absence of unspecific adsorptions are the TEM images images shown in Fig. 2. When the assay is carried out in the presence of the nonspecific antigen (goat IgG—Fig. 2A) only MBs are observed with a very low amount of AuNPs nonspecifically bonded. However, if the assay is performed with the specific antigen (human IgG—Fig. 2B), a high quantity of AuNPs is observed around the MBs, which indicates that the immunological reaction has taken place.

3.2. Catalytic effect of AuNPs on the silver electrodeposition

The silver enhancement method, based on the catalytic effect of AuNPs on the chemical reduction of silver ions, has been widely used to improve the detection limits of several metalloimmunoassays. In these assays (Karin et al., 2006; Guo et al., 2005; Chu et al., 2005) the silver ions are chemically reduced onto the electrode surface in the presence of AuNPs connected to the studied bioconjugates, without the possibility to discriminate between AuNP or electrode surface. Furthermore, these methods are time consuming and two different mediums are needed in order to obtain the analytical signal: the silver/chemical reduction medium to ensure the silver deposition and the electrolytic medium necessary to the silver-stripping step.

However, in this work, for the first time, the selective electrocatalytic reduction of silver ions on AuNPs is clarified, and the advantages of using MBs as bioreaction platforms combined with the electrocatalytic method are used to design a novel sensing device.

The principle of the electrocatalytic method is resumed in Fig. 3A. Cyclic voltammograms, obtained by scanning from +0.30 to −1.20 V in aqueous 1.0 M NH_3/2.0×10^{-4} M $AgNO_3$, for an electrode without (a) and with (b) AuNPs previously adsorbed during 15 min are shown. It can be observed that the half-wave potential of the silver reduction process is lowered when AuNPs are previously deposited on the electrode surface. Under these conditions, there is a difference (ΔE) of 200 mV between the half-wave potential of the silver reduction process on the electrode surface without (a) and with (b) AuNPs adsorbed on the electrode surface. The amount of the catalytic current related to silver reduction increases with the amount of AuNPs adsorbed on the electrode surface (results not shown).

Taking this fundamental behavior into account, a novel analytical procedure for the sensitive detection of AuNPs is designed. It consists in choosing an adequate deposition potential, i.e. −0.12 V, at which the direct electroreduction of silver ions, during a determined time, would take place on the AuNPs surface instead of the bare electrode surface. At the beginning of the process, the electrocatalytical reduction of silver ions onto the AuNPs surface occurs and once a silver layer is already formed more silver ions are going to be reduced due to a self-enhancement deposition. The electrocatalytic process is effective due to the large surface area of AuNPs

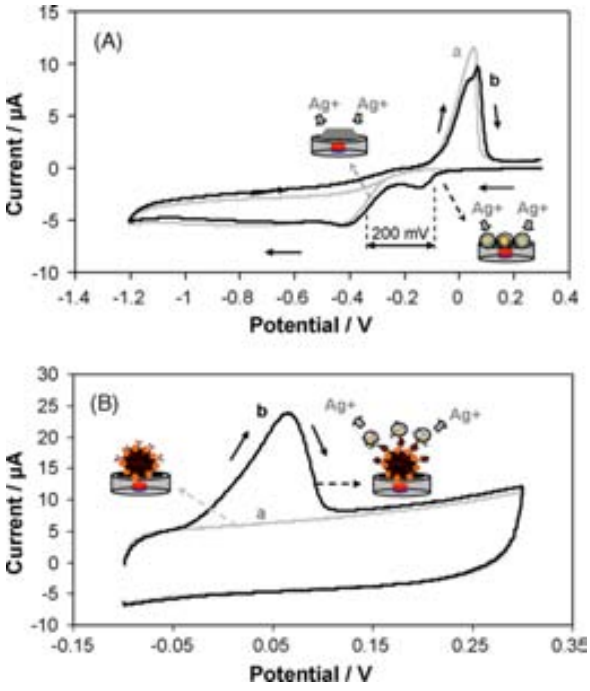

Fig. 3. (A) Cyclic voltammograms, scanned from +0.30 to −1.20 V in aqueous 1.0 M NH_3—2.0×10^{-4} M $AgNO_3$, for an electrode without deposited AuNPs (a curve) and for an electrode where previously AuNPs have been deposited from the synthesis solution for 15 min (b curve). (B) Cyclic voltammograms recorded in aqueous 1.0 M NH_3—2.0×10^{-4} M $AgNO_3$, from −0.12 to +0.30 V for the sandwich type assay described in Section 2, with an human IgG concentration of 5.0×10^{-7} μg/mL (b curve) and with the same concentration of the nonspecific antigen (goat IgG – blank assay – a curve). Silver deposition potential: −0.12 V; silver deposition time: 60 s; scan rate: 50 mV/s.

allowing an easy diffusion and reduction of the silver ions. The proposed mechanism is the following:

In a first step, while applying a potential of −0.12 V during 60 s, the silver from the ammonia complex, is reduced to a metallic silver layer onto the AuNP surface:

$$Ag(NH_3)_2^+ + 1e^- \xrightarrow{AuNP, E=-0.12\,V} Ag\,(\text{deposited on AuNPs}) + 2NH_3$$

In a second step an anodic potential scan is performed (from −0.12 to +0.30 V) in the same medium, during which the re-oxidation of silver at +0.10 V is recorded:

$$Ag\,(\text{deposited onto AuNPs}) + 2NH_3 \xrightarrow{E(-0.12\,\text{to}\,+0.30\,V)} Ag(NH_3)_2^+ + 1e^-$$

The amount of silver electrodeposited at the controlled potential (corresponding to deposition onto AuNP surface only) is proportional to the adsorbed AuNPs. Consequently the re-oxidation peak at +0.10 V, produces a current the amount of which is proportional to the AuNPs quantity. The obtained re-oxidation peak constitutes thus the analytical signal, used later on for the AuNPs and consequently the protein quantification. The designed AuNP and protein sensing system based on the electrocatalytic reduction of silver presents advantages over the previously reported chemical reduction procedures in terms of higher signal to background ratio and the reduction of the unspecific silver depositions. This behavior is improved by using MBs as platforms of the bioreactions, since the unspecific AuNPs adsorptions are minimized and at an adequate deposition potential, the silver electrodeposition on the electrode surface is blocked by the MBs.

Thus, following the analytical procedure described in Section 2 the selective silver deposition onto the AuNPs surface is achieved. The potential and the time of the silver electrodeposition have been previously optimized (see Fig. S2 in the *Supplementary Material*).

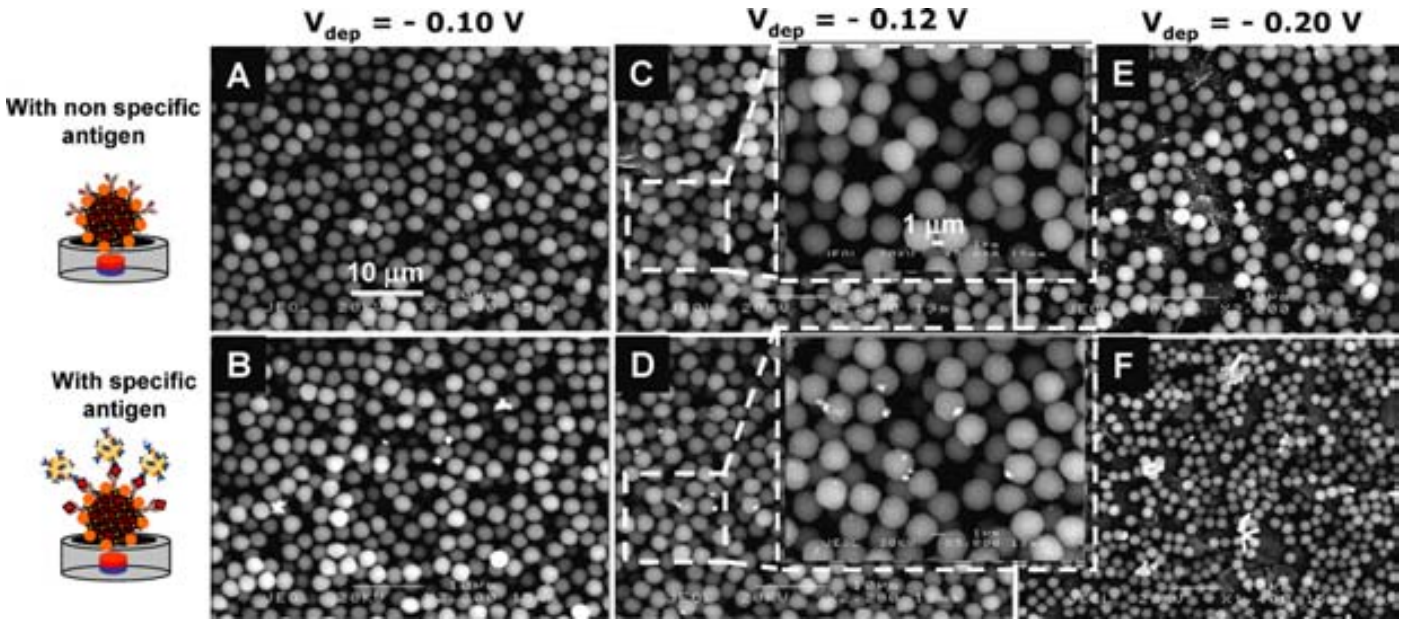

Fig. 4. Scanning electron microscopy (SEM) images of the MB deposited on the electrode surface, after the silver electrodeposition in aqueous 1.0 M NH_3—2.0×10^{-4} M $AgNO_3$, at −0.10 V (A and B), −0.12 (C and D) and −0.20 V (E and F) during 1 min, for the sandwich type assay performed as described in Section 2, with the nonspecific antigen (goat IgG – blank assays – A, C, E) and for the specific antigen (human IgG) at concentration of 1.0×10^{-3} μg/mL (B, D, F).

The application of a −0.12 V potential during 60 s resulted the best as a compromise between the higher sensitivity and analysis time.

Typical analytical signals obtained for the sandwich type assay performed with an human IgG concentration of 5.0×10^{-7} μg/mL (a) and for the blank assay performed with the same concentration of goat IgG (b) are shown at Fig. 3B.

The electrocatalytic deposition of silver ions onto the surface of the magnetic electrode versus the applied potential used for silver deposition is studied also by SEM. Fig. 4 shows SEM images of the MBs deposited onto the magnetic electrode surface, after performing silver electrodeposition at different deposition potentials (−0.10, −0.12 and −0.20 V) during 1 min. The upper images of Fig. 4(A, C, E) correspond to the sandwich type assays performed with the nonspecific antigen (goat IgG—blank assays), and the lower part images (B, D, F) correspond to the assays with an specific antigen (human IgG). In both cases, the protein concentration was 1.0×10^{-3} μg/mL. It can be observed that at a deposition potential of −0.10 V, (A) no silver crystals are formed in the absence of the specific antigen while low amounts of silver crystals (white structures in the B image) are observed for the assay performed with the specific antigen. This means that the silver deposition has scarcely occurred to the AuNPs anchored onto the MBs through the immunological reaction (B). The formation of these silver crystals is much more evident when the same assay (with specific antigen) is performed at deposition potential of −0.12 V (D) where a bigger amount of MBs appears to be covered with silver crystals—the same phenomena not observed for the blank assay (C). The obtained image is clear evidence that the used potential has been adequate for the silver deposition onto the AuNPs attached to the MBs through the immunological reaction. The EDX analysis (provided by SEM instrument) is also performed and the results are in agreement with the SEM images. The EDX results confirm the presence of gold and silver only in the assay performed with the specific antigen (see Fig. S3 in the Supplementary Material). By using more negative deposition potentials (i.e. −0.20 V) the deposition of silver takes place in a high extent also on the electrode surface as it was expected (*E*). This phenomenon can be appreciated by bigger cluster like white silver crystals that may be associated not only with silver deposited onto the AuNPs but also onto the surface of the magnetic

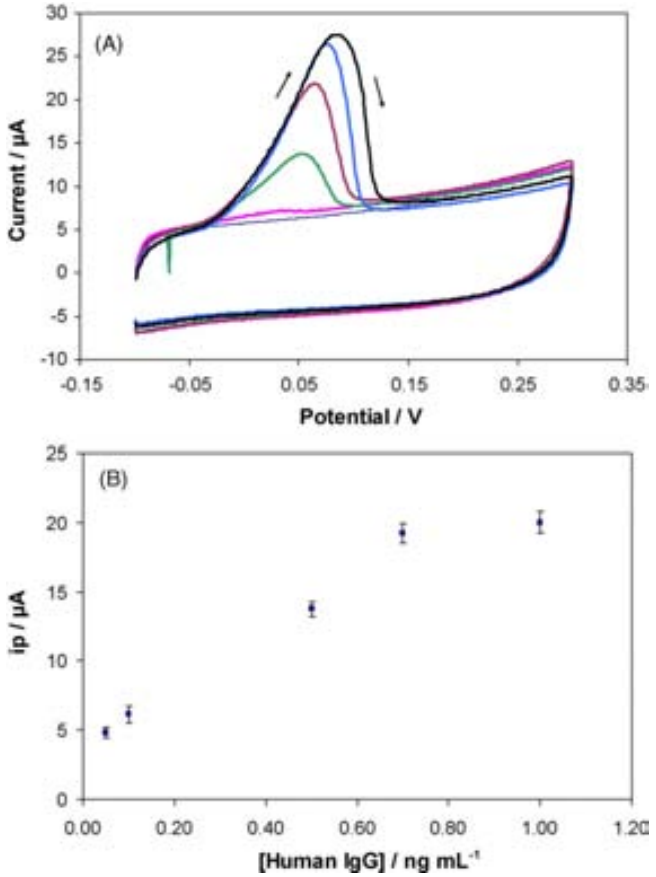

Fig. 5. (A) Cyclic voltammograms recorded in aqueous 1.0 M NH_3—2.0×10^{-4} M $AgNO_3$, from −0.12 to +0.30 V, for the sandwich type assay described in Section 2 with 1.0×10^{-6} μg/mL of the nonspecific antigen (goat IgG—thin line) and for increasing specific antigen (human IgG) concentrations: 5.0×10^{-8}, 1.0×10^{-7}, 5.0×10^{-7}, 7.5×10^{-7} and 1.0×10^{-6} μg/mL. Silver electrodeposition potential: −0.12 V; silver deposition time: 60 s; scan rate: 50 mV/s. (B) The corresponding relationship between the different concentrations of the human IgG and the obtained peak currents used as analytical signals.

electrode. This potential (−0.20 V) is not adequate to quantify the specific antigen due to false positive results that can be generated. The −0.12 V has been used in our experiments as the optimal deposition potential that can not even discriminate between the assays and the blank but also be able to do protein quantification at a very low detection limit.

Similar silver structures formed onto AuNPs have been reported earlier after chemical silver(I) reduction for a DNA array-based assay (Park et al., 2002) or an immunoassay (Gupta et al., 2007) but this is the first time that such potential controlled silver deposition induced by the electrocatalytical effect of AuNP is being evidenced. Moreover the relation between the current produced by the oxidation of the selectively deposited silver layer and the quantity of AuNP is demonstrated as shown in the following part.

In Fig. 5A are shown cyclic voltammograms for different concentrations of human IgG following the procedure explained in Section 2. Fig. 5B represents the corresponding peak heights used as analytical signals. As observed in this figure a good linear relationship for the concentrations of human IgG, in the range from 5.0×10^{-8} to 7.5×10^{-7} μg/mL, with a correlation coefficient of 0.9969, according to the following equation:

$$ip\,(\mu A) = 21.436\,\mu A/(\mu g/mL) \times [\text{human IgG}]\,(\mu g/mL) + 3.750\,\mu A\,(n = 3)$$

is obtained.

The limit of detection (calculated as the concentration corresponding to three times the standard deviation of the estimate) of the antigen was 23 fg of human IgG for milliliter of sample. The reproducibility of the method shows a RSD around 4%, obtained for a series of 3 repetitive immunoreactions for 5.0×10^{-7} μg human IgG/mL.

These results indicate that with the silver enhancement method can be detected 1000 times lower concentrations of antigen than with the direct differential pulse voltammetry (DPV) gold detection (as done by Ambrosi et al., 2007).

4. Conclusions

In this work, for the first time, the selective electrocatalytic reduction of silver ions onto the surface of AuNPs is clarified. This catalytic property is combined with the use of microparamagnetic beads as platform for the immobilization of biological molecules, and advantages used to design a novel sensing device. The electrochemical measurement accompanied by scanning electron microscopy images reveal the silver electrocatalysis enhancement by the presence of nanoparticles anchored to the electrode surface through specific antigen–antibody interactions.

In the sensing device, AuNP as label is used to detect human IgG as a model protein and the excess/non-linked reagents of the immunological reactions are separated using a permanent magnet, allowing the electrochemical signal coming from AuNPs to be measured, and thus the presence or absence of protein be determined. The magnetic separation step significantly reduces background signal and gives the system distinct advantages for alternative detection modes of antigens. Finally, the sensible electrochemical detection of the AuNPs is achieved, based on their catalytic effect on the electroreduction of silver ions.

Several problems inherent to the silver electrocatalysis method are resolved by using the magnetic beads as platforms of the bioassays: (i) the selectivity inherent to the use of magnetic beads avoids unspecific adsorptions of AuNPs on the electrode surface, that could give rise to unspecific silver electrodeposition due to the high sensitivity of the amplification method and (ii) in this method, a critical parameter is the silver electrodeposition potential, in order to achieve the silver deposition only on the surface of the AuNPs and not on the electrode surface. In this way, the magnetic beads can block the electrode surface, so the silver electrodeposition on that surface is minimized.

The developed electrocatalytic method allows to achieve low levels of AuNPs, so very low protein detection limits, up to 23 fg/mL, are obtained, that are 1000 times lower in comparison to the method based on the direct detection of AuNPs. The novel detection mode allows the obtaining of a novel immunosensor with low protein detection limits, with special interest for further applications in clinical analysis, food quality and safety as well as other industrial applications.

This system establishes a general detection methodology that can be applied to a variety of immunosystems and DNA detection systems, including lab-on-a-chip technology. Currently, this methodology is being applied in our lab for the detection of low concentrations of proteins with clinical interest in real samples.

Acknowledgments

MEC (Madrid) for the projects MAT2008-03079/NAN, CSD2006-00012 “NANOBIOMED” (Consolider-Ingenio 2010) and Juan de la Cierva scholarship (A. de la Escosura) is acknowledged.

Appendix A. Supplementary data

Supplementary data associated with this article can be found, in the online version, at doi:10.1016/j.bios.2008.12.028.

References

Ambrosi, A., Castañeda, M.T., Killard, A.J., Smith, M.R., Alegret, S., Merkoçi, A., 2007. Anal. Chem. 79, 5232–5240.
Bradley, J.S., 1994. Clusters Colloids, 459 (Chapter 6).
Cai, H., Wang, Y., He, P., Fang, Y., 2002. Anal. Chim. Acta 469, 165–172.
Cai, H., Shang, C., Hsing, I.M., 2004. Anal. Chim. Acta 523, 61–68.
Cespedes, F., Martinez-Fabregas, E., Bartroli, J., Alegret, S., 1993. Anal. Chim. Acta 273, 409–417.
Cha, D.Y., Parravano, G., 1970. J. Catal. 18, 238–320.
Chu, X., Fu, X., Chen, K., Shen, G.L., Yu, R.Q., 2005. Biosens. Bioelectron. 20, 1805–1812.
Daniel, M.C., Astruc, D., 2004. Chem. Rev. 104, 293–346.
Das, J., Abdul-Aziz, M., Yang, H.A., 2006. J. Am. Chem. Soc. 128, 16022–16023.
De la Escosura-Muñiz, A., González-García, M.B., Costa-García, A., 2004. Electroanalysis 16, 1561–1568.
De la Escosura-Muñiz, A., González-García, M.B., Costa-García, A., 2006. Sens. Actuators B 114, 473–481.
De la Escosura-Muñiz, A., González-García, M.B., Costa-García, A., 2007. Biosens. Bioelectron. 22, 1048–1054.
De la Escosura-Muñiz, A., Ambrosi, A., Merkoçi, A., 2008. Trends Anal. Chem. 27, 568–584.
Dequaire, M., Degrand, C., Limoges, B., 2000. Anal. Chem. 72, 5521–5528.
Dequaire, M.R., Limoges, B., Brossier, P., 2006. Analyst 131, 923–929.
Fritzsche, W., Taton, T.A., 2003. Nanotechnology 14, R63–R73.
González-García, M.B., Costa-García, A., 1995. Bioelectrochem. Bioenerg. 38, 389–395.
Grunes, J., Zhu, J., Somorjai, G.A., 2003. Chem. Commun. 18, 2257–2260.
Guo, H., He, N., Ge, S., Yang, D., Zhang, J., 2005. Talanta 68, 61–66.
Gupta, S., Huda, S., Kilpatrick, P.K., Velev, O.D., 2007. Anal. Chem. 79, 3810–3820.
Hernández-Santos, D., González-García, M.B., Costa-García, A., 2000a. Electroanalysis 12, 1461–1466.
Hernández-Santos, D., González-García, M.B., Costa-García, A., 2000b. Electrochim. Acta 46, 607–615.
Karin, Y., Torres, C., Dai, Z., Rubinova, N., Xiang, Y., Pretsch, E., Wang, J., Bakker, Y., 2006. J. Am. Chem. Soc. 128, 13676–13677.
Katz, E., Willner, I., Wang, J., 2004. Electroanalysis 16, 19–44.
Kawde, A.N., Wang, J., 2004. Electroanalysis 16, 101–107.
Kerman, K., Morita, Y., Takamura, Y., Ozsoz, M., Tamiya, E., 2004. Anal. Chim. Acta 510, 169–174.
Kim, J.H., Seo, K.S., Wang, J., 2006. IEEE Sens. J. 6, 248–253.
Lang, H.F., Maldonado, S., Stevenson, K.J., Chandler, B.D., 2004. J. Am. Chem. Soc. 126, 12949–12956.
Lee, T.M.H., Cai, H., Hsing, I.M., 2004. Electroanalysis 16, 1628–1631.
Lee, T.M.H., Cai, H., Hsing, I.M., 2005. Analyst 130, 364–369.
Li, L.L., Cai, H., Lee, T.M.H., Barford, J., Hsing, I.M., 2004. Electroanalysis 16, 81–87.
Liao, K.T., Huang, H.J., 2005. Anal. Chim. Acta 538, 159–164.

Liu, G., Wang, J., Kim, J., Rasul-Jan, M., Collins, G.E., 2004. Anal. Chem. 76, 7126–7130.
Liu, G., Wu, H., Wang, J., Lin, Y., 2006. Small 2, 1139–1143.
Merkoçi, A., Aldavert, M., Marín, S., Alegret, S., 2005. Trends Anal. Chem. 24, 341–349.
Merkoçi, A., 2007. FEBS J. 274, 310–316.
Park, S.J., Taton, T.A., Mirkin, C.A., 2002. Science 295, 1503–1506.
Piras, L., Reho, S., 2005. Sens. Actuators B 111, 450–454.
Reetz, M.T., Schulenburg, H., López, M., Spliethoff, B., Tesche, B., 2004. Chimia 58, 896–899.
Santandreu, M., Cespedes, F., Alegret, S., Martinez-Fabregas, E., 1997. Anal. Chem. 69, 2080–2085.
Seydack, M., 2005. Biosens. Bioelectron. 20, 2454–2469.
Turkevich, J., Stevenson, P., Hillier, J., 1951. Discuss. Faraday Soc. 11, 55–75.
Wang, J., Xu, D., Kawde, A.N., Polsky, R., 2001a. Anal. Chem. 73, 5576–5581.
Wang, J., Polsky, R., Xu, D., 2001b. Langmuir 17, 5739–5741.
Wang, J., Liu, G., Polsky, R., Merkoçi, A., 2002a. Electrochem. Commun. 4, 722–726.
Wang, J., Xu, D., Polsky, R., 2002b. J. Am. Chem. Soc. 124, 4208–4209.
Wang, J., Liu, G., Merkoçi, A., 2003a. Anal. Chim. Acta 482, 149–155.
Wang, J., Liu, G., Merkoçi, A., 2003b. J. Am. Chem. Soc. 125, 3214–3215.
Wang, M., Sun, C., Wang, L., Ji, X., Bai, Y., Li, T., Li, J., 2003c. J. Pharm. Biomed. Anal. 33, 1117–1125.

Rapid identification and quantification of tumor cells using an electrocatalytic method based on gold nanoparticles

A.
de la Escosura-Muñiz, C. Sánchez-Espinel, B. Díaz-Freitas, A. González-Fernández, **M. Maltez-da Costa**, A. Merkoçi

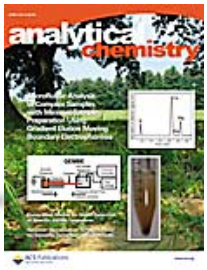

Analytical Chemistry

2009, 81, 10268-1027

Anal. Chem. **2009,** *81,* 10268–10274

Rapid Identification and Quantification of Tumor Cells Using an Electrocatalytic Method Based on Gold Nanoparticles

Alfredo de la Escosura-Muñiz,[†,‡] Christian Sánchez-Espinel,[§] Belén Díaz-Freitas,[§] África González-Fernández,[§] Marisa Maltez-da Costa,[†] and Arben Merkoçi*[,†,∥]

Nanobioelectronics & Biosensors Group, Catalan Institute of Nanotechnology, CIN2 (ICN-CSIC), Barcelona, Spain, Aragon Institute of Nanoscience, University of Zaragoza, Zaragoza, Spain, Immunology Group and Unidad Compartida del Complejo Hospitalario Universitario de Vigo, Edificio de Ciencias Experimentales, Universidade de Vigo, Vigo, Spain, and ICREA, Barcelona, Spain

There is a high demand for simple, rapid, efficient, and user-friendly alternative methods for the detection of cells in general and, in particular, for the detection of cancer cells. A biosensor able to detect cells would be an all-in-one dream device for such applications. The successful integration of nanoparticles into cell detection assays could allow for the development of this novel class of cell sensors. Indeed, their application could well have a great future in diagnostics, as well as other fields. As an example of a novel biosensor, we report here an electrocatalytic device for the specific identification of tumor cells that quantifies gold nanoparticles (AuNPs) coupled with an electrotransducing platform/sensor. Proliferation and adherence of tumor cells are achieved on the electrotransducer/detector, which consists of a mass-produced screen-printed carbon electrode (SPCE). In situ identification/quantification of tumor cells is achieved with a detection limit of 4000 cells per 700 μL of suspension. This novel and selective cell-sensing device is based on the reaction of cell surface proteins with specific antibodies conjugated with AuNPs. Final detection requires only a couple of minutes, taking advantage of the catalytic properties of AuNPs on hydrogen evolution. The proposed detection method does not require the chemical agents used in most existing assays for the detection of AuNPs. It allows for the miniaturization of the system and is much cheaper than other expensive and sophisticated methods used for tumor cell detection. We envisage that this device could operate in a simple way as an immunosensor or DNA sensor. Moreover, it could be used, even by inexperienced staff, for the detection of protein molecules or DNA strands.

The development and application of biosensors is one of the leading sectors of state-of-the-art nanoscience and nanotechnology. Biosensors are under commercial development for numerous applications, including the detection of pathogens, the measurement of clinical parameters, the monitoring of environmental pollutants, and other industrial applications. The most effective way of providing biosensors to potential customers, especially those with limited budgets, might be to modify the technology so that it can run on everyday equipment, rather than on specialized apparatuses.[1] Enzymatic biosensors represent an already consolidated class of biosensors, with glucose biosensors among the most successful on the market. Nevertheless, research is still needed to find novel alternative strategies and materials, so that affinity biosensors—immunosensors and genosensors—could be used in more successful applications in everyday life.

Early detection of cancer is widely acknowledged as the crucial key for an early and successful treatment. The detection of tumor cells is an increasingly important issue that has received wide attention in recent years,[2−7] mainly for two reasons: (i) new methods are allowing the identification of metastatic tumor cells (for example, in peripheral blood), with special relevance both for the evolution of the disease and for the response of the patient to therapeutic treatments, and (ii) diagnosis based on cell detection is, thanks to the use of monoclonal antibodies,[8] more sensitive and specific than that based on traditional methods.

Detecting multiple biomarkers and circulating cells in human body fluids is a particularly crucial task for the diagnosis and prognosis of complex diseases, such as cancer and metabolic disorders.[9] An early and accurate diagnosis is the key to an effective and ultimately successful treatment of cancer, but it

* Corresponding author. E-mail: arben.merkoci.icn@uab.es. Phone: +34935868014. Fax: +34935813797.

† Catalan Institute of Nanotechnology, CIN2 (ICN-CSIC).

‡ University of Zaragoza.

§ Universidade de Vigo.

∥ ICREA.

(1) Erickson, J. S.; Ligler, F. S. *Nature* **2008**, *456*, 178–179.
(2) Yucai, X.; Yin, T.; Wiegraebe, W.; He, X. C.; Miller, D.; Stark, D.; Perko, K.; Alexander, R.; Schwartz, J.; Grindley, J. C.; Park, J.; Haug, J. S.; Wunderlich, J. P.; Li, H.; Zhang, S.; Johnson, T.; Feldman, R. A.; Li, L. *Nature* **2009**, *457*, 97–101.
(3) Savage, P. A.; Vosseller, K.; Kang, C.; Larimore, K.; Riedel, E.; Wojnoonski, K.; Jungbluth, A. A.; Allison, J. P. *Science* **2008**, *319*, 215–220.
(4) Manganas, L. N.; Zhang, X.; Li, Y.; Hazel, R. D.; Smith, S. D.; Wagshul, M. E.; Henn, F.; Benveniste, H.; Djuri, P. M.; Enikolopov, G.; Maleti-Savati, M. *Science* **2007**, *318*, 980–985.
(5) Smith, J. E.; Medley, C. D.; Tang, Z.; Shangguan, D.; Lofton, C.; Tan, W. *Anal. Chem.* **2007**, *79*, 3075–3082.
(6) Cortez, C.; Tomaskovi-Crook, E.; Ohnston, A. P. R.; Scout, A. M.; Nice, E. C.; Heath, J. K.; Caruso, F. *ACSNano* **2007**, *1*, 93–102.
(7) Medley, C. D.; Smith, J. E.; Tang, Z.; Wu, Y.; Bamrungsap, S.; Tan, W. *Anal. Chem.* **2008**, *80*, 1067–1072.
(8) Rector, I.; Rektorova, I.; Kubova, D. J. *Neurol. Sci.* **2006**, *248*, 185–191.
(9) Sidransky, D. *Nat. Rev. Cancer* **2002**, *2*, 210–219.

10.1021/ac902087k CCC: $40.75
Published on Web 11/13/2009

requires new sensitive methods for detection. Many current methods for the routine detection of tumor cells are time-consuming (e.g., immunohistochemistry), expensive, or require advanced instrumentation (e.g., flow cytometry[10]). Hence, alternative cost-effective methods that employ simple/user-friendly instrumentation and are able to provide adequate sensitivity and accuracy would be ideal for point-of-care diagnosis. Therefore, in recent years, there have been some attempts at cell analysis using optical-based biosensors.[11−14] In addition to optical biosensors, sensitive electrochemical DNA sensors,[15−20] immunosensors,[20−22] and other bioassays have all recently been developed by our group and others,[23] using nanoparticles (NPs) as labels and providing direct detection without prior chemical dissolution.[24,25]

Herein, we present the design and application of a new class of affinity biosensor. Based on a new electrotransducing platform, this is a novel cell sensor inspired by DNA sensors and immunosensors. This platform consists of a screen-printed carbon electrode (SPCE), coupled to a new nanoparticle-based electrocatalytic method that allows rapid and consecutive detection/identification of in situ cell proliferation. Detection is based on the reaction of cell surface proteins with specific antibodies conjugated to gold nanoparticles (AuNPs). Use of the catalytic properties of the AuNPs on hydrogen formation from hydrogen ions[26] makes it possible to quantify the nanoparticles and, in turn, to quantify the corresponding attached cancer cells. This catalytic effect has also been observed for platinum[26] and palladium[27] nanoparticles, but AuNPs are more suitable for biosensing purposes, because of their simple synthesis, narrow size distribution, biocompatibility, and easy bioconjugation. The catalytic current generated by the reduction of the hydrogen ions is chronoamperometrically recorded and related to the quantity of the cells of interest. The basis of the method is that the protons are catalytically reduced to hydrogen in the presence of AuNPs at an adequate potential in acidic medium. This approach, using the catalytic current resulting from the reduction of hydrogen ions, has been employed for the detection of both platinum(II)[28] and gold(I)[29] complexes used as labels in genosensor designs. However, to our knowledge, the present study is the first where the chronoamperometric method is used for AuNPs, with all the advantages that the latter bring to biosensing applications.

To evaluate the efficacy of this cell sensor as a probing tool for the detection of tumor cells, we studied whether the human tumor HMy2 cell line (HLA-DR class II positive B cell) could indeed be detected and whether another human tumor PC-3 cell line (HLA-DR class II negative prostate carcinoma) was not detected. Tumor cells can be grown on the surface of SPCEs, showing a similar morphology to those in other conventional cell growth substrates. Incubation of cells with AuNPs conjugated to antibodies was carried out in either a direct or indirect way. In the former, a commercial mouse monoclonal antibody (mAb) directed against DR molecules was conjugated to AuNPs, whereas in the indirect method, incubation with unconjugated anti-DR monoclonal antibody was followed by secondary antibodies attached to AuNPs. In both cases, the immunosensor was able to identify DR-positive tumor cells, but not the negative cells. As expected, the indirect method gave a higher signal, because of the amplification mediated by several secondary antibodies attached to the primary antibody.

We propose this cell sensor as a new class of biosensor device for the specific identification of cells in general and, more particularly, for the identification of tumor cells. The method does not require expensive equipment, it provides an adequate sensitivity and accuracy, and it would be an ideal alternative for point-of-care diagnosis in the future.

Given the increased use of various metallic nanoparticles, we envisage possible further applications of these smart nanobiocatalytic particles for other diagnostic purposes. The simultaneous detection of several kinds of cells (e.g., to perform blood tests, detect inflammatory or tumoral cells in biopsies or fluids) could be carried out, including multiplexed screening of cells, proteins, and even DNA.

MATERIALS AND METHODS

Chemicals and Equipment. Hydrogen tetrachloroaurate(III) trihydrate ($HAuCl_4 \cdot 3H_2O$, 99.9%) and trisodium citrate were purchased from Sigma-Aldrich (Spain). Unless otherwise stated, all buffer reagents and other inorganic chemicals were supplied by Sigma, Aldrich, or Fluka (Spain). All chemicals were used as received, and all aqueous solutions were prepared in doubly distilled water. The phosphate buffer solution (PBS) consisted of 0.01 M phosphate buffered saline, 0.137 M NaCl, and 0.003 M KCl (pH 7.4). Analytical grade (Merck, Spain) HCl was used. The solutions were prepared with ultrapure water.

The human tumor cell lines used as targets in this study were HMy2, a tumoral B cell line that expresses surface HLA-DR molecules (class II of major histocompatibility complex), and PC-3, a tumoral prostate cell line that does not express the DR protein.

(10) Vermes, I.; Haanen, C.; Reutelingsperger, C. *J. Immunol. Methods* **2000**, *243*, 167–190.
(11) Fang, Y.; Ferrie, A. M.; Fontaine, N. H.; Yuen, P. K. *Anal. Chem.* **2005**, *77*, 5720–5725.
(12) Knauer, S. K.; Stauber, R. H. *Anal. Chem.* **2005**, *77*, 4815–4820.
(13) Skivesen, N.; Horvath, R.; Thinggaard, S.; Larsen, N. B.; Pedersen, H. C. *Biosens. Bioelectron.* **2007**, *22*, 1282–1288.
(14) Lin, B.; Li, P.; Cunninghamb, B. T. *Sens. Actuators B* **2006**, *114*, 559–564.
(15) Wang, J.; Liu, G.; Merkoçi, A. *J. Am. Chem. Soc.* **2003**, *125*, 3214–3215.
(16) Wang, J.; Polsky, R.; Merkoçi, A.; Turner, K. L. *Langmuir* **2003**, *19*, 989–991.
(17) Pumera, M.; Castañeda, M. T.; Pividori, M. I.; Eritja, R.; Merkoçi, A.; Alegret, S. *Langmuir* **2005**, *21*, 9625–9629.
(18) Castañeda, M. T.; Merkoçi, A.; Pumera, M.; Alegret, S. *Biosens. Bioelectron.* **2007**, *22*, 1961–1967.
(19) Marin, S.; Merkoçi, A. *Nanotechnology* **2009**, *20*, 055101.
(20) Ambrosi, A.; Merkoçi, A.; de la Escosura-Muñiz, A.; Castañeda, M. T. In *Biosensing Using Nanomaterials*; Merkoçi, A., Ed.; Wiley Interscience: New York, 2009; Chapter 6, pp 177−197.
(21) Ambrosi, A.; Castañeda, M. T.; Killard, A. J.; Smyth, M. R.; Alegret, S.; Merkoçi, A. *Anal. Chem.* **2007**, *79*, 5232–5240.
(22) de la Escosura-Muñiz, A.; Maltez-da Costa, M.; Merkoçi, A. *Biosens. Bioelectron.* **2009**, *24*, 2475–2482.
(23) de la Escosura-Muñiz, A.; Ambrosi, A.; Merkoçi, A. *Trends Anal. Chem.* **2008**, *27*, 568–584.
(24) Pumera, M.; Aldavert, M.; Mills, C.; Merkoçi, A.; Alegret, S. *Electrochim. Acta* **2005**, *50*, 3702–3707.
(25) Merkoçi, A.; Marcolino-Junior, L. H.; Marín, S.; Fatibello-Filho, O.; Alegret, S. *Nanotechnology* **2007**, *18*, 035502.
(26) Chikae, M.; Idegami, K.; Kerman, K.; Nagatani, N.; Ishikawa, M.; Takamura, Y.; Tamiya, E. *Electrochem. Commun.* **2006**, *8*, 1375–1380.
(27) Meier, J.; Schiøtz, J.; Liu, P.; Nørskov, J. K.; Stimming, U. *Chem. Phys. Lett.* **2004**, *390*, 440–444.
(28) Hernández-Santos, D.; González-García, M. B.; Costa-García, A. *Anal. Chem.* **2005**, *77*, 2868–2874.
(29) Díaz-González, M.; de la Escosura-Muñiz, A.; González-García, M. B.; Costa-García, A. *Biosens. Bioelectron.* **2008**, *23*, 1340–1346.

All cells were cultured in RPMI 1640 medium (Gibco, Life Technologies, Scotland) supplemented with 10% heat-inactivated fetal calf serum (FCS) (PAA, Austria), penicillin (100 U/mL), and glutamine (2 mM) (Gibco) at 37 °C in a humidified atmosphere containing 5% CO_2.

Measurement of HLA-DR expression was carried out with a commercial FITC-mouse antihuman HLA-DR mAb (Immunotech, France) and BH1, a human IgM mAb produced by the Immunology group of Vigo,[30−32] which recognizes human HLA-class II molecules on the surface of human monocytes, B lymphocytes, tumor B cell lines (HMy2, Raji, and Daudi), and tumor cells from patients suffering from hematological malignancies. As a control for positive recognition of both cell lines tested, the human mAb 32.4 was used, also produced by the Immunology group of Vigo. For the BH1 and 32.4 mAbs, FITC-conjugated rabbit antihuman IgM polyclonal antibodies (DakoCytomation, Spain) were used as secondary antibodies.

Electrochemical measurements were taken using an Ivium Potentiostat (The Netherlands) connected to a PC.

Cells were visualized under inverted and directed microscopes (Olympus IX50 and BX51, respectively, Olympus Optical, Japan), and photographs were taken with an Olympus DP71 camera.

A DEK248 semiautomatic screen-printing machine (DEK International, Switzerland) was used for the fabrication of the screen-printed carbon electrodes (SPCEs), as electrochemical transducers. The reagents used for this process were Autostat HT5 polyester sheet (McDermid Autotype, U.K.) and Electrodag 423SS carbon ink, Electrodag 6037SS silver/silver chloride ink, and Minico 7000 Blue insulating ink (Acheson Industries, The Netherlands).

The chambers used for cell incubation on the working area of the surface of the SPCEs were Lab-Tek eight-well chamber slides (Nunc, Thermo Fisher Scientific, Spain).

A JEOL JEM-2011 transmission electron microscope (JEOL Ltd., Japan) was used to characterize the gold nanoparticles.

Philips XL30 and JEOL JSM 6700F scanning electron microscopes were used to obtain images of cell growth on the surface of the sensor.

A Cytomics FC 500 Series Flow Cytometry Systems and CXP and MXP software (Beckman Coulter, Fullerton, CA) was used for the cell fluorescence measurements.

The electrochemical transducers used for the in situ growth and detection of the cells were homemade screen-printed carbon electrodes (SPCEs), prepared as described in the Supporting Information.

Preparation and Modification of Gold Nanoparticles. The 20-nm gold nanoparticles (AuNPs) were synthesized by reducing tetrachloroauric acid with trisodium citrate, a method pioneered by Turkevich et al.[33] (see the experimental procedure for AuNP synthesis, transmission electron microscopy (TEM) images, and the Gaussian distribution of sizes in the Supporting Information).

The conjugation of AuNPs to FITC-mouse anti human DR mAb (αDR) and polyclonal rabbit antihuman IgM (αIgM) antibodies was performed according to the following procedure:[21] Two milliliters of AuNP suspension was mixed with 100 μL of 100 μg/mL solutions of each antibody and incubated at 25 °C for 20 min. Subsequently, a blocking step with 150 μL of 1 mg/mL BSA incubating at 25 °C for 20 min was undertaken. Finally, centrifugation was carried out at 14000 rpm for 20 min, and AuNP/αDR and AuNP/αIgM conjugates were reconstituted in PBS solution.

Effect of Gold Nanoparticles on Hydrogen Ion Reduction. Cyclic votammetric measurements were made to study the catalytic effect of gold nanoparticles on hydrogen ion reduction. A total of 25 μL of a 2 M HCl solution was mixed with 25 μL of a solution of AuNPs (different concentrations), the mixture was placed onto the surface of the electrodes, and cyclic voltammograms were recorded from +1.35 to −1.40 V at a scan rate of 50 mV/s. The background was recorded by placing 50 μL of a 1 M HCl solution onto the surface of the electrodes, following the same electrochemical procedure.

Qualitative analyses were carried out taking advantage of the chronoamperometric mode. Chronoamperograms were obtained by placing a mixture of 25 μL of 2 M HCl and 25 μL of the AuNP solution (different concentrations) onto the surface of the electrodes and, subsequently, holding the working electrode at a potential of +1.35 V for 1 min and then a negative potential of −1.00 V for 5 min. The cathodic current generated was recorded. The background (blank curve) was recorded by placing 50 μL of a 1 M HCl solution onto the electrode surface and following the same electrochemical protocol.

Similar measurements were taken for the AuNP/αDR and AuNP/αIgM conjugates.

Incubation of Cells. *Incubation of Cells in Flasks.* HMy2 and PC-3 cell lines were cultured in medium at 37 °C in a humidified atmosphere containing 5% CO_2 in tissue culture flasks (Falcon, Becton Dickinson and Company, Franklin Lakes, NJ). The PC-3 cells were removed from the flasks using a cell scrapper, whereas the HMy2 cells were removed mechanically by mixing the flask, and the cells were counted in the presence of Trypan blue.

Incubation of Cells onto the Surface of Screen-Printed Carbon Electrodes (SPCEs). Only the working electrode surfaces were introduced into Lab-Tek eight-well chamber slides (Nunc, Thermo Fisher Scientific) after gasket removal and then fixed with mounting. (Supporting Information, Figure S1B,C). A fixed amount of cells was added into each well in a volume of 700 μL of culture medium and incubated for 24 h at 37 °C in a humidified atmosphere containing 5% CO_2.

Detection/Quantification of Cells. *Immunological Reaction with Specific Antibodies.* (a) For the direct immunoassay, once cells had grown onto the electrode surface, they were washed with PBS, and 50 μL of AuNP/αDR was added onto the working electrode area and left there for 30 min at 37 °C.

(b) For the indirect immunoassay, cells were incubated with primary antibodies (either BH1 or 32.4 mAbs) for 30 min, washed with PBS, and then incubated with AuNP/αIgM for 30 min.

(30) Magadán, S.; Valladares, M.; Suarez, E.; Sanjuan, I.; Molina, A.; Ayling, C.; Davies, S.; Zou, X.; Williams, G. T.; Neuberger, M. S.; Brüggeman, M.; Gambón, F.; Díaz-Espada, F.; González-Fernández, Á. *Biotechniques* **2002**, *33*, 680–690.

(31) Suárez, E.; Magadán, S.; Sanjuán, I.; Valladares, M.; Molina, A.; Gambón, F.; Díaz-Espada, F.; González-Fernández, A. *Mol. Immunol.* **2006**, *43*, 1827–1835.

(32) Díaz, B.; Sanjuan, I.; Gambón, F.; Loureiro, C.; Magadán, S.; González-Fernández, A. *Cancer Immunol. Immunother.* **2009**, *58*, 351–360.

(33) Turkevich, J.; Stevenson, P.; Hillier, J. *Discuss. Faraday Soc.* **1951**, *11*, 55–75.

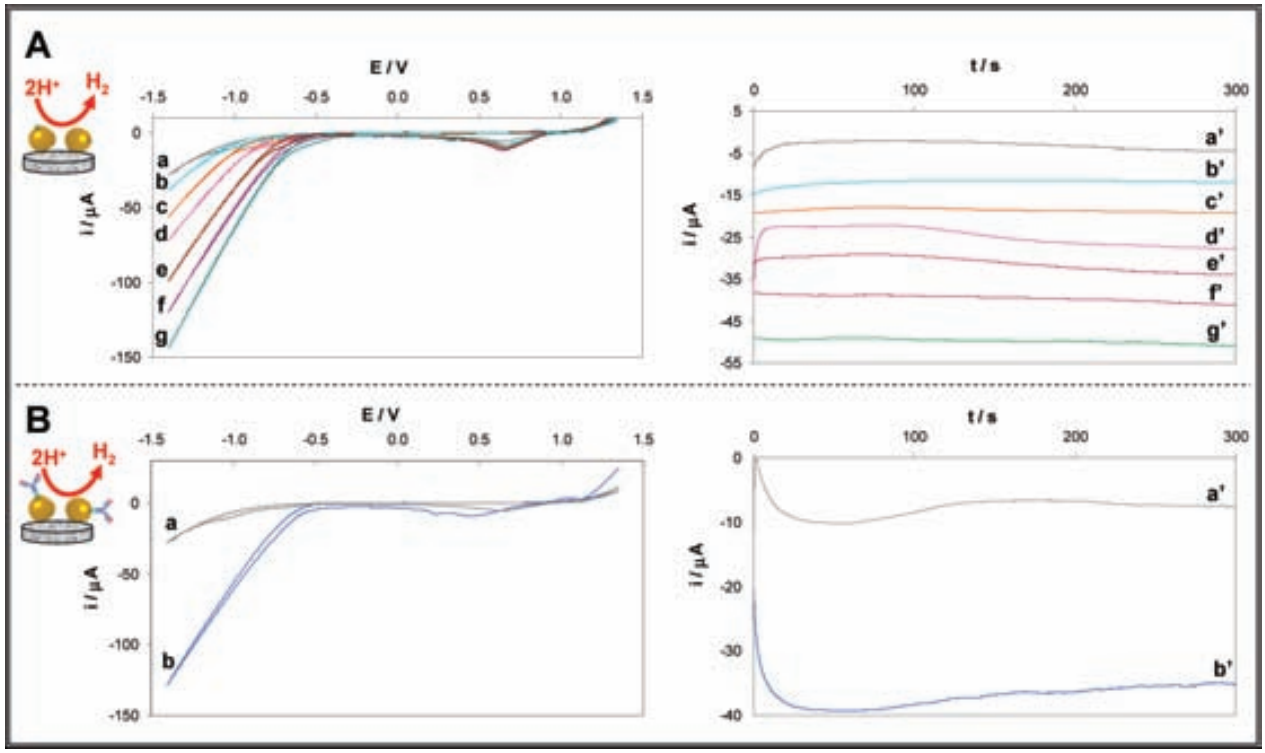

Figure 1. (A) Left: Cyclic voltammograms recorded from +1.35 to −1.40 V at a scan rate of 50 mV/s for a 1 M HCl solution (blank curve, a) and for increasing concentrations of AuNPs in 1 M HCl: (b) 0.96, (c) 4.8, (d) 24, (e) 120, (f) 600, and (g) 3000 pM. Right: Chronoamperograms recorded by applying a potential of −1.00 V for 5 min, using a 1 M HCl solution (blank curve, a′) and the same AuNP concentrations in 1 M HCl as detailed above (b′−g′). (B) Left: Cyclic voltammograms recorded under the same conditions as in A, left, for the blank (curve a) and for a solution of the conjugate AuNP/αDR (curve b). Right: Chronoamperograms recorded under the same conditions as in A, right, for the blank (a′) and for the conjugate AuNP/αDR (b′).

Analytical Signal Based on Hydrogen Evolution Catalyzed by AuNPs. Cells (after direct or indirect immunoassays) were washed with PBS solution to remove unbound AuNP/antibodies, and then 50 μL of 1 M HCl solution was applied to the SPCE surface. Subsequently, the electrode was held at a potential of +1.35 V for 1 min, and then a negative potential of −1.00 V was applied for 5 min. The cathodic current generated was recorded, and the value of the current at 200 s was chosen as the analytical signal.

Flow Cytometry. Flow cytometry analysis was carried out using 2×10^5 cells (HMy2 or PC-3) incubated at 4 °C for 40 min in the presence of commercial FITC-anti human DR mAb (αDR) or concentrated hybridoma supernatant containing BH1 and 32.4 mAbs. Cells were washed twice with PBS, and for indirect immunofluorescence, cells were stained with FITC-rabbit anti HuIgM (αIgM) Abs (Dako) at 4 °C for 30 min. The stained cells were washed five times with PBS, and the cellular fluorescence was measured using a flow cytometer.

RESULTS AND DISCUSSION

Catalytic Effect of AuNPs on Hydrogen Evolution. The catalytic properties of AuNPs, deposited onto SPCEs, are shown in Figure 1. Figure 1A (left) displays cyclic voltammograms (CVs) in 1 M HCl solutions recorded from +1.35 to −1.40 V, and Figure 1A (right) shows the corresponding chronoamperometric responses plotted at a fixed potential of −1.00 V. Curve a is the background CV that corresponds to the SPCE without AuNP, whereas curves b−g correspond to SPCEs with increasing concentrations of deposited AuNPs present in the HCl solution. The background CV (curve a) shows that the reduction of the medium's protons to hydrogen starts at approximately −0.60 V. In the presence of the AuNPs (curves b−g) on the surface of the electrode, the potential for hydrogen ion reduction shifts (by up to 500 mV, depending on the concentration of AuNPs) toward less negative potentials. Moreover, it can also be seen that, because of the catalytic effect of the AuNPs, a higher current is generated (up to 100 μA higher, as evaluated for the potential value of −1.40 V, depending on the concentration of AuNPs). The oxygen reduction on SPCE at very negative potentials (lower than −1.40 V) is not of great importance; therefore, the background signals are not affected.

The results obtained show that, if an adequate potential is fixed (i.e., −1.00 V), the intensity of the current recorded in chronoamperometric mode during the stage of hydrogen ion electroreduction (Figure 1A, right) can be related to the presence (curves b′−g′) or absence (curve a′) of AuNPs on the surface of the SPCE. A proportional increase of catalytic current was observed with corresponding increases in the concentration of AuNPs (from 3 nM (3000 pM) to 0.96 pM). The absolute value of the current generated at 200 s (response time of the sensor) was chosen as the analytical signal and used for quantification of the AuNPs.

The effect of other sources of hydrogen ions (e.g., HNO_3, H_2SO_4 at different concentrations ranging from 0.1 to 1 M) on the current intensity corresponding to the AuNPs was also studied (results not shown). The use of HNO_3 was avoided because of its corrosive effect on the transducer (screen-printed electrode based on carbon ink). Moreover, at the same

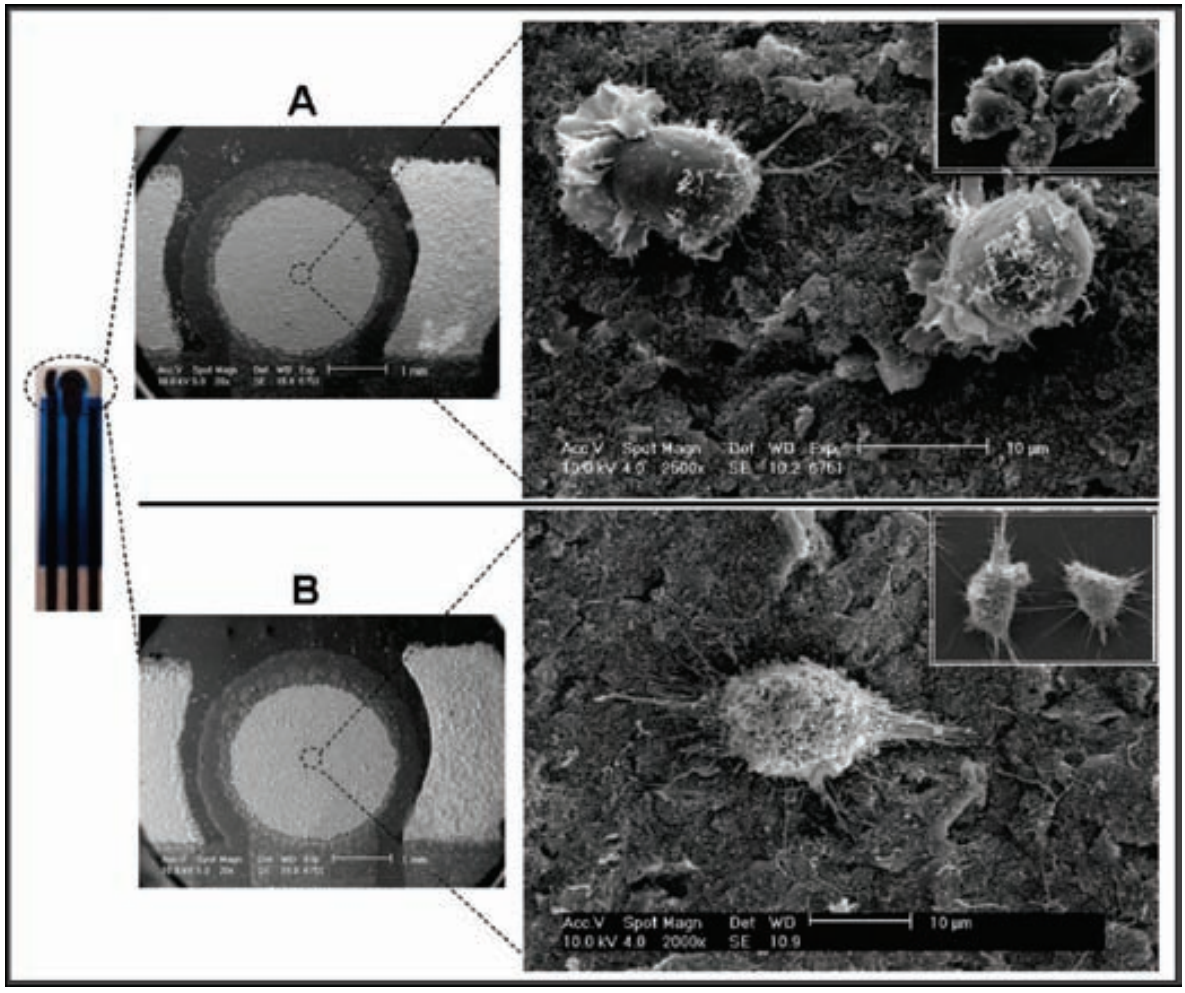

Figure 2. SEM images of the electrotransducer (SPCE) (left) with its three surfaces and details of the (A) HMy2 and (B) PC-3 cell lines on the carbon working electrode (right). Inset images correspond to cell growth on the plastic area of the SPCEs.

concentration, H_2SO_4 gave lower sensitivity than was obtained for HCl.

The pretreatment at +1.35 V was also optimized. It was found that this previous oxidation is necessary for obtaining the best electrocatalytic effect in the further reduction step (hydrogen ion reduction at −1.00 V for 5 min). During the application of this oxidative potential, some of the AuNPs are transformed into Au(III) ions (released from the AuNP surface). These ions could also exert a catalytic effect on hydrogen evolution,[29] as could the significant number of AuNPs still remaining (results not shown) after the oxidation step.

The behavior of AuNPs modified with antibodies was also evaluated for conditions similar to those used for the nonmodified AuNPs. A very similar response (see both CVs at Figure 1B, left, and corresponding chronoamperograms in Figure 1B, right) was observed for AuNPs modified with anti-DR mAb (AuNP/αDR).

Cell Growth on the Surface of SPCEs. After the evaluation of the SPCE to detect AuNPs using the catalytic mode, the next step was to study whether tumor cells can grow or attach themselves on top of the same electrodes. Two adherent human tumor cells (HMy2 and PC-3) that differ in the expression of surface HLA-DR molecules were used. HMy2 (a B-cell line) presents surface HLA-DR molecules, whereas PC-3 (a tumoral prostate cell line) is negative to this marker; they were used as target cells and "blank/control assay" cells, respectively. The growth of both cell lines on SPCEs was compared with that in flasks, the routine environment used in cell culture.

A total of 2×10^5 cells were placed onto the surface of the SPCEs through a small chamber with a window over the electrode area. Cell growth was allowed to take place on the surface of the working electrode. Figure 2 shows scanning electron microscopy (SEM) images of both cell lines attached to the working electrode of the SPCEs. Both types of cells were able to grow on the carbon surface, and most interestingly, they showed morphological features similar to those of cells growing on the plastic surface (inset images).

Identification of Cells Based on the Catalytic Detection of AuNPs. Scheme 1 shows the cell assay used to specifically identify tumoral cells starting from the SPCE electrotransducer. Both types of cell, HMy2 (Scheme 1A) and PC-3 (Scheme 1B), were initially introduced onto the surface of the SPCEs and allowed to grow (a,a′), prior to incubation with antibody-modified AuNPs (b,b′). Finally, analysis by electrocatalytic detection based on hydrogen ion reduction (d,d′) was carried out. Taking advantage of the catalytic properties of AuNPs on hydrogen evolution, antibodies conjugated with AuNPs were used to discriminate positive or negative cells for one specific marker. The presence of HLA-DR proteins on the surface of HMy2 cells was compared with PC-3 cells used as blanks. Two different antibodies were used for this purpose: a commercial anti-DR mAb

Scheme 1. (A) Tumoral Cell Line (HMy2) Expressing Surface HLA-DR Molecules Compared to a (B) Cell Line That Is Negative to This Marker (PC-3)[a]

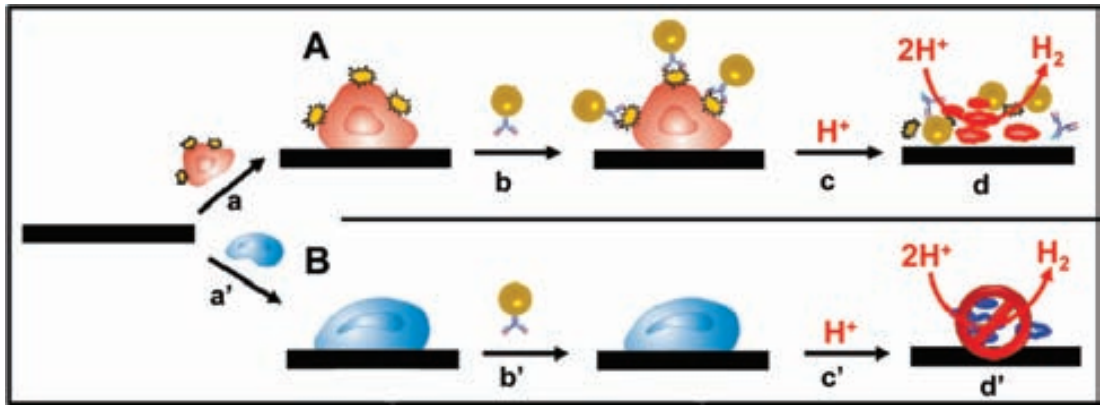

[a] Cells were (a,a′) attached to the surface of the electrodes and (b,b′) incubated with AuNP/αDR, (c,c′) an acidic solution was added, and (d,d′) the hydrogen generation was electrochemically measured.

(αDR) and a homemade BH1 mAb, both able to recognize HLA-DR class II molecules. For the commercial sample, αDR antibodies were directly labeled with AuNPs, whereas for the homemade BH1 antibody, a second step was necessary using AuNPs conjugated to secondary antibodies (αIgM). Another homemade antibody (32.4 mAb) that recognizes both types of cells was used as a positive control.

After addition of 50 μL of a 1 M HCl solution, when a negative potential of −1.00 V was applied, the hydrogen ions of the medium were reduced to hydrogen, and this reduction was catalyzed by the AuNPs attached through the immunological reaction. The current produced was measured. The electrochemical response in the presence of AuNP/αDR antibodies was positive in HMy2 (DR-positive cells), but not, as expected, in PC-3 (DR-negative cells) (Supporting Information, Figure S3A). This response was greatly increased by the use of secondary antibodies, as was observed for the BH1 mAb followed by AuNP/αIgM. For the control antibody (32.4 mAb), the electrochemical signals suggested that the PC-3 cells grew on the SPCEs and that recognition took place to a higher extent for these cells than for the HMy2 cell line.

These results concur with those for both cell lines in the immunofluorescence analysis by flow cytometry (Supporting Information, Figure S3B). The figure shows that, whereas HMy2 cells are positive to both the commercial αDR and the BH1 mAbs, PC-3 cells are negative to these antibodies. The same result was found for the positive control undertaken with the antibody 32.4, which recognizes both types of cells by immunofluorescence but has a higher intensity of recognition for PC-3 cells.

Effect of the Number of Cells on the Electrocatalytical Signal. To minimize the analysis time, the commercial αDR mAb was chosen for the quantification studies, even though the BH1 mAb had a higher response. Different quantities of HMy2 cells, ranging from 10000 to 400000, were incubated on the SPCEs and, subsequently, recognized by the AuNP/αDR. Figure 3A shows the effect of the number of cells on the electrocatalytical signal. An increase can be seen in the value of the analytical signal obtained that is correlated to the amount of HMy2 cells cultured. Although, because of the scale, no major differences can be appreciated in Figure 3A, a difference of around 170 nA was observed between control cells (blank) and 10000 cells. The inset curve shows that there is a very good linear relationship between

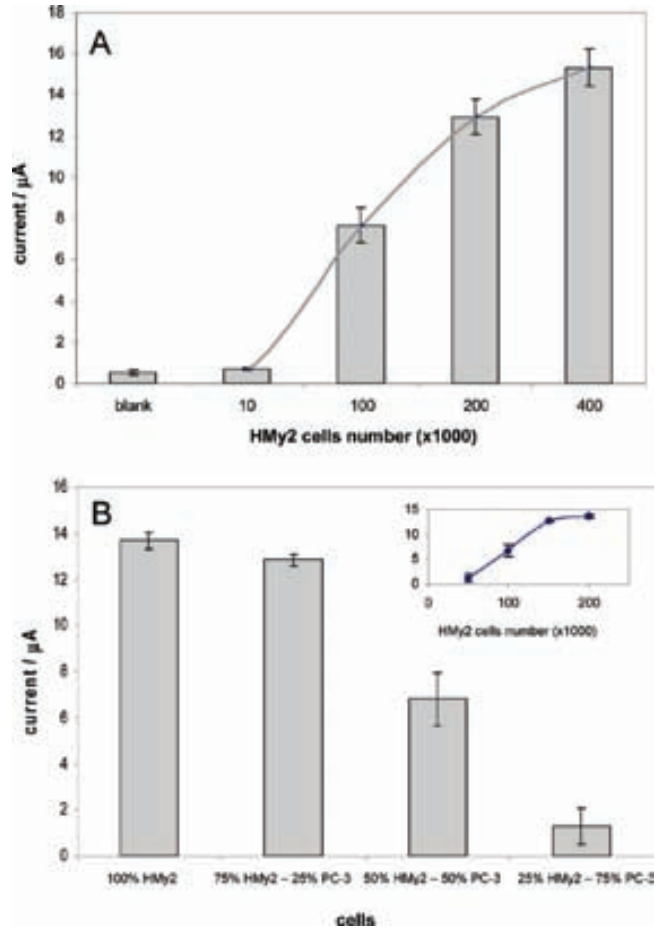

Figure 3. (A) Effect of the number of HMy2 cells on the electrocatalytical signals, after incubation with AuNP/αDR. (B) Electrocatalytical signals obtained with HMy2 cells, after incubation with AuNP/αDR in the presence of PC-3 cells at different HMy2/PC-3 ratios (the first bar, "100% HMy2", corresponds to 200000 HMy2 cells, whereas the last bar "25% HMy2−75% PC-3" corresponds to 50000 HMy2 cells and 150000 PC-3 cells).

the two parameters in the range of 10000−200000 cells, with a correlation coefficient of 0.9955, according to the equation

$$\text{current } (\mu\text{A}) = 0.0641(\text{cell number}/1000) + 0.497\ (\mu\text{A})\ (n = 3)$$

The limit of detection (calculated as the concentration of cells corresponding to 3 times the standard deviation of the estimate)

was 4000 cells in 700 μL of sample. The reproducibility of the method shows a relative standard deviation (RSD) of 7%, obtained for a series of three repetitive assay reactions for 100000 cells.

In addition, the ability of the method to discriminate HMy2 in the presence of PC-3 cells was also demonstrated. Figure 3B shows the values of the analytical signal after incubation with AuNP/αDR for mixtures of HMy2 and PC-3 cells at different ratios (100% corresponds to 200000 cells). The presence of PC-3 cells does not significantly affect the analytical signal coming from the recognition of HMy2 cells, and once again, a good correlation was obtained for the signal detected and for the amount of positive cells on the electrode. This could pave the way for future applications to discriminate, for example, tumor cells in tissues or blood, as well as biopsies, where at least 4000 cells express a specific marker on their surface.

Further technological improvements, such as reducing the size of the working electrode, could lead to a reduction in the volume of sample required for analysis, thereby allowing the detection of even lower quantities of cells. In addition, amplification strategies could be implemented; for example, micro-/nanoparticles could be simultaneously used as labels and carriers of AuNPs, making it possible to obtain an enhanced catalytic effect (more than one AuNP per antibody would be used) that would produce improved sensitivities and detection limits.

The developed methodology could be extended for the discrimination/detection of several types of cells (tumoral, inflammatory) expressing proteins on their surface, by using specific monoclonal antibodies directed at these targets. For example, the methodology could be applied for the diagnosis of metastasis. Metastatic tumor cells can express specific membrane proteins different from those in the healthy surrounding tissue, where they colonize. It could also be used for those primary tumors that exhibit specific tumor markers or overexpress others than those that are normally absent or have very low expression in healthy tissues. The breast cancer receptor (BCR) could possibly fall into this category, as it appears at low levels in healthy cells, but is overexpressed in some types of breast cancer. With a positive response, the identification of tumor cells could be very useful for an early treatment of the patient with monoclonal antibodies specifically targeted against this cancer receptor.

CONCLUSIONS

A novel cell sensor design has been developed coupled with a new electrocatalytic detection method for AuNPs, making possible specific identification of tumor cells. The proposed cell sensor is a rapid and simple cell detection device, on which cell growth occurs in situ, followed by detection on the same platform. The method's electrochemical detection mode is a more sensitive alternative to the direct detection of AuNPs reported earlier for DNA or protein sensing. Chronoamperometric plotting of the analytical signal is much simpler than the stripping analysis or differential pulse voltammetries described in previous reports.[17−19,21] In our particular example, we show that HLA-DR molecules on the surface of HMy2 cells are recognized by specific antibodies, previously conjugated with AuNPs. Their catalytic effect on hydrogen ion reduction is measured, allowing for specific cell identification, with a detection limit of 4000 cells.

In conclusion, we have demonstrated a tumor cell sensor based on gold nanoparticle immunoconjugates that, in combination with a screen-printed electrode, provides an efficient sensing platform, achieving both detection and identification of analytes. This strategy uses the electrocatalytic properties of gold nanoparticles to impart efficient transduction of the cell-binding event. A rapid, efficient, and generalized identification and quantification of cells is made possible by the use of this cell sensor. We have shown here that it can be used in the detection of surface molecules on tumoral cells, but more research is under way to determine whether this cell sensor could also be used for the detection of intracellular antigens and in cell suspensions. This would increase the possible uses of this device even more. The robust characteristics of the nanoparticles and transducing platform, combined with the diversity of surface functionality that can be readily obtained using nanoparticles, make this approach a promising technique for biomedical diagnostics. This approach could pave the way for further applications, such as the detection of cancer or inflammatory cells in diagnostic procedures (e.g., in needle aspiration biopsies in the operating room), using a simple miniaturized system. This method can also be extended to DNA detection based on conjugated AuNPs. As the cell sensor is produced by standard screen-printing fabrication, it can be readily mass produced at low cost and as disposable units. The use of magnetic nanoparticles could soon bring inherent signal amplification in a manner similar to that previously reported for DNA[19] or protein detection.[21,22]

Finally, efforts are under way to fabricate a lab-on-a-chip system that will include the use of magnetic particles as antibody immobilization platforms and could be used for protein and cell analysis. We envisage that the resulting cell sensor will be broadly applicable to sensing different cells, biomarkers, and biological species with enhanced sensitivity and specificity. Furthermore, it will be a truly portable, low-cost, easy-to-use device for point-of-care use.

ACKNOWLEDGMENT

We acknowledge funding from the MEC (Madrid, Spain) for Projects MAT2008-03079/NAN and CSD2006-00012 "NANOBIOMED" (Consolider-Ingenio 2010) and the Juan de la Cierva scholarship (A.E.-M.) and from the Xunta de Galicia (PGIDIT06TMT31402PR). We also thank Jesús Mendez (CACTI, Universidad de Vigo, Vigo, Spain) for his help with the SEM images and Ted Cater and Teresa Carretero for English corrections and editorial comments.

SUPPORTING INFORMATION AVAILABLE

Additional information as noted in text. This material is available free of charge via the Internet at http://pubs.acs.org.

Received for review June 2, 2009. Accepted October 29, 2009.

AC902087K

Detection of Circulating Tumor Cells Using Nanoparticle

M. Maltez-da Costa, A de la Escosura-Muniz, Carme Nogués, Leonard Barrios, Elena Ibáñez A. Merkoçi

Submitted to Small

DOI: 10.1002/smll.((please add manuscript number))

Detection of Circulating Tumor Cells Using Nanoparticles

*Marisa Maltez-da Costa, Alfredo de la Escosura-Muñiz, Carme Nogués, Leonard Barrios, Elena Ibáñez, Arben Merkoçi **

[*] Prof. Arben Merkoçi
ICREA, Institució Catalana de Recerca i Estudis Avançats and Nanobioelectronics & Biosensors Group, CIN2 (ICN-CSIC), Catalan Institute of Nanotechnology, Campus de la UAB Bellaterra (Barcelona), 08193 Spain
E-mail: arben.merkoci@icn.cat

Marisa Maltez-da Costa, Dr. Alfredo de la Escosura-Muñiz
Nanobioelectronics & Biosensors Group, CIN2 (ICN-CSIC), Catalan Institute of Nanotechnology, Campus de la UAB Bellaterra (Barcelona), 08193 Spain

Prof. Carme Nogués, Prof. Lleonard Barrios, Dr. Elena Ibáñez
Departament de Biologia Cel•lular, Fisiologia i Immunologia, Universitat Autònoma de Barcelona, Campus UAB-Facultat de Biociències

Supporting Information is available on the WWW under http://www.small-journal.com or from the author.

Keywords: cancer diagnosis • hydrogen catalysis •circulating tumor cell • gold nanoparticles • electrochemical properties

Discrimination of circulating cancer cells from normal blood cells offers a high potential in tumor diagnosis and fast scanning non-invasive methods are needed to achieve early diagnosis and prognosis in cancer patients. A rapid cancer cell detection and quantification assay, based on the electrocatalytic properties of gold nanoparticles towards the Hydrogen Evolution Reaction is described. The selective labeling of cancer cells is performed in suspension allowing a fast interaction between electrochemical labels (gold nanoparticles) and the target proteins expressed at the cell membrane. The subsequent electrochemical detection is accomplished with small volumes of sample and user-friendly equipment through a simple

electrochemical method that originates a fast electrochemical response used for the quantification of nanoparticle-labeled cancer cells.

The selective labeling of cancer cells by gold nanoparticles is also monitored by cytometry and microscopic techniques. This system establishes an efficient cell-detection assay capable of detecting 4 x10^3 Caco2 cells in suspension (used as target cells in a proof-of-concept sensing assay) and is able to discriminate between the target cells and other circulating cells (monocytes) that may interfere in real sample analysis. In addition, to further verify the efficiency of this sensing system, we apply the SEM-Backscattering imaging for the observation of cells without the need of metallization or any other procedure, that would change or mask the nanosized gold nanoparticles modified with antibodies and used to label the cancer cell membrane. The developed CTC sensing assay and imaging mode can be extended to several other cells detection scenarios in addition to nanoparticles based drug delivery and nanotoxicology studies.

1. Introduction

Circulating Tumor Cells (CTCs) are blood-travelling cells that detach from a main tumor or from metastasis. CTCs quantification is under intensive research for examining cancer metastasis, predicting patient prognosis, and monitoring the therapeutic outcomes of cancer.[1–5] Although extremely rare, CTCs detection/quantification in physiological fluids represents a potential alternative to the actual invasive biopsies and subsequent proteomic and functional genetic analysis.[6,7] Therefore their discrimination from normal blood cells offers a high potential in tumor diagnosis.[4,8] Established techniques for CTC identification include

labeling cells with antibodies (immunocytometry) or detecting the expression of tumor markers by reverse-transcriptase polymerase chain reaction (RT-PCR).[9]

Cancer cells overexpress specific proteins at their plasma membrane and using the information available for the different types of cancer cells, the reported proteins are often used as targets in CTCs sensing methodologies.[10] An example of these target proteins is the Epithelial Cell Adhesion Molecule (EpCAM), a 30-40 kDa type I glycosylated membrane protein expressed at low levels in a variety of human epithelial tissues and overexpressed in most solid cancers.[11] Decades of studies have revealed the roles of EpCAM in tumorigenesis and it has been identified to be a cancer stem cell marker in a number of solid cancers, as for example in colorectal adenocarcinomas cancer where it is found in more than 98%, and its expression is inversely related to the prognosis. [12,13]

The objective of this work is to develop a rapid electrochemical biosensing strategy for cancer cells identification/quantification using antibody-functionalized gold nanoparticles (AuNPs) as labels. AuNPs have shown to be excellent labels in both optical (e.g. ELISA) and electrochemical (e.g. differential pulse voltammetry) detection of DNA or proteins. [14–19] The use of the electrocatalytic properties of the AuNPs on hydrogen formation from hydrogen ions (Hydrogen Evolution Reaction, HER) also enables an enhanced quantification of nanoparticles or anti-hepatitis B virus antibodies.[20,21] We also reported HER reaction to be very useful in the detection of human tumor HMy2 cell line (HLA-DR class II positive B cell) in the presence of another human tumor PC-3 cell line (HLA-DR class II negative prostate carcinoma) while being immobilized onto a carbon electrode platform.[22]

Given the importance of CTC detection we combine now the capturing capability of AuNPs modified with antibodies with the sensitivity of the HER detection mode in a novel and

simple 'in-situ' like sensing format that can be used for the rapid quantification of AuNPs-labeled cancer cells (see scheme in **Figure 1**).

2. Results and discussion

Synthesis and biofunctionalization of AuNPs to achieve specificic cell labeling

Since the CTCs detach from a primary tumor we chose an adherent tumor cell line, Human Colon Adenocarcinoma Cell line (Caco2), as a model CTC. Similarly to other adenocarcinomas, colon adenocarcinoma cells have a strong expression of EpCAM (close to 100%) and for this reason this glycoprotein was used as target.[11] Several commercial antibodies were tested by flow cytometry in order to choose the one that allows a better labeling of cells, and that would later be conjugated to the AuNPs forming a biofunctionalized specific label for the electrochemical detection of Caco2.

The biofunctionalized electrochemical labels were prepared by conjugation of AuNPs (20nm prepared using Turkevich's citrate capped modified synthesis[23]) with anti-EpCAM antibody following a previously optimized protocol.[15] The nanoparticles were characterized by Transmission Electron Microscopy (TEM) and also UV/Vis Absorbance spectroscopy, to check both the size distribution, and the presence of the antibody layer around them after biofunctionalization (**Figure 2**). We observed a size distribution of 19.2 ± 1.37 nm and a typical absorbance maximum at 520 nm that shifts to 529 nm after biofunctionalization. This red-shift in the absorbance is explained by the changes in the AuNPs-surface plasmon resonance, indicative of a different composition of the surface and evidencing the formation of the conjugate.

Microscopy images and cytometry analysis of cell interaction with biofunctionalized AuNPs

To assess the effectiveness of AuNPs/anti-EpCAM-conjugate labels their specific interaction with cells was evaluated. Caco2 cells were used in suspension.

The free anti-EpCAM antibody proved to have high affinity for EpCAM at Caco2 surface, but it was necessary to verify that after conjugation with AuNPs the antibody maintains the ability to recognize the target protein. Therefore, fluorescence microscopy imaging of cell samples before and after incubation with biofunctionalized AuNPs, using a fluorescent-tagged secondary antibody, was performed. Prior to the incubation, cells (10^6 cells/mL) were centrifuged (1000rpm, 5min) and the pellet was re-suspended in PBS-BSA 0.1%. Afterwards, cells (200 x10^3 cells) were incubated with 50μL of AuNPs/anti-EpCAM-conjugate, as prepared solution. After incubation (30 minutes/ 25ºC, under agitation) labeled cells were centrifuged, washed two times to eliminate the excess of AuNPs/anti-EpCAM-conjugate, resuspended in PBS-BSA 0.1% and incubated with FITC-conjugated anti-rabbit antibody used as a label for fluorescence analysis.

As shown in **Figure 3**, fluorescence at the cell membrane allows assuring the specific biorecognition of the Caco2 cells with the anti-EpCAM antibody functionalized AuNPs. This fact is also evidenced by flow cytometry analysis of cell samples. This method is well suited to check the affinity of different antibodies to several cell proteins and by using the proper controls it can also be used to quantify both labeled and unlabeled cells. Using the same protocol of sample preparation as for optical microscopy, cell samples were analyzed using a flow cytometry. Similarly to the previous method, only when the cells were labeled with AuNPs/anti-EpCAM-conjugate, besides the staining with fluorescent secondary antibody, a strong increase in cell fluorescence was observed (**Figure 3c**). Several controls were

performed for both methods. Caco2 cells were incubated with anti-EpCAM antibody both free and conjugated to AuNPs. Controls were also performed with citrate modified AuNPs without anti-EpCAM, and with AuNPs conjugated to another polyclonal anti-EpCAM antibody which proved to be non-specific to Caco2 cells.

Electrochemical detection of AuNPs labeled Caco2 cells

After the optimization of several incubation related steps (time, temperature, agitation, etc.) the cell samples were analyzed by the electrochemical method. After the incubation protocol (detailed in experimental section), Caco2 cells were detected through the chronoamperometric measurement of the HER in 1M HCl that was electrocatalyzed by AuNPs labels. **Figure 4a** displays the relation between the analytical signal and the concentration of Caco2 cells, in the range between 0 and 1.5 $x10^5$ cells. A linear relation was observed between 1 $x10^3$ and 5 $x10^4$ cells with a limit of detection (LOD) of 4.41 $x10^3$ cells (calculated as the amount corresponding to three times the standard deviation of the estimate) with a correlation coefficient of 0.9902 and a RSD of around 4% for three repetitive assays performed with 5 $x10^4$ cells.

To demonstrate the specificity of the electrochemical detection a selectivity test was devised. CTCs circulate in the blood flow among thousands of other human cells and their detection must be selective enough to avoid false positive results. Thus we chose a circulating blood cell line (monocytes) to simulate the possible interference caused by other cells in our detection. Samples were prepared by mixing in suspension the Caco2 cells with monocytes (THP-1 cells) in different proportions. The cell samples were then incubated with the AuNPs/anti-EpCAM-conjugate (50μL). After removing the excess of conjugate by

centrifugation, samples were analyzed by the electrochemical method described above. The total quantity of cells was fixed at $5x10^4$, and different ratios between Caco2 cells and monocytes were evaluated. No analytical signal was obtained from the sample containing 100% of monocytes. Furthermore, the increasing percentage of Caco2 cells assayed in the presence of decreasing quantities of monocytes resulted in an increase in the analytical signal independent of the monocytes quantity, demonstrating the specificity of the assay.

The statistical analysis reported an LOD of 5.42 $x10^3$ Caco2 cells, with a correlation coefficient of 0.9928 in a linear range from 1 $x10^3$ to 5 $x10^4$ cells, with an RSD = 2% for 5 $x10^4$ cells (3 replicates). The results demonstrate that this method is selective for the target cells and that the electrochemical signal is not affected by the presence of other circulating cells.

Scanning Electron Microscopy (SEM) images of cel interaction with biofunctionalized AuNPs

Although Scanning Electron Microscopy (SEM) is a well-known cell characterization technique, its use for liquid suspensions that involve interaction of cells with small nanometer-sized materials is rather difficult. Due to the requirements of structure stability and electron conductivity necessary for high magnification SEM images, it is often necessary to perform sample metallization that would hide the low nanometer nanoparticles interacting with the cell surface, in addition to changing its outer-layer chemical composition. To perform cell analysis, after their incubation with AuNPs/anti-EpCAM-conjugate, the cells were kept in suspension and treated with glutaraldehyde solution followed by sequential dehydration with ethanol and resuspended in hexamethyldisilazane solution. This protocol allowed a good fixation of cells (from suspension) while maintaining cell shape (**Figure 5**) and the membrane

outer structure intact. The obtained results proved this protocol to be well suited for the observation of cells without the need of metallization or any other procedure that would change or mask the nanosized conjugate (AuNPs/anti-EpCAM) used to label the cell membrane. Figure **5a** shows SEM-Backscattered images of CaCo2 cells while figure **5b** and **5c** show the SEM-Backscattered images of both Caco2 and THP-1 cells contained in the mixture 70%-Caco2/30%-THP1 after their incubation with AuNPs/anti-EpCAM-conjugate. In figure **5b** it is possible to observe the cell membrane with enough detail to discriminate the small nanoparticles attached. We used the Backscattered Electrons mode to be sure that these small structures are indeed the specifically attached AuNPs. Since heavy elements backscatter electrons more strongly than light elements, they appear brighter in the image enhancing the contrast between different chemical compositions.

Both Caco2 cells in suspension and monocytes have a round shape and it is difficult to differentiate them by optical microscopy techniques. But with the optimized SEM preparation protocol we obtained high quality images where we can clearly observe the detail of Caco2 plasma membrane and perceive the numerous particles all around the cell surface.

3. Conclusions

In conclusion, a novel electrochemical strategy to detect and quantify CTCs based on the selective labeling with biofunctionalized AuNPs has been achieved and its efficiency followed by flow cytometry and SEM-Backscattering imaging. The proposed sensor is a rapid and simple CTC detection device that uses specific antibody/AuNPs conjugate to recognize tumor cells in suspension followed by detection in a user-friendly platform.

In our particular example, the observations proved that the labeling with anti-EpCAM-functionalized AuNPs is selective for Caco2 cells and therefore, the catalytic electrochemical detection method developed is specific for the target cells despite the presence of other circulating cells. The electrocatalytic detection of AuNPs/anti-EpCAM labeled Caco2 cells resulted in a limit of detection near 4 $x10^3$ cells.

Our strategy can be adapted for the detection of other tumor cells that also overexpress Ep-CAM, or to other cancer cell receptors by redesigning the AuNPs conjugate. We believe this is a big input in the CTC quantification state of the art techniques that struggle to achieve novel tools for "liquid biopsies" in order to perform patient prognosis, predict metastasis formation and monitor the therapeutic outcomes of cancer. In addition we expect that this method can be combined with cell separation/filtration fluidic platforms, in order to obtain portable and cost-effective alternative CTC quantification devices in the optic of point-of-care sensing systems.

4. Experimental section

Chemicals and equipment

Rabbit polyclonal antibodies to EpCAM were purchased from Abnova (D01P) and from Abcam (ab65052), mouse monoclonal mouse antibody (B302(323/A3)) to EpCAM was purchased from Abcam (ab8601), and FITC-conjugated anti-rabbit antibody was purchased from Sigma (F0382). Hydrogen tetrachloroaurate (III) trihydrate ($HAuCl_4.3H_2O$, 99.9%) and trisodium citrate ($Na_3C_6H_5O_7.2H_2O$) were purchased from Sigma-Aldrich (Spain). Unless otherwise stated, all buffer reagents and other inorganic chemicals were supplied by Sigma-Aldrich (Spain). All chemicals were used as received

and all aqueous solutions were prepared in double-distilled water. The phosphate buffer solution (PBS) was composed of 0.01M phosphate buffered saline, 0.137M NaCl, 0.003M KCl (pH 7.4). Samples for SEM analysis were prepared by using glutaraldehyde and hexamethyldisilazane (HMDS) microscopy grade solutions, Sigma-Aldrich (Spain).

A semi-automatic screen-printing machine DEK248 (DEK International, Switzerland) was used for the fabrication of the screen printed carbon electrodes (SPCEs). The electrodes were printed over Autostat HT5 polyester sheet (McDermid Autotype, UK) using Electrodag 423SS carbon ink for working and counter electrodes, Electrodag 6037SS silver/silver chloride ink for reference electrode and Minico 7000 Blue insulating ink (Acheson Industries, The Netherlands) to insulate the contacts and define the sample interaction area.

The electrochemical experiments where performed with a μAutolab II (Echo Chemie, The Netherlands) potentiostat/galvanostat connected to a PC and controlled by Autolab GPES software. All measurements were carried out at room temperature, with a working volume of 50μL, which was enough to cover the three electrodes contained in the home made SPCE used as electrotransducer, connected to the potentiostat by a home made edge connector module.

Flow cytometry analysis of cells was undertaken with a BD FACSCalibur, Becton Dickinson. For optical microscopy analysis an Olympus IX85 motorized inverted microscope was used and SEM analysis was undertaken with a Merlin®FE-SEM.

Cell culture

Since the CTCs detach from a primary tumor we chose an adherent tumoral cell line, Human

Colon Adenocarcinoma Cell line (Caco2), as a model for CTCs. Caco2 cells (European Collection of Cells Culture, No: 86010202) were maintained in Earle's MEM supplemented with 10%(v/v) foetal bovine serum (FBS) and 2 mM L-glutamine. Cells were grown in a humidified incubator (95% air and 5% CO2 at 37ºC). Adherent cells in exponential phase were harvested by treatment with trypsin in order to detach the cells from the growth surface. Human monocytes (THP-1), which grow in suspension, were used as blank and obtained from ECACC (88081201) and cultivated at 37ºC in a 5% CO_2 atmosphere.

Synthesis and biofunctionalization of gold nanoparticles

The 20-nm AuNPs were synthesized by an adapted method of the one pioneered by Turkevich *et al*. A total of 50 mL of 0.01% $HAuCl_4$ solution was heated with vigorous stirring and 1.25mL of a 1% trisodium citrate solution was added quickly to the boiling solution. When the solution turned deep red, indicating the formation of gold nanoparticles, it was left stirring and cooling down. In this way, a dispersed solution of near 20-nm AuNPs was obtained. .

The conjugation of AuNPs to anti-EpCAM antibody was performed according to the following procedure, previously optimized by our group. AuNPs suspension (1mL) was mixed with 100 μL of 100 μg/mL antibody solution and incubated at 25ºC for 20 min with gentle stirring. Subsequently, a blocking step with 5% BSA for 20 min at 25ºC was undertaken. Finally, a centrifugation at 14000 rpm and 5ºC, for 20 min was carried out and the AuNPs/anti-EpCAM conjugate was reconstituted in PBS-BSA (0.1%) solution and kept at 4ºC.

Microscopy images and cytometry analysis of cell interaction with biofunctionalized AuNPs

A fluorescent tagged secondary antibody that recognizes anti-EpCAM antibody allowed the detection of AuNPs/anti-EpCAM-conjugate at the cell membrane by both fluorescence microscopy imaging and flow cytometry analysis. The preparation of samples for both methods was the same. Prior to the incubation, cells (suspension with 1x 10^6 cells.mL^{-1}) were isolated from the culture medium by centrifugation (1000 rpm, 5min) and the pellet was resuspended in PBS-BSA 0.1%. In both methods, two samples of 2x 10^5 cells were incubated with 50μL of AuNPs/anti-EpCAM-conjugate, as prepared solution. After incubation (30 minutes/ 25ºC, with agitation) labeled cells were centrifuged, washed two times to eliminate the excess of anti-EpCAM functionalized AuNPs and redispersed in buffer. After washing by centrifugation the pellet was resuspended and incubated with FITC-conjugated anti-rabbit secondary antibody used as a label for fluorescence analysis. Controls were performed with citrate modified AuNPs without anti-EpCAM antibody, and also with AuNPs conjugated to another antibody that proved to be non-specific to Caco2 cells.

Electrochemical detection of AuNPs labeled Caco2 cells and selectivity test

The electrochemical detection of Caco2 cells based on the electrocatalytic detection of AuNP labeled anti-EpCAM was performed in HCl 1M by chronoamperometry. Samples were prepared by incubation of different amounts of Caco2 cells (from 0 to 1.5x 10^5 Caco2 cells) with 50μL of AuNPs/anti-EpCAM conjugate (30 minutes, 25ºC, with agitation). After removing the excess of AuNPs by centrifugation washing steps, samples were analyzed by chronoamperometry.

The samples used in the selectivity test were prepared by mixing in suspension the Caco2 cells with monocytes (THP-1 cells) in different proportions. They were then incubated with

the AuNPs/anti-EpCAM conjugate (50μL of AuNPs/anti-EpCAM conjugate, 30 minutes, 25ºC, with agitation). After removing the excess of AuNPs by centrifugation washing steps, samples were detected by the electrochemical method described above. Samples with 100, 70, 50, 20 and 0 % of Caco2 cells were tested with the 100% corresponding to 5x 10^4 cells (0% of Caco2 means that the sample had only monocytes).

Scanning Electron Microscopy (SEM) images of cel interaction with biofunctionalized AuNPs

The technical advances in electron microscopy allow the achievement of excelent characterization tools both in the micro and nano domain. Scanning Electron Microscopy (SEM) is a well known characterization technique for cells, which have relative large dimensions, but the interactions of cells with small nanometer sized materials in liquid suspension its not so easy to observe. Cells often lack the requirements of structure stability and electron conductivity necessary for high magnification SEM images, and its often necessary to apply metalization procedures that cover all the sample with a nano/micro layer of material that would hide the low nanometer rugosity of small nanoparticles interacting with the cell surface, in addition to changing its outer-layer chemical composition.

The accurate characterization of the interaction Caco2 cell-biofunctionalized AuNPs is very important to elucidate the specifity and selectivity of the sensing system presented here. Therefore, after incubation of cell samples with anti-EpCAM functionalized-AuNPs as described above, the cells were kept in suspension and treated with glutaraldehyde solution folowed by sequential ethanol solutions with increasing purity, and they were finally resuspended in HMDS solution. This protocol allows a good fixation of cells in suspension while mantaining cell shape and the membrane outer structure, and proved to be well suited

for the observation of cells without the need of metalization or any other procedure that would change or mask the nanosized conjugate (AuNPs/anti-EpCAM) used to label the cell membrane.

Acknowledgements

We acknowledge MICINN (Madrid) for the projects PIB2010JP-00278 and IT2009-0092, the E.U.'s support under FP7 contract number 246513 ''NADINE'' and the NATO Science for Peace and Security Programme's support under the project SfP 983807.

We also thank the SCAC-IBB members: Manuela Costa, for the technical support on cytometry experiments and data analysis, Francisca Garcia and Francisco Cortes, for the technical support on cell culture; The Servei de Microscòpia UAB members: Onofre Castell and Marcos Rosado for the technical support with SEM imaging and for the important inputs on the sample preparation protocols.

[1] T. G. Lugo, S. Braun, R. J. Cote, K. Pantel, V. Rusch, *Journal of clinical oncology : official journal of the American Society of Clinical Oncology* **2003**, *21*, 2609-15.

[2] S. Nagrath, L. V. Sequist, S. Maheswaran, D. W. Bell, D. Irimia, L. Ulkus, M. R. Smith, E. L. Kwak, S. Digumarthy, A. Muzikansky, P. Ryan, U. J. Balis, R. G. Tompkins, D. a Haber, M. Toner, *Nature* **2007**, *450*, 1235-9.

[3] P. Paterlini-Brechot, N. L. Benali, *Cancer letters* **2007**, *253*, 180-204.

[4] K. Pantel, C. Alix-Panabières, *Trends in molecular medicine* **2010**, *16*, 398-406.

[5] N. Bednarz-Knoll, C. Alix-Panabières, K. Pantel, *Breast cancer research : BCR* **2011**, *13*, 228.

[6] B. Taback, a D. Chan, C. T. Kuo, P. J. Bostick, H. J. Wang, a E. Giuliano, D. S. Hoon, *Cancer research* **2001**, *61*, 8845-50.

[7] S. Wang, H. Wang, J. Jiao, K.-J. Chen, G. E. Owens, K.-ichiro Kamei, J. Sun, D. J. Sherman, C. P. Behrenbruch, H. Wu, H.-R. Tseng, *Angewandte Chemie (International ed. in English)* **2009**, *48*, 8970-3.

[8] J. den Toonder, *Lab on a chip* **2011**, *11*, 375-7.

[9] K. Li, R. Zhan, S.-S. Feng, B. Liu, *Analytical Chemistry* **2011**, *83*, 2125-2132.

[10] M. Perfézou, A. Turner, A. Merkoçi, *Chemical Society reviews* **2011**, DOI 10.1039/c1cs15134g.

[11] P. T. H. Went, A. Lugli, S. Meier, M. Bundi, M. Mirlacher, G. Sauter, S. Dirnhofer, *Human Pathology* **2004**, *35*, 122-128.

[12] C. Patriarca, R. M. Macchi, A. K. Marschner, H. Mellstedt, *Cancer treatment reviews* **2011**, DOI 10.1016/j.ctrv.2011.04.002.

[13] L. Belov, J. Zhou, R. I. Christopherson, *Cell Surface Markers in Colorectal Cancer Prognosis.*, **2010**.

[14] J. Wang, *Small (Weinheim an der Bergstrasse, Germany)* **2005**, *1*, 1036-43.

[15] J. Das, M. A. Aziz, H. Yang, *Journal of the American Chemical Society* **2006**, *128*, 16022-3.

[16] D. Tang, R. Yuan, Y. Chai, *Analytical chemistry* **2008**, *80*, 1582-8.

[17] D. a Giljohann, D. S. Seferos, W. L. Daniel, M. D. Massich, P. C. Patel, C. a Mirkin, *Angewandte Chemie (International ed. in English)* **2010**, *49*, 3280-94.

[18] M. Pumera, M. T. Castañeda, M. I. Pividori, R. Eritja, A. Merkoçi, S. Alegret, *Langmuir : the ACS journal of surfaces and colloids* **2005**, *21*, 9625-9.

[19] A. Ambrosi, M. T. Castañeda, A. J. Killard, M. R. Smyth, S. Alegret, A. Merkoçi, *Analytical chemistry* **2007**, *79*, 5232-40.

[20] M. Maltez-da Costa, A. De La Escosura-Muñiz, A. Merkoçi, *Electrochemistry Communications* **2010**, *12*, 1501-1504.

[21] A. De La Escosura-Muñiz, M. Maltez-da Costa, C. Sánchez-Espinel, B. Díaz-Freitas, J. Fernández-Suarez, Á. González-Fernández, A. Merkoçi, *Biosensors and Bioelectronics* **2010**, *26*, 1710-1714.

[22] A. De La Escosura-Muñiz, C. Sánchez-Espinel, B. Díaz-Freitas, A. González-Fernández, M. Maltez-da Costa, A. Merkoçi, *Analytical Chemistry* **2009**, *81*, 10268-10274.

[23] J. Turkevich, P. C. Stevenson, J. Hillier, **1953**, *57*, 670-673.

Received: ((will be filled in by the editorial staff))
Revised: ((will be filled in by the editorial staff))
Published online on ((will be filled in by the editorial staff))

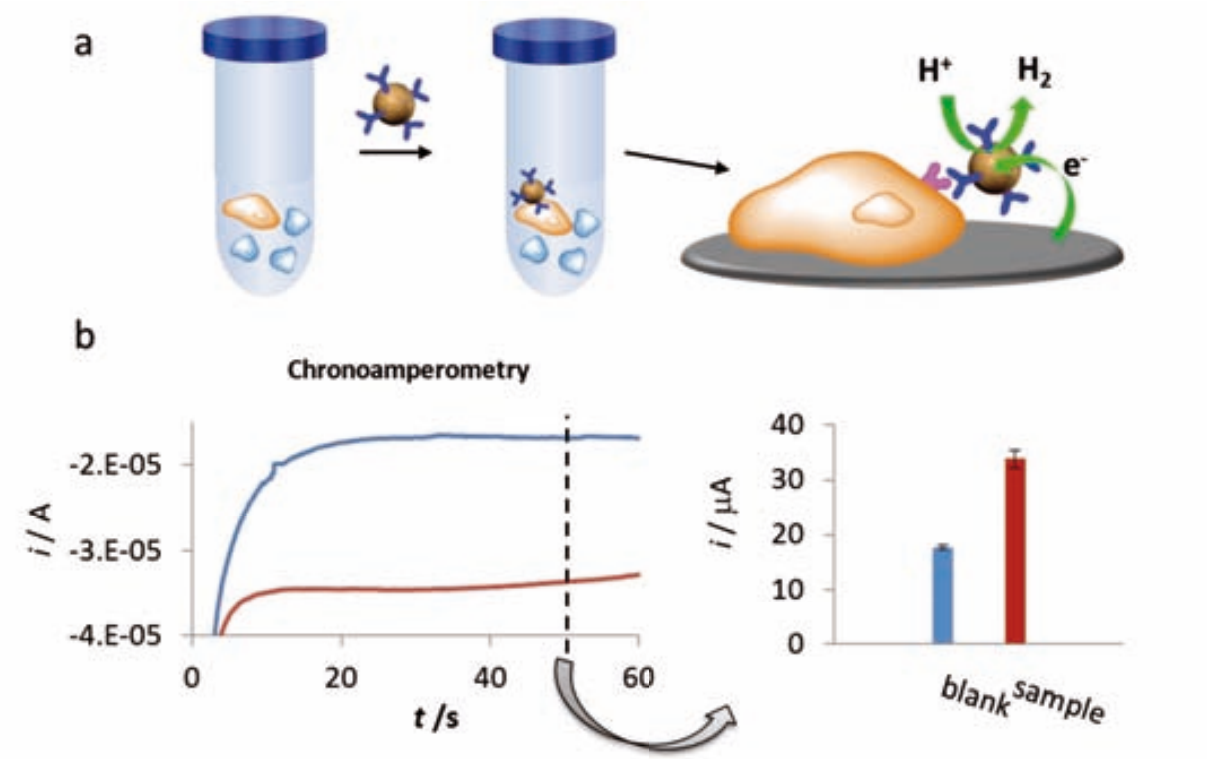

Figure 1.(a) Scheme of the CaCo2 cells biorecognition with AuNPs/anti-EpCAM-antibodies and further detection through the Hydrogen Evolution Reaction (HER) electrocatalyzed by the AuNPs labels; b) Left: Chronoamperograms registered in 1M HCl, during the HER applying a constant voltage of -1.0V, for AuNPs-labeled CaCo2 cells (3.5 x10^4 - red curve) and for the control (PBS/BSA - blue curve). Right: Comparison of the corresponding analytical signals (absolute value of the current registered at 50 seconds) of the blank and sample.

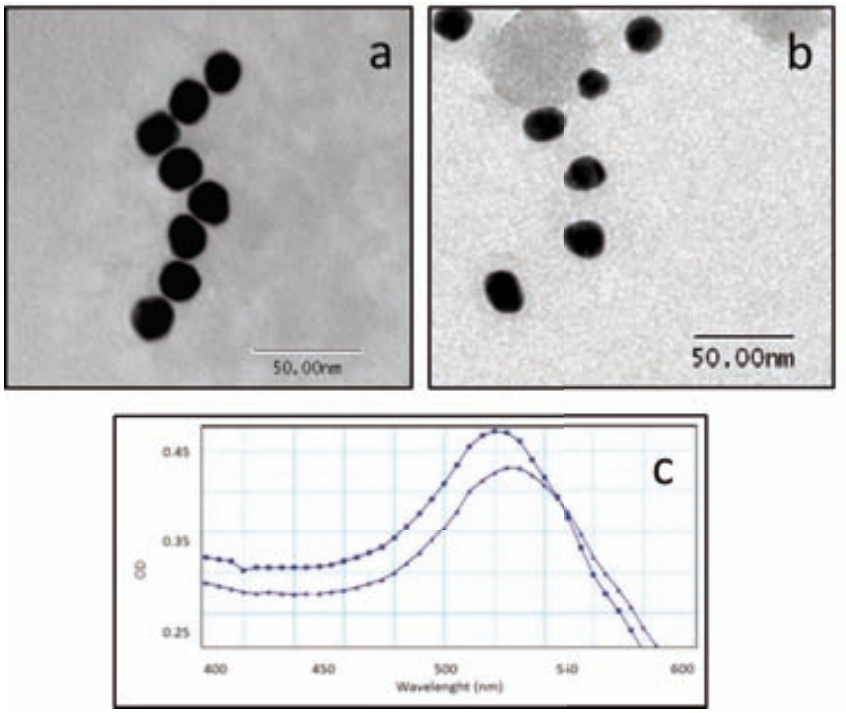

Figure 2. TEM images of AuNPs, before (a) and after (b) biofunctionalization with anti--EpCAM antibody. (c) UV-Vis spectra of AuNPs before (■) and after (▲) biofunctionalization with anti-EpCAM.

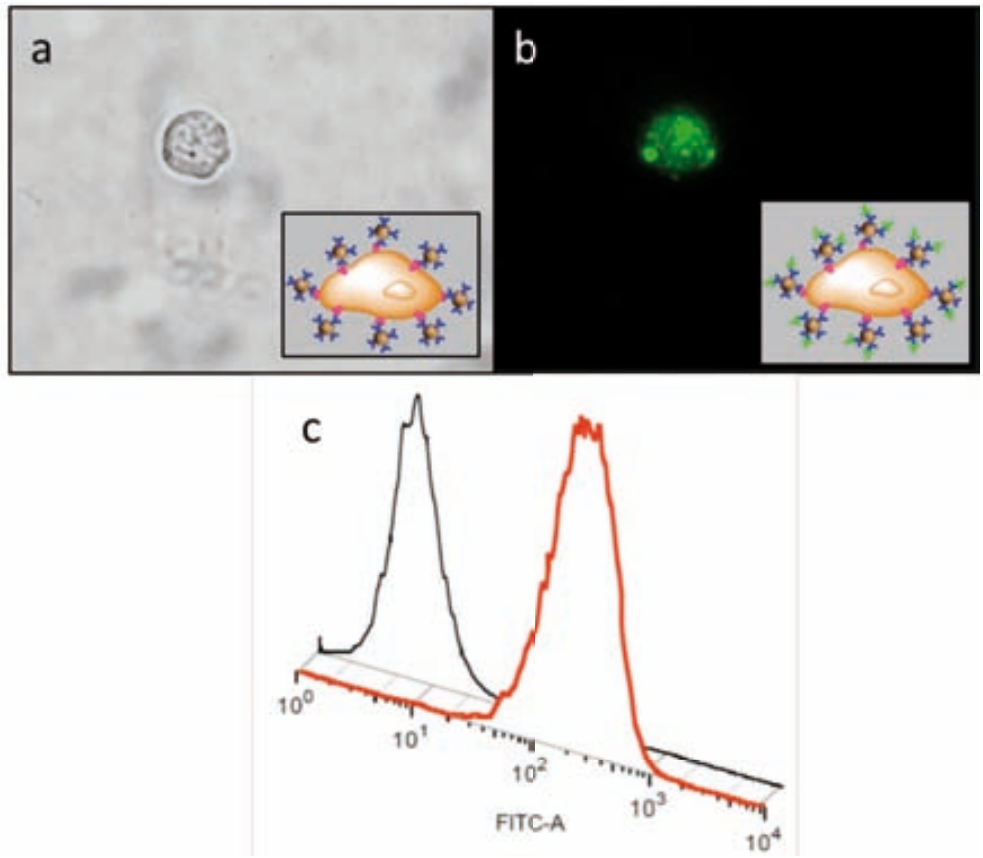

Figure 3. (a, b) Microscopy imaging of Caco2 cells incubated sequentially with AuNPs/anti-EpCAM and a FITC conjugated secondary anti-rabbit antibody, at bright field a) and fluorescence mode b). (c) Flow cytometry analysis of Caco2 cells labeled with AuNPs/anti-EpCAM. Histogram count of unlabeled (black) vs. labeled (red) cells using the same FITC secondary antibody as in 2a, b).

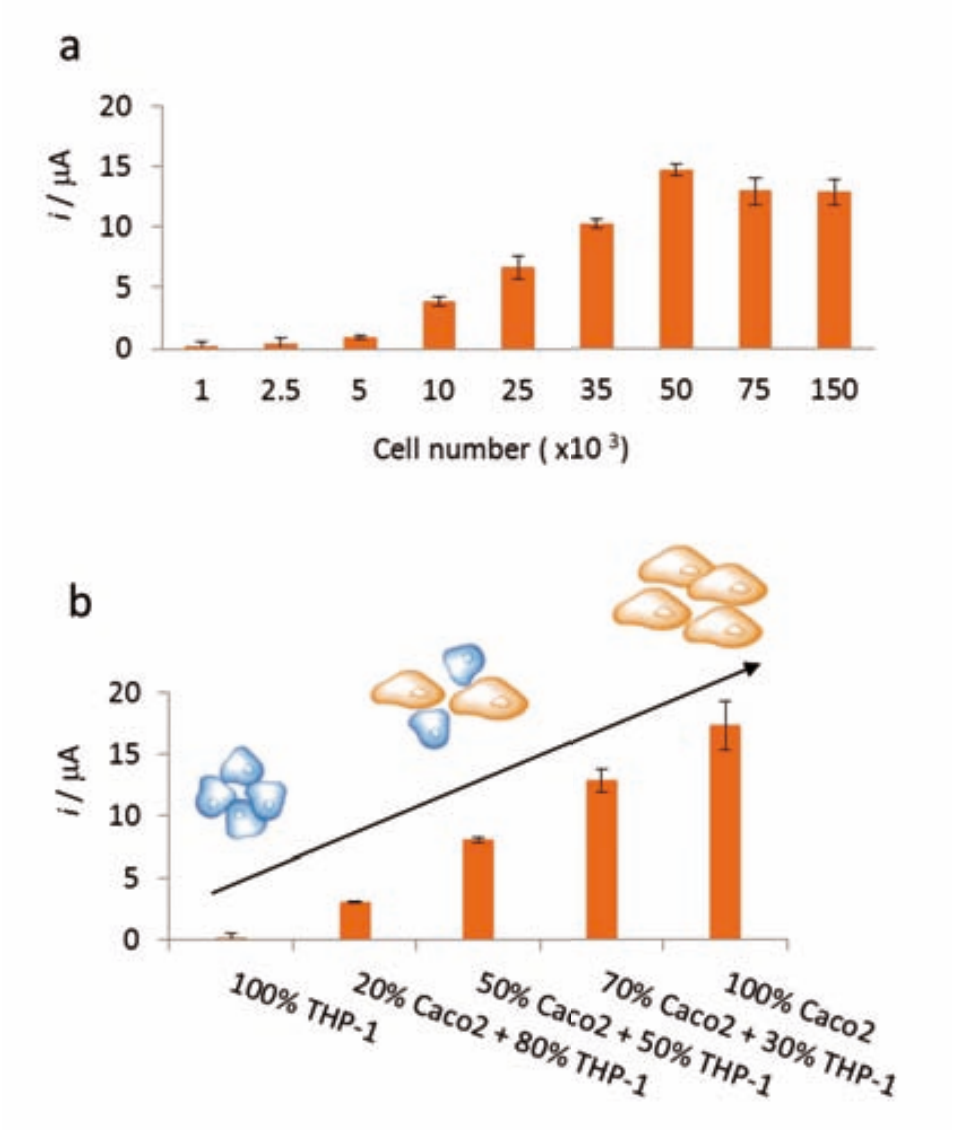

Figure 4. Electrochemical results obtained for increasing number of Caco2 cells after incubation with AuNPs/anti-EpCAM (a) and for mixed suspensions of Caco2 and monocytes (THP-1 cells) at different Caco2/THP-1 ratios (total cells amount: 5 x10^4) after incubation with AuNPs/anti-EpCAM (b).

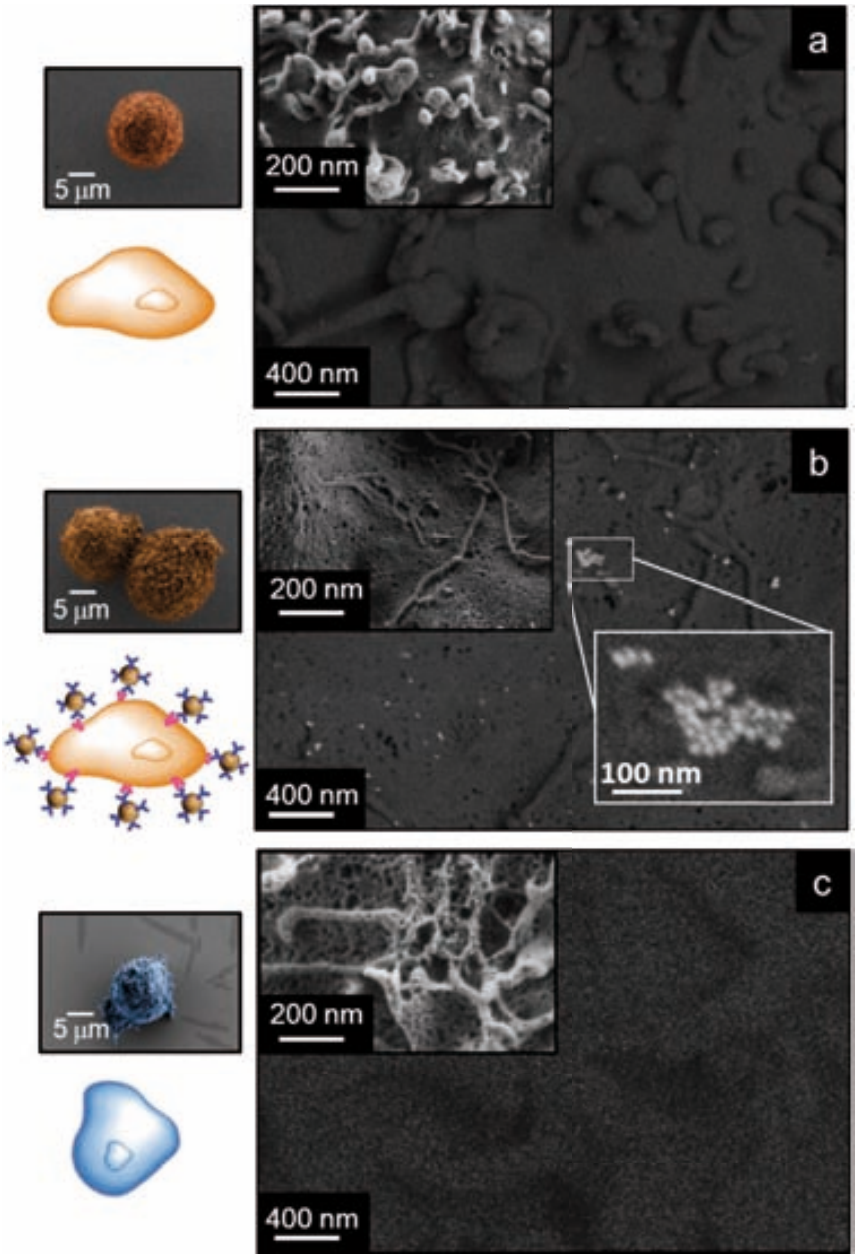

Figure 5. Right: SEM-Backscattered images of the cell surfaces of (a): Caco2 cells before incubation with AuNPs/anti-EpCAM; (b) Caco2 and (c) monocytes after incubation with AuNPs/anti-EpCAM in the same sample. The zoom in (b) corresponds to a detail of AuNPs/anti-EpCAM at CaCo2 surface (insets of scattered images of the same cell area are also shown for comparison purposes). Left: SEM full images of Caco2 and monocytes and the corresponding schematic cartoons.

A novel electrochemical strategy to detect and quantify Circulating Tumor Cells (CTCs) based on the selective labeling with electrocatalytic nanoparticles has been achieved. The proposed sensor is a rapid and simple detection device that uses specific antibody/AuNPs conjugate to recognize tumor cells in suspension followed by fast electrochemical detection in a user-friendly platform.

TOC Keyword:

M. Maltez-da Costa, A. de la Escosura-Muñiz, C. Nogués, L. Barrios, E. Ibañez, A. Merkoçi

Detection of Circulating Tumor Cells Using Nanoparticles

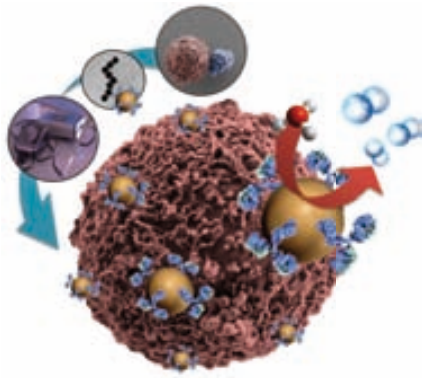

Cover proposal

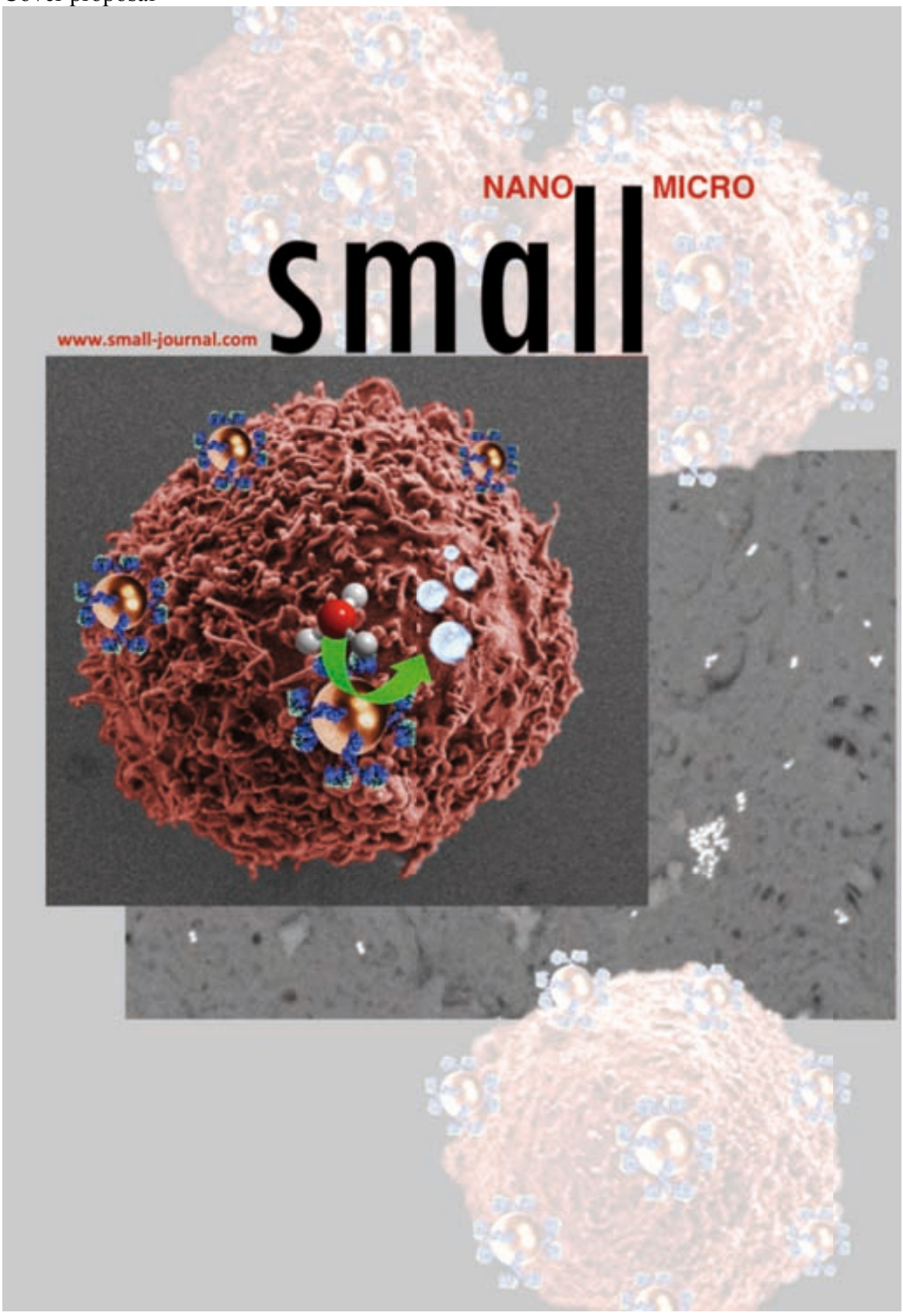

Supporting information

Detection of Circulating Tumor Cells Using Nanoparticles **

*Marisa Maltez-da Costa, Alfredo de la Escosura-Muñiz, Carme Nogués, Leonard. Barios, Elena Ibáñez, Arben Merkoçi **

[*] Prof. Arben Merkoçi
ICREA, Institució Catalana de Recerca i Estudis Avançats and Nanobioelectronics & Biosensors Group, CIN2 (ICN-CSIC), Catalan Institute of Nanotechnology, Campus de la UAB Bellaterra (Barcelona), 08193 Spain
E-mail: arben.merkoci.icn@uab.es

Marisa Maltez-da Costa, Dr. Alfredo de la Escosura-Muñiz
Nanobioelectronics & Biosensors Group, CIN2 (ICN-CSIC), Catalan Institute of Nanotechnology, Campus de la UAB Bellaterra (Barcelona), 08193 Spain

Prof. Carmen Nogués, Prof. Leonard Barrios, Dr. Elena Ibáñez
Departament de Biologia Cel•lular, Fisiologia i Immunologia, Universitat Autònoma de Barcelona, Campus UAB-Facultat de Biociències

Scanning Electron Microscopy (SEM) images of cell interaction with biofunctionalized AuNPs

In **Figure S1**, we can see several SEM images of Caco2 cells. In the images acquired with higher magnification (a-d) it is possible to observe the cell membrane both before (a,c) and after (b,d) Caco2 incubation with anti-EpCAM-functionalized AuNPs. In image b we can observe the cell membrane with enough detail to discriminate the small nanoparticles attached. To be sure that this small structures are anti-EpCAM-functionalized AuNPs we used the Backscattered Electrons mode (BSE) to diferentiate between elements (c,d). Since heavy elements backscatter electrons more strongly than light elements, they appear brighter in the image enhancing the contrast between different chemical compositions. In the image from

Caco2 sample incubated with AuNPs (d) the nanoparticles are visualized wit a much better contrast indicating the presence of a much heavier nanosized element than the background.

The samples used in the selectivity test were also characterized by SEM using the same sample preparation protocol. In **Figure S2** we can see SEM images obtained for the sample containing 70% of Caco2 and 30% of monocytes. Both cells have a round shape which makes it difficult to differentiate them by optical microscopy techniques. But with the optimized SEM preparation protocol we obtained high quality images where we can observe the detail of the plasma membrane and, using the Backscattered Electrons mode (BSE), observe the presence of anti-EpCAM-functionalized AuNPs only at the surface of Caco2 cells. No AuNPs were found in the several monocytes present in the sample and all the Caco2 cells displayed numerous particles all around the cell surface.

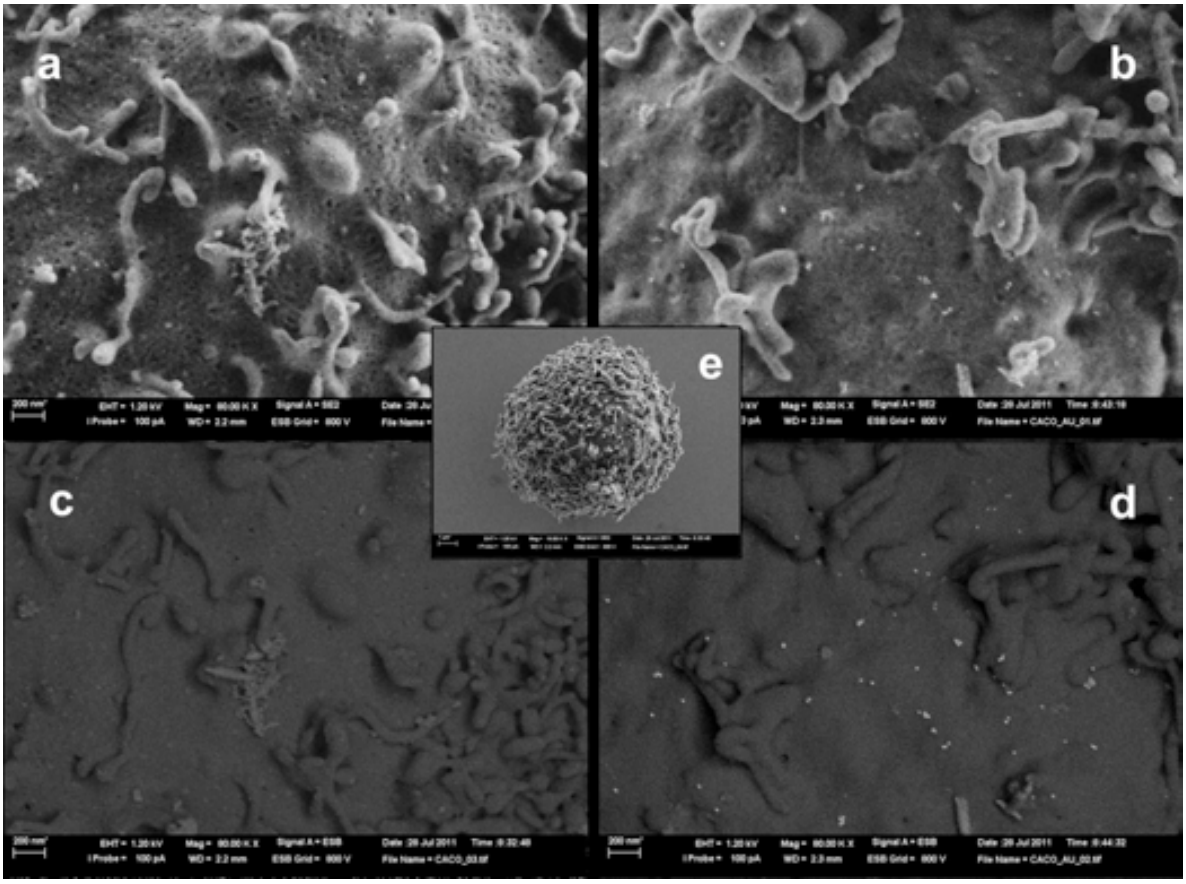

Figure S1: SEM images of Caco2 cells. Full cell image (e) and higher magnification images of cell membrane before (a,c) and after (b,d) their incubation with anti-EpCAM-functionalized AuNPs . Images c and d were acquired with backscatered electrons mode.

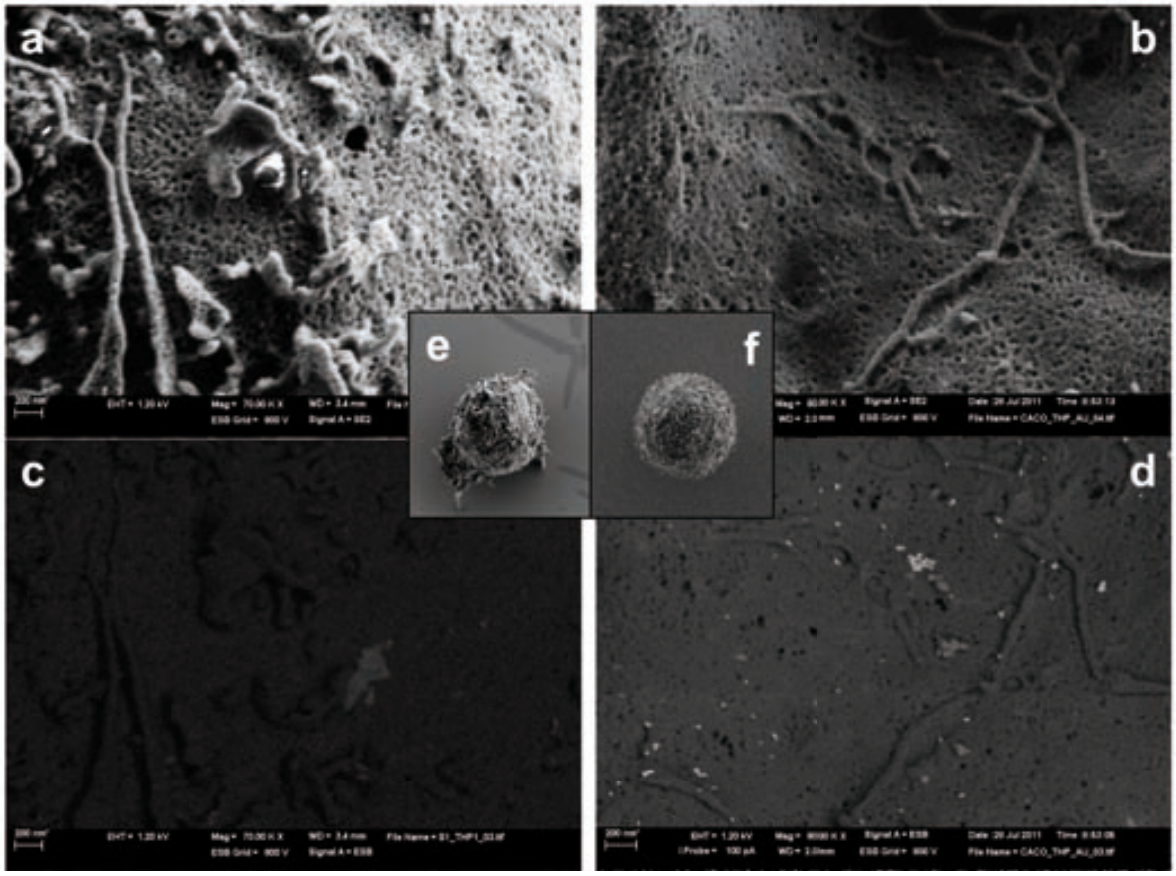

Figure S2: SEM images for the samples containing monocytes (THP-1) and Caco2 cells. Images showing a THP-1 cell (e) and a Caco2 cell (f) and higher magnification images of cell plasma membrane from THP-1 (a,c) and Caco2 (b,d) after incubation with anti-EpCAM-functionalized AuNPs. Images c and d were acquired with backscattered electrons mode.

Magnetic cell assay with electrocatalytic gold nanoparticles for rapid CTCs electrochemical detection

M. Maltez-da Costa, A de la Escosura-Muniz, Carme Nogués, Leonard Barrios, Elena Ibáñez A. Merkoçi

Submitted to Nature Methods

Magnetic cell assay with electrocatalytic gold nanoparticles for rapid Circulating Tumor Cells electrochemical detection

Marisa Maltez-da Costa[1], Alfredo de la Escosura-Muñiz[1], Carme Nogués[2], Leonard Barrios[2], Elena Ibáñez[2], Arben Merkoçi[1,3]

ABSTRACT

Here we present a new strategy for the simultaneous isolation and labeling of circulating tumor cells (CTCs) applied to their fast electrochemical quantification. The human colon adenocarcinoma cell line Caco2 was chosen as a model of CTC. Similarly to other adenocarcinomas, colon adenocarcinoma cells show a strong expression of Epithelial Cell Adhesion Molecule (EpCAM) in the plasma membrane. We combine the capturing capability of anti-EpCAM antibody functionalized magnetic beads and the specific labeling through antibody-modified gold nanoparticles (AuNPs), with the sensitivity of the AuNPs-electrocatalyzed Hydrogen Evolution Reaction detection technique. The full-optimized process was used for the electrochemical detection of Caco2 cells in presence of monocytes, other circulating cells which could potentially interfere in real blood samples.

Therefore, we obtained a novel and simple '*in- situ*'-like sensing format that we applied for the rapid quantification of AuNPs-labeled CTCs in presence of other human cells.

In addition, we applied the SEM-Backscattering imaging for the observation of cells without the need of metallization or any other procedure, that would change or mask the nanosized gold nanoparticles modified with antibodies and used to label the cancer cell membrane. The developed CTC capture and sensing assay and the characterization outfits can be extended to several other cells detection scenarios in addition to nanoparticles based drug delivery and nanotoxicology studies.

INTRODUCTION

Circulating Tumor Cells (CTCs) are traveling cells that detach from a main tumor or from metastasis. CTCs quantification is under intensive research for examining cancer dissemination, predicting patient prognosis, and monitoring the therapeutic outcomes of cancer [1–3]. Although CTCs are extremely rare, their detection/quantification in physiological fluids represents a potential alternative to the actual invasive biopsies and subsequent proteomic and functional genetic analysis [4,5]. In fact, isolation of CTCs from peripheral blood, as a 'liquid biopsy', is

expected to be able to complement conventional tissue biopsies of metastatic tumors for therapy guidance [1,6]. A particularly important aspect of a 'liquid biopsy' is that it is safe and can be performed frequently, because repeated invasive procedures may be responsible for limited sample accessibility [7]. Established techniques for CTC identification include labeling cells with tagged antibodies (immunocytometry) and subsequent examination by fluorescence analysis or detecting the expression of tumor markers by reverse-transcriptase polymerase chain reaction (RT-PCR)[8]. However, the required previous isolation of CTCs from the human fluids is limited to complex analytic approaches that often result in a low yield and purity [9,10].

Cancer cells overexpress specific proteins at their plasma membrane which are often used as targets in CTCs sensing methodologies using the information available for the different types of cancer cells [11]. An example of these target proteins is the Epithelial Cell Adhesion Molecule (EpCAM), a 30-40 kDa type I glycosylated membrane protein expressed at low levels in a variety of human epithelial tissues and overexpressed in most solid carcinomas [12]. Decades of studies have revealed the roles of EpCAM in tumorigenesis and it has been identified to be a cancer stem cell marker in a number of solid cancers, such as in colorectal adenocarcinomas, where it is found in more than 98% of them, and its expression is inversely related to the prognosis[13,14]. Another example of a tumor associated protein is the Carcinoembryonic antigen (CEA), a 180-200 kDa highly glycosylated cell surface glycoprotein which overexpression was originally thought to be specific for human colon adenocarcinomas. Nowadays it is known to be associated with other tumors, and the large variations of serum CEA levels and CEA expression by disseminated tumor cells have been strongly correlated with the tumor size, its state of differentiation, the degree of invasiveness and the extent of metastatic spread[14,15].

The objective of this work is to develop a rapid electrochemical biosensing strategy for CTCs quantification using antibody-functionalized gold nanoparticles (AuNPs) as labels and magnetic beads (MBs) as capture platforms in liquid suspensions.

AuNPs have shown to be excellent labels in both optical (e.g. ELISA) and electrochemical (e.g. differential pulse voltammetric) detection of DNA[16] or proteins[17,18]. The use of the electrocatalytic properties of the AuNPs on hydrogen formation from hydrogen ions (Hydrogen Evolution Reaction, HER) also enables an enhanced quantification of nanoparticles[19] allowing the detection, for example, of anti-hepatitis B virus antibodies in human serum through their labeling with nanoparticle conjugates[20]. We also reported HER reaction to be very useful in the detection of the human tumor HMy2 cell line (HLA-DR class II positive B cells) in the presence of another human tumor PC-3 cell line (HLA-DR class II negative prostate carcinoma) while being immobilized onto a carbon electrode platform[21].

Since human fluid samples are complex and contain a variety of cells and metabolites, the fast detection of CTCs becomes quite a difficult task. To get through this obstacle, several attempts of filtration, pre-concentration or other purification steps are actually being reported by researchers that work in this field and each of them has advantages and drawbacks [22,23]. The only FDA (U.S. Food and Drug Administration) approved method for the detection of CTCs is the Cell Search System® that first enriches the tumor cells immunomagnetically by means of ferrofluidic nanoparticles conjugated to EpCAM and then, after immunomagnetic capture and enrichment, allows the identification and enumeration of CTCs using fluorescent staining [24,25]. When sample processing is complete, images are presented to the user in a gallery format for final cell classification. Because this is an expensive, time consuming and complex analysis, our objective is to design and evaluate an electrochemical detection system based on the electrocatalytic properties of the AuNPs, in combination with the use of superparamagnetic microparticles (MBs) modified with anti-EpCAM as a cell capture agent (**Fig. 1**). The integration of both systems, the capture with MBs and the labeling with electrocatalytic AuNPs, should provide a selective and sensitive method for the detection and quantification of CTCs in liquid suspensions.

The human colon adenocarcinoma cell line Caco2, was chosen as a model CTC. Similarly to other adenocarcinomas, colon adenocarcinoma cells, show a strong expression of EpCAM (close to 100%)[12] and for this reason this glycoprotein was used as the capture target. In relation to AuNPs labeling, we explored two different protein targets: EpCAM and CEA, both expressed by Caco2 cells. Two separate electrochemical detections were performed, each one using a different antibody conjugated to AuNPs, in order to choose the one that achieves a better electrochemical response in terms of both sensitivity and selectivity.

RESULTS

Biofunctionalization of electrochemical labels

The biofunctionalized electrochemical labels were prepared by conjugation of AuNPs (20 nm sized prepared using Turkevich's citrate capped modified synthesis[26]) with rabbit polyclonal anti-EpCAM antibody or mouse monoclonal anti-CEA antibody following a previously optimized protocol.[20] The nanoparticles were characterized by Transmission Electron Microscopy (TEM) and also UV/Vis absorbance spectroscopy, to check both the size distribution and the presence of the antibody layer around them after biofunctionalization. We observed a mean size of 19.2 ± 1.4 nm and a typical maximum of absorbance at 520 nm that shifted to 529 nm after biofunctionalization (**Supplementary Fig. 1)**. This red-shift in the absorbance is explained by the changes in the AuNPs-surface plasmon resonance, indicating a different composition of the surface and evidencing the formation of the conjugate.

Evaluation of the interaction between Caco2 cells and electrochemical labels

To assess the effectiveness of AuNPs/antibody-conjugate labels, their specific interaction with Caco2 cells in suspension was evaluated. With this aim, fluorescence microscopy imaging of cell samples before and after incubation with biofunctionalized AuNPs, using a fluorescent tagged secondary antibody, was performed. The free anti-EpCAM antibody proved to have high affinity for EpCAM at Caco2 surface (data not shown), but it was necessary to verify that after conjugation with AuNPs the antibody maintains its ability to recognize the target protein. The resulting fluorescence at the cell membrane (**Fig. 2**) confirmed the specific biorecognition of the Caco2 cells by the AuNPs/anti-EpCAM. This fact was also evidenced by flow cytometry analysis of the cell samples. Flow cytometry is well suited to check the affinity of different antibodies to several cell proteins and, by using the proper controls, it can also be used to quantify both labeled and

unlabeled cells. Using the same protocol for sample preparation as for optical microscopy, Caco2 samples were analyzed (**Fig. 3**). When the cells were labeled with AuNPs/rabbit-anti-EpCAM-conjugate, followed by a fluorescent secondary anti-rabbit antibody, a strong increase in cell fluorescence was observed (**Fig. 3a**). Several controls were performed for both methods. Caco2 cells were incubated with rabbit-anti-EpCAM antibody both free and conjugated to AuNPs. Controls were also performed with AuNPs/anti-EpCAM without fluorescent-tagged secondary antibody (**Supplementary Fig. 2a**), and with AuNPs conjugated to another rabbit polyclonal anti-EpCAM antibody which proved to be non-specific to Caco2 cells (**Supplementary Fig. 2b**).

Optimization of Caco2 cells magnetic capture and labeling

For the magnetic capture of Caco2, we first used 4.5 μm MBs conjugated to a monoclonal anti-EpCAM antibody. Although 4.5 μm MBs are generally used for cell applications, due to their large size and high magnetic mobility, our experiments with anti-EpCAM functionalized 4.5 μm MBs resulted in discrepancies both in flow cytometry analysis and electrochemical detection. After MBs and AuNPs incubation, Caco2 cells seemed damaged and/or agglomerated when analyzed by fluorescence microscopy and flow cytometry (**Supplementary Fig. 3 and 4**). This damage may be due to the large size of these MBs, which promotes higher flow-induced shear stress during the cleaning steps performed with stirring[27,28] . Since CTCs are reported to be vulnerable cells which viability is easily compromised after capture[6], we tested smaller MBs (tosylactivated 2.8μm) that are recommended for extremely fragile cells, due to their smaller size and lower magnetophoretic mobility, and can reduce the possibility of interference between the nearest particles[29]. These are uniform polystirene beads (with a magnetic core), coated with a polyurethane layer modified with sulphonyl ester groups, that can subsquently react covalently with proteins or other ligands containing amino or sulfhydryl groups. MBs were functionalized with a monoclonal anti-EpCAM antibody previously tested by flow cytometry analysis. The electrochemical

measurements and the cytometry analyses were in agreement: these MBs can capture the cells without perceived damage (**Fig. 3b and 3c**) and allow for better electrochemical results.

We also performed optimization of the ratio MBs/cell, as well as the cell incubation sequence with both MBs/anti-EpCAM and AuNPs/anti-EpCAM conjugates to improve the AuNPs electrochemical signal. The ratio between MB and AuNPs/anti-EpCAM used in the detection assay is very important, because MBs/anti-EpCAM quantity should be minimized to allow the maximum labeling by AuNPs/anti-EpCAM conjugate that will in turn give the detection signal. Regarding the incubation sequence with conjugates, if a separate incubation is performed using MBs/anti-EpCAM in the first place, the EpCAM at the cell surface could be "blocked" for the further labeling with AuNPs/anti-EpCAM, resulting in a loss of AuNPs electrochemical signal. In the case that a simultaneous incubation is performed, both MBs and AuNPs conjugates would compete for the same protein and consequently, the aforementioned blocking effect could also occur. To test this, several ratios of MBs/AuNPs conjugates (1:1, 2:1, 4:1 and 14:1 MBs/cell) , using two incubation protocols (MBs/anti-EpCAM and AuNPs/anti-EpCAM simultaneous and separate incubations) were evaluated. Flow cytometry results (**Supplementary Fig. 5**) showed that a high MB/cell ratio is associated not only to more cell damage/death (cells are exposed to a higher magnetic attraction) but also to a higher number of cells without the MBs/anti-EpCAM. Therefore, it seems that an excess of MBs/anti-EpCAM (14:1 MBs/cell) is not favorable to the detection, and the best results were achieved with a 2:1 MBs/cell ratio. It is also important to clarify that when MBs/anti-EpCAM were not used (only AuNPs/anti-EpCAM labeling) the flow cytometry analysis reported 98% of AuNPs/anti-EpCAM-labeled cells with a low value of dead cells. This result was obtained for cells incubated with a large excess of AuNPs/anti-EpCAM (3nM AuNPs) (**Supplementary Fig. 6a**), which leads to the conclusion that, contrary to MBs/anti-EpCAM, an excess of AuNPs/anti-EpCAM does not affect cell integrity, probably due to their smaller size. Finally, concerning the incubation sequence, we chose

the simultaneous one as the optimal in order to obtain a fast capture/labeling of cells with both conjugates (**Supplementary Fig. 6b**). Moreover, when using the 2:1 MBs/cell ratio the flow cytometry analysis did not indicate major differences between the two tested incubations.

Evaluation of Caco2 cell capture and labeling in the presence of control cells

The accurate study of the Caco2 cell-biofunctionalized AuNP interaction is very important to elucidate the specifity and selectivity of the sensing system presented here. The use of scanning electron microscopy (SEM) is a well known characterization technique for cells with relative large dimensions. However, its application in the case of cells interaction with small nanometer sized materials in liquid suspension is not an easy task. Cells often lack the requirements of structure stability and electron conductivity necessary for high magnification SEM images, and it is usually necessary to cover all the sample with a nano/micro layer of conductive material. This metallization process will mask the small nanoparticles attached to the cell surface. Therefore, we adapted a SEM sample preparation protocol to fulfill two requirements: the cells should always be kept in suspension, so that the characterization is done in exactly the same conditions than the electrochemical detection, and no sample coating should be performed, to avoid the masking of AuNPs/anti-EpCAM that should be present at the cell surface. Accordingly, cell samples were kept in suspension while treated with glutaraldehyde fixative with subsequent dehydration solutions, and finally resuspended in hexamethyldisilazane (HMDS) solution prior to the drop-deposition onto a silicon dioxide wafer. No metal-oxides were used and the critical-point drying procedure was not performed nor the final metallization step. HMDS is generally used in photolitography techniques, as an adhesion promoter between silicon dioxide films and the photoresist. However, in the present method, HMDS is used as a substitute of the critical-point, as it is reported to be a time-saving alternative without introducing additional artefacts in SEM images.[30,31] We

processed samples in which Caco2 cells were incubated in the presence or absence of AuNPs/anti-EpCAM conjugate.

With the optimized SEM preparation protocol and the Field Emission-SEM (FE-SEM) precise technical settings, we obtained high quality images (**Fig. 4a**). At high magnification we could see the detail of the plasma membrane and using the Backscattered Electrons mode (BSE) we could discriminate the small AuNPs attached onto the Caco2 cell membrane through the immunoreaction (**Fig. 4b**). Since heavy elements backscatter electrons more strongly than light elements, they appear brighter in the obtained image, thus enhancing the contrast between objects of different chemical compositions. In addition, as we did not use metal-oxides during the fixation of cells, the only metal-origin element in the samples should be the gold from the AuNPs used as labels. When the same procedure was performed for monocytes (**Fig. 4c and d**), no AuNPs were observed, demonstrating the specificity of the AuNPs anti-EpCAM.

We processed other samples in which Caco2 cells were mixed with the THP-1 control cells in a 70% Caco2 and 30% THP-1 proportion, and then incubated with MBs/anti-EpCAM with and without labeling of AuNPs/anti-EpCAM. As expected, no monocytes were found in the SEM sample (**Fig. 5**) since they were supposed to be removed during the magnetic separation steps. At higher magnification, using the BSE mode (**Fig. 5c and d**), the presence of AuNPs/anti-EpCAM dispersed onto the Caco2 surface could be observed. Several membrane protrusions were also observed in all the SEM images when MBs/anti-EpCAM were used as capture conjugates (**Fig. 5b**). These are finger like structures that epithelial cells can develop in cell-matrix adherent processes [32–34] and in which Ep-CAM can also be involved [34,35]. It is important to note that this protusions are enhanced when MBs are used **(Supplementary Fig. 8)**, whereas in the samples of Caco2 and Caco2-labelled only with AuNPs/anti-EpCAM (**Supplementary Fig. 7**) the cell structure seems well confined. Although this evidence is not directly related to the assay performance, we believe these effects may be related to the different sizes of MBs and AuNPs, being MBs aproximately 1.4 $x10^3$ times larger.

Electrochemical detection of Caco2 cells

The full-optimized process was used for the electrochemical detection of Caco2 cells in presence of monocytes (THP-1), other circulating cells which could interfere in real blood samples. The use of the electrocatalytic properties of the AuNPs on hydrogen formation from hydrogen ions (HER) makes it possible to quantify the AuNPs and, in turn, to quantify the corresponding labelled cancer cells (through the proteins to which these are connected)[19]. Chronoamperometric plotting of the analytical signal is much simpler, from signal acquisition point of view, than the stripping analysis or differential pulse voltammetry described in previous works[16,17]. To evaluate the selectivity of the assays, Caco2 cells were mixed with the THP-1 control cells in different proportions, and then incubated with both MB/anti-EpCAM and AuNPs/anti-EpCAM in a one-step incubation. After magnetic separation and cleaning steps, the samples were analyzed following the electrocatalytic method explained. Samples with 100%, 70%, 50% and 20% of Caco2 cells (**Fig. 6a**) were tested (100% corresponds to 5 $x10^4$ cells), achieving a limit of detection (LOD) of 8.34 $x10^3$ Caco2 cells, with a correlation coefficient (R) of 0.91 and a linear range from 1 $x10^4$ to 5 $x10^4$ cells with Relative Standard Deviation (RSD) = 4.92% for 5 $x10^4$ cells. LOD was determined by extrapolating the concentration at blank signal plus 3 s.d. of the blank. The results proved that this method is selective for Caco2 cells. However, the achieved limit of detection is not enough to guarantee the application of the method. This is probably due to the aforementioned competition between antibody-modified MBs and AuNPs for the EpCAM protein. Furthermore, EpCAM is considered a general marker for a large variety of epithelial cells, so the selection of a more specific target was required to improve both the specificity and the sensitivity of the assay. Concretely, the CEA protein was chosen as it is reported to be strongly associated with the invasiveness of cancer cells, and it is known to be overexpressed by colon adenocarcinoma cells[14,15]. The AuNPs were biofunctionalized with a mouse anti-CEA and used as electrochemical labels. The incubation of Caco2 cells with the AuNPs/anti-CEA was done simultaneously with

the capturing by MBs/anti-EpCAM followed by the electrocatalytic detection. The electrochemical analysis of Caco2 cells (**Fig. 6c**) resulted in a LOD of 1.6 $x10^2$ cells with R= 0.993, in a linear range from 1 $x10^3$ to 3.5 $x10^4$ cells. LOD was determined by extrapolating the concentration at blank signal plus 3 s.d. of the blank. The RSD = 5.6 % for 5 $x10^4$ cells, evidences a very good reproducibility of the results if we take into consideration that the number of nanoparticles attached to the cells due to the interaction between the antibody and CEA depends primarily on the number and distribution of the antigen molecule over the surface, which may vary from cell to cell and from batch to batch[36]. The results obtained using AuNPs/anti-CEA as the detection labels were much better, in terms of LOD, than those with AuNPs/anti-EpCAM.

When changing the AuNPs-conjugate antibody to anti-CEA the goal was to have better specificity in the detection without losing the sensitivity. Consequently, the AuNPs/anti-CEA was also tested for the electrochemical detection of Caco2 cells in the presence of THP-1 control cells (**Fig. 6b**). Caco2 cells were mixed with THP-1 in different proportions (100, 70, 50, 20% of Caco2 cells; 100% corresponds to 5 $x10^4$ cells) and then incubated with both MB/anti-EpCAM and AuNPs/anti-CEA in a one-step incubation. After magnetic separation and cleaning steps, samples were analysed by the same electrochemical procedure previously mentioned. The statistical analysis reported a LOD of 2.2 $x10^2$ Caco2 cells, with a correlation coefficient of 0.968 in a linear range from 1 $x10^4$ to 5 $x10^4$ cells with RSD = 6.3% for 5 $x10^4$ cells. This value is quite similar to that obtained in the absence of THP-1, evidencing the high selectivity obtained thanks to the CEA recognition together with the magnetic separation/purification.

DISCUSSION

The use of nanoparticles as labeling agents in immunoassays results in an improvement of sensitivity over the traditional enzyme or dye based assays[37]. Nanometer-sized particles such as metal and iron-oxide nanoparticles display

optical, electrochemical, magnetic or structural properties that the materials in molecular or bulk state do not have. When these particles are conjugated with specific antibodies they can target tumor-expressed proteins with high affinity and specificity. For example, AuNPs of 20 nm diameter have large surface areas that promote a good conjugation to antibodies and provide a fast interaction with nanometer sized antigens at the cell surface. The labeled tumor cells can then be detected and quantified through the appropriate methods for AuNPs detection, which can be optical, electric or electrochemical. From the several methods available, the electrochemical routes hold several advantages related to the gold nanoparticles specific characteristics, such as their own redox properties and excellent electroactivity towards other reactions. Exploiting the latest, advantages can be taken from the electrocatalytic effect that AuNPs have over several reactions, which exclude the need for contact between the electrode surface and the nanoparticle[37], and is suitable when detecting particles used as labels for relatively large dimensions such as the tumor cells.

The electrochemical detection of metal nanoparticles in general, and AuNPs in particular, can be accomplished using simple and portable apparatus that do not require large volume samples, time-consuming steps or high skilled users if thinking on point of care applications. After optimization, the detection can be seen as a semi-automated technique that could be integrated in small lab-on-a-chip platforms with the additional improvements related to the required volumes and time of analysis inherent to these systems[38].

The developed CTC detection technology includes several parameter optimizations as for example the size of the magnetic particles, their functionalization with antibodies, or the specificity of the antibody used to functionalize the AuNPs labels, including other protocol related parameters (e.g. incubation times) and the respective parameters related to the characterization by microscopy (optical and electronic) and flow cytometry.

Using the technical advances in electron microscopy to better characterize the cell-nano and -microparticle interactions, we processed samples in which Caco2

cells were mixed with THP-1 control cells (other circulating cells which could interfere in real blood samples) and were then incubated with AuNPs/anti-EpCAM and MB/anti-EpCAM conjugates. Using the Backscattered Electrons mode (BSE) mode we confirmed the presence of AuNPs/anti-EpCAM all around the Caco2 cell surface, whereas no monocytes were present in the sample. These observations proved that the capture and labeling with anti-EpCAM-functionalized particles is selective for Caco2 cells and thus a specific detection of target cells in the presence of other circulating cells can be achieved.

The full-optimized process was used for the electrochemical detection of Caco2 cells in the presence of THP-1. Although the results proved that the method was selective for Caco2 cells, the achieved limit of detection was not enough to guarantee the application of the method. The fact that the capture and detection labels were oriented to the same target protein, could hinder our detection due to the possible blocking effect that MBs could exert over the small AuNPs. For this reason, we believed that the detection could be improved using a different antibody in the detection conjugated label, specific to other protein in the cell plasma membrane. To pursuit this goal, other antigens/proteins that are also present at Caco2 cells surface, and assumed to be relevant in the study/quantification of CTCs, were also considered. Since EpCAM is a general marker for a large variety of epithelial cells, another more specific detection using CEA as the target for the AuNPs-conjugate label was performed. We obtained better LOD values, in the absence and presence of other control cells, that are nearer the desirable for a valuable CTCs detection. One of the possible explanations for the better results achieved, is the fact that CEA is a much bigger protein than EpCAM (180kDa vs. 40kDa). Even though both CEA and EpCAM are transmembrane proteins, the first one presents a larger extracelular domain, more similar in size to the antibody (150kDa). Even though the anti-CEA Fab fragment size, which is mainly responsible for the antigen recognition, has an equivalent size to the Fab' from anti-EpCAM, the possible steric effects related to the antigen size[39,40] can help to elucidate why a better signal is obtained when using CEA as target at the cell

membrane. The electrochemical detection and the characterization results demonstrate that this method is selective for Caco2 cells, and that the electrochemical signal is not affected by the presence of other circulating cells. So we conclude that the achieved detection through the AuNPs/anti-CEA is more selective for the target tumor cells and can exclude the false positive results related to the EpCAM marker.

We envision the application of the presented method to the quantification of CTCs in real human samples where besides cells (cancerous and non-cancerous ones), also proteins and metabolites are present. Although the anti-CEA antibody is not specific for CTCs (in fact, it can also recognize the CEA that is frequently found in the serum of patients with several types of cancer), its combination with MBs/anti-EpCAM provides a selective capture and labeling of cells that express both antigens. This principle can also be adapted for other cancer cells by redesigning both micro- and nano-conjugates with the appropriate antibodies. Furthermore, the potential incorporation of the presented method for isolation, labeling and sensitive electrochemical detection/quantification of Caco2 cells in lab-on-a-chip systems[3,41] could contribute to the desired standardization of CTCs detection technologies.

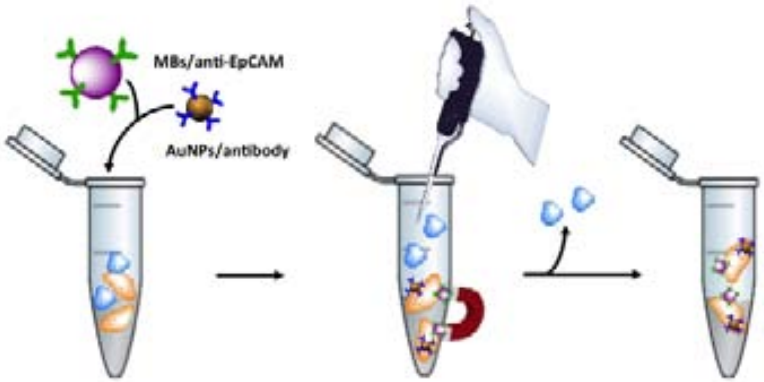

Figure 1a. Overall scheme of Caco2 cells capture by MBs-anti-EpCAM and simultaneous labeling with AuNPs/specific antibodies in the presence of control cells;

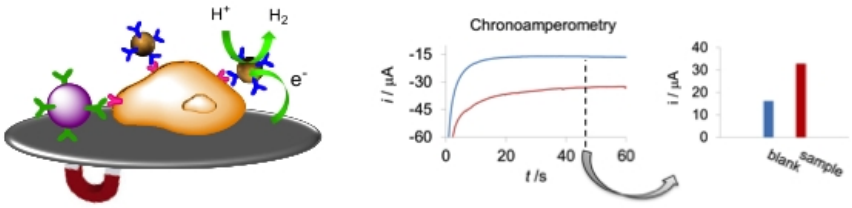

Figure 1b. Detection of labeled Caco2 cells through the Hydrogen Evolution Reaction (HER) electrocatalyzed by the AuNP labels. Right: Chronoamperograms registered in 1M HCl, during the HER applying a constant voltage of -1.0V, for AuNP labeled CaCo2 cells (3.5 x104 - red curve) and for the blank (PBS/BSA - blue curve). Right: Comparison of the corresponding analytical signals (absolute value of the current registered at 50 seconds).

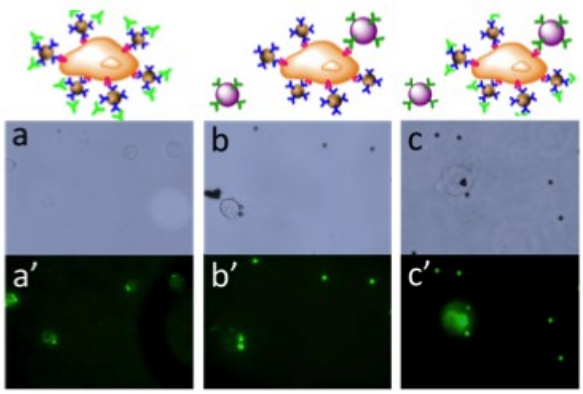

Figure 2. Figure 2 lFluorescence microscopy characterization. (a-c) Microscopy imaging of Caco2 cells in bright field (a, b, c), and fluorescence modes (a', b', c'). (a, a') Cells in suspension labeled with AuNPs/rabbit-anti-EpCAM and sequential labeling with FITC-conjugated secondary anti-rabbit antibody; (b, b') cells captured with MBs/mouse-anti-EpCAM and simultaneous labeling with AuNPs/rabbit-anti-EpCAM showing the autofluorescence of MBs; (c, c') cells in the same conditions as in b after sequential labeling with FITC-conjugated secondary anti-rabbit antibody.

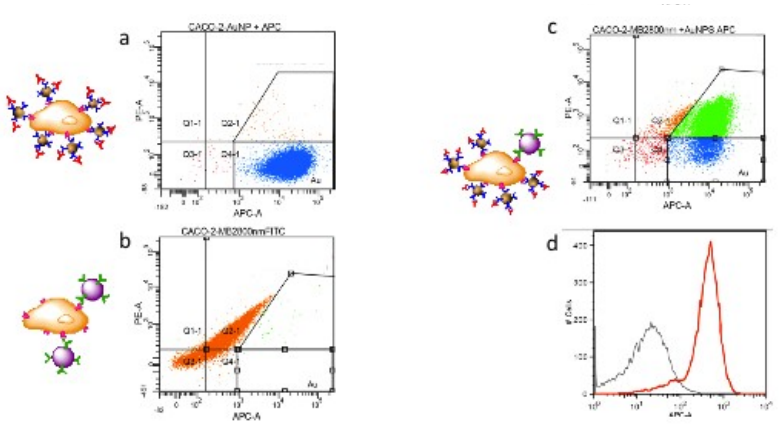

Figure 3. Figure 3 l Flow Cytometry analysis performed after 30 minute incubations, as described in the methods section. After appropriate forward and sideward scatter gating, the Caco2 cells were evaluated using PE-A and APC-A signals. (a) Representative dot plots of Caco2 cells labeled with AuNPs/anti-EpCAM ; (b) Caco2 cells captured by MBs/anti-EpCAM; (c) Caco2 cells captured with MBs/anti-EpCAM and simultaneously labeled with AuNPs/anti-EpCAM. (d) Representative histogram count of Caco2 cells captured with MBs/anti-EpCAM, unlabeled (black) vs. labeled (red) with AuNPs/anti-EpCAM using the APC-conjugated secondary antibody.

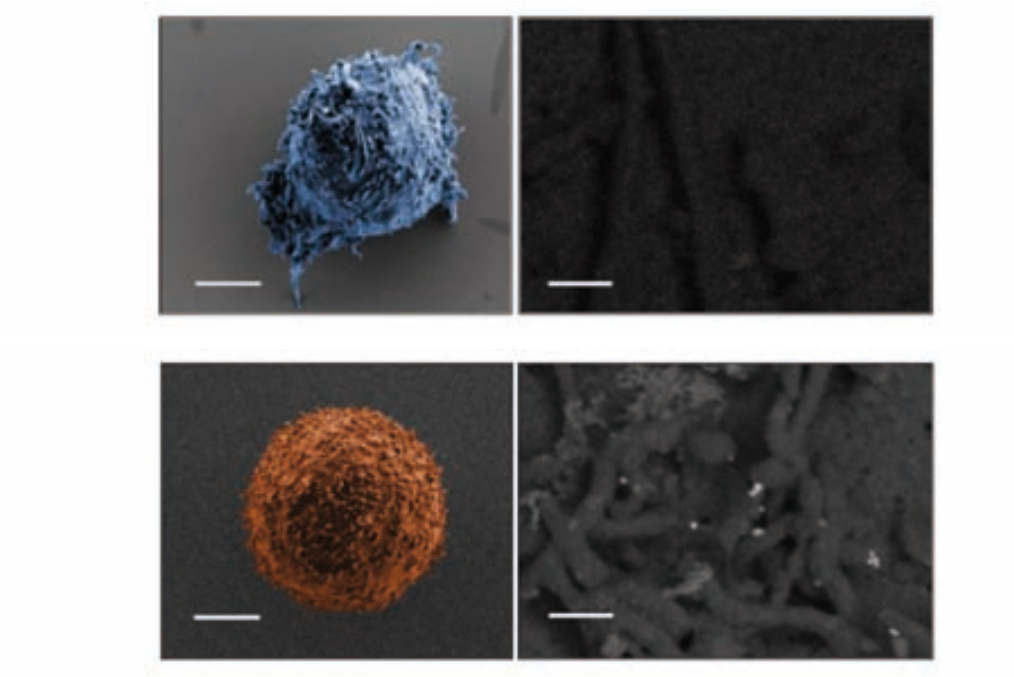

Figure4. Figure 4 | Scanning electron microscopy. (a) SEM image (false colored with Corel Paint Shop Pro) of Caco2 cell incubated with AuNPs/anti-EpCAM conjugates; (b) Higher magnification image, using backscattered electrons mode, showing AuNPs distributed along the cell plasma membrane. (c) SEM image (false colored with Corel Paint Shop Pro) of control cell (THP-1); (d) Higher magnification image of THP-1 cell in backscattered electrons mode. Scale bars, 3 mm (a and c) and 200 nm (b-d).

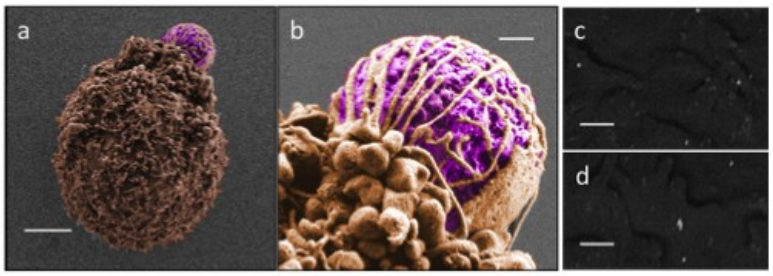

presence of THP-1 cells.(a, b) SEM images (false colored with Corel Paint Shop Pro) of a Caco2 cell captured by MBs/anti-EpCAM. (c, d) Higher magnification backscattered images of the Caco2 cell surface showing AuNPs distributed along the cell plasma membrane. Scale bars, 3 mm (a), 400 nm (b) and 200 nm (c, d).

METHODS

Cell culture. The human colon adenocarcinoma cell line Caco2 was used as a model CTC. Caco2 cells (European Collection of Cell Cultures (ECACC), No: 86010202) were maintained in Earle's Minimal Essential Medium (MEM) supplemented with 10% (v/v) fetal bovine serum (FBS) and 2 mM L-glutamine in a humidified incubator (5% CO_2 at 37ºC). Prior to each experiment, Caco2 cells were trypsinized in order to dettach them from the culture flask. Human monocytes (THP-1 cell line from ECACC, No: 88081201), which grow in suspension, were used as blank and cultivated in RPMI medium supplemented with 10% FBS (5% CO_2 at 37ºC). Culture media and supplements from PAA LaboratoriesGmBh.

Synthesis and biofunctionalization of gold nanoparticles. The 20-nm AuNPs were synthesized by an adapted method of the one pioneered by Turkevich *et al*[26]. The glass material was washed overnight with freshly prepared Aqua Regia solution (1 part nitric acid: 3 parts hydrochloric acid). The Aqua Regia solution was then washed off thoroughly four times with MilliQ water. A total of 50 mL of 0.01% Hydrogen tetrachloroaurate (III) trihydrate (Sigma-Aldrich) prepared in MilliQ water was heated under vigorous stirring and 1.25mL of 1% trisodium citrate (Sigma-Aldrich) prepared in MilliQ water was added quickly to the solution when the temperature reached 98ºC. When the solution turned deep red, indicating the formation of gold nanoparticles, it was left cooling down under stirring. In this way, a dispersed solution of near 20-nm AuNPs was obtained.

Two different proteins, EpCAM (Epithelial Cell Adhesion Molecule) and CEA (Carcinoembryonic Antigen), both expressed by Caco2 cells, were used as targets for AuNPs labeling. Rabbit polyclonal anti-EpCAM (D01P, Abnova) or mouse monoclonal (1C7) anti-CEA (Ab10039, Abcam) antibodies were used for each biofuntionalization in order to create two different labels suitable for the electrochemical detection. The conjugation of AuNPs to anti-EpCAM or anti-CEA antibodies was performed according to the following procedure, previously

optimized by our group [19,20]. Briefly, 1 mL of 1.5nM AuNPs suspension, with the pH corrected to 8.5 with Borate Buffer (BB; pH 9, 0.01M), was mixed with 100 mL of a 100 mg/mL antibody solution and incubated at 25ºC for 20 min with gentle stirring. Subsequently, a blocking step with 5% BSA (Sigma-Aldrich) for 20 min at 25ºC was undertaken. Finally, two centrifugation steps at 14000 rpm and 5ºC for 20 min were carried out in order to remove the free antibody, and the AuNPs/antibody conjugates were reconstituted in 0.1M PBS-0.1% BSA solution and kept at 4ºC. To verify that the free antibody was removed from the conjugates solution, the supernatants from each centrifugation step were inspected using UV/Vis spectroscopy. Buffer compounds from Sigma-Aldrich.

Biofunctionalization of Superparamagnetic Tosylactivated microbeads (MBs). Superparamagnetic microbeads (M280 Tosylactivated, Dynal-Biotech) are uniform polystirene beads with a magnetic core, coated with a polyurethane layer. The surface of these beads is modified with sulphonyl ester groups that can react covalently with proteins or other ligands containing amino or sulfhydryl groups.

EpCAM glycoprotein was used as a target for MB capture, and mouse monoclonal anti-EpCAM (Ab8601, Abcam) was chosen to create biofunctionalized MBs for CTCs capture. The functionalization was performed by following the manufacturer recommended instructions. Briefly, the MBs (2μL, stock solution) were washed with 0.1M BB pH9.5 and resupended in 200μL of 0.1M BB pH9.5 to achieve a concentration of 2 x10^7 MB/mL. An excess of mouse monoclonal anti-EpCAM antibody (20μg) was then incubated with the MB suspension with gentle agitation (37ºC, 2h) in 0.1M BB pH9.5. The MBs/anti-EpCAM conjugates were then separated from solution, washed with 0.1M BB pH9.5, and blocked with 0.01M PBS-0.5% BSA solution pH7.4 (37ºC, 2h). Afterwards, MBs/anti-EpCAM conjugates were separated from blocking solution, washed and resuspended in 0.01M PBS -0.1% BSA pH7.4, and stored at 4ºC until needed. Buffer compounds from Sigma-Aldrich.

Labeling of Caco2 cells with AuNPs/antibody conjugates. Different amounts of Caco2 cells (from 0 to 5 x 10^4), resuspended in 0.01 M PBS-0.1% BSA, were incubated with 50μL of AuNPs/anti-CEA or AuNPs/anti-EpCAM conjugates (30 min, 25ºC, with agitation). After removing the excess of AuNPs with three centrifugation-washing steps (5 min, 1000 rpm), cells were resuspended in 0.01M PBS -0.1% BSA.

Capture of Caco2 cells by MB/anti-EpCAM and simultaneous labeling with AuNPs/antibody. Different amounts of Caco2 cells (from 0 to 5 x 10^4), resuspended in 0.01M PBS-0.1% BSA, were simultaneously incubated with MB/anti-EpCAM (2.5mL) and AuNPs/antibody (50μL) conjugates. After incubation (30 min, 25ºC, with agitation), captured cells were separated from the solution using a magnetic separation platform. They were washed two times to eliminate the excess of antibody functionalized AuNPs, resuspended in 0.01M PBS, and then analized.

Flow cytometry and microscopy analyses of cell interaction with anti-EpCAM modified MBs and biofunctionalized AuNPs. Caco2 cells (2 x 10^5 resuspended in 0.01M PBS-0.1%BSA) were incubated with MBs/anti-EpCAM (2.5μL) or AuNPs/anti-EpCAM (50μL) conjugates, or simultaneously with of AuNPs/anti-EpCAM (50μL) and MB/anti-EpCAM (2.5μL) conjugates. After incubation (30 min, 25ºC, with agitation), labelled cells were separated from solution using a magnetic separation platform (when MBs were used) or by centrifugation (when no MBs were used). They were washed two times to eliminate the excess of antibody functionalized AuNPs, and redispersed in 0.01M PBS.

Finally, cells were incubated (30 min, 4ºC) with the secondary antibody, which was different for cytometry (APC-conjugated anti-rabbit antibody, sc3846, Santa Cruz) than for microscopy (FITC-conjugated anti-rabbit antibody, F0382, Sigma) analyses. Controls were performed with citrate modified AuNPs (without anti-EpCAM antibody), and also with AuNPs conjugated to another rabbit polyclonal

anti-EpCAM antibody (ab65052, Abcam) that proved to be non-specific to Caco2 cells. In cytometry analysis, the isotype controls were also performed using anti-Human IgG1 isotype non-specific to EpCAM.
Flow cytometry analysis of cells was undertaken with a BD FACSCalibur, Becton Dickinson, and optical microscopy analysis with an Olympus IX85 motorized inverted microscope.

Fabrication of screen-printed carbon electrodes (SPCEs). The electrochemical transducers were homemade screen-printed carbon electrodes (SPCEs) consisting of three electrodes in a single strip: working electrode (WE), reference electrode (RE) and counter electrode (CE). The full size of the sensor strip was 29mm x 6.7mm, and the WE diameter was 3mm. The fabrication of the SPCEs was carried out in three steps in the semi-automatic screen-printing machine DEK248 (DEK International, Switzerland), using a different stencil, with the corresponding patterns, for each layer. First, a graphite layer (Electrodag 423SS carbon ink for WE and CE) was printed onto the polyester sheet (Autostat HT5, McDermid Autotype, UK). After curing for 30 min at 95ºC, a second layer was printed with silver/silver chloride ink (Electrodag 6037SS for the RE). After another curing for 30 min at 95ºC, the insulating layer was printed using insulating ink (Minico 7000 Blue, Acheson Industries, The Netherlands) to protect the contacts and define the sample interaction area. Finally, the SPCEs were cured again at 95ºC for 20 min.

Electrochemical detection of AuNPs labelled Caco2 cells by chronoamperometry. The electrochemical quantification of Caco2 cells based on the electrocatalytic detection of biofunctionalized AuNPs was performed in 1M HCl by chronoamperometry. All measurements were carried out at room temperature with a working volume of 50μL, which was enough to cover the three electrodes contained in the homemade SPCE used as electrotransducer, connected to the potentiostat (μAutolab II, Echo Chemie, The Netherlands) by a homemade edge connector module.

Different amounts of Caco2 cells (from 0 to 5 x10^4) labelled with the AuNPs/antibody conjugates were placed (25μL) onto the working electrode surface and HCl was added to obtain a 50μL drop. Chronoamperograms were registered applying a constant voltage of -1.0V during 60 seconds. The analytical signal of each sample was obtained by the subtraction of the blank (the absolute of both current values registered at 50 seconds).

Electrochemical detection of AuNPs labeled Caco2 cells in the presence of interferent cells. To demonstrate the specificity of the detection, a selectivity test was performed. CTCs circulate in the blood flow among thousands of other human cells and their detection must be selective enough to avoid false positive results. Thus, a circulating cell line (monocytes) was chosen to simulate the possible interference caused by other cells in our Caco2 cell detection.

A total of 5 x 10^4 cells were prepared by mixing Caco2 cells in suspension with monocytes (THP-1 cells) at different proportions (100, 70, 50 and 20% of Caco2 cells). They were then simultaneously incubated with 50μL of AuNPs/antibody conjugate and 2.5μL of MBs/anti-EpCAM (30 min, 25ºC with slow agitation). After removing the excess of AuNPs by magnetic separation and two subsequent washing steps with 0.01M PBS, samples were analyzed by the electrochemical method described above.

Sample preparation for Scanning Electron Microscopy (SEM) analysis. Caco2 cell samples, in the presence or absence of THP-1 control cells, were prepared following the same protocol. A suspension of 2 x 10^5 cells incubated with anti-EpCAM functionalized-AuNPs and/or MBs/anti-EpCAM conjugates, was fixed with 2.5% glutaraldehyde in 0.1M cacodilate buffer, during 1 h at 25ºC. After each of the following steps, cells labelled with AuNPs/anti-EpCAM conjugates and attached to MBs were recovered by magnetic separation, whereas cells labelled only with AuNPs/anti-EpCAM conjugates were recovered by centrifugation. After removing the supernatant solution, pellets were dehydrated sequentially in ethanol increasing

series (30, 50 and 96 %, 5 min each, 25ºC) . To complete the dehydration process, samples were incubated three times in 100% ethanol (5 min, 25ºC), and finally resuspended in hexamethyldisilazane (Sigma-Aldrich) solution and kept at 4ºC until analysis. The volume of all reagents used was always 10x the pellet volume, and slow agitation was performed to promote a better difusion. Prior to SEM analysis (Merlin®FE-SEM, Zeiss), 4μL of each sample were deposited onto a 0.5 x 0.5mm silicon dioxide wafer placed over a typical SEM sample holder. This protocol avoids the use of metallization steps while mantaining the cellular structure intact, and allows a direct visualization of small metallic nanoparticles onto the cell surface.

ACKNOWLEDGEMENTS

We acknowledge MICINN (Madrid) for the projects PIB2010JP-00278 and IT2009-0092, the E.U.'s support under FP7 contract number 246513 ''NADINE'' and the NATO Science for Peace and Security Programme's support under the project SfP 983807.

We also thank the SCAC-IBB members: Manuela Costa, for the technical support on cytometry experiments, Francisca Garcia and Francisco Cortes, for the technical support on cell culture; Servei de Microscopia-UAB member, Onofre Castell for the technical support with SEM imaging and for the important inputs on the sample preparation protocol.

AUTHOR AFFILIATIONS

[1]Nanobioelectronics & Biosensors Group, CIN2 (ICN-CSIC), Catalan Institute of Nanotechnology, Campus de la UAB Bellaterra (Barcelona), 08193 Spain

[2]Departament de Biologia Cel•lular, Fisiologia i Immunologia, Universitat Autònoma de Barcelona, Campus UAB-Facultat de Biociències

[3]ICREA, Institució Catalana de Recerca i Estudis Avançats

CORRESPONDING AUTHOR

Correspondence should be addressed to Arben Merkoçi (arben.merkoci@icn.cat)

AUTHOR CONTRIBUTIONS

A.M., A.E.M., C.N. and L.B. conceived the idea and coordinated the project.

A.M., A.E.M., M.M.C., C.N., L.B. designed the method.

M.M.C. performed the experiments

M.M.C., A.E.M., A.M. analyzed and interpreted the data with contribution from C.N., L.B., and E.I. that also provided biological insight.

M.M.C. wrote the manuscript and edited it under supervision of A.E.M. and A.M..

All authors revised the manuscript.

COMPETING FINANCIAL INTERESTS

The authors declare no competing financial interests.

1. Pantel, K. & Alix-Panabières, C. Circulating tumour cells in cancer patients: challenges and perspectives. *Trends in molecular medicine* **16**, 398-406 (2010).

2. Bednarz-Knoll, N., Alix-Panabières, C. & Pantel, K. Clinical relevance and biology of circulating tumor cells. *Breast cancer research : BCR* **13**, 228 (2011).

3. Nagrath, S. *et al.* Isolation of rare circulating tumour cells in cancer patients by microchip technology. *Nature* **450**, 1235-9 (2007).

4. Taback, B. *et al.* Detection of occult metastatic breast cancer cells in blood by a multimolecular marker assay: correlation with clinical stage of disease. *Cancer research* **61**, 8845-50 (2001).

5. Wang, S. *et al.* Three-dimensional nanostructured substrates toward efficient capture of circulating tumor cells. *Angewandte Chemie (International ed. in English)* **48**, 8970-3 (2009).

6. den Toonder, J. Circulating tumor cells: the Grand Challenge. *Lab on a chip* **11**, 375-7 (2011).

7. Allard, W.J. *et al.* Tumor cells circulate in the peripheral blood of all major carcinomas but not in healthy subjects or patients with nonmalignant diseases. *Clinical cancer research : an official journal of the American Association for Cancer Research* **10**, 6897-904 (2004).

8. Li, K., Zhan, R., Feng, S.-S. & Liu, B. Conjugated polymer loaded nanospheres with surface functionalization for simultaneous discrimination of different live cancer cells under single wavelength excitation. *Analytical Chemistry* **83**, 2125-2132 (2011).

9. Zieglschmid, V., Hollmann, C. & Böcher, O. Detection of disseminated tumor cells in peripheral blood. *Critical reviews in clinical laboratory sciences* **42**, 155-96 (2005).

10. Nagrath, S. *et al.* Isolation of rare circulating tumour cells in cancer patients by microchip technology. *Nature* **450**, 1235-9 (2007).

11. Perfézou, M., Turner, A. & Merkoçi, A. Cancer detection using nanoparticle-based sensors. *Chemical Society reviews* (2011).doi:10.1039/c1cs15134g

12. Went, P.T.H. *et al.* Frequent EpCam Protein Expression in Human Carcinomas. *Human Pathology* **35**, 122-128 (2004).

13. Patriarca, C., Macchi, R.M., Marschner, A.K. & Mellstedt, H. Epithelial cell adhesion molecule expression (CD326) in cancer: A short review. *Cancer treatment reviews* (2011).doi:10.1016/j.ctrv.2011.04.002

14. Belov, L., Zhou, J. & Christopherson, R.I. *Cell surface markers in colorectal cancer prognosis. International journal of molecular sciences* **12**, 78-113 (2010).

15. Shi, Z.R., Tsao, D. & Kim, Y.S. Subcellular Distribution , Synthesis , and Release of Carcinoembryonic Antigen in Cultured Human Colon Adenocarcinoma Cell Lines Subcellular Distribution , Synthesis , and Release of Carcinoembryonic. *Cancer Research* **43**, 4045-4049 (1983).

16. Pumera, M. *et al.* Magnetically trigged direct electrochemical detection of DNA hybridization using Au67 quantum dot as electrical tracer. *Langmuir : the ACS journal of surfaces and colloids* **21**, 9625-9 (2005).

17. Ambrosi, A. *et al.* Double-codified gold nanolabels for enhanced immunoanalysis. *Analytical chemistry* **79**, 5232-40 (2007).

18. Ambrosi, A., Airò, F. & Merkoçi, A. Enhanced gold nanoparticle based ELISA for a breast cancer biomarker. *Analytical chemistry* **82**, 1151-6 (2010).

19. Maltez-da Costa, M., De La Escosura-Muñiz, A. & Merkoçi, A., Electrochemical quantification of gold nanoparticles based on their catalytic properties toward hydrogen formation: Application in magnetoimmunoassays. *Electrochemistry Communications* **12**, 1501-1504 (2010).

20. De La Escosura-Muñiz, A. *et al.* Gold nanoparticle-based electrochemical magnetoimmunosensor for rapid detection of anti-hepatitis B virus antibodies in human serum. *Biosensors and Bioelectronics* **26**, 1710-1714 (2010).

21. De La Escosura-Muñiz, A. *et al.* Rapid identification and quantification of tumor cells using an electrocatalytic method based on gold nanoparticles. *Analytical Chemistry* **81**, 10268-10274 (2009).

22. Sergeant, G., Penninckx, F. & Topal, B. Quantitative RT-PCR detection of colorectal tumor cells in peripheral blood--a systematic review. *The Journal of surgical research* **150**, 144-52 (2008).

23. Riethdorf, S., Wikman, H. & Pantel, K. Review: Biological relevance of disseminated tumor cells in cancer patients. *International journal of cancer. Journal international du cancer* **123**, 1991-2006 (2008).

24. Cohen, S.J. *et al.* Isolation and characterization of circulating tumor cells in patients with metastatic colorectal cancer. *Clinical colorectal cancer* **6**, 125-32 (2006).

25. Riethdorf, S. *et al.* Detection of circulating tumor cells in peripheral blood of patients with metastatic breast cancer: a validation study of the CellSearch system. *Clinical*

cancer research : an official journal of the American Association for Cancer Research **13**, 920-8 (2007).

26. Turkevich, J., Stevenson, P.C. & Hillier, J. The formation of colloidal gold. **57**, 670-673 (1953).

27. Zborowski, M. & Chalmers, J.J. Magnetic Cell Separation. *Laboratory Techniques in Biochemistry and Molecular Biology* (2008).

28. Mccloskey, K.E., Chalmers, J.J. & Zborowski, M. Magnetic Cell Separation : Characterization of Magnetophoretic Mobility to enrich or deplete cells of interest from a heterogeneous. *Society* **75**, 6868-6874 (2003).

29. Varadan, V., Chen, L. & Xie, J. *Nanomedicine : design and applications of magnetic nanomaterials, nanosensors and nanosystems*. *The FASEB Journal* (Wiley: 2008).doi:10.1002/9780470715611

30. Nation, L. A new method using hexamethyldisilazane for preparation of soft insect tissues for scanning electron microscopy. *Stain Technology* **58**, 347-351 (1983).

31. Bray, D.F., Bagu, J. & Koegler, P. Comparison of hexamethyldisilazane (HMDS), Peldri II, and critical-point drying methods for scanning electron microscopy of biological specimens. *Microscopy Research and Technique* **26**, 489-495 (1993).

32. Guillemot, J.C. *et al.* Ep-CAM transfection in thymic epithelial cell lines triggers the formation of dynamic actin-rich protrusions involved in the organization of epithelial cell layers. *Histochemistry and cell biology* **116**, 371-8 (2001).

33. Gupton, S.L. & Gertler, F.B. Filopodia: The Fingers That Do the Walking. *Science Signaling* re 5 (2007).doi:10.1126/stke.4002007re5

34. Trzpis, M., McLaughlin, P.M.J., de Leij, L.M.F.H. & Harmsen, M.C. Epithelial cell adhesion molecule: more than a carcinoma marker and adhesion molecule. *The American journal of pathology* **171**, 386-95 (2007).

35. Baeuerle, P. a & Gires, O. EpCAM (CD326) finding its role in cancer. *British journal of cancer* **96**, 417-23 (2007).

36. Loureiro, J. *et al.* Magnetoresistive chip cytometer. *Lab on a chip* **11**, 2255-61 (2011).

37. De La Escosura-Muñiz, A. & Merkoçi, A. Electrochemical detection of proteins using nanoparticles: applications to diagnostics. *Expert Opinion on Medical Diagnostics* **4**, 21-37 (2010).

38. Whitesides, G.M. The origins and the future of microfluidics. *Nature* **442**, 368-73 (2006).

39. Hlavacek, W.S., Posner, R.G. & Perelson, a S. Steric effects on multivalent ligand-receptor binding: exclusion of ligand sites by bound cell surface receptors. *Biophysical journal* **76**, 3031-43 (1999).

40. Bongini, L. *et al.* A dynamical study of antibody-antigen encounter reactions. *Physical biology* **4**, 172-80 (2007).

41. El-Ali, J., Sorger, P.K. & Jensen, K.F. Cells on chips. *Nature* **442**, 403-11 (2006).